EXCURSION GUIDE

InterRad XV in Niigata 2017

Niigata University (JAPAN)

Oct/22–Oct/27, 2017

Edited by Atsushi Matsuoka & Tsuyoshi Ito

EXCURSION GUIDE

InterRad XV in Niigata 2017

Edited by Atsushi Matsuoka & Tsuyoshi Ito

Editorial: Progress in radiolarian research during the last two decades

Atsushi MATSUOKA* and Tsuyoshi ITO**

"Radiolarian Revolution"—This term indicates the rapid development of radiolarian research in 1980s and the overturn of previously-believed scenarios for geological history by interpreting newly accumulated radiolarian fossil evidence. Many radiolarian studies had been performed in Japan, so that Japan was at the major stage of the revolution in 1980s. In October, 1994, the 7th International Radiolarian Symposium (InterRad VII) was held in Osaka, Japan. The excursion guidebook containing three articles for the InterRad VII was published (Ishiga, 1994; Matsuoka et al., 1994; Sakai and Aita, 1994), presenting the latest achievements of radiolarian research at that time.

For the first time in 23 years, the InterRad returns to Japan in October for its fifteenth gathering. Since the last InterRad in Japan, numerous radiolarian studies have been continued and research results have been accumulated steadily. Five excursions (two pre-conference, two mid-day, and one post-conference excursions) are designated in the InterRad XV (Fig. 1). This volume, the supplement volume of no. 32 of *Science Reports of Niigata University (Geology)*, comprises six articles for the excursions of InterRad XV. We here introduce an outline of each article and its significance.

The article by Motoyama et al. (2017a) deals with the Boso Peninsula in Chiba Prefecture. Cenozoic strata with various sedimentological and tectonic settings are well exposed in the Boso Peninsula facing to both Tokyo Bay and the Pacific Ocean. The article introduces these Cenozoic strata, such as uplifted fore-arc cover sediments, trench-slope basin deposits, and accretionary complexes of the trench–fore-arc system. This is the first report of radiolarian occurrences from the Tabuchi section, which is a hopeful candidate of the Global Boundary Stratotype Section and Point (GSSP) of the Middle Pleistocene Stage with the transition from the reversed-polarity Matuyama Chron to normal-polarity Brunhes Chron.

The article by Motoyama et al. (2017a) also describes the Bandai area in the Aizu region, Fukushima Prefecture. The area is well-known for the Bandaisan Geopark. One of the main

* Department of Geology, Faculty of Science, Niigata University, Niigata 950-2181, Japan

** Stratigraphy and Tectonics Research Group, Research Institute of Geology and Geoinformation, Geological Survey of Japan, AIST, Tsukuba 305-8567, Japan
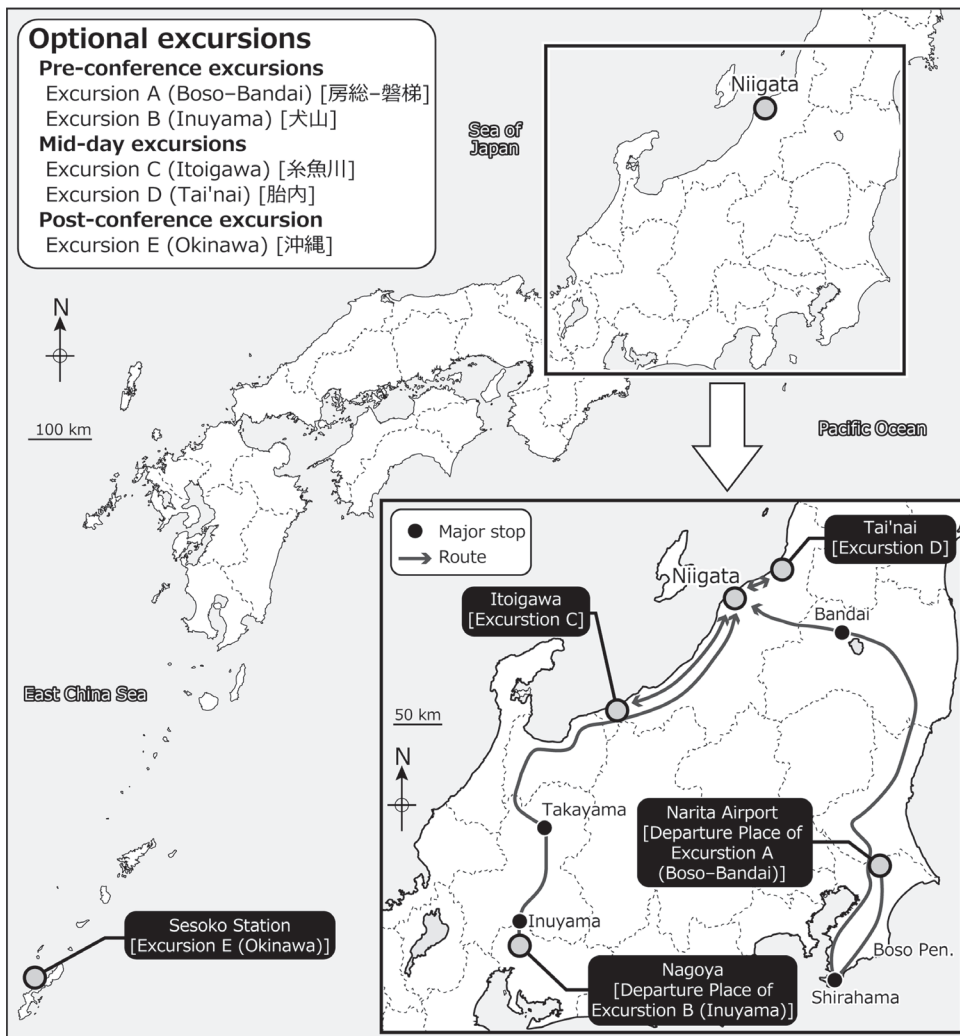
Fig. 1. Optional excursions of InterRad XV in Niigata 2017.

features of the geopark is the Bandai Volcano, an active stratovolcano. Although the Bandai volcano had collapsed several times by eruption in the past and had caused terrible volcanic disasters, it also formed beautiful and magnificent landscapes.

The article by Onoue et al. (2017) compiles numerous studies of Mesozoic radiolarians and accretionary complexes in the southern part of the Mino area. The Triassic–Jurassic chert sequences in the area are one of the most significant and complete records of the Panthalassan pelagic ocean environments. Onoue et al. (2017) show several themes in the area including Early Triassic ocean anoxia and its recovery, Late Triassic Pluvial Event, Late Triassic bolide impact and radiolarian faunal turnover, end-Triassic radiolarian extinction, and Triassic–Jurassic astronomical cycles recorded in the chert sequences. By reviewing the article by Matsuoka et al. (1994), which demonstrated the latest achievements

in research at that time in the same area, the participants will easily realize a great progress in research of these pelagic sequences during the last two decades.

The article by Ito et al. (2017) introduces an outline and history of the Itoigawa UNESCO Global Geopark in Itoigawa, Niigata Prefecture. The geopark was approved as a Global Geopark in 2009, becoming one of the first Global Geoparks in Japan. In fact, the word "geopark" was first coined in Itoigawa when the Fossa Magna Park opened in 1990. One of the main attraction of the Itoigawa UNESCO Global Geopark is the exposures of various rocks in a wide range in origin and age, including various-aged radiolarian occurrences.

The article by Motoyama et al. (2017b) deals with Middle Miocene–Pliocene biosiliceous and microfossil-bearing-silisiclastic sediments at the Natsui section along the Tainai River, Niigata Prefecture. Several biostratigraphies have been constructed in the Natsui section based on microfossils, such as pollen, diatom, planktonic foraminifera, calcareous nannofossil, and ostracod. Motoyama et al. (2017b) newly present Middle to Upper Miocene radiolarian biostratigraphy for the Natsui section. The radiolarian faunas are typical in the Sea of Japan in the Neogene.

The article by Matsuoka et al. (2017) shows previous studies on living radiolarians resulted from annual workshops called "Okinawa Radiolarian Tour" at the Sesoko station (Tropical Biosphere Research Center of the University of the Ryukyus) in Sesoko Island, Okinawa Prefecture. The successive tours have provided valuable knowledge on living radiolarians (e.g., faunal characteristics, biological activities, skeletal growth, and molecular phylogeny); therefore, the station is one of the most important research stations for living radiolarian studies in the world. In addition, the article compiles brief histories of radiolarian biological research and introduces practical information on oceanographic conditions, travel, safety, and handling and storage procedures for radiolarian studies in the Sesoko Station. For beginners of living radiolarian study, the article can contribute to handle living radiolarians as a first step.

The article by Ito and Matsuoka (2017) describes the geology and radiolarian occurrences in Ie Island, Okinawa Prefecture. Mesozoic accretionary complexes are exposed in the Okinawa Islands, but its exposure is scattered because the Pleistocene Ryukyu Group covers them. Ie Island is therefore the valuable area for Paleozoic and Mesozoic radiolarian researches in the Okinawa Islands. The bedded cherts of the Gusukuyama Formation in Mt. Gusuku in the central part of the island contain late Permian–Late Jurassic radiolarians; siliceous mudstones in the southern flank of Mt. Gusuku yield latest Jurassic–earliest Cretaceous radiolarians. Red chert clasts within the Pleistocene Ryukyu Group at Waji in the north coast of Ie Island contain Permian radiolarians including dimorphic pairs of Albaillellaria, which are rarely reported worldwide.

The above-mentioned articles include not only the compilation of numerous previous studies but also valuable unpublished data. The participants may realize that "Radiolarian

Revolution" is still ongoing in Japan. Moreover, the articles cover subjects of general interest, such as regional geology and geoparks. We hope these articles will help all participants to enjoy the excursions.

Acknowledgements

References

Ishiga, H., 1994, Late Paleozoic bedded cherts and Permian and Triassic boundary in the Tanba Terrane, Southwest Japan. *Guide Book for INTERRAD VII Field Excursion*, Organizing committee of INTERRAD VII, Osaka, 1–18.

Ito, T., Ibaraki, Y. and Matsuoka, A., 2017, Outline and history of the Itoigawa UNESCO Global Geopark in Niigata Prefecture in central Japan, with radiolarian occurrences in Itoigawa. *Sci. Rep. Niigata Univ. (Geol.)*, no. 32 (Supplement), 71–90.

Ito, T. and Matsuoka, A., 2017, Permian–Cretaceous radiolarians from Ie Island, Okinawa Prefecture, Japan. *Sci. Rep. Niigata Univ. (Geol.)*, no. 32 (Supplement), 125–136.

Matsuoka, A., Hori, R., Kuwahara, K., Hiraishi, M., Yao, A. and Ezaki, Y., 1994, Triassic-Jurassic radiolarian-bearing sequences in the Mino terrane, central Japan. *Guide Book for INTERRAD VII Field Excursion*, Organizing committee of INTERRAD VII, Osaka, 19–61.

Matsuoka, A., Suzuki, N., Ito, T., Kimoto, K., Tuji, A., Ichinohe, R. and Li, X., 2017, Excursion guide to radiolarians in the East China Sea near Sesoko Island, Okinawa, Japan: A distinguishing research station for living radiolarian studies. *Sci. Rep. Niigata Univ. (Geol.)*, no. 32 (Supplement), 103–123.

Motoyama. I., Itaki, T., Kamikuri, S., Taketani, Y. and Okada, M., 2017a, Cenozoic biostratigraphy, chronostratigraphy and paleoceanography in the Boso Peninsula and Bandai Volcano in the Aizu region, East Japan. *Sci. Rep. Niigata Univ. (Geol.)*, no. 32 (Supplement), 1–27.

Motoyama, I., Kurihara, T. and Itaki, T., 2017b, Neogene biosiliceous sedimentary sequence and radiolarian biostratigraphy in the Tainai area, Niigata Prefecture. *Sci. Rep. Niigata Univ. (Geol.)*, no. 32 (Supplement), 91–102.

Onoue, T., Hori, R. S. and Kojima, S., 2017, Triassic and Jurassic radiolarian response to global catastrophic events in the Panthalassa Ocean, as recorded in the Mino Belt, central Japan. *Sci. Rep. Niigata Univ. (Geol.)*, no. 32 (Supplement), 29–69.

Sakai, T. and Aita, Y., 1994, Neogene siliceous microfossil-bearing sequence of the Northern Kanto District. *Guide Book for INTERRAD VII Field Excursion*, Organizing committee of INTERRAD VII, Osaka, 63–88.

Cenozoic biostratigraphy, chronostratigraphy and paleoceanography in the Boso Peninsula and Bandai Volcano in the Aizu region, East Japan

Isao MOTOYAMA*, Takuya ITAKI**, Shin'ichi KAMIKURI***,
Yojiro TAKETANI**** and Makoto OKADA*****

Abstract

The Boso Peninsula is a geologically active region where Cenozoic marine sediments formed in a wide variety of depositional and tectonic environments, including ocean basins, trench, trench-slope basins, forearc basins, and shelf to coastal zones. Radiolarians are key to dating most of these sedimentary rocks. In the northern part of the peninsula, Quaternary sedimentary sequences consisting mainly of siltstone and sandstone crop out along canyons of the Yoro and other rivers. There is no better place in the world than the Yoro canyon to correlate the Pleistocene geomagnetic polarity records to marine micro-biostratigraphy, oxygen isotope records, and radiometric ages from volcanic ash layers. This feature is of great benefit to establishing the boundary stratotype of the lower and middle parts of the Pleistocene Stage. In the more mountainous area to the south, visitors can trace the geological history back to middle Miocene through continuous sedimentary sequences. The earliest fossils imprinted in the rock of the peninsula are of early Cretaceous radiolarians from the Mineoka ophiolite complex. Since the Early Miocene the southern part of the peninsula was covered by seas and close to the trench where the Philippine Sea Plate subducts under the North American Plate. Continual subduction of the oceanic plate resulted in a pile of accreted Miocene sedimentary rocks in the southern part of the peninsula. Cover sediments unconformably resting on those accretionary prisms are thought to represent trench-slope basin deposits. Well-developed uplifted marine terraces in the

   * Faculty of Science, Yamagata University, Yamagata 990-8560, Japan
  ** Geological Survey of Japan, AIST, Tsukuba, Ibaraki 305-8567, Japan
 *** Faculty of Education, Ibaraki University, Bunkyo 2-1-1, Mito, Ibaraki 310-8512, Japan
 **** Fukushima Museum, Aizuwakamatsu, Fukushima 965-0807, Japan
***** Faculty of Science, Ibaraki University, Bunkyo 2-1-1, Mito, Ibaraki 310-8512, Japan
      Corresponding author: I. Motoyama,
      i-motoyama@sci.kj.yamagata-u.ac.jp

southern portion of the peninsula represent the Holocene-continuing seismic activity associated with the earthquake cycle.

Mount Bandai is a cone-shaped active stratovolcano. Past eruptions and collapses of mountain body formed a dammed lake, Lake Inawashiro, the fourth largest lake in Japan, to the south and created the numerous beautiful lakes in the forest land to the north. Bandai Volcano and its surrounding area was registered as a Japanese Geopark in 2011.

Key words: fore-arc basin, trench-slope deposit, Radiolaria, microfossil, Global Boundary Stratotype Section and Point (GSSP), Tabuchi section, Bandaisan Geopark

Introduction

The Boso Peninsula in Chiba Prefecture is bordered by the Tokyo Metropolitan City in the northwest, facing Tokyo Bay to the west and the Pacific Ocean to the south and east (Fig. 1). Although its elevation (highest peak of 408 m) is quite low, vigorous erosion by river flows have formed lots of creeks displaying excellent exposures in this region, because of the rapid uplift and humid climate during the Quaternary. Such good conditions for geological observation make the Boso Peninsula one of the most well-known geological fields of the upper Cenozoic sedimentary sequence in Japan, encompassing raised fore-arc and trench-slope basin deposits and an accretionary complex of the trench–fore-arc system near the triple junction of trenches that is unique in the world. At the junction, one continental (North American Plate) and two oceanic (Philippine Sea Plate and Pacific Plate) plates meet, with the latter subducting under the former plate. The fore-arc deposits represent the Middle Miocene to Pleistocene sedimentologic, micropaleontologic, and magnetostratigraphic records, including the lower and middle parts of the Pleistocene Stage with the transition between the Matuyama and Brunhes polarity chrons – a hopeful candidate of the Global Boundary Stratotype Section and Point (GSSP). Microfossils are common to abundant in these upper Cenozoic strata. Both the siliceous and calcareous microfossils have been documented from them to determine depositional ages. These microfossils contain both low-latitude and boreal faunal and floral elements, because of the close proximity to the confluence zone of the warm Kuroshio Current and the cold Oyashio Current through time, so they provide an effective clue to reconstructing the paleoceanographic evolution of the mid-latitude western Pacific Ocean since the Middle Miocene. However, little effort has been made on this issue in the field. The accretionary prism and the trench-slope basin-fill deposits also yield well-preserved siliceous microfossils that have been studied for the reconstruction of the structural development of the trench-slope system.

Bandai Volcano is an active stratovolcano located in the Aizu area, Northeast Japan (Figs. 1, 2). Because of its beautiful conical shape it is sometimes called ʻAizu Fujiʻ. The mountain
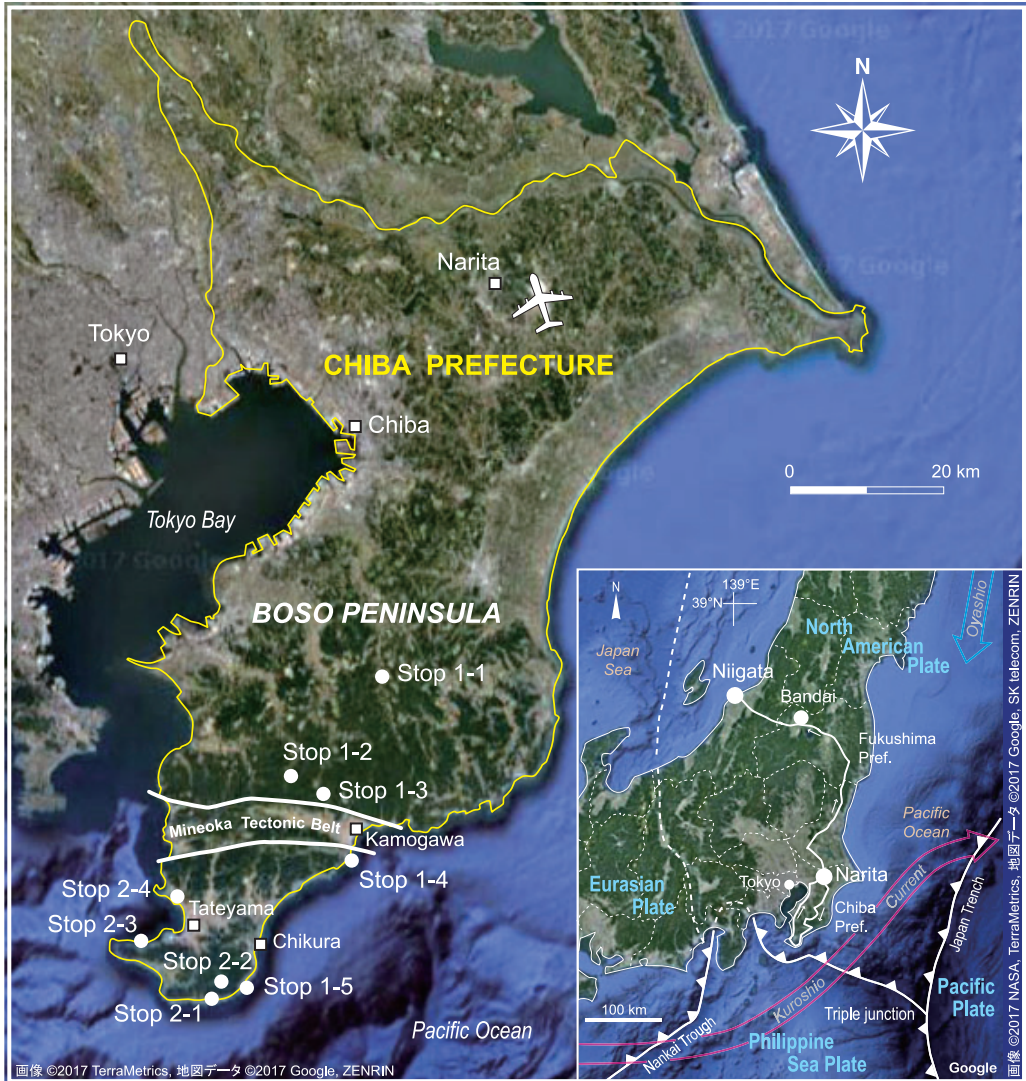
Fig. 1. Index map.

body collapsed many times during past eruptions, especially the eruption in 1888, which was the most terrible volcanic disaster within the last 150 years (i.e., since the beginning of the Meiji Era) in Japan. However, it resulted in a beautiful and magnificent landscape, and so the Bandai Volcano area was admitted to the Japan Geopark Network in 2011.

Fig. 2. Locality of Bandaisan (Bandai Volcano).

Geology and Micropaleontology

1. Boso Peninsula

The Boso Peninsula can be divided into three geological zones: the northern area where the Middle Miocene to Pleistocene normal sediments distribute, the Mineoka tectonic belt characterized by an ophiolitic complex and Lower Miocene accretionary prism, and the southern area associated with a Miocene to Pliocene accretionary prism that are unconformably overlain by Middle Miocene to Pleistocene cover sediments (Figs. 1, 3). These zones are bordered by major faults extending in an E-W direction. Across the Mineoka belt the sedimentary facies, deformation of strata, and geologic history change abruptly. The northern area is of interest for biostratigraphy and chronostratigraphy. The Mineoka belt and the southern portion compose a unique field where we can see the young trench-slope tectonic system in onshore sections. Much attention has recently been focused on the origin and evolution of the system through studies of sedimentology and structural geology. Microfossils have contributed in dating these sediments and reconstructing a detailed tectonic and sedimentological history.

Northern area: A thick marine sedimentary sequence of the Awa, Kazusa, and Shimosa Groups in ascending order distribute in this area. These groups represent the history of fore-arc basins and display evidence of a progressive shoaling of marine environments from slope to shelf environments through the Middle Miocene to Quaternary (Kitazato, 1997; Ito et al., 2016). These strata become progressively younger to the north, but are gently folded with E–W axes near the Mineoka tectonic belt.

The Awa Group with a thickness of 3,000 m, ranging in age from 16 to 3 Ma, is subdivided into the Kanigawa, Kinone, Amatsu, Kiyosumi, and Anno Formations. The Miura Group, whose stratotype is placed in the Miura Peninsula, is an equivalent unit to the Awa Group. The facies of the Kanigawa to Kinone Formations indicates an upward deepening trend and the Amatsu Formation consists mainly of hemipelagic mudstone. The Kiyosumi and Anno Formations consist of alternations of sandstone and mudstone representing flysh facies deposited in submarine fan environments (Tokuhashi, 1979; Nakajima et al., 1981). Micropaleontological evidence suggests deposition of the Awa Group in the fore-arc basin began in the mid Miocene (16–15 Ma). The Amatsu Formation is a thick (1,000 m) hemipelagic sequence that deposited during 12 to 5.5 Ma and intercalates numerous ash layers of which characteristic ones are numbered from AM1 to AM98. This formation yields calcareous and siliceous microfossils and has been dated by a lot of biostratigraphic works (planktonic foraminifera, Oda, 1977; calcareous nannofossils, Kanie et al., 1991; Mita and Takahashi, 1998; Kameo et al., 2002, 2010; Kameo and Sekine, 2013; Radiolaria, Motoyama and Takahashi, 1997; Sawada et al., 2009; diatoms, Haga and Kotake, 1996; Watanabe and Takahashi, 1997, 2000; Takahashi et al., 1999). Kitazato (1997) estimated paleodepths of 1,000 to 2,000 m for the Amatsu to Anno Formations.

The Awa Group is separated from the overlying Kazusa Group by a gently angular unconformity called the Kurotaki Unconformity. The Kazusa Group was formed by sediment accumulation in a fore-arc basin during 2.4 to 0.45 Ma (Ito et al., 2016). The best exposures of this group are found along the Yoro River where 3,000 m of north-dipping mudstones, sandstones, and tuff beds are displayed. The basal conglomerate of the Kurotaki Formation unconformably overlays the Awa Group. Erosion of the underlying sediments by this unconformity becomes greater to the east. Calcareous microfossils are abundant in the Kazusa Group and have been well investigated in biostratigraphic and paleoceanographic works (e.g., Aoki, 1963, 1968; Kitazato, 1977; Nishida, 1977; Oda, 1977; Takayama and Ikeno, 1977; Sato et al., 1988, 1999; Igarashi, 1994), while diatom biostratigraphic study is restricted to Cherepanova et al. (2002) and no radiolarian works have been published, so that much more work is needed to clarify the nature of siliceous fauna and flora. Studies on the oxygen isotope stratigraphy has been done by Okada and Niitsuma (1989), Pickering et al. (1999) and Tsuji et al. (2005). The lower part of the Kazusa Group was deposited in bathyal environments with a maximum paleodepth of ~1,500 m (Kitazato, 1997) and the middle part

of this group of late Pleistocene age represents the final phase of deep-sea deposition in the Boso area (Ito and Katsura, 1992). The overlying Shimosa Group of late Pleistocene age is composed mainly of sandstone deposited in shelf to coastal environments. This group has yielded abundant fossil marine molluscan shells. A few fossil mammals have been discovered from this group.

We have preliminarily investigated radiolarian assemblages from the middle to upper Miocene Amatsu Formation using samples collected by Sawada et al. (2009) to discuss paleoceanography. The radiolarian assemblages comprising 95 taxa include 17 warm-water (low latitude) taxa (*Anthocyrtidium* spp., *Calocycletta caepa*, *Carpocanium* spp., *Collosphaera* spp., *Dictyocoryne* spp., *Diartus hughesi*, *D. petterssoni*, *Didymocyrtis laticonus*, *D. penultima*, *Heliodiscus* spp., *Lithopera renzae*, *L. thornburgi*, *Lophocyrtis pentagona*, *Phormostichoartus corbula*, *P. doliolum*, *Phorticium pylonium* group, *Stylodictya multispina* group), and 12 cool-water (high latitude/cosmopolitan) taxa (*Amphistylus angelinus*, *Axoprunim bispiculum*, *Cyrtocapsella japonica*, *C. tetrapera*, *Larcopyle polyacantha* group, *Lithelius minor* group, *Lophocyrtis aspera*, *Spongodiscus gigas*, *S. sol, Stylosphaera timmsi*, *Thecosphaera dedoensis*, *T. pseudojaponica*). The faunal composition suggests the studied region was in the temperate climatic zone influenced by both warm and cool water currents. The fluctuation patterns in the relative abundance of warm-water taxa indicate that the Kuroshio Current was strengthened during three intervals (12.5 Ma, 11.5 to 10.5 Ma, and 9.5 to 8.5 Ma).

Mineoka tectonic belt: This zone represents 'basement rocks' of the Boso Peninsula. It involves the Mineoka ophiolitic complex comprising various sized exotic blocks of ultramafic rocks (peridotite, serpentinite), basalt, dolerite, diorite, sandstone, shale, chert, and limestone (Takahashi et al., 2012, 2016). Middle Eocene radiolarians occurred from a siliceous mudstone nodule (Kawakami, 2004); Paleocene to Oligocene planktonic foraminifers were found from limestone blocks (Mohiuddin and Ogawa, 1996, 1998a, b); and bedded chert yielded early Cretaceous radiolarians (Ogawa and Sashida, 2005). These suggest that the Mineoka ophiolitic complex includes the oldest rocks in the Boso Peninsula. A great deal of attention has been focused on the origin and evolution of this ophiolitic complex through petrological and geochronological studies (e.g., Ogawa and Naka, 1984; Arai, 1991; Fujioka et al., 1995; Hirano et al., 2003; Takahashi et al., 2012). Some of these investigations link the origin of the complex to the Philippine Sea Plate, while some implicate the lost Mineoka Plate, which is thought to have existed in the western Pacific during the Paleogene, but has now disappeared because of subduction of the plate into the mantle (Hirano et al., 2003). The ophiolitic complex might have been squeezed out to the surface from great depths along a major thrust fault system.

The Mineoka ophiolite complex is surrounded by the Hota Group, which consists of mudstone, sandstone and tuffs associated with deformational structures such as thrusts, folds, repetitions, and shared structures indicative of an accretionary prism (Takahashi et al.,
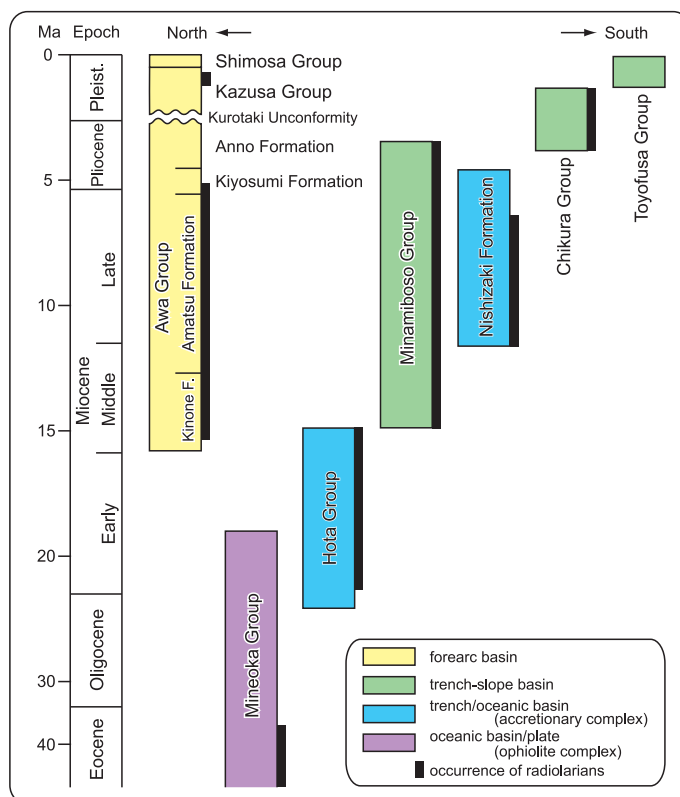
Fig. 3. Subdivision and correlation of Cenozoic rocks in Boso Peninsula.

2016). Radiolarians from the Hota Group indicate an early Miocene age (Saito, 1992).

Southern area: The oldest rocks in this area are represented by the accretionary complex Hota Group. Mudstones of this group yield latest Oligocene diatoms (Suzuki et al., 1996) and Early Miocene radiolarians (Saito, 1992) while Paleogene radiolarians were reported from gravels of tuff and mudstone included in the group (Kawakami, 2004). There is a younger accretionary prism called the Nishizaki Formation. Radiolarians indicate a Late Miocene age for this formation (Kawakami, 2001; Yamamoto and Kawakami, 2005). These accretionary complexes are unconformably overlain by cover sediments that are assigned to the Minamiboso, Chikura and Toyofusa Groups. The Minamiboso Group consists of eight formations that represent separated small trench-slope basins varying in age from the Middle Miocene to Pliocene (Kawakami and Shishikura, 2006). The Chikura Group in this area consists of Upper Pliocene to Lower Pleistocene marine deposits (siltstone, sandstone, and conglomerate) and is divided into the Shirahama, Shiramazu, Mera, and Hata Formations, in ascending order (Kawakami and Shishikura, 2006). These strata are gently folded with E–W axes becoming progressively younger to the north. Molluscan fossils including *Calyptogena*, which represents cold seep communities in deeps-sea environments,
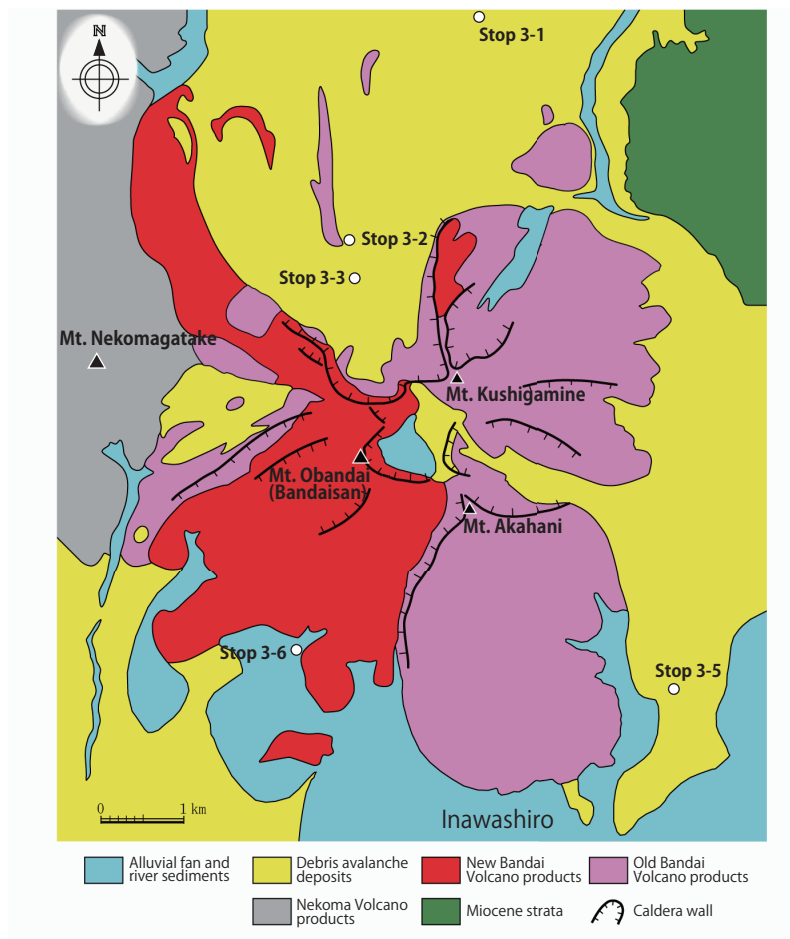
Fig. 4. Geological map of Bandai Volcano. After Taketani et al. (2015), simplified from Chiba and Kimura (2001).

and various microfossils including foraminifera, calcareous nannofossils, radiolarians, and diatoms occur in these formations. The Toyofusa Group is a Pleistocene representative of the cover sediments in the trench-slope system.

2. Bandai Volcano and Bandaisan Geopark

Bandai Volcano, an active volcano on the east Japan volcanic front, is located in the Aizu area of Fukushima Prefecture, Northeast Japan (Fig. 2). The volcano has three peaks: Mt. Obandai (Bandaisan) (1,816 m), the highest peak of the volcano, Mt. Kushigamine (1,636 m), and Mt. Akahani (1,427 m) (Fig. 4).

Bandai Volcano is covered with thick layers of pyroclastic flow sediments in addition to andesitic lavas. The eruptive history of Bandai Volcano has been researched mainly by tephrochronology (Yamamoto and Suto, 1996; Chiba and Kimura, 2001). The volcano became

active about 700,000 years ago (Mimura, 1994). First, a large mountain body (Old Bandai Volcano), which includes Mt. Kushigamine and Mt. Akahani, was formed (Fig. 4). About 50,000 years ago a large part of the southwestern slope of Old Bandai volcano collapsed during a Plinian eruption (Yamamoto and Suto, 1996). The debris avalanche spread across a large area and Lake Inawashiro was born by natural damming of a river (Nagahashi et al., 2016). In the collapsed area, volcanic activity became high, which led to the formation of Mt. Obandai and its northern neighbor Mt. Kobandai (New Bandai Volcano) (Chiba and Kimura, 2001) (Fig. 4).

Most of Mt. Kobandai collapsed during a phreatic explosion in 1888 and a large horseshoe-shaped caldera was formed (Sekiya and Kikuchi, 1889). The collapse brought rapid debris avalanches to the north this time, burying many villages and killing 477 people (Nakamura, 1978). On the other hand it formed about 300 beautiful dammed lakes, magnificent landscapes and a characteristic natural environment. The area around Bandai Volcano was designated as Bandai Asahi National Park in 1950.

In 2010 the Bandaisan Geopark Council was established for conservation and utilization of natural and cultural resources related to Bandai Volcano. The Bandai Volcano area was admitted to the Japan Geopark Network in 2011 by the Japan Geopark Committee. The main theme of the Bandaisan Geopark is to clarify the birth and transition of Bandai Volcano, especially large scale change of topography and natural environment caused by mountain collapse and the following debris avalanche, and furthermore to study the volcano's influence on regional history and culture. The Bandaisan Geopark Council is now making an effort to join the UNESCO Global Geopark Network.

<center>Description of field stops</center>

STOP 1
Stop 1-1: Tabuchi section—Boundary section of the Lower/Middle Pleistocene, Plio-Pleistocene fore-arc basin deposits (Kokumoto Formation, Kazusa Group)

The Tabuchi section is located about 40 km south of Narita Airport (Fig. 1). Here a sequence of Pleistocene marine sedimentary strata is exposed in its most complete succession. The sedimentary sequence at the Tabuchi section is a hopeful candidate of the GSSP for the Lower/Middle Pleistocene (Aida, 1997), which is in competition with the other candidates from Italy toward the formal certification of the GSSP and the 'Chibanian Stage' by the IUGS. The boundary of the Lower/Middle Pleistocene is defined by the youngest geomagnetic polarity reversal, the Matuyama–Brunhes reversal event, dated at 0.78 Ma when the Earth's magnetic field switched from the reversed to the normal mode. The Tabuchi section is superior to the others in having a detailed magnetic polarity record around the transition from Matuyama to Brunhes in a high-sedimentation-rate (200 cm /

Fig. 5. Massive siltstone of the Kokumoto Formation, Kazusa Group, recording the youngest geomagnetic polarity reversal, the Matuyama-Brunhes boundary, on a cliff of the Tabuchi section along the Yoro River. Byakubi-E tephra gently dipping to the left (north) just above the third red mark from the bottom has been dated to 772.7 ±7.2 kiloyears ago using U–Pb zircon dating (Suganuma et al., 2015).

kiloyear) sedimentary sequence (Okada and Niitsuma, 1989; Kazaoka et al., 2015; Nishida et al., 2016; Okada et al., 2017). Most recently this magnetostratigraphic record has been correlated with an oxygen isotope chronology using foraminiferal tests from the same section (Suganuma et al., 2015), suggesting that the polarity transition falls within the marine isotope stage (MIS) 19. The polarity boundary has been calibrated at 770.2 ±7.3 ka based on radiometric (U–Pb) dating for a tephra (Byakubi-E) just below the polarity boundary. The Tabuchi section is placed in a gorge along the Yoro River where fine-grained deep-sea sediments of the Kokumoto Formation, Kazusa Group, is well exposed. These sediments yield marine calcareous and siliceous microfossils as well as pollen derived from terrestrial environments. Although some low-resolution biostratigraphic study has been published for the Kazusa Group along the Yoro River (e.g., Aoki, 1963, 1968; Oda, 1977; Takayama and Ikeno, 1977; Nishida, 1977; Igarashi, 1994), it is expected that new microfossil-based studies will provide high-resolution paleoclimatic and paleoceanographic reconstructions for mid-Pleistocene central Japan.

When we stand on the dry river floor the escarpment on our left marks the position of the polarity boundary (Fig. 5). We can see colored pins that mark stratigraphic horizons of samples for magnetostratigraphy, of which red and green ones are of reversed and normal polarity, respectively, and yellow ones are of transitional nature. Byakubi-E tephra, gently
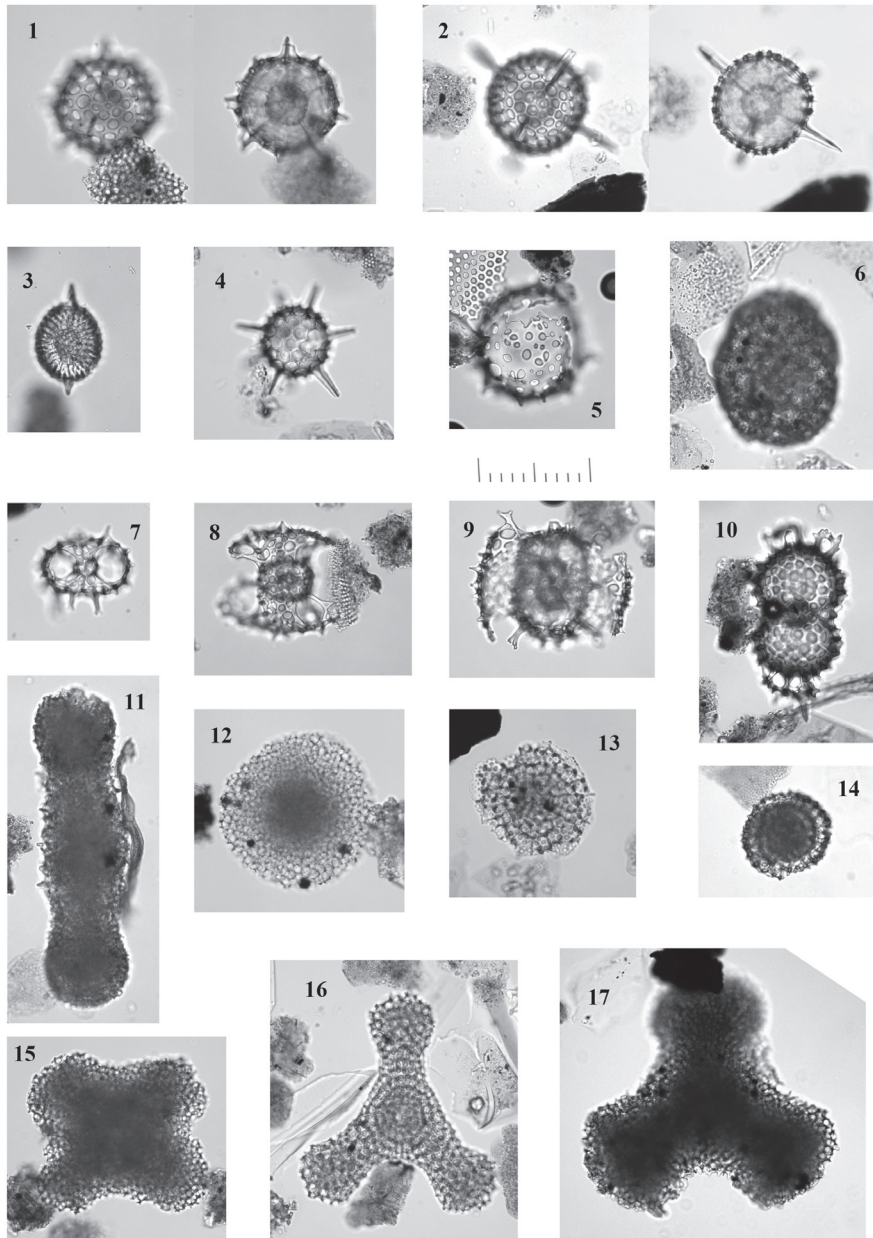
Fig. 6. Radiolarians from the Kokumoto Formation (Early-Middle Pleistocene): **1.** *Actinomma leptodermum* (Jørgensen) (sample KG7), **2.** *Hexacontium pachydermum* Jørgensen (sample KG13), **3.** *Druppatractus irregularis* Popofsky (sample YW11), **4.** *Acanthosphaera circopora* Popofsky (sample YN7), **5.** *Acrosphaera spinosa* (Haeckel) (sample YW11), **6.** *Larcopyle buetschlii* Dreyer (sample KG11), **7.** *Tetrapyle* sp. (sample KG13), **8.** *Tetrapyle circularis* Haeckel (sample YW5), **9.** *Phorticium pylonium* Haeckel (sample YW1), **10.** *Didymocyrtis* sp. (sample YW3), **11.** *Spongocore cylindrica* (Haeckel) (sample KG29), **12.** *Spongodiscus resurgens* Ehrenberg (sample KG7), **13.** *Stylochlamydium venustum* (Bailey) (sample KG17), **14.** *Larcospira minor* (Jørgensen) (sample YN9), **15.** *Spongaster tetras tetras* Ehrenberg (sample YW5), **16.** *Dictyocoryne profunda* Ehrenberg (sample YN9), **17.** *Dictyocoryne truncatum* (Ehrenberg) (sample YN8). Scale equals 100 μm. All specimens were collected from around Stop 1-1. See Okada et al. (2017) for sample horizons.
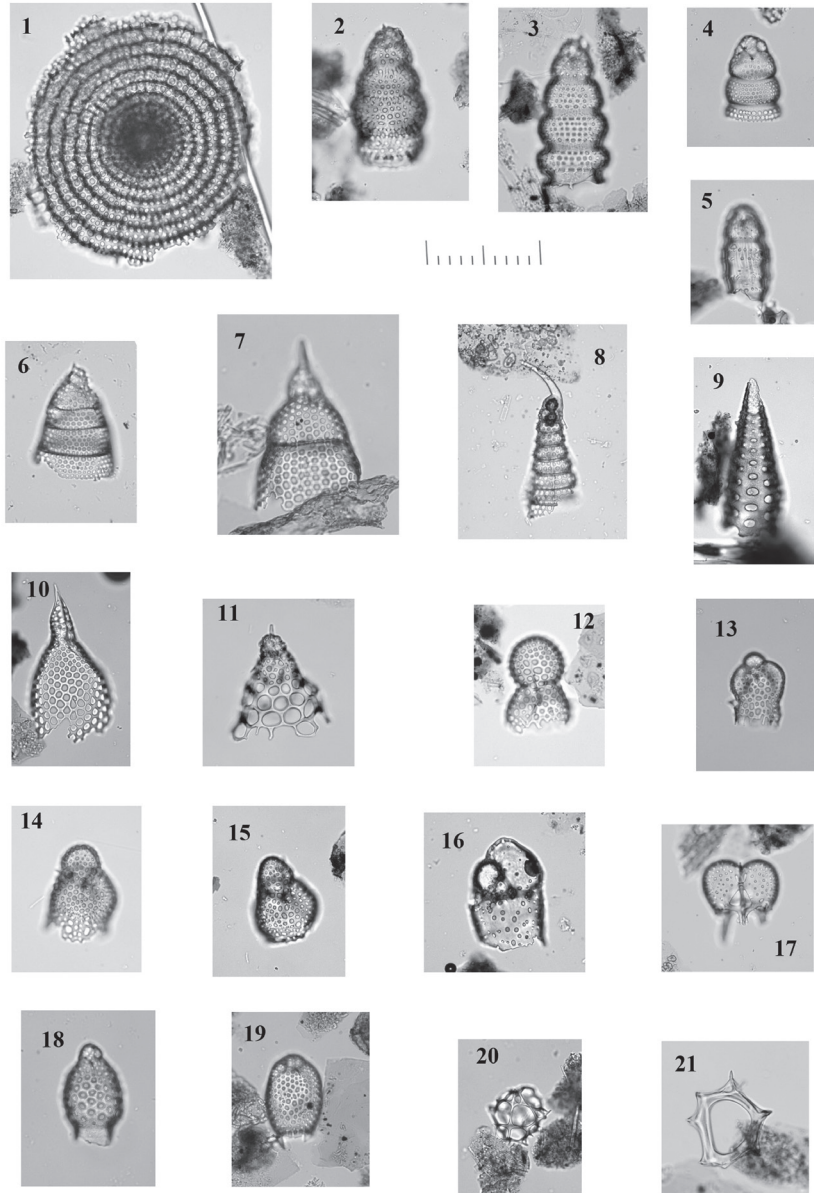
Fig. 7. Radiolarians from the Kokumoto Formation (Early-Middle Pleistocene): **1.** *Flustrella* sp. (sample YW3), **2.** *Botryostrobus aquilonaris* (Bailey) (sample YN7), **3.** *Botryostrobus auritus/australis* (Ehrenberg) group (sample YN7), **4.** *Lithamphora furcaspiculata* Popofsky (sample KG13), **5.** *Siphocampe arachnea* (Ehrenberg) (sample KG5), **6.** *Eucyrtidium hexastichum* (Haeckel) (sample KG11), **7.** *Pterocorys clausus* (Popofsky) (sample KG17), **8.** *Cyrtolagena cuspidata* (Bailey) (sample YN7), **9.** *Cornutella profunda* Ehrenberg (sample YN8), **10.** *Anthocyrtidium zanguebaricum* (Ehrenberg) (sample YN4), **11.** *Cycladophora davisiana* Ehrenberg (sample YN11), **12.** *Dimelissa thoracites* (Haeckel) (sample KG5), **13.** *Trisulcus* sp. (sample YN9), **14.** *Lithomelissa setosa* Jørgensen (sample YN9), **15.** *Lithomelissa setosa* Jørgensen (sample YN11), **16.** *Botryopyle cribosa* (Popofsky) group (sample YW7), **17.** *Phormospyris stabilis* (Goll) *scaphipes* (Haeckel) (sample YN9). **18.** *Carpocanarium papillosum* (Ehrenberg) (sample KG7), **19.** *Carpocanistrum* sp. (sample KG17), **20.** *Plectacantha oikiskos* Jørgensen (sample YW7), **21.** *Zygocircus productus* (Hertwig) group (sample YN9). All specimens were collected from around Stop 1-1. See Okada et al. (2017) for sample horizons.

Fig. 8. Upper part of the Amatsu Formation including a wide-spread tephra, Am78, so called 'OK Tuff', Koitogawa River.

dipping to the north, is placed just below the transitional horizon.

    Takuya Itaki and his coworkers have started paleoceanographic work based on radiolarian assemblages from the Tabuchi section. Radiolarian fossils collected from this section are shown in Figs. 6 and 7. Their assemblages are mainly composed of warm water taxa (e.g., *Dictyocoryne* spp., *Didymocyrtis* spp., and *Tetrapyle* spp.) related to the subtropical Kuroshio Current. Cold water species such as *Lithomelissa setosa* and *Stylochlamydium venustum* are also recognized during the glacial intervals suggesting influence of the cold Oyashio Current.

Stop 1-2: Koito River—Upper Miocene fore-arc basin deposits (Awa Group)

    The upper course of the Koito River is characterized by extensive exposures of Neogene marine deposits named as the Amatsu, Kiyosumi, and Anno Formations. The portion at Stop 1-2 (key ash layers AM66 to AM78) represents the coarse grained facies of the upper part of the Amatsu Formation (Fig. 8) and displays evidence of a decrease in sedimentation rate around 8 to 6 Ma. Radiolarian assemblages from this facies indicate zones RN7 (*Didymocyrtis antepenultima* Zone) to RN9 (*Stichocorys peregrina* Zone) (Sawada et al., 2009). The upper course of the Koito River is generally inaccessible except by trail because of a deep valley with vertical cliffs. At this stop there are excellent exposures of sandstone and sandy mudstone beds with many ash layers along the trail. On the cliff there are number plates pinned to the key ash layers.
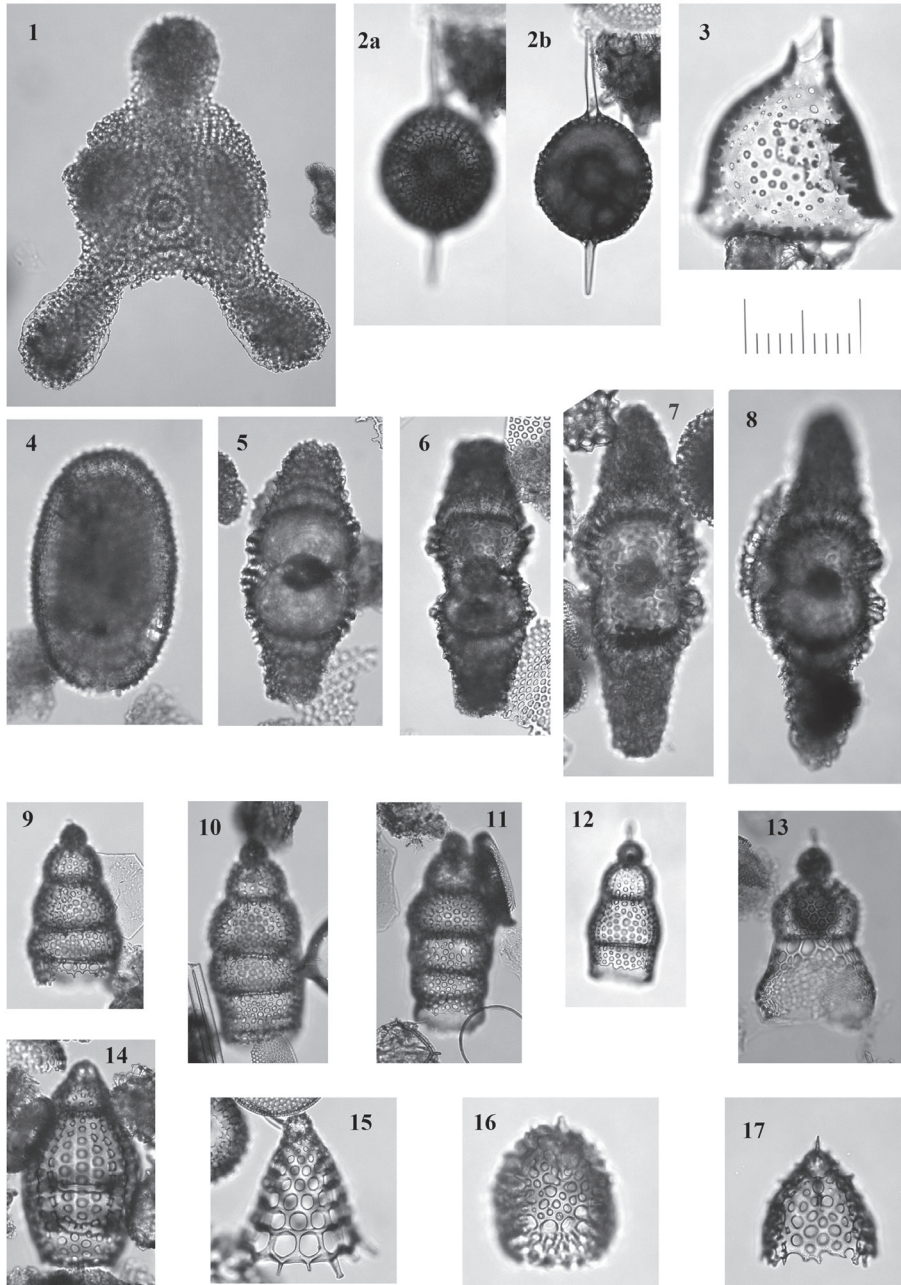
Fig. 9. Radiolarians from the lower part of the Amatsu Formation (middle Miocene): **1.** *Dictyocoryne agrigentina* Stöhr, **2.** actinommid gen. et sp. indet. (Sanfilippo et al., 1985, Fig. 5-2), **3.** *Trisolenia megalactis megalactis* Ehrenberg, **4.** *Larcopyle polyacantha polyacantha* (Campbell and Clark), **5–8.** *Didymocyrtis laticonus* (Riedel), **9–10.** *Stichocorys peregrina* (Riedel), **11–12.** *Stichocorys delmontensis* (Campbell and Clark), **13.** *Stichocorys* aff. *johnsoni* Caulet, **14.** *Eucyrtidium inflatum* Kling, **15.** *Cycladophora cosma cosma* Lombari and Lazarus, **16.** *Ceratocyrtis stoermeri* Goll and Bjørklund, **17.** *Ceratocyrtis* sp. Scale equals 100 μm. All specimens were collected from sample Boso-8 (calcareous concretion between ash layers Am1 and Am2, Meigawa River).

Stop 1-3: Meigawa River—Middle Miocene fore-arc basin deposits (Awa Group)

The Meigawa River (called as 'Kanigawa section' in some literatures), a tributary of the Kamogawa River, is located 4.5 km southeast from Stop 1-2. Along the river the Middle Miocene part of the Awa Group (Kanigawa, Kinone, and lower Amatsu Formations) is well exposed and the integrated biostratigraphy of multiple microfossil groups has been established by Takahashi et al. (1999). This stop is at the bottom of the Amatsu Formation which is defined by the first occurrence of scoria ash layers, Am1. This stratigraphic horizon is correlated to the radiolarian *Eucyrtidium inflatum* Zone and *Dorcadospyris alata* Zone (Motoyama and Takahashi, 1997). We collected a sample of a calcareous concretion between ash layers Am1 and Am2 and herein illustrate the characteristic species found in it (Figs. 9 and 10).

Stop 1-4: Futomi-hama—Lower Miocene accretionary prism (Hota Group)

This is where we can take rock samples containing radiolarians of zones RN2 (*Stichocorys delmontensis* Zone) or RN3 (*Stichocorys wolffii* Zone). The Hota Group is composed of fairly deformed mudstone and sandstone intercalating ash layers. The absence of calcareous microfossils suggests that it deposited in deep-sea environments below the calcium carbonate compensation depth (CCD) (Yamamoto et al., 2017). This group ranges from the Early Miocene to the earliest Middle Miocene in age (RN1 to RN5), indicating progressively younger sediments toward the north (Saito, 1992) and is thought to have been accreted to the island arc during 17 to 15 Ma (Yamamoto et al., 2017). The rocks here are folded mudstone and thin tuff beds cut by numerous small faults and repetitions of units can be observed (Fig. 11).

Stop 1-5: Shiramazu—Plio-Pleistocene trench-slope basin deposit (Chikura Group)

On the coast from Chikura to Shirahama, there are good exposures of the Chikura Group. These outcrops are designated as the stratotypes of the Shirahama and Shiramazu Formations. The Shirahama Formation is 100 m in thickness and consists of an alternation of sandstone and mudstone with minor conglomerate. This formation is characterized by reddish brown colored sandstone comprising volcaniclastic coarse grains and poorly preserved microfossils, presumably of Pliocene age, although no biostratigraphic works have been done yet. The Shiramazu Formation (200 m thickness) is composed of an alternation of sandstone and tuffaceous siltstone. Scoria sandstone beds are intercalated in these sediments. These sandstones often show slump structures and Bouma sequences suggesting that they are products of debris flows and turbidity currents. On the basis of calcareous nannofossil biostratigraphy and magnetostratigraphy, the Shiramazu Formation is late Pliocene in age (3.68–3.31 Ma) (Kotake et al., 1995; Kanie et al., 1997; Kameo et al., 2003). Kotake (1988) and Kotake et al. (1995) reported the occurrence of a radiolarian species
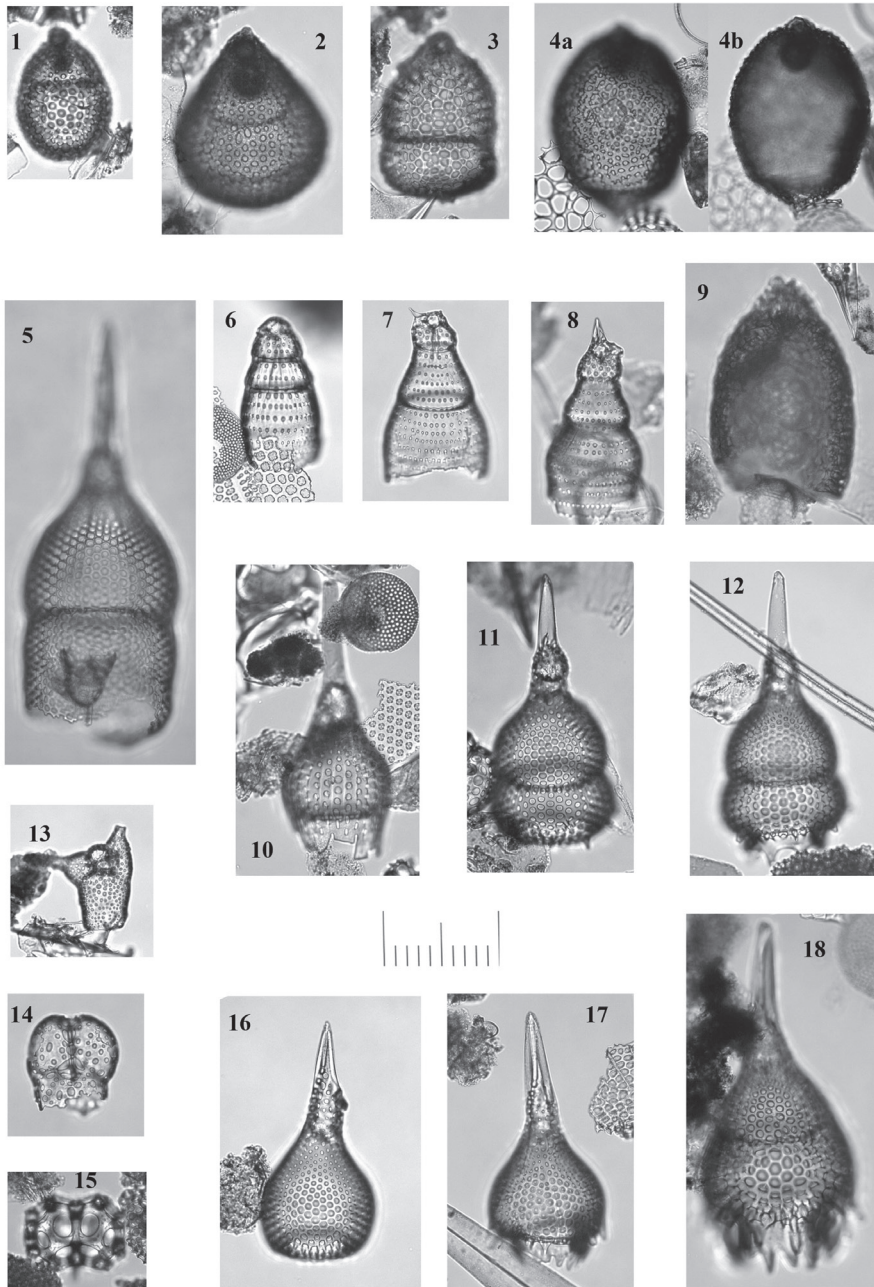
Fig. 10. Radiolarians from the lower part of the Amatsu Formation (middle Miocene): **1.** *Cyrtocapsella japonica* (Nakaseko), **2.** *Cyrtocapsella cornuta* Haeckel, **3.** *Lithopera renaze* Sanfilippo and Riedel, **4.** *Lithopera baueri* Sanfilippo and Riedel, **5.** *Calocycletta caepa* Moore, **6.** *Phormostichoartus marylandicus* (Martin), **7–8.** *Siphostichartus corona* (Haeckel), **9.** *Lithopera thornburgi* Sanfilippo and Riedel, **10.** *Calocycletta costata* (Riedel), **11–12.** *Lamprocyclas* sp., **13.** *Acrobotrys disolenia* Haeckel, **14.** *Phormospyris stabilis stabilis* (Goll), **15.** *Tholospyris anthophora* (Haeckel), **16–17.** *Anthocyrtidium ehrenbergi* (Stöhr), **18.** *Lamprocyclas margatensis* (Campbell and Clark). Scale equals 100 μm. All specimens were collected from sample Boso-8 (calcareous concretion between ash layers Am1 and Am2, Meigawa River).

Fig. 11. Lower Miocene siltstone intercalating tuff beds, Hota Group. Scale = 14 cm.
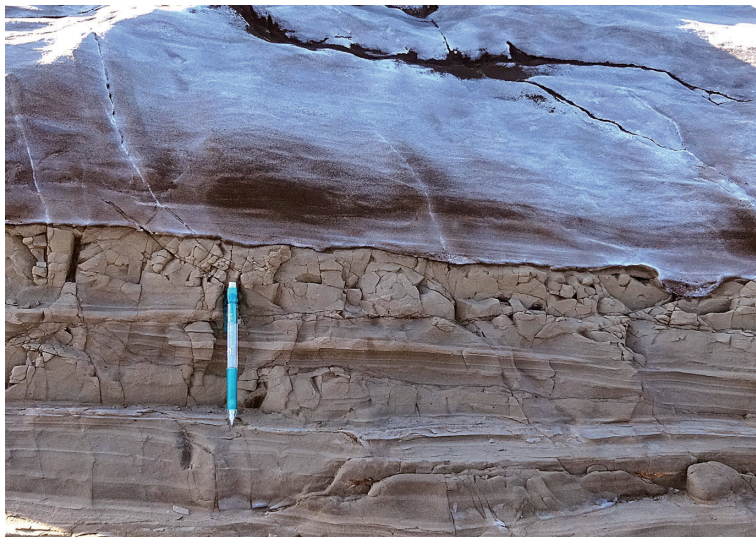
Fig. 12. The contact between the Shirahama Formation and the overlying Shiramazu Formation, which are characterized by brown-colored volcaniclastic sandstone and light gray-colored tuffaceous siltstone, respectively. Scale = 14 cm.

Stichocorys peregrina from the inland sections of the Shiramazu Formation.

At Shiramazu point, roadside rocky shore, it is possible to observe the upper part of the Shirahama Formation and the overlying basal part of the Shiramazu Formation and the conformable contact between them (Fig. 12). The contact can be easily identified because of their colors with good contrast.

Fig. 13. The Nojimazaki Conglomerate Member comprising gravity flow deposits at Cape Nojima-zaki.

STOP 2

Stop 2-1: Nojima-zaki—Pliocene trench-fill deposit (Chikura Group)

Cape Nojima-zaki is the southern tip of the Boso Peninsula. It is possible to observe a member of the Shirahama Formation, Nojimazaki Conglomerate Member, which distributes in the restricted area on the west side of the cape (Fig. 13). This conglomerate is composed of pebble- to cobble-sized gravels representing a channel fill deposit that could have been formed in the paleo-deep-sea trench. Most of the gravels are poorly sorted volcaniclastics. Minor components include plutonic rocks, sandstone, siltstone, chert and green tuff. Mud clasts are frequently observed. Early Cretaceous radiolarians have been found in the chert gravels. Both the lithofacies and shallow water fossils from the conglomerate indicate that they are gravity-transported shelf sediments, which flowed down the continental slope to the deep-sea trough.

Stop 2-2: Green Road—Pleistocene slope deposit (Chikura Group)

A 300 m thick sequence, Hata Formation, is dominated by interbedded tuffaceous sandstone and siltstone with frequent intercalation of pumice and scoria layers. A remarkable feature of this formation is the occurrence of large slumped sedimentary bodies. Calcareous nannofossils and magnetic polarity records indicate a late Pliocene to early Pleistocene (1.95–0.85 Ma) age for this formation (Kotake, 1988; Kotake et al., 1995). They also reported the occurrence of an early Pleistocene radiolarian species, *Eucyrtidium matuyamai*.

The roadside outcrop at this locality shows a remarkable example of chaotic sediments that consist of fragmented strata of various sizes within a sandy matrix (Fig. 14). This was

Fig. 14. Chaotic deformation features within the trench-slope cover sediments of the Hata Formation, Chikura Group.

introduced by Yamamoto et al. (2007) who suggested that a large earthquake could have triggered the sliding of slope deposits that moved down the paleo-slope surface as a liquefied sediment flow.

Stop 2-3: Kenbutsu—Coastal terrace uplifted during the 1923 Kanto Earthquake (Magnitude 7.9)

The Kanto Earthquake was one of the most catastrophic events generated by megathrust activities in modern Japan. This event devastated metropolitan Tokyo and its nearby areas and killed more than 100,000 people. Such major earthquakes in the Kanto region result in sudden coseismic uplift in the southern Boso Peninsula. Accumulations of these geomorphic changes affect the long-term evolution of coastal topography marked by coastal terraces. Fifteen or more steps have been detected that were formed during the Holocene and reflect the earthquake cycle. The highest terrace of the Holocene reaches 30 m above today's sea level.

An excellent place to see such uplifted coastal terraces is the Kenbutsu coast (Shishikura et al., 2016) (Fig. 15). The first step, called 'Taisho bench', above today's wave cut bench represents the coseismic uplift of the 1923 Kanto Earthquake. This vertical movement was 1.5 m. The second step of 3 m is larger than the first reflecting the larger magnitude of the related earthquake. This event is correlated to the Genroku Earthquake (M 7.9–8.5) that happened in 1703 and the terrace platform is called Genroku Terrace. The rock body of the terraces at this locality is the Kagamigaura Formation, the Minamiboso Group (Yamamoto and Kawakami, 2005; Kawakami and Shishikura, 2006).

Fig. 15. Uplifted coastal terraces on the Kenbutsu coast. Here a couple of steps reflecting two major earthquakes that occurred in 1923 and 1703 are clearly visible.

Fig. 16. Tilted tuffaceous sandstone bed set of the Chikura Group dominates the background of the Gake-Kannon temple.

Fig. 17. Locality of the stops in Bandai Volcano. The base graphic map is provided from the Bandaisan Geopark Council.

Stop 2-4: Gake-Kannon—Pleistocene slope basin deposit (Chikura Group)

We will meet the Chikura Group again at this point. The vertical cliff exposes stratified tuffaceous sandstone strata (Fig. 16). A red colored temple dedicated to Kannon (Guanyin in Chinese), known as 'Gake-Kannon' (formally Daifukuji Temple), is placed at a high point on the cliff. 'Gake' means 'cliff' and 'Kannon' is a Goddess of Mercy in Buddhism.

STOP 3 (Fig. 17)

Stop 3-1: Bishamon-numa ―Lake born by the 1888 eruption of Bandai Volcano

Bishamon-numa is the largest lake (150,000 m²) in the Goshiki-numa area. This area contains over 30 various sized lakes and swamps which were born when water collected in the hollows among flow mounds (small conical hills) formed by the debris avalanche of the 1888 eruption. The water of each swamp is a mixture of the acidic ground water from the Aka-numa swamp located near the 1888 explosion caldera and other neutral ground water. Therefore Goshiki-numa swamps have various water qualities and show many beautiful colors.

Stop 3-2: Urabandai Ski Slope ―The flow way of the 1888 debris avalanche

The 1888 phreatic eruption of Bandai Volcano caused Kobandai's collapse and debris avalanche. The way the debris avalanche ran is the present ski slope. Lake Hibara viewed to the north of this site was born after the damming of a river by the debris avalanche. On

Fig. 18. Explosion caldera and Aka-numa swamp formed by the collapse of Mt. Kobandai in 1888.

Lake Hibara there are several islands. They are flow mounds, called Nagare-yama in Japanese, formed by the debris avalanche, many of which are now under the water surface.

Stop 3-3: Aka-numa and Explosion Caldera 一Site of the Kobandai collapse in 1888

A big horseshoe-shaped caldera with a sheer cliff of bare rock was created by the collapse of Kobandai in the 1888 phreatic explosion (Fig. 18). Many strata of lava, volcanic breccia and volcanic ash seen on the surface of the cliff show the history of the past eruptions of Bandai Volcano. Aka-numa swamp was formed right after the collapse of Kobandai. The water of the swamp is strongly acidic and looks reddish brown, because mud containing iron hydroxide accumulates at the bottom of the swamp.

Stop 3-4: Museum of the Mt. Bandai Eruption

This museum is located on the northern slope of Bandai Volcano, called Urabandai. The museum mainly collects materials of the 1888 eruption of Bandai Volcano and natural environment around Mt. Bandai. The exhibition themes of the museum are as follows: the 1888 eruption of Mt. Bandai, villages swallowed up by rising lake waters, materials from the Mt. Bandai eruption, animals and plants around Mt. Bandai, volcanoes around the world, and the first seismograph in the world.

Stop 3-5: Mine-no-Oishi 一A large rock carried by the debris avalanche in 1888

When Bandai Volcano erupted in 1888, large andesitic rocks were carried by a debris avalanche from the place near the summit of Bandai Volcano to Mine Village through the Biwasawa River. Mine-no-Oishi is one of these rocks (Fig. 19). This giant rock has a height of 3.1 m and a length of 8.2 m. Because its present location is evidence that it was carried a

Fig. 19. Mine-no-Oishi, a large andesitic rock carried to Mine village by the debris avalanche in the 1888 eruption of Bandai Volcano.

much longer distance during the eruption than expected, this rock was designated as a National Monument of Natural History in 1941.

Stop 3-6: Resort Ski Slope ─View point of the flow mound topography formed by the Okinajima debris avalanche

A lot of Nagare-yama (flow mounds) can be seen at the southwestern foot of Bandai Volcano. They are formed by a debris avalanche which was caused by a large-scale mountain collapse during a Plinian-style eruption about 50,000 years ago. Some flow mounds are around 500 m in diameter. The debris avalanche, called the Okinajima debris avalanche, also resulted in the damming of a river that flowed from the Inawashiro basin into the Aizu basin and gave birth to a large lake, the present Lake Inawashiro.

Stop 3-7: South of JR Bandai-machi Station ─Internal structure of a flow mound formed by the Okinajima debris avalanche

This outcrop is one of the Nagare-yama formed by the Okinajima debris avalanche. At this site the rock facies and structure inside of the flow mound can be seen. A mass of large rocks of andesitic lava, which was once part of the old mountain of Bandai Volcano is surrounded by a muddy matrix (Fig. 20). Cracks like a jigsaw puzzle, called a jigsaw crack, can be seen on the rock surface. These are characteristic features of a debris avalanche.

Fig. 20. The internal structure of a flow mound formed by the Okinajima debris avalanche, which occurred about 50,000 years ago. A mass of large andesite rocks is surrounded by a muddy matrix.

Acknowledgements

Referecnces

Aida, N., 1997, Paleomagnetic stratigraphy of the type section (proposed site) for the Lower/Middle Pleistocene Boundary—Kokumoto Formation. *In* Kawamura, M., Oka, T. and Kondo, T., eds., *Commemorative volume for Professor Makoto Kato*, 275–282*.

Aoki, N., 1963, Pliocene and Pleistocene foraminifera from along the Yoro River, Boso Peninsula-vertical faunal change-. *Sci. Rep. Tokyo Kyoiku Daigaku, Sec. C*, **8**, 203–227.

Aoki, N., 1968, Benthonic foraminifera of Kazusa Group, Boso Peninsula. *Trans. Proc. Palaeontol. Soc. Japan*, N. S., no. 70, 238–266.

Arai, S., 1991, The circum-Izu Massif peridotite, central Japan, as back-arc basin mantle fragments of the Izu-Bonin arc system. *In* Peters, Tj. et al., eds., *Ophiolite Genesis and Evolution of the Oceanic Lithosphere*, Kluwer Acad. Pub., Dordrecht, 807–822.

Cherepanova, M. V., Pushkar, V. S., Razjigaeva, N., Kumai, H. and Koizumi, I., 2002, Diatom biostratigraphy of the Kazusa Group, Boso Peninsula, Honshu, Japan. *Quatern. Res. (Daiyonki Kenkyu)*, **41**, 1–10.

Chiba S. and Kimura, J., 2001, Geology and growth history of Bandai volcano, Tohoku-Honshu arc, Japan − Analysis of volcanic activity by tephrochronology–. *Japan. Magazine Mineral. Petrol. Sci.*, **30**, 126–156*.

Fujioka, K., Tanaka, T. and Aoike, K., 1995, Serpentine seamount in Izu-Bonin and Mariana forearcs— Observation by a submersible and its relation to onland serpentinite belt. *Jour. Geogr. (Chigaku Zasshi)*, **104**, 473–494*.

Haga, M. and Kotake, N., 1996, Diatom age of the lower part of the Miocene Amatsu Formation, Boso Peninsula, southern-central Japan. *Jour. Geol. Soc. Japan*, **102**, 758–760*.

Hirano, N., Ogawa, Y., Saito, K., Yoshida. T., Sato, H. and Taniguchi, H., 2003, Multi-stage evolution of the Tertiary Mineoka Ophiolite in the NW Pacific as revealed by new geochemical and age constraints. *In* Dilek, Y. and Robinson, P. T., eds., *Ophiolites in Earth's History*, Geol. Soci. London, Spec. Pub., **218**, 279–298.

Igarashi, A., 1994, Paleoceanographic changes during the deposition of the middle Pleistocene Kazusa Group, central Japan: Estimation based on the principal components analysis of planktonic foraminifera. *Jour. Geol. Soc. Japan*, **100**, 348–359*.

Ito, M., Kameo, K., Satoguchi, Y., Masuda, F., Hiroki, Y., Takano, O., Nakajima, T. and Suzuki, N., 2016, Neogene–Quaternary sedimentary successions. *In* Moreno, T., Wallis, S., Kojima, T. and Gibbons, W. eds., *The Geology of Japan*, The Geological Society, London, 309–337.

Ito, M. and Katsura, Y., 1992, Inferred glacio-eustatic control for high-frequency depositional sequences of the Plio-Pleistocene Kazusa Group, a forearc basin fill in Boso Peninsula, Japan. *Sediment. Geol.*, **80**, 67–75.

Kameo, K., Mita, I. and Fujioka, M., 2002, Calcareous nannofossil biostratigraphy of the Amatsu Formation (Middle Miocene to Lower Pliocene), Awa Group, distributed in the central part of the Boso Peninsula, central Japan. *Jour. Geol. Soc. Japan*, **108**, 813–828*.

Kameo, K., Saito, K., Kotake, N. and Okada, M., 2003, Late Pliocene sea surface environments in the Pacific side of central Japan based on calcareous nannofossils from the lower part of the Chikura Group, southernmost part of the Boso Peninsula. *Jour. Geol. Soc. Japan*, **109**, 478–488*.

Kameo, K. and Sekine, T., 2013, Calcareous nannofossil biostratigraphy and the geologic age of the Anno Formation, the Awa Group in the Boso Peninsula, central Japan. *Jour. Geol. Soc. Japan*, **119**, 410–420*.

Kameo, K., Shindo, R. and Takayama, T., 2010, Calcareous nannofossil biostratigraphy and geologic age of the Kiyosumi Formation of the Awa Group, Boso Peninsula, central Japan: Age determination based on size variations of *Reticulofenestra* specimens. *Jour. Geol. Soc. Japan*, **115**, 563–574*.

Kanie, Y., Hattori, M., Kuramochi, T., Okada, H., Ohba, T. and Honma, C., 1997, Two vesicomyid bivalvia from the Shiramazu Formation of the Chikura Group in the southernmost part of the Boso Peninsula. *Jour. Geol. Soc. Japan*, **103**, 794–797*.

Kanie, Y., Okada, H., Sasahara, Y. and Tanaka, H., 1991, Calcareous nannoplankton age and correlation of the Neogene Miura Group between the Miura and Boso Peninsulas, southern-central *Japan. Jour. Geol. Soc. Japan*, **97**, 135–155*.

Kawakami, S., 2001, Upper Miocene radiolarians from the Nishizaki Formation and Ishido Group in the southern part of Boso Peninsula, Japan, and their geological significance. *News of Osaka Micropaleontologists (NOM), Spec. Vol.*, no. 12, 343–358*.

Kawakami, S., 2004, Reexamined geology of Mineoka Tectonic Zone, Boso Peninsula, Japan, from the age of Tertiary radiolarians and gravelly rocks. *News of Osaka Micropaleontologists (NOM), Spec. Vol.*, no. 13, 197–204*.

Kawakami, S. and Shishikura, M., 2006, *Geology of the Tateyama District. Quadrangle Series, 1:50.000*, Geological Survey of Japan, AIST, 82p*.

Kazaoka, O., Suganuma, Y., Okada, M., Kameo, K., Head, M. J., Yoshida, Y., Sugaya, M., Kameyama, S., Ogitsu, I., Nirei, H., Aida, N. and Kumai, H., 2015, Stratigraphy of the Kazusa Group, Boso Peninsula: An expanded and highly-resolved marine sedimentary record from the Lower and Middle Pleistocene of central Japan. *Quatern. Internat.*, **382**, 116–135.

Kitazato, H., 1977, Vertical and lateral distributions of benthic foraminiferal fauna and the fluctuation of warm and cold waters in the middle Pleistocene of the Boso Peninsula, Central Japan. *Sci. Repts. Tohoku Univ. 2nd ser.*, **47**, 7–41.

Kitazato, H., 1997, Paleogeographic changes in central Honshu, Japan, during the late Cenozoic in relation to the collision of the Izu-Ogasawara Arc with the Honshu Arc. *Island Arc*, **6**, 144–157.

Kotake, N., 1988, Upper Cenozoic marine sediments in southern part of the Boso Peninsula, central Japan. *Jour. Geol. Soc. Japan*, **94**, 187–206*.

Kotake, N., Koyama, M. and Kameo, K., 1995, Magnetostratigraphy and biostratigraphy of the Plio-Pleistocene Chikura and Toyofusa Groups, southernmost part of the Boso Peninsula, central Japan. *Jour. Geol. Soc.*

Japan, **101**, 515–531*.

Mimura, K., 1994, Radiometric ages of Bandai Volcano − the reconnaissance − . *Bull. Geol. Surv. Japan*, **45**, 565–571*.

Mita, I. and Takahashi, M., 1998, Calcareous nannofossil biostratigraphy of the Middle Miocene Kinone and lower Amatsu Formation in the Boso Peninsula, central Japan. *Jour. Geol. Soc. Japan*, **104**, 877–890*.

Mohiuddin, M.M. and Ogawa, Y., 1996, Middle Eocene to early Oligocene planktonic foraminifers from the micritic limestone beds of the Heguri area, Mineoka Belt, Boso Peninsula, Japan. *Jour. Geol. Soc. Japan*, **102**, 611–625.

Mohiuddin, M.M. and Ogawa, Y., 1998a, Early Miocene pelagic sequences in the Mineoka Belt, Boso Peninsula, Japan. *Jour. Geol. Soc. Japan*, **104**, 1–12.

Mohiuddin, M.M. and Ogawa, Y., 1998b, Late Paleocene-middle Miocene pelagic sequences in the Boso Peninsula, Japan: New light on northwest Pacific tectonics. *Island Arc*, **7**, 301–314.

Motoyama, I. and Takahashi, M., 1997, Radiolarian biostratigraphy of the Middle Miocene Kinone and Amatsu Formations, Boso, Japan, with a synthesis of siliceous and calcareous microfossil stratigraphy. *Jour. Japan. Assoc. Petroleum Technol.*, **62**, 226–238*.

Nagahashi, Y., Kataoka, K. and Nakazawa, N., 2016, Formation and geologic history of Lake Inawashiro-ko based on stratigraphy and sedimentary facies of the INW2012 core sediments. *In* Tsutsumi, T., ed., *Environmental study in Urabandai-Inawashiro area*, 17–31. Fukushima Mimpo-sha (in Japanese).

Nakajima, T., Makimoto, H., Hirayama, J. and Tokuhashi, S., 1981, *Geology of the Kamogawa District, Quadrangle Series, scale 1:50,000*. Geol. Surv. Japan, 107p*.

Nakamura, Y., 1978, Geology and petrology of Bandai and Nekoma volcanoes. *Sci. Rep. Tohoku Univ., Ser. 3*, **14**, 67–119.

Nishida, N., Kazaoka, O., Izumi, K., Suganuma, Y., Okada, M., Yoshida, Y., Ogitsu, I., Nakazato, H., Kameyama, S., Kagawa, A., Morisaki, M. and Nirei, H., 2016, Sedimentary processes and depositional environments of a continuous marine succession across the Lower Middle Pleistocene boundary: Kokumoto Formation, Kazusa Group, central Japan. *Quatern. Internat.*, **397**, 3–15.

Nishida, S., 1977, Late Cenozoic calcareous nannoplankton biostratigraphy in the southern Kwanto region, Japan. *Bull. Nara Univ. Educ.*, **26**, 19–38*.

Oda, M., 1977, Planktonic foraminiferal biostratigraphy of the late Cenozoic sedimentary sequence, Central Honsyu, Japan. *Sci. Rep. Tohoku Univ., 2nd ser.*, **48**, 1–76.

Ogawa, Y. and Naka, J., 1984, Emplacement of ophiolitic rocks in forearc areas: Examples from central Japan and Izu-Mariana-Yap island arc system. *In* Gass, I. G. et al., eds, *Ophiolites and Oceanic Lithosphere*, Geol. Soc. London Spec. Pub., no. 13, 291–301.

Ogawa, Y. and Sashida, K., 2005, Lower Cretaceous radiolarian bedded chert from the Mineoka Belt, Boso Peninsula, Japan. *Jour. Geol. Soc. Japan*, **111**, 624–627.

Okada, M. and Niitsuma, N., 1989, Detailed paleomagnetic records during the Brunhes-Matuyama geomagnetic reversal and a direct determination of depth lag for magnetization in marine sediments. *Physics of the Earth and Planetary Interiors*, **56**, 133–150.

Okada, M., Suganuma, Y., Haneda, Y. and Kazaoka, O., 2017, Paleomagnetic direction and paleointensity variations during the Matuyama–Brunhes polarity transition from a marine succession in the Chiba composite section of the Boso Peninsula, central Japan. *Earth, Planets and Space,* 69:45. DOI 10.1186/s40623-017-0627-1

Pickering, K.T., Souter, C., Oba, T., Taira, A., Schaaf, M. and Platzman, E., 1999, Glacioeustatic control on deep-marine clastic forearc sedimentation, Pliocene-mid-Pleistocene (c. 1180-600 ka) Kazusa Group. SE Japan. *Jour. Geol. Soc., London*, **156**, 125–136.

Saito, S., 1992, Stratigraphy of Cenozoic strata in the southern terminus area of Boso Peninsula, Central Japan. *Contr. Inst. Geol. Paleontol., Tohoku Univ.*, no. 93, 1–37*.

Sato, T., Kameo, K. and Mita, I., 1999, Validity of the latest Cenozoic calcareous nannofossil datums and its application to the tephrochronology. *Earth Science* (*Chikyu Kagaku*), **53**, 265–274*.

Sato, T., Takayama, T., Kato, M., Kudo, T. and Kameo, K., 1988, Calcareous microfossil biostratigraphy of the uppermost Cenozoic formations distributed in the coast of the Japan Sea, Part 4: conclusion. *Jour. Japan. Assoc. Petrol. Technol.*, **53**, 474–491*.

Sawada, T., Shindo, R., Motoyama, I. and Kameo, K., 2009, Geology and radiolarian biosratigraphy of the Miocene and Pliocene Series exposed along the Koitogawa River, Boso Peninsula, Japan. *Jour. Geol. Soc. Japan*, **115**, 206–222*.

Sekiya S. and Kikuchi, Y., 1889, The eruption of Bandaisan. *Jour. Coll. Sci. Imp. Univ. Tokyo, Japan*, **3**, 91–172.

Shishikura, M., Kamataki, T. and Fujiwara, O., 2016, History of the Kanto earthquakes recorded in marine terraces and tsunami deposits in the southern coast of the Boso Peninsula, central Japan. *Jour. Geol. Soc. Japan*, **122**, 357–370*.

Suganuma, Y., Okada, M., Horie, K., Kaiden, H., Takehara, M., Senda, R., Kimura, J., Kawamura, K., Haneda, Y., Kazaoka, O. and Head, M. J., 2015, Age of Matuyama-Brunhes boundary constrained by U-Pb zircon dating of a widespread tephra. *Geology*, **43**, 491–494.

Suzuki, Y., Akiba, F. and Kamiya, M., 1996, Latest Oligocene siliceous microfossils from Hota Group in southern Boso Peninsula, eastern Honshu, Japan. *Jour. Geol. Soc. Japan*, **102**, 1068–1071.

Takahashi, M., Mita, I., Watanabe, M. and Motoyama, I., 1999, Integrated stratigraphy of the Middle Miocene marine sequence in the Boso Peninsula, central Japan: a review. *Bull. Geol. Surv. Japan*, **50**, 225–243.

Takahashi, N., Arai, S. and Niida, S., 2012, Geology and tectonic evolution of the Mineoka belt, Boso Peninsula, Central Japan. *Res. Rep. Kanagawa prefect. Mus. Nat. Hist.*, **14**, 25–56*.

Takahashi, N., Shibata, K., Hirata, D. and Niida, S., 2016, Geologic traverse from the Mineoka Belt to the Hayama Belt, Central Japan. *Jour. Geol. Soc. Japan*, **122**, 375–395*.

Takayama, T. and Ikeno, N., 1977, Chronological variations in the calcareous nannofossil assemblage from the sequence along the Yoro River, Chiba Prefecture. *Professor Kazuo Huzioka Memorial Volume*, 413–423*.

Taketani, Y., Kobiyama, R., Kaneta, Y. and Sato, H., 2015, *Bandaisan Geopark Area Guidebook H, Central Inawashiro Area*. 14 p. Bandaisan Geopark Council (in Japanese).

Tokuhashi, S., 1979, Three dimensional analysis of a large sandy-flysch body, Mio-Pliocene Kiyosumi Formation, Boso Peninsula, Japan. *Mem. Fac. Sci., Kyoto Univ., Ser. Geol. Mineral.*, **46**, 1–60.

Tsuji, T., Miyata, Y., Okada, M., Mita, I., Nakagawa, H., Sato, Y. and Nakamizu, M., 2005, High-resolution chronology of the lower Pleistocene Otadai and Umegase Formations of the Kazusa Group, Boso Peninsula, central Japan: chronostratigraphy of the JNOC TR-3 cores based on oxygen isotope, magnetostratigraphy and calcareous nannofossil. *Jour. Geol. Soc. Japan*, **111**, 1–20*.

Watanabe, M. and Takahashi, M., 1997, Diatom biostratigraphy of the Middle Miocene Kinone and lower Amatsu Formations in the Boso Peninsula, central Japan. *Jour. Japan. Assoc. Petrol. Technol.*, **62**, 215–225*.

Watanabe, M. and Takahashi, M., 2000, Diatom biostratigraphy of the middle Miocene marine sequence of the Kawadani section in the Kamogawa area, Boso Peninsula, central Japan. *Jour. Geol. Soc. Japan*, **106**, 489–500*.

Yamamoto, T. and Suto, S., 1996, Eruptive history of Bandai volcano, NE Japan, based on tephrastratigraphy. *Bull. Geol. Surv. Japan*, **47**, 335–359*.

Yamamoto, Y., Chiyonobu, S., Kamiya, N., Hamada, Y. and Saito, S., 2017, Structural characteristics of shallow portion of plate subduction zone: A forearc system in the southern Boso Peninsula, central Japan. *Jour. Geol. Soc. Japan*, **123**, 41–55*.

Yamamoto, Y. and Kawakami, S., 2005, Rapid tectonics of the Late Miocene Boso accretionary prism related to the Izu-Bonin arc collision. *Island Arc*, **14**, 178–198.

Yamamoto, Y., Ogawa, Y., Uchino, T., Muraoka, S. and Chiba, T., 2007, Large-scale chaotically mixed sedimentary body within the Late Pliocene to Pleistocene Chikura Group, Central Japan. *Island Arc*, **16**, 505–507.

*: in Japanese with English abstract

Triassic and Jurassic radiolarian response to global catastrophic events in the Panthalassa Ocean, as recorded in the Mino Belt, central Japan

Tetsuji ONOUE*, Rie S. HORI** and Satoru KOJIMA***

Abstract

The field trip will focus on the radiolarian response to global catastrophic events (e.g., bolide impact, large-scale volcanism, and anoxia) recorded in Triassic and Jurassic radiolarian chert of the Mino Belt, central Japan. The radiolarian chert of the Mino Belt records the sedimentary history of an oceanic plate in the Panthalassa Ocean prior to accretion at the trench. The topics presented and discussed in the field are: (1) the end-Permian mass extinction and recovery from the event; (2) Early Triassic anoxia and subsequent recovery in the Middle Triassic; (3) paleoenvironmental changes across the Early–Late Carnian boundary (Carnian Pluvial Event); (4) collapse of marine ecosystems triggered by a Norian impact event; (5) ocean acidification at the Triassic–Jurassic boundary; and (6) Early Jurassic (Toarcian) anoxia and the formation of black chert. In addition to these topics, this trip will consider aspects of the accretion process of oceanic plate sediments during the Middle to Late Jurassic.

Key words: Triassic, Jurassic, Radiolaria, chert, Mino Belt, accretionary complex

   * Department of Earth and Environmental Sciences, Faculty of Advanced Science and Technology, Kumamoto University, Kumamoto 860-8555, Japan

 ** Department of Earth Sciences, Graduate School of Science and Engineering, Ehime University, Matsuyama 790–8577, Japan

*** Department of Civil Engineering, Faculty of Engineering, Gifu University, Gifu 501–1193, Japan
Corresponding author: T. Onoue,
onoue@sci.kumamoto-u.ac.jp

Introduction

The aim of this field trip is to introduce the stratigraphy and micropaleontology of sections through Lower Triassic–Middle Jurassic sequences of the Mino Belt in central Japan. The Mino Belt is a Middle to Late Jurassic subduction-generated accretionary complex in central Japan that strikes approximately east-northeast (Fig. 1). The belt is characterized by a coherent sequence comprising Lower Triassic to Middle Jurassic bedded chert and overlying Middle Jurassic terrigenous clastic rocks (Matsuda and Isozaki, 1991). The absence of carbonate rocks and coarse terrigenous grains in the bedded chert suggests that its primary depositional site was deeper than the calcium carbonate compensation depth and beyond the reach of terrigenous clastic grains. Previous paleomagnetic studies of the Triassic bedded chert successions of the Mino Belt suggested that these sediments accumulated in a pelagic, open-ocean setting within a low- to middle-latitude part of the Panthalassa Ocean (Shibuya and Sasajima, 1986; Ando et al., 2001; Uno et al., 2015). The Triassic–Jurassic cherts accreted within an accretionary complex on the eastern margin of the Asian continent during the Middle to Late Jurassic (Matsuda and Isozaki, 1991).

The Triassic–Jurassic chert sequences of the Mino Belt in the Inuyama–Kamiaso area, central Japan, preserve one of the most significant and complete records of Triassic–Jurassic pelagic environments in the Panthalassa Ocean. The three-day field trip will focus on the radiolarian response to global catastrophic events (e.g., bolide impact, large-scale volcanism, and anoxia) recorded in the Triassic to Jurassic radiolarian chert in the Inuyama–Kamiaso area. Equally importantly, we hope to provide the participants with knowledge of aspects of the accretion process of oceanic plate sediments during the Middle to Late Jurassic.

Geologic outline of the Inuyama–Kamiaso area

1. General overview

The Mino Belt consists of Jurassic accretionary complexes that strike east–northeast in central Japan (Fig. 1). The belt is juxtaposed against the Circum–Hida (Hida Gaien) Belt to the north, which is tectonically overlain by the metamorphosed correlative of the Mino Belt that occurs to the south (the Ryoke Belt).

The accretionary complexes in the Mino Belt are subdivided into seven tectonostratigraphic units based on lithology, structure, and age of accretion (Fig. 2: Wakita, 1988; Wakita et al., 1992). The complexes consist of two coherent units (the Samondake and Kamiaso units) and five melange units (the Sakamoto-toge, Funafuseyama, Kuze, Nabi, and Kanayama units). The coherent units are composed of imbricate thrust sheets of sedimentary sequences that retain their primary stratigraphic coherency in most parts. The
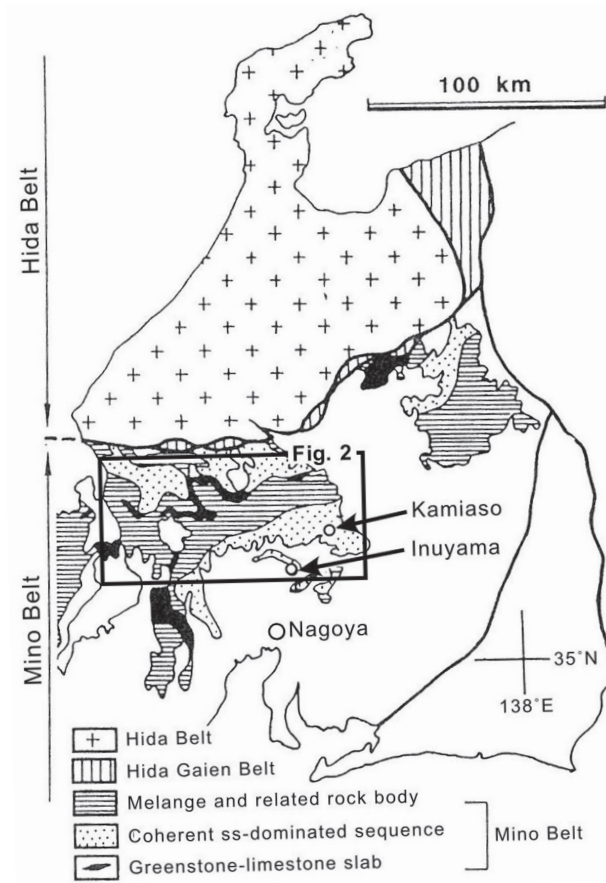
Fig. 1. Index map showing the Inuyama–Kamiaso area (modified from Matsuoka et al., 1994).

melange units consist of mixed rock assemblages in which numerous blocks and lenses of various lithologies (e.g., basaltic rocks, limestone, and bedded chert) and size are complexly mingled with terrigenous clastic rocks (Wakita, 1988; Nakae, 2000; Sano and Kojima, 2000; Sano et al., 2017). The ages of accretion of these units become younger from north to south, as the structurally lower units occur in the southern area (Wakita, 1988; Wakita et al., 1992).

The field trip will visit seven localities in the Inuyama–Kamiaso area, eastern Gifu Prefecture, central Japan (Figs. 2, 3). This area is distributed in the southern part of the coherent Kamiaso Unit of the Mino Belt, which strikes east–northeast. The Kamiaso Unit in this area consists of thrust piles of sedimentary sequences containing Triassic to Lower Jurassic bedded chert and overlying Middle Jurassic clastic rocks (i.e., a chert–clastic sequence: Matsuoka et al., 1994). The chert–clastic sequence is interpreted to have accumulated in a pelagic, deep-sea setting below the carbonate compensation depth and within a tapering wedge of trench-fill turbidites with distal facies. Paleomagnetic analysis of the bedded chert in the study area indicates that the site of deposition changed from a low-latitude zone in the Middle Triassic to a mid-latitude zone in the Late Triassic (Fig. 4:
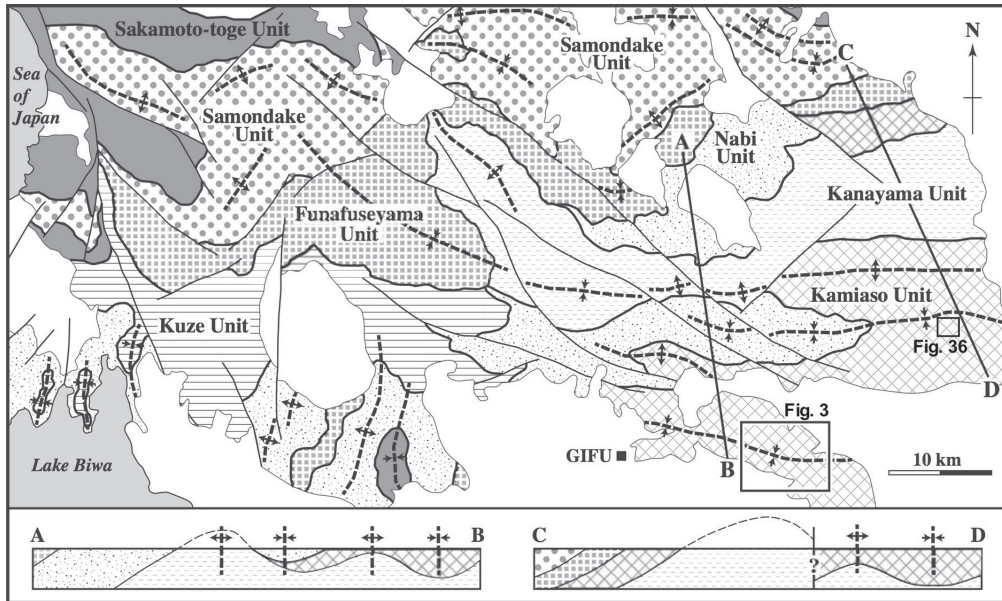
Fig. 2. Map showing the tectonostratigraphic subdivision of the accretionary complexes in the Mino area and geological cross-sections along the lines A–B and C–D. After Kojima et al. (2016).
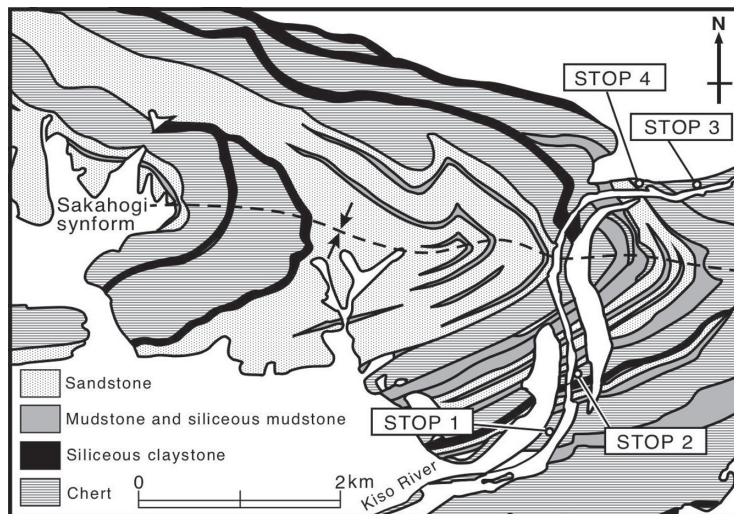
Fig. 3. Geologic and location maps of the field stops along the Kiso River. Modified after Wakita (1988).
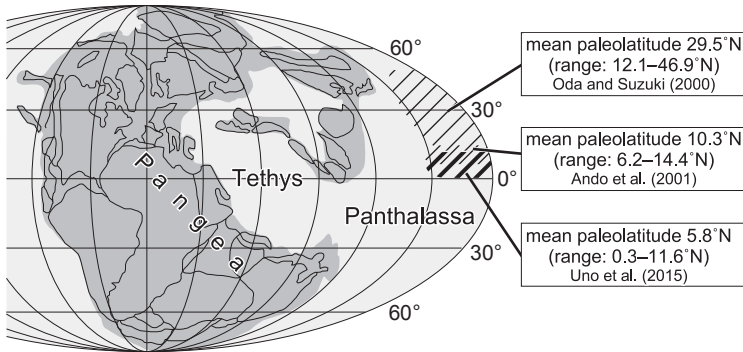
Fig. 4. Late Triassic paleogeography showing the paleolatitudes for the site of deposition of the Inuyama chert (after Uno et al., 2015). The data for the Inuyama chert is of Norian age.
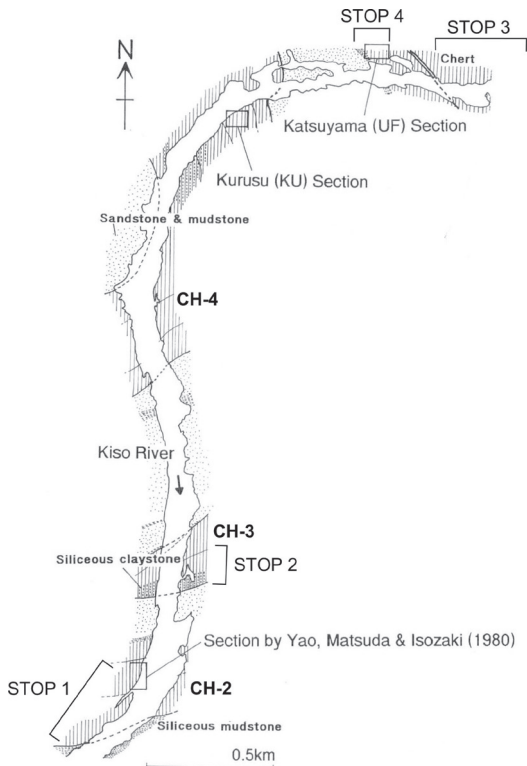
Fig. 5. Route map of the chert-clastic sequence along the Kiso River in the Inuyama area. Modified after Hori (1992).

Shibuya and Sasajima, 1986; Oda and Suzuki, 2000; Ando et al., 2001; Uno et al., 2015). Previous studies have compiled a detailed radiolarian biostratigraphy of the Triassic to Middle Jurassic bedded chert of the area (e.g., Yao et al., 1982; Hori, 1990, 1992; Sugiyama, 1992, 1997).

The chert–clastic sequence in the Inuyama–Kamiaso area occurs as a stack of thrust sheets (Wakita, 1988; Kimura and Hori, 1993) that formed during accretion (Matsuda and Isozaki, 1991) and are named CH-1, CH-2, CH-3, and CH-4, in structurally ascending order (Yao et al., 1980). The complexly stacked wedges of the thrust sheets form a large syncline (the Sakahogi Synform) that plunges to the west (Fig. 5).
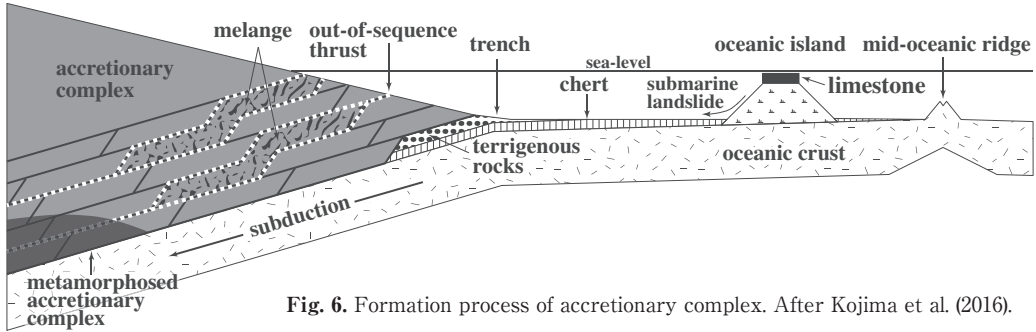
Fig. 6. Formation process of accretionary complex. After Kojima et al. (2016).
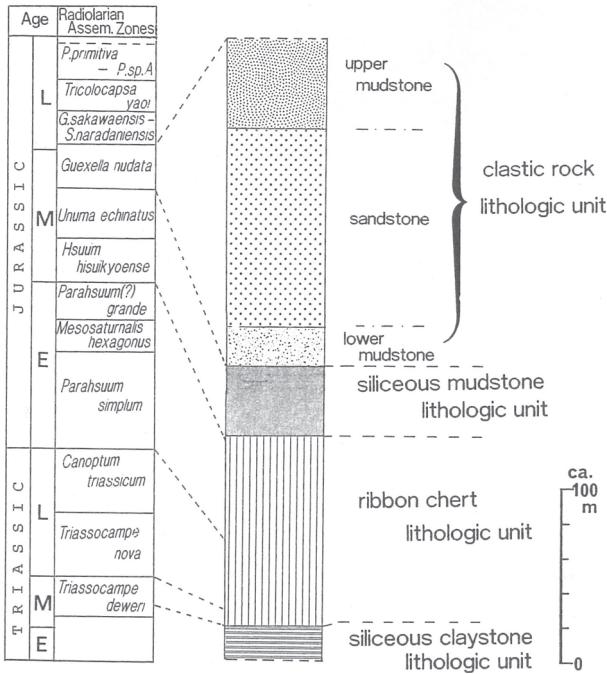
Fig. 7. Generalized columnar section of Triassic–Jurassic chert–clastic sequence in the Inuyama area (modified after Kimura and Hori, 1993). Radiolarian assemblage zones are after Yao et al. (1980) and Hori (1990).

2. Deep-water oceanic plate stratigraphy

The chert–clastic sequence records the sedimentary history upon an oceanic plate prior to accretion at the trench (Matsuda and Isozaki, 1991). The reconstructed ocean floor sequence found in ancient accretionary complexes is called "oceanic plate stratigraphy" and records the history of the oceanic plate from its initiation at a mid-ocean ridge to a trench where accretionary complexes are formed through offscraping and underplating of the oceanic plate (Fig. 6).

The chert–clastic sequence in the Inuyama–Kamiaso area is lithostratigraphically subdivided into lower siliceous claystone (ca. 19 m thick), middle bedded chert (ca. 110 m), upper siliceous mudstone (ca. 38 m), and uppermost clastic rocks (ca. 190 m) units in ascending order (Fig. 7: Kimura and Hori, 1993; Matsuoka et al., 1994). The stratigraphic

base and top of the sequence are truncated by thrust faults (Kimura and Hori, 1993). Studies of radiolarian and conodont biostratigraphy (e.g., Yao et al., 1982; Hori, 1990; Matsuda and Isozaki, 1991; Sugiyama, 1997) have revealed that the lower, middle, upper, and uppermost units of the chert–clastic sequence can be assigned to the upper Spathian to lower Anisian, middle Anisian to upper Toarcian, upper Toarcian to Bathonian, and Bathonian to lower Callovian, respectively.

The lower to upper units of the chert–clastic sequence record a Lower Triassic to Middle Jurassic sequence (~80 Myr). The lithostratigraphic change within the uppermost unit of the chert–clastic sequence indicates a lateral shift of the depositional sites as the oceanic plate migrated, from a pelagic setting during the deposition of the Lower Triassic to Lower Jurassic bedded chert to a hemipelagic setting, in which airborne tephras and fine-grained terrestrial materials were deposited, during Middle Jurassic time (Matsuda and Isozaki, 1991). The age of accretion of the chert–clastic sequence is best approximated as Middle Jurassic, as inferred from the youngest age of radiolarians obtained from black mudstone.

3. Triassic and Jurassic radiolarian biostratigraphy

Bedded cherts in the Mino Belt commonly yield Triassic–Jurassic radiolarians and Triassic conodonts. The depositional ages of the chert–clastic sequence in the Kamiaso Unit were initially dated using conodonts in the late 1970s and early 1980s (Igo and Koike, 1975; Koike, 1979; Isozaki and Matsuda, 1982, 1983; Yao et al., 1982). However, conodonts are so scarce in these cherts that the ages of the deposits were predominantly determined from the radiolarian biostratigraphy. Because the Triassic–Jurassic bedded chert successions in the Inuyama–Kamiaso area represent one of the most complete and well-preserved stratigraphic records in the Mino Belt, many radiolarian biostratigraphies have been established for the Triassic and Jurassic bedded cherts in this area (e.g., Nakaseko and Nishimura, 1979; Yao et al., 1980, 1982; Yao, 1982; Kido et al., 1982; Mizutani and Kido, 1983; Yoshida, 1986; Hori, 1990, 1992, 1997; Matsuda and Isozaki, 1991; Sugiyama, 1992, 1997).

In a landmark study of Triassic radiolarian biozones, Sugiyama (1997) established 18 radiolarian zones ranging from the Spathian (late Olenekian) to the end of the Triassic in siliceous rocks (chert and siliceous claystone) in the Inuyama–Kamiaso area of central Japan (Fig. 8). Sugiyama (1997) determined the total ranges of 247 selected radiolarian taxa based on high-resolution analyses of 534 samples from 26 sections along the Kiso and Hida rivers. He correlated these ranges with nine previously reported biozones worldwide and then determined the chronology of the radiolarian zones by compiling existing age data. This is the most comprehensive study on the subject to date, and the zonation scheme reported is the only one to span almost the whole Triassic with relatively high resolution (O'Dogherty et al., 2010). To calibrate Sugiyama's Triassic radiolarian zonation with the conodont zones
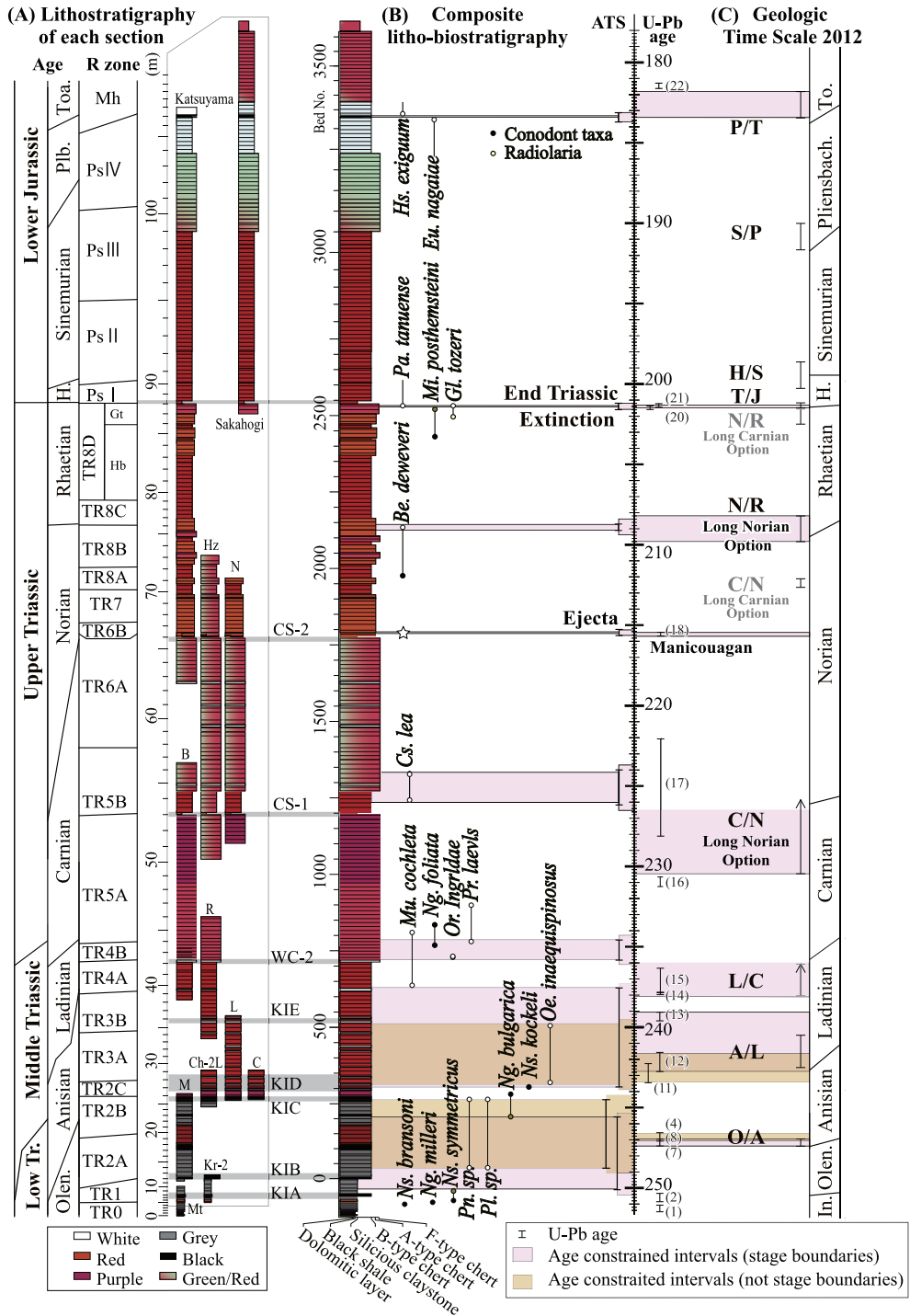
Fig. 8. The lithostratigraphy of the study sections and the composite litho-biostratigraphy for the Lower Triassic to Lower Jurassic deep-sea sequence in the Inuyama area, Japan. Lithologic types are from Sugiyama (1997), Ikeda et al. (2010) and Sakuma et al. (2012). After Ikeda and Tada (2014).

and the standard Triassic timescale, the Late Triassic conodont biostratigraphy was recently investigated in the same sections as those used by Sugiyama (1997) as type sections for radiolarian biozones (Nakada et al., 2014; Uno et al., 2015).

The first comprehensive work on the biostratigraphy of Jurassic radiolarians in the Inuyama–Kamiaso area was carried out by Yao et al. (1980). Subsequently, Yao (1982) described three Triassic and one Jurassic radiolarian assemblages in the CH-2 thrust sheet along the Kiso River in the Inuyama area. As a result of extensive research on Lower and Middle Jurassic bedded cherts, Hori (1990) established five radiolarian assemblage-zones in this area. In chronological order, these are the *Parahsuum simplum* I, *P. simplum* II, *P. simplum* III, *P. simplum* IV, *Mesosaturnalis hexagonus*, *Parahsuum* (?) *grande*, and *Hsuum hisuikyoense* zones (Fig. 8). The calibration for the Jurassic radiolarian zonation proposed by Hori (1990) with the standard Jurassic timescale is based on indirect correlation with ages determined from European and North American radiolarian biostratigraphies (Carter and Hori, 2005; Carter et al., 2010).

Stop descriptions

Figure 9 shows the localities visited during this field trip. Figures 3 and 5 presents a geological map of the Inuyama area showing the locations of Stops 1 to 4.
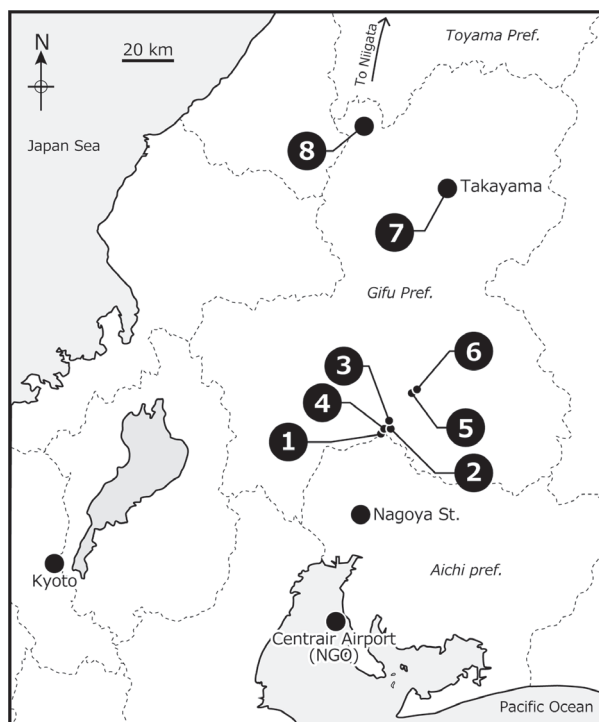
Fig. 9. Index map showing the field stops.

STOP 1. Unuma

GPS coordinates: 35° 23′54″N, 136° 57′33″E.

Unuma is well-known type locality of the genus *Unuma* described by Ichikawa and Yao (1976). The section at the Unuma locality consists of a ~60-m-thick sequence of bedded cherts of the CH-2 thrust sheet described by Yao et al. (1980). This is the renowned section where Yao et al. (1982) first established the four Middle Triassic to Lower Jurassic radiolarian zones in Japan. After their work, many studies of stratigraphy (Matsuda and Isozaki, 1991; Ikeda et al., 2010), structural geology (Kimura and Hori, 1993; Kameda et al., 2012), geochemistry (Takiguchi et al., 2006; Yamaguchi et al., 2016), and paleomagnetism (Shibuya and Sasajima, 1986; Ando et al., 2001) have been carried out at Unuma.

Stop 1-1: Recovery from superanoxia

The section at Unuma begins with carbonaceous claystone and black chert at the base (Ujiie et al., 2015), but the exposure of these rocks is now covered by gravel and sand.
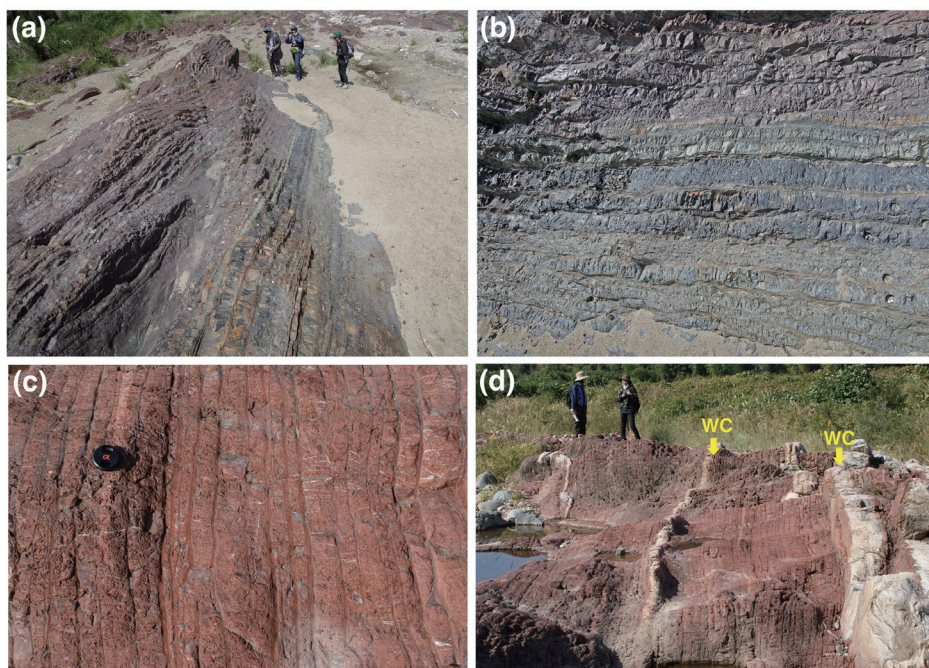
Fig. 10. Field occurrence of Middle Triassic bedded chert in the Unuma section. **(a)** Lower Middle Triassic (Anisian) bedded chert showing a remarkable redox change in deep-sea sediment; recovery from the dark gray anoxic chert to reddish oxic chert. **(b)** Sedimentary transition between gray to purple/brick red chert, reflecting an upward increase in hematite content. **(c)** Bedded chert consists of rhythmic alternations of chert and shale beds, which is considered to have resulted from cyclic changes in the accumulation rate of biogenic SiO_2 within a background of slow accumulation of eolian clay. **(d)** Rhythmic white chert (WC) layers interbedded with red cherts.
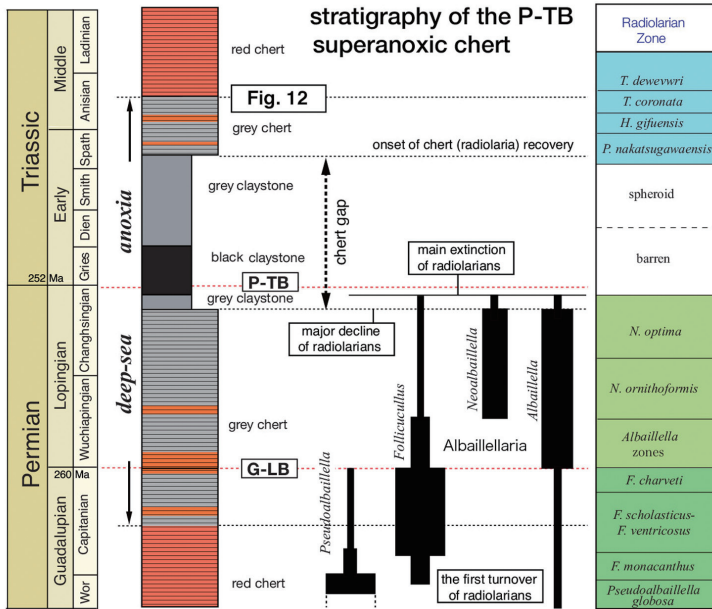
Fig. 11. Composite stratigraphic column of the Permian–Triassic boundary section in pelagic chert facies of Panthalassa (after Isozaki, 2014).
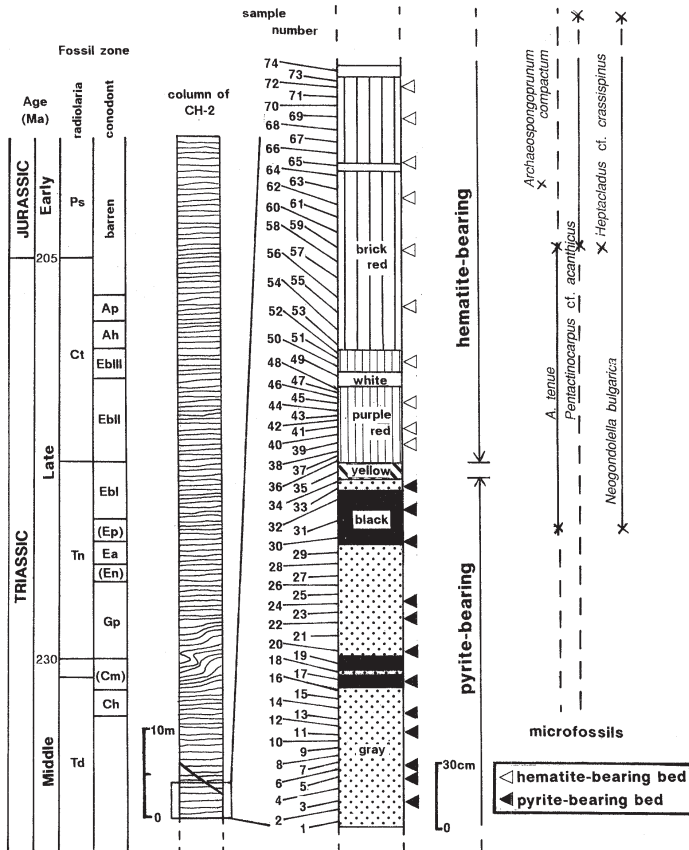
Fig. 12. Stratigraphic column of the study section showing distribution of hematite and pyrite (after Nakao and Isozaki, 1994).

Where depositional contacts occur, middle Anisian gray bedded chert overlies black chert. The gray bedded chert in the lowermost part gradually changes upward to red bedded chert (Fig. 10a, b), which represents the middle Triassic recovery from the deep-sea anoxic event that occurred across the Permian–Triassic boundary (Fig. 11: Isozaki, 1997). Based on Fe-mineral identification by Mössbauer spectroscopy, accessory Fe-bearing minerals in deep-sea cherts, such as pyrite and hematite, have been used as redox indicators for ancient deep-sea environments (Sato et al., 2011, 2012). Kubo et al. (1996) revealed that the occurrence of pyrite and hematite in the gray and red cherts essentially indicates primary reducing and oxidizing depositional conditions, respectively (Fig. 12). It is important to note that the oxygen-depleted interval was not restricted to the Permian–Triassic boundary, but had a much longer duration, until the middle Anisian (~10 Myr of the Triassic).

Stop 1-2: Milankovitch cycles

Middle Triassic red bedded cherts are continuously exposed along the Kiso River (Fig. 10c). The chert consists of rhythmically alternating beds of chert (5–135 mm in thickness) and thin beds of shale (1–80 mm thick). The processes that result in chert–shale couplets of alternating SiO_2-rich (chert) and SiO_2-poor (shale) beds have long been discussed. Hori et al. (1993) proposed that the chert beds were produced by radiolarian blooms against a background of constant, extremely slow accumulation of clay, based on the 10–100 times higher abundance of cosmic microspherules in shale than in chert (Fig. 13). They also
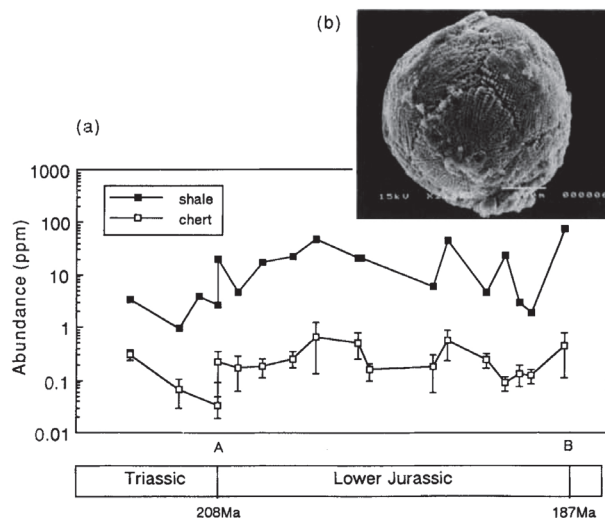
Fig. 13. The temporary change of magnetic microspherule abundance from shale and chert beds in the bedded cherts of the KU Section. Abundance is shown in ppm of volume from a pair of shale–chert couplet. The abundance value of cherts indicates the average of five samples. (b) Scanning electron micrograph of a representative magnetic microspherule which was obtained from the measured section. It has a characteristic dendritic form surface. Scale bar = 100 μm. After Hori et al. (1993).
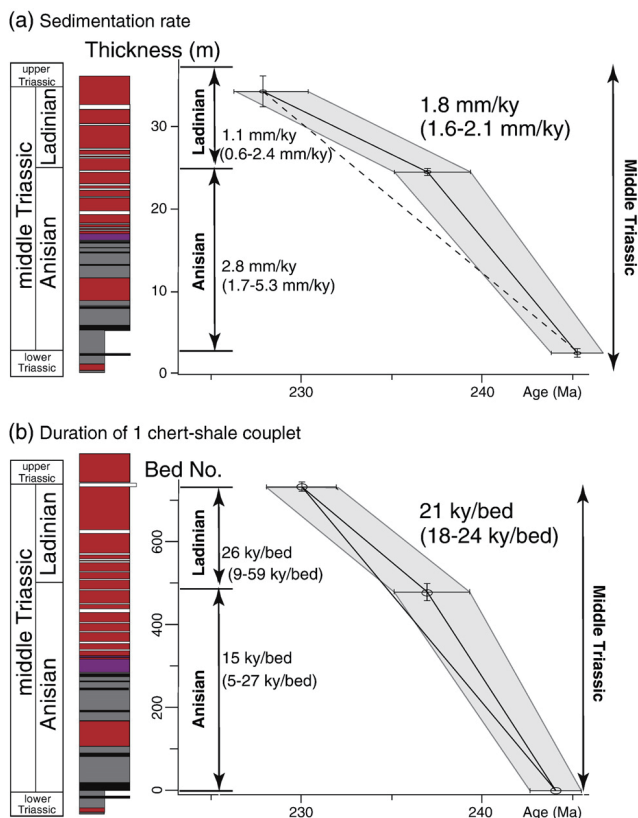
Fig. 14. (a) The estimated average sedimentation rates based on the relationship between thickness and age. (b) The estimated average duration of individual chert–shale couplets based on the relationship between bed number and age for the Anisian, Ladinian, and entire middle Triassic bedded chert in the Inuyama area, Central Japan. After Ikeda et al. (2010).

suggested that the bed-thickness cycles recognized in the bedded cherts were formed by periodic variations in radiolarian productivity related to the Milankovitch climatic cycle. Recently, spectral analysis of a bed-number series of thickness variations in chert beds was performed assuming that each chert–shale couplet represents a 20-kyr precession cycle in the Middle Triassic (Fig. 14: Ikeda et al., 2010). The results of spectral analysis revealed cycles involving approximately 200, 20, 5, and 2–3 beds, corresponding to periodicities of approximately 4000, 400, 100, and 40–60 kyr, respectively. By further assuming that the 20-bed cycle represents a 405-kyr eccentricity cycle of constant and stable periodicity, spectral analysis of the time series of thickness variations of chert beds revealed distinct 38-kyr obliquity and 97- and 117-kyr eccentricity cycles in addition to a 405-kyr eccentricity cycle (Ikeda et al., 2010). Although radiolarian productivity probably affected variations in chert bed thickness, further studies are required to understand the relationship between Milankovitch cycles and radiolarian productivity in the Triassic pelagic realm.

Stop 1-3: Origin of white chert

Rhythmically repeated white chert layers (~20 cm thick) are visible in the Anisian red bedded cherts at Unuma (Fig. 10d). The white chert is characterized by outcrop-scale
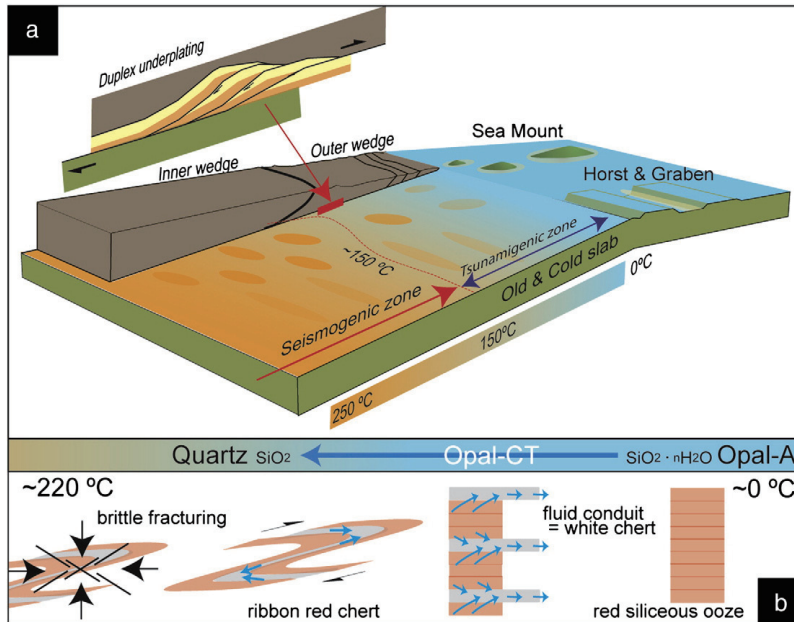
Fig. 15. Cartoon showing the setting of deformation/diagenesis of bedded cherts in a cold subduction zone (after Kameda et al., 2012). **(a)** Thermal conditions of a cold subduction zone. The temperature around seamounts (petit hot spot) and horst–grabens may be higher than that of normal oceanic plate due to volcanism, thereby representing hot patches in the subduction zone (future coupling areas). **(b)** Diagenesis of siliceous ooze (opal-A), resulting in its conversion to chert (i.e., quartz via an intermediate stage of opal-CT) accompanied by dehydration. White cherts represent fossilized fluid conduits during diagenesis. Brittle fracturing of the chert occurred after duplex-underplating under temperatures of ~220 °C.

ductile folding with ENE–WSW trending axial traces, and is composed mainly of thin crack-filling mineral veins that were precipitated in multiple stages. Kameda et al. (2012) suggested that the ductile deformation was facilitated by silica dehydration–precipitation, and is represented by multiple phases of vein networks.

   The outcrop clearly shows that the white chert was formed prior to the ductile deformation. There are several hypotheses regarding the origin of the white cherts. Tsukamoto (1989) proposed that they were derived originally from limestones and were subsequently silicified during later burial diagenesis. In contrast, Kameda et al. (2012) suggested that the white cherts acted as conduits for SiO_2-oversaturated fluid and became silicified through multiple veining events and the precipitation of SiO_2 minerals, due to intense brittle fracturing and fluid flow (Fig. 15). Yamaguchi et al. (2016) estimated that the amount of water necessary to precipitate SiO_2 in the white chert is ~10^2 times larger than that produced from compaction and silica/clay diagenesis of pelagic siliceous sediment (chert). They pointed out that water released by dehydration during silica diagenesis and fluid from various other sources (e.g., smectite–illite transition, saponite–chlorite transition, and serpentine dehydration) would pass through the chert layer.

STOP 2. Momotaro Shrine

GPS coordinates: 35° 24'16"N, 136° 57'48"E.

The outcrop at STOP 2 is located near the Momotaro Shrine (Jinja) on the east side of the Kiso River in Inuyama City (Fig. 5). A widespread exposure of the Lower Triassic siliceous claystone and overlying Middle Triassic chert in the chert–clastic sequence of the CH-3 thrust sheet is visible (Fig. 16). Higher in the section, the Middle to Upper Triassic (Ladinian to Carnian) bedded chert is exposed.

Stop 2-1: Early Triassic anoxia

The Early to Middle Triassic radiolarian biostratigraphy at Momotaro Shrine was documented by Yao and Kuwahara (1997). This section was called the "Momotaro–Jinja section" (Fig. 17: Yao and Kuwahara, 1997). Three radiolarian biozones are recognized in the Lower Triassic siliceous claystone of this section: the Olenekian "Sphaeroides" and *Parentactinia nakatsugawaensis* zones, and the Anisian *Hozmadia gifuensis* zone. Takahashi et al. (2009) established conodont biozones in the same section as Yao and Kuwahara (1997): the "Sphaeroides" zone corresponds to the late Olenekian (Spathian), the *P. nakatsugawaensis* zone is late Olenekian (Spathian), and the *H. gifuensis* zone is Anisian (Fig. 18). After their conodont biostratigraphic work, Sakuma et al. (2012) correlated $\delta^{13}C_{org}$ records in the Momotaro–Jinja section with high-resolution isotopic profiles of carbonate carbon ($\delta^{13}C_{carb}$) from shallow-marine carbonate sequences in southern China (e.g., Payne

Fig. 16. Aerial photograph of the Unuma section showing the location of Lower Triassic bedded chert sequence described by Yao and Kuwahara (1997).

et al., 2004) to establish a higher-resolution age model.

The basal 3 m of the section is composed of gray siliceous claystone (Bed groups 2 and 3 of Takahashi et al., 2009: Fig. 18) and red siliceous claystone (Bed group 4), both of which belong to the "Sphaeroides" zone. The middle part of the section (~3 m thick), which belongs to the *P. nakatsugawaensis* zone, consists of red siliceous claystone (Bed group 5), gray siliceous claystone interbedded with chert (Bed groups 6–10, 13), and two black chert beds (Bed groups 11–12). The upper part (~1.5 m thick) contains thick alternating gray chert and siliceous claystone (Bed groups 14–15), and corresponds to the *H. gifuensis* zone (Anisian).

The Momotaro–Jinja section provides valuable insights into the relationship between redox history and radiolarian diversity in the Panthalassa Ocean across the Early–Middle Triassic transition. As discussed at Unuma (STOP 1), the total duration of the Early Triassic oxygen-depleted episode was probably a maximum of 10 million years until recovery in the Anisian (Fig. 11). Takahashi et al. (2009) analyzed organic molecules from siliceous claystones and cherts from the Momotaro–Jinja section to clarify the redox conditions during the Early to Middle Triassic (Fig. 18). Their geochemical analysis revealed low pristane/phytane ratios
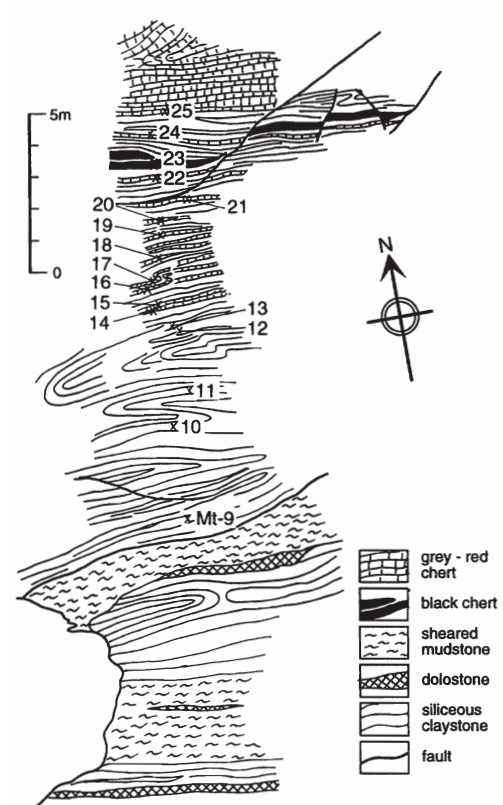
Fig. 17. Sketch of outcrop of the Momotaro-Jinja section at STOP 2-1. After Yao and Kuwahara (1997).
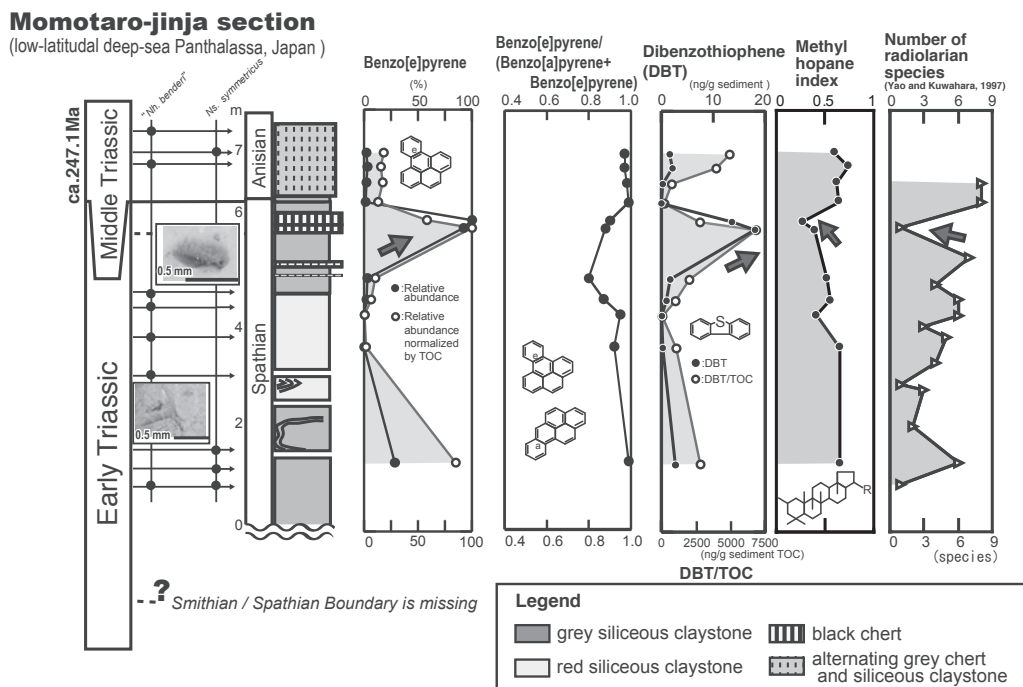
Fig. 18. Study results between Early Triassic and Middle Triassic from the Momotaro-Jinja section of the low latitudinal pelagic deep-sea (after Takahashi, 2013). Data are from Takahashi et al. (2009).

(a measure of redox conditions) in the Momotaro-Jinja section (<1), indicating the prevalence of deep-sea anoxia during the late Olenekian to Anisian. In addition, high concentrations of dibenzothiophene (an index of anoxic depositional environments) are present in the strata deposited at the end of the Spathian, which suggests the development of anoxic deep water. This anoxia event coincided with a decrease in cyanobacterial abundance in the photic zone, as indicated by the $2a$-methylhopane index, and low radiolarian diversity. These results suggest that the anoxic deep water in the Panthalassa Ocean reached intermediate water depths at the end of the Early Triassic (Fig. 19), killing marine planktonic organisms including radiolaria (Takahashi et al., 2009).

Stop 2-2: Carnian Pluvial Event

As the stratigraphic sequence youngs from south to north at STOP 2, the Ladinian–Carnian bedded chert sequence was visible in the northern part of the previous stop. The Ladinian and Carnian represent a time of relative stability, interrupted only by an episode of more humid conditions known as the Carnian Pluvial Event (CPE). The CPE occurred in the latest Julian (Early Carnian) and is indicated by several lines of evidence, including a sudden input in coarse siliciclastic material observed in most shallow-water Carnian
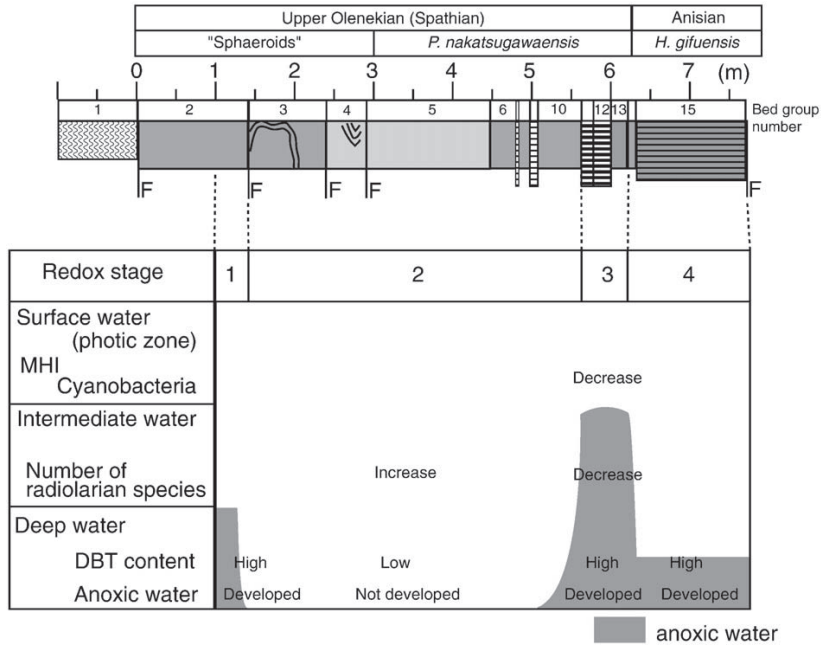
Fig. 19. Conceptual diagram of Panthalassic oceanic environmental stages from the upper Olenekian to lower Anisian. After Takahashi et al. (2009).

successions of Europe (Simms and Ruffell, 1989). The event was characterized by a temporary shutdown of carbonate systems across the western Tethyan realm (Rigo et al., 2007) and high extinction rates of several groups, such as ammonoids, crinoids, bryozoa, and conodonts (Simms and Ruffell, 1989, 1990; Rigo et al., 2007). It has been suggested that the CPE was caused by the major flood-basalt volcanism of the Wrangellia large igneous province in the Panthalassa Ocean (Dal Corso et al., 2012).

To reveal the pelagic sedimentary response to Carnian climate change, Nakada et al. (2014) observed stratigraphic changes in Fe-bearing minerals in the upper Julian–lower Tuvalian interval of the bedded chert sequence from "Section R" (Sugiyama, 1997) at the Momotaro Shrine locality (Fig. 20). They revealed that the stratigraphic change in the Fe-bearing compositions can be divided into three stages: (I) a stage in which a relatively stable mineral composition (chlorite + illite + hematite) is observed in cherts deposited during the lower to middle Julian; (II) an abrupt change in mineral composition (absence of chlorite and appearance of smectite) in upper Julian–lower Tuvalian strata; and (III) recovery of the previous stable mineral composition in the middle to upper Tuvalian (Fig. 21). According to Nakada et al. (2014), the sudden disappearance of chlorite and the presence of smectite during the second stage occurred as a result of increasing rainfall, corresponding to the CPE period. They inferred that the primary formation of chlorite would have decreased, whereas smectite should have formed as a result of the increasing humidity in the continental area.
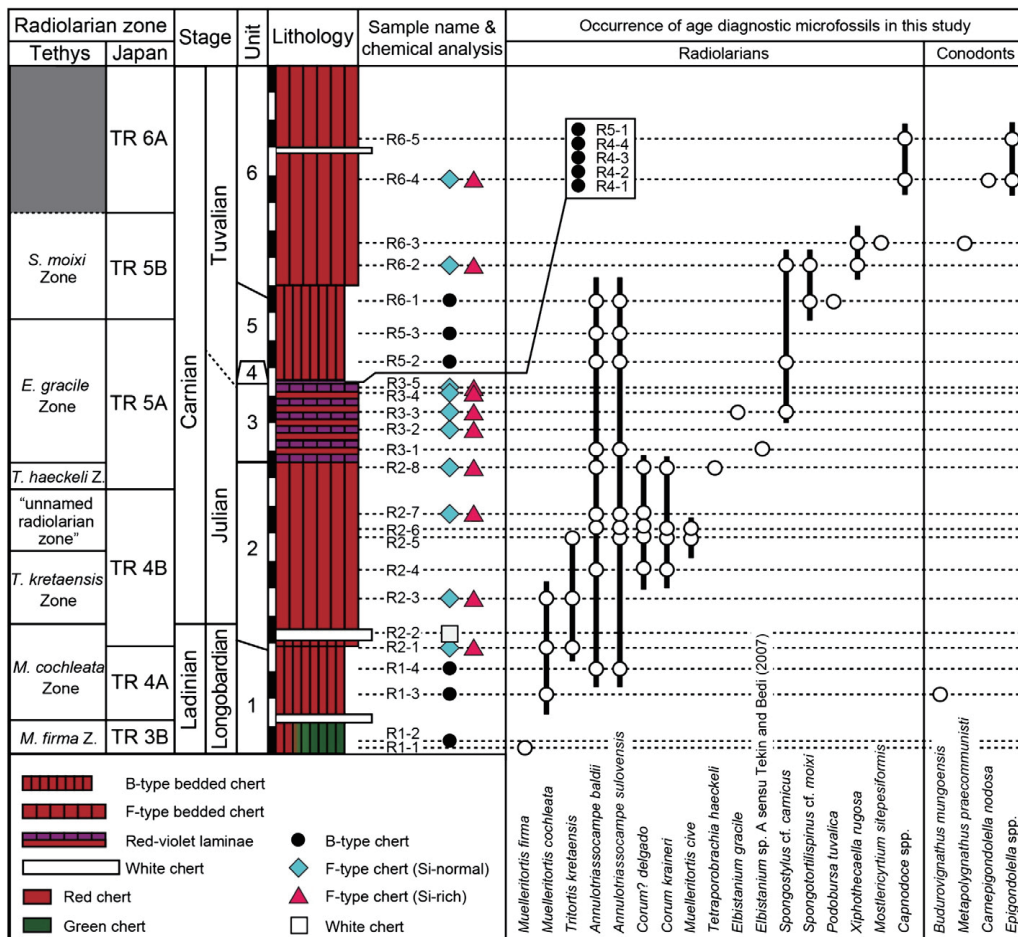
Fig. 20. Summary of lithostratigraphic, biostratigraphic, geochronologic, and examined samples (after Nakada et al., 2014). It is noted that this section is one of the type sections of the Triassic standard radiolarian biostratigraphy by Sugiyama (1997). Radiolarian zones are from Kozur and Mostler (1994) and Kozur (2003) in Tethys and from Sugiyama (1997) in Japan after our examinations of radiolarians and conodonts. The subdivision in the Carnian is based on Ogg (2012). The litholigic types of bedded chert are from Imoto (1984); the B-type bedded chert shows a clear repetition of distinct siliceous and muddy layers at levels of several centimeters and the F-type bedded chert has boundaries that are indistinct due to amalgamation.
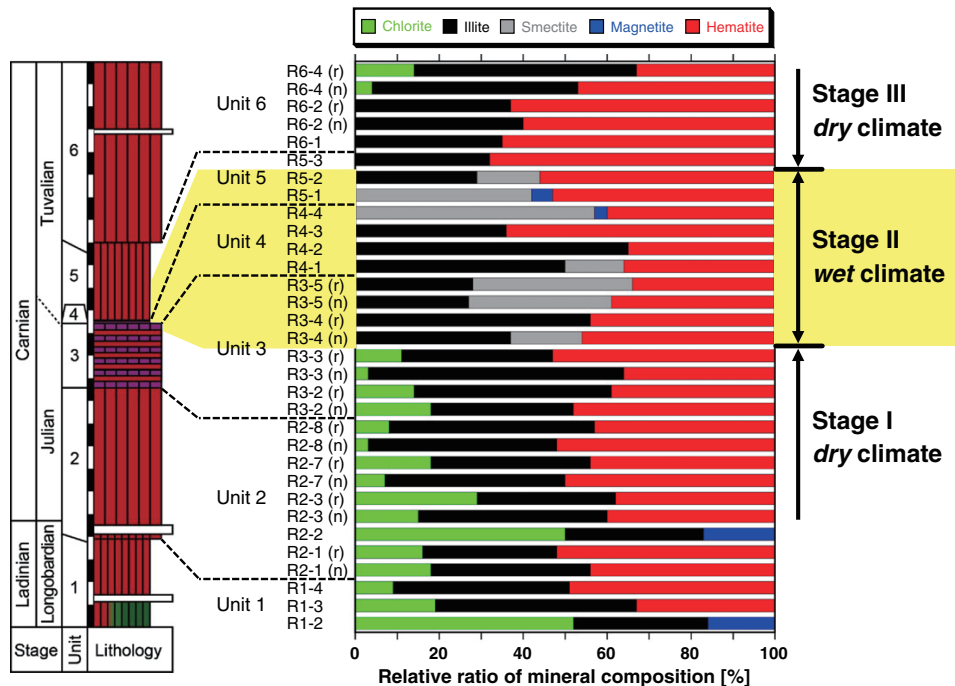
Fig. 21. Summary of XANES- and EXAFS-LCF results for chert samples collected from Section R. The mineral composition determined by EXAFS-LCF prevailed over the XANES-LCF results. Note that (n) and (r) denote the Si-normal and the Si-rich parts of F-type chert, respectively. After Nakada et al. (2014).

Fig. 22. Aerial photograph of the Sakahogi section showing the location of Norian impact ejecta layer.
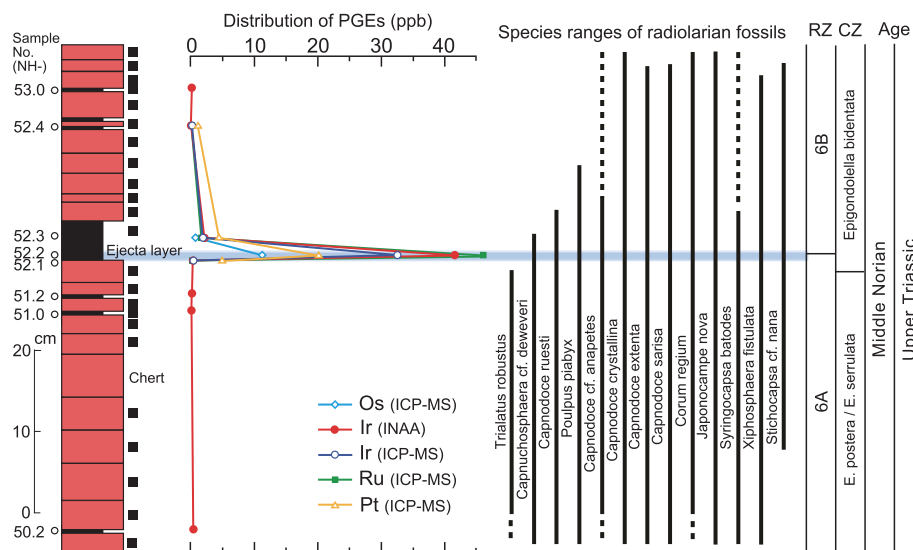
Fig. 23. PGE abundances and biostratigraphy of radiolarians from the middle Norian section (Sakahogi) at STOP 3. Solid squares beside the lithologic section indicate the occurrence of conodonts and radiolarians in cherts and claystones. The radiolarian ranges are used to constrain the age of the ejecta deposit. The claystone contains anomalously high iridium concentrations, of up to 41.5 parts per billion (ppb), which are comparable with the levels found at the K/Pg boundary. Modified after Onoue et al. (2012).

STOP 3. Sakahogi

GPS coordinates: 35° 25'18"N, 136° 58'27"E.

An excellent exposure of Upper Triassic bedded chert (= CH-2 thrust sheet of Yao et al., 1980) is observed in the Sakahogi locality along the Kiso River (Fig. 22). "Section N" (Sugiyama, 1997) exposes a ~20-m-thick sequence of bedded chert. Sugiyama (1997) established six radiolarian zones (the *Capnuchosphaera* to *Praemesosaturnalis multidentatus* zones) from the Carnian–Norian bedded chert in this section.

Stop 3-1: Norian impact event

We will see and discuss a possible link between the late Middle Norian radiolarian extinction and a large impact event. Such an event has been inferred from anomalous concentrations of platinum-group elements (PGEs) and negative osmium (Os) isotope excursions in a claystone layer in an Upper Triassic bedded chert succession in Section N (Figs. 23, 24: Onoue et al., 2012; Sato et al., 2013). The claystone layer is 4–5 cm thick and contains a lower and an upper sublayer (Fig. 25a). The lower sublayer contains microspherules in a matrix of clay minerals (mainly illite), cryptocrystalline quartz, and hematite (Fig. 25b). The upper sublayer is composed of undisturbed clay minerals (illite) and
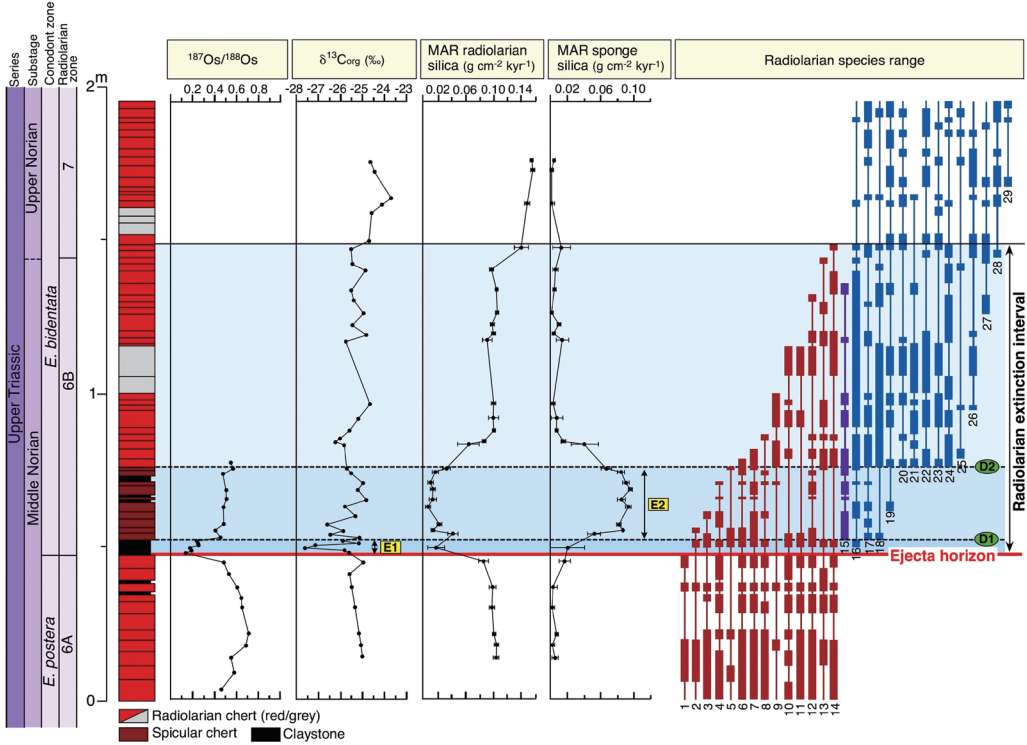
Fig. 24. Stratigraphic profiles of Os isotope ratios, organic carbon isotopes, mass accumulation rates of biogenic silica, and radiolarian biostratigraphy in bedded cherts of the Sakahogi section. Biostratigraphic ranges of 29 radiolarian species in the study interval at Sakahogi show extinctions of middle Norian species (red) corresponding with successive blooms of opportunistic species (purple) and radiations of new species (blue). Dashed lines mark the initial (D1) and second (D2) phases of diversification of upper Norian radiolarian species. Modified after Onoue et al. (2016).

cryptocrystalline quartz.

Biostratigraphic and magnetostratigraphic studies (Sugiyama, 1997; Onoue et al., 2012; Uno et al., 2015) have revealed that the claystone layer occurs in the upper Middle Norian bedded chert. Given that the constant average sedimentation rate of the Middle Norian chert is 1.0 mm kyr^{-1} (Onoue et al., 2012), the deposition of the claystone layer occurred ~1 Myr before the Middle–Late Norian boundary (~214 Ma; Ogg, 2012).

The late Middle Norian age of the clay layer suggests that the PGE anomalies and microspherules in the lower sublayer originated from an extraterrestrial source, related to an impact event that formed the 90-km-diameter Manicouagan crater in Canada (214–215 Ma). In addition, a magnetostratigraphic analysis yielded a normal polarity interpretation for the clay layer, which is consistent with paleomagnetic data for the Manicouagan melt rock (Uno et al., 2015). Studies of PGEs and Os isotopes have revealed that the anomalously high PGE abundances in the lower sublayer resulted from a large chondritic impactor with a diameter of 3.3–7.8 km (Sato et al., 2016). An impactor of this size would produce a crater
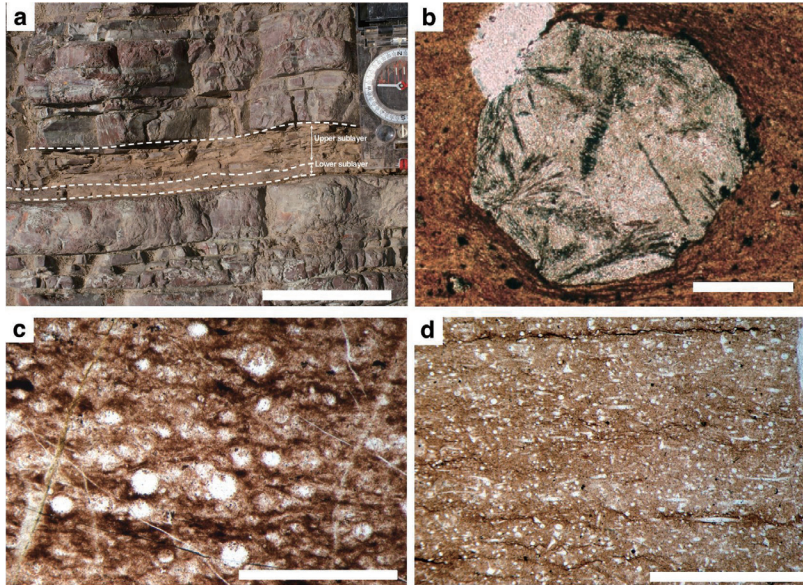
Fig. 25. (a) Photograph showing detail of claystone layer at Sakahogi locality, modified after Onoue et al. (2012). The claystone layer is 4–5 cm thick and contains a lower and an upper sublayer. The lower sublayer contains microspherules in a matrix of clay minerals (mainly illite), cryptocrystalline quartz, and hematite. The upper sublayer is composed of undisturbed clay minerals (illite) and cryptocrystalline quartz. **(b)** Photomicrographs of microspherules from the ejecta deposit. Plane-polarized light. (Scale bar: 500 μm.) **(c, d)** Photomicrographs showing spicular (c) and radiolarian (d) cherts from the Sakahogi section. Plane polarized light. NHR 46 (a); NHR 38 (b). Scale bars = 1 mm.

~56–101 km in diameter, assuming an impactor entry velocity of 20 km s^{-1}, an entry angle of 45°, and a crystalline target (density = 2750 kg m^{-3}). The size range of such a crater is consistent with the size of the Manicouagan crater (diameter = ~90 km).

Stop 3-2: Radiolarian faunal turnover across the Middle–Upper Norian transition

A biostratigraphic study of section N at Sakahogi indicated that extinctions of Middle Norian radiolarian species occurred in a stepwise fashion in the ~1-myr interval above the ejecta horizon (Onoue et al., 2016). Furthermore, high-resolution paleontological and geochemical data (Fig. 24) have revealed that two paleoenvironmental events occurred during the initial phase of the radiolarian extinction interval. The first event (E1) consisted of the post-impact shutdown of primary productivity and a remarkable decline in the amount of biogenic silica preserved before the first phase of diversification (D1). The second event (E2) consisted of a large and sustained reduction in the sinking flux of radiolarian silica and the proliferation of siliceous sponges, which occurred before the second phase of diversification (D2) and lasted for ~0.3 Myr after the impact (Fig. 24). The primary cause of this decline is difficult to identify, but the relatively long period of the E2 interval (~0.3 Myr after the impact) largely excludes the possibility that the decline was triggered by instantaneous environmental stresses (e.g., extended darkness, global cooling, or acid rain)
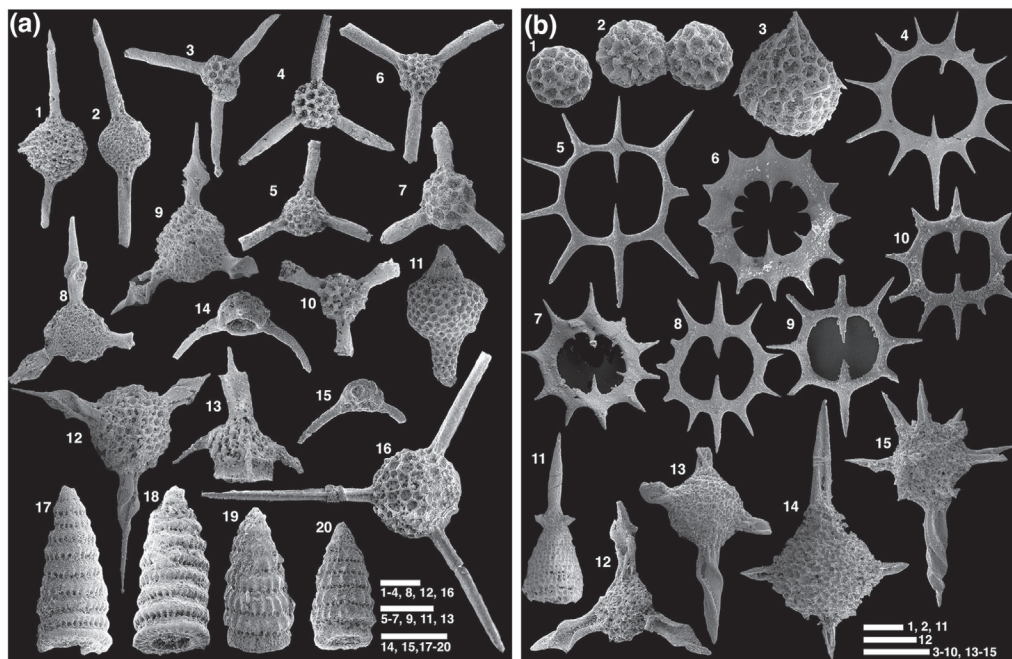
Fig. 26. Radiolarian fossils from the bedded cherts in the middle–upper Norian section at Sakahogi (Modified after Onoue et al., 2016). **(a)** Middle Norian radiolarians from the Sakahogi section. Scale bars = 100 μm. **1–2,** *Xiphosphaera fistulata* Carter. NHR30 (1); NHR49 (2). **3–4,** *Capnodoce sarisa* De Wever. NH52-R6. **5,** *Capnodoce extenta* Blome. NHR50. **6,** *Capnodoce* sp. cf. *C. ruesti* Kozur and Mock. NH52-R6. **7,** *Capnodoce crystallina* Pessagno. NHR43. **8–9,** *Capnuchosphaera* sp. cf. *C. deweveri* Kozur and Mostler. NHR36 (8); NHR53 (9). **10,** *Capnodoce* sp. cf. *C. anapetes* De Wever. NHR31. **11,** *Syringocapsa batodes* De Wever. NH52-R6. **12,** *Sarla hadrecaena* (De Wever). NHR57. **13,** *Trialatus robustus* (Nakaseko and Nishimura). NHR33. **14–15,** *Poulpus piabyx* De Wever. NHR37 (14); NH52-R6 (15). **16,** *Sepsagon longispinosus* (Kozur and Mostler). NHR42. **17–18,** *Japonocampe nova* (Yao). NHR36 (17); NH52-R6 (18). **19–20,** *Corum regium* Blome. NHR43 (19); NH52-R6 (20). **(b)** Upper Norian radiolarians from the Sakahogi section. Scale bars = 100 μm. **1–2,** Spumellaria gen. et sp. indet. A. NHR42. **3,** *Pentactinocarpus sevaticus* Kozur and Mostler. NHR42. **4,** *Palaeosaturnalis harrisonensis* (Blome). NHR52. **5,** *Palaeosaturnalis* sp. aff. *P. dotti* (Blome). NHR81. **6,** *Pseudoheliodiscus heisseli* (Kozur and Mostler) NHR91. **7,** *Pseudoheliodiscus finchi* Pessagno. NHR62. **8,** *Palaeosaturnalis* sp. aff. *P. harrisonensis* (Blome). NHR60. **9,** *Palaeosaturnalis largus* (Blome) NHR57. **10,** *Palaeosaturnalis dotti* (Blome) NHR57. **11,** *Lysemelas olbia* Sugiyama. NHR80. **12,** *Sarla prietoensis* Pessagno. NHR57. **13,** *Plafkerium* sp. A. NHR60. **14,** *Plafkerium* (?) sp. B. NHR74. **15,** *Discofulmen* sp. NHR90.

that would have been caused by a bolide impact.

Decreases in the sinking flux of radiolarian silica during the E1 and E2 events may reflect a decline in radiolarian production in Middle Norian taxa, including in *Capnodoce* and *Capnuchosphaera* species (Fig. 26a). These Middle Norian radiolarians are rare above the E1 interval, whereas a small spumellarian species is abundant within the E2 interval; this spumellarian species is reported as Spumellaria gen. et sp. indet. A, and its occurrence can be used to identify the stratigraphic position of the ejecta layer in other Triassic chert sections within the Jurassic accretionary complexes in Japan (Sato et al., 2013). These taxa can be considered to be short-lived opportunistic species, as they disappeared at the end of
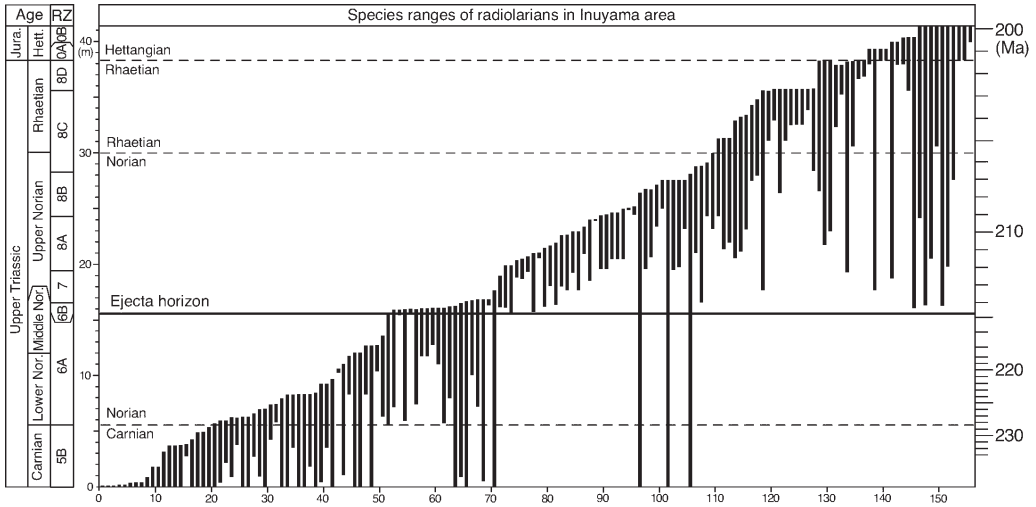
Fig. 27. Stratigraphic ranges of Late Triassic radiolarian species in the Inuyama area, projected onto a composite section, after Onoue et al. (2016). Species numbers are shown on the x-axis. Radiolarian zones (RZ) are from Sugiyama (1997).
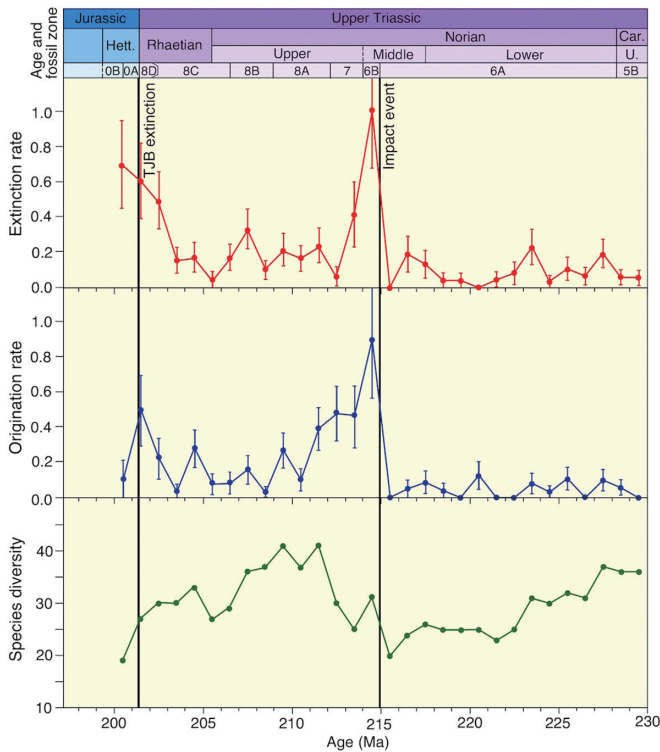
Fig. 28. Extinction and origination rates of Late Triassic radiolarian species in the Panthalassa Ocean. The extinction rate of the middle Norian impact event is substantially higher than the rate at the Triassic–Jurassic boundary (TJB). Error bars are one standard deviation, estimated from bootstrap resampling of the stratigraphic ranges of species with 1000 iterations. After Onoue et al. (2016).

the radiolarian faunal turnover interval. Ito et al. (2017) raised the possibility that these spherical radiolarians represent colonial radiolarians in the Triassic.

The biostratigraphic analysis also revealed that the radiation of Late Norian taxa (Fig. 26b) was contemporaneous with a temporary bloom in the numbers of opportunistic spumellarian species in the E2 interval (Onoue et al., 2016). The timing of these radiation events suggests that the decrease in radiolarian biomass in the Middle Norian taxa enhanced the bloom of opportunistic radiolarian species and the evolutionary radiation of Late Norian taxa in the E1 and E2 intervals. Hence, the gradual extinction of Middle Norian radiolarian taxa during the ~1-Myr period could be explained by ecological pressures imposed by Late Norian taxa, provided that the Late Norian taxa were more rapidly growing and more efficient phytoplankton feeders than the Middle Norian taxa.

Onoue et al. (2016) analyzed a large dataset of Upper Triassic radiolarian occurrences in the Inuyama area to assess the magnitude of the extinction event caused by the Middle Norian impact and to compare this event with extinction events at other stage boundaries (Fig. 27). An analysis of the stratigraphic ranges of radiolarian species indicated that a dramatic increase in extinction and origination rates is observed in the 1-Myr interval following the impact event (Fig. 28). These results suggest that the Middle Norian impact triggered the extinction and contemporaneous evolutionary radiation of the radiolarian fauna in the equatorial Panthalassa Ocean.

STOP 4. Katsuyama
GPS coordinates: 35° 25'21"N, 136° 58'16"E.

A well-exposed outcrop of the bedded chert sequence (CH-3 of Yao et al., 1982) spanning the Middle Triassic to Upper Jurassic, including the Triassic–Jurassic boundary and Toarcian OAE level, is located in the left bank of the Kiso River near Katsuyama, Sakahogi Town, Gifu Prefecture, Japan. This section was originally described by Hori (1990, 1992), and is called the Katsuyama (UF) section. The whole sketch map and stratigraphy of this section were shown in the excursion of Osaka InterRad VII Meeting 1994 (Figs. 29, 30: Matsuoka et al., 1994). Eight radiolarian assemblage zones are recognized: the *Hozmadia gifuensis, Triassocampe coronata,* "*Triassocampe*" *nova, Canoptum triassicum, Parahsuum simplum,* "*Mesosaturnalis*" *(Hexasaturnalis) hexagonus*, and *Parahsuum* (?) *grande* zones.

Stop 4-1: Triassic–Jurassic boundary
The Triassic–Jurassic boundary in the Katsuyama (UF) section is clearly recognized in the CH-3 bedded chert sequence, visible as a color change in the chert facies and an associated thick (<10 cm) shale bed (Hori, 1992). A distinctive dusty red (purplish) chert is developed just above the Upper Triassic brick-red chert sequences, the former is correlated
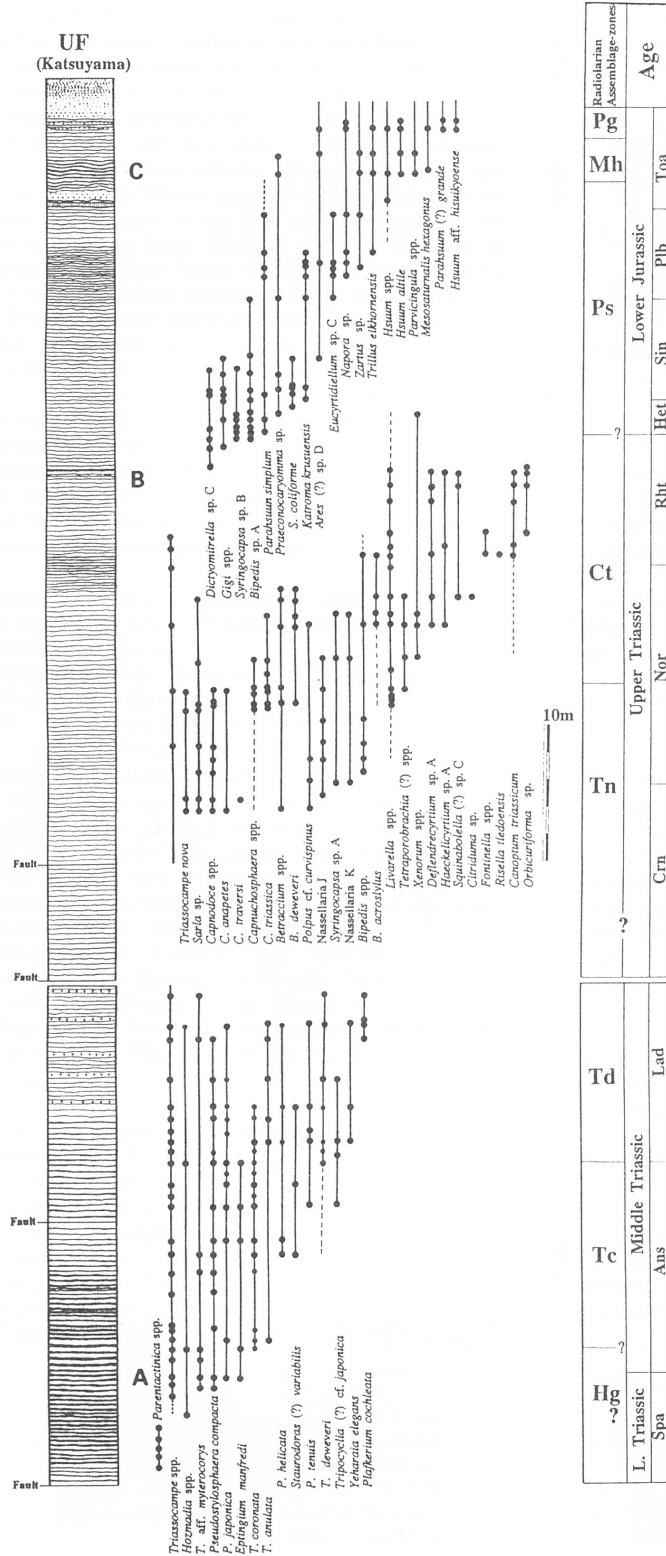
Fig. 29. Lithologic column and stratigraphic distribution of selected radiolarian species in the Katsuyama (UF) section. After Matsuoka et al. (1994).
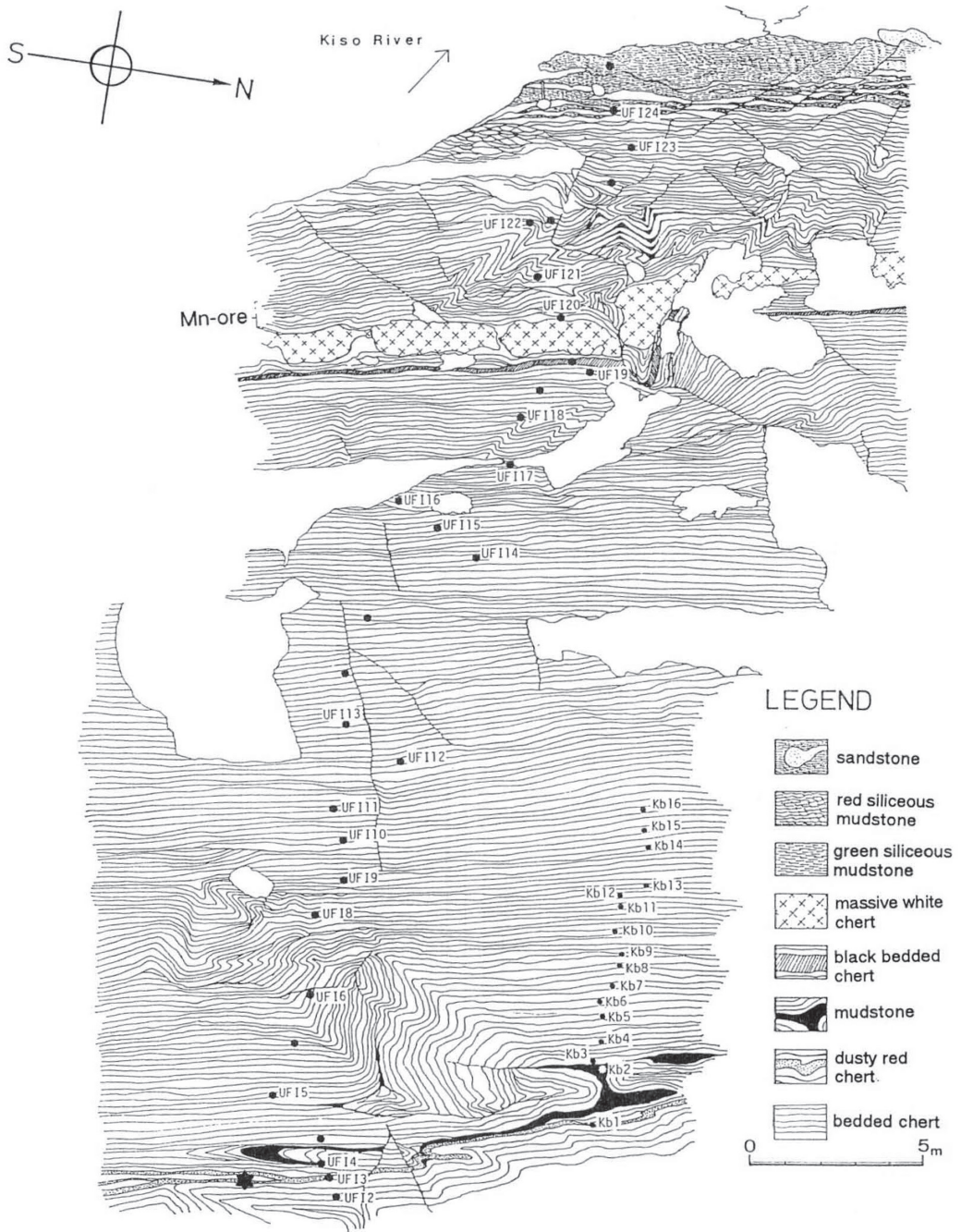
Fig. 30. Sketch map of the Katsuyama (UF) section showing sample localities (solid circles) for radiolarian biostratigraphy of the section. After Hori (1992).
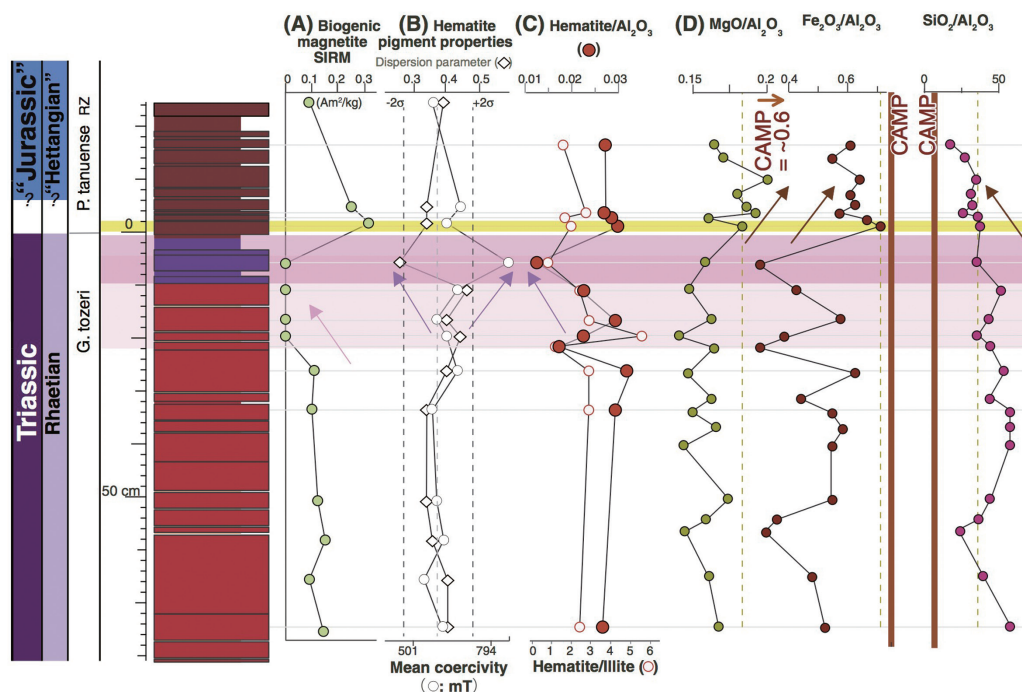
Fig. 31. Stratigraphic changes in magnetic, mineralogical, and geochemical data across the Triassic–Jurassic (T–J) transition at the Katsuyama (UF) section. After Ikeda et al. (2015). (A) Biogenic magnetite saturation isothermal remnant magnetization (SIRM; mA m²/kg) (Abrajevitch et al., 2013). (B) Hematite pigment properties (Mean coercivity (mT, logarithmic scale; open circle) and Dispersion parameter (DP; diamond)). Dashed red lines indicate range of ± 2 standard deviations from mean for both values (Abrajevitch et al., 2013). (C) Hematite/illite (open circle) and hematite/Al_2O_3 (closed circle) (D) MgO/Al_2O_3, Fe_2O_3/Al_2O_3, and SiO_2/Al_2O_3 ratios. Yellow dotted thin line and brown thick lines indicate the chemical compositions of the base of dusty red chert and the Central Atlantic magmatic province (CAMP) basalts, respectively.

with the final occurrence of the conodont species *Misikella posthernsteini*. The radiolarian faunal change from Triassic to Jurassic taxa occurred after the extinction of *M. posthernsteini* (Carter and Hori, 2005). Distinctive changes in clay and magnetic mineral compositions in the Triassic–Jurassic boundary strata are recognized (Fig. 31), suggesting a short-lived environmental change (pH change?) in the latest Triassic marked by the disappearance of biogenic magnetite (Abrtajevitch et al., 2013) and a reduction in authigenic hematite (Ikeda et al., 2015). The results of Os and C_{org} isotopic analyses on the Triassic–Jurassic boundary chert sequences indicate that similar excursion curves of these isotope ratios have been recognized in Triassic–Jurassic boundary sequences from the Panthalassa such as in New Zealand and the Kurusu section of the Inuyama area (Okada et al., 2015; Hori et al., 2016). These results reveal a long-lived reduction of primary production in the Panthalassa during Late Triassic time and a subsequent increased influx of continental material just before the radiolarian faunal turnover.

Fig. 32. Detailed lithostratigraphic log, organic carbon isotope record ($\delta^{13}C_{org}$), and biostratigraphy of the Katsuyama (UF) section. Radiolarian biostratigraphy is from Hori (1997) and modified according to Carter et al. (2010). The major difference between these two zonations is based on the presence of only one species (*Hsuum exiguum*) to define to the middle Toarcian. Modified after Gröcke et al. (2011).

Stop 4-2: Toarcian OAE

This section comprises a Toarcian OAE (T-OAE) black chert sequence containing fine, occasionally framboidal, pyrite crystals between the *Parahsuum simplum* and "*Mesosaturnalis*" (*Hexasaturnalis*) *hexagonus* radiolarian zones of the Katsuyama (UF) section. The black chert contains extremely high levels of organic carbon (100 times higher than those of the red cherts from the Inuyama area, which normally contain 0.01–0.03 wt.% organic carbon), with associated overlying thick, massive, white, Mn-rich chert beds. Stable C isotope analysis of organic carbon of bulk cherts yielded a distinctive negative shift at this T-OAE (Fig. 32), indicating an influx of an extremely light carbon source such as methanotrophic bacteria at the time of the T-OAE (Gröcke et al., 2011). A marked radiolarian faunal turnover occurred across this T-OAE level, characterized by disappearance of the *Parahsuum simplum* assemblage radiolarian taxa and a high diversity of multi-segmented nassellarians such as *Hsuum*, *Parahsuum*, *Parvicingula* s.l., and *Elodium* (Hori, 1997). Astronomical cycle analyses of chert bedding revealed that the age and

duration of the T-OAE in the Inuyama chert sequences show good agreement with those of the Karoo–Ferrar volcanism (Ikeda and Hori, 2014).

STOP 5. Kamiaso conglomerate

GPS coordinates: 35° 31'34"N, 137° 6'58"E.

We will observe the Kamiaso conglomerate sandwiched between trench-fill turbidites in the Kamiaso area. The Kamiaso conglomerate is well known because the gneiss clasts within it have yielded the oldest radiometric age in Japan. The conglomerate, together with the sandstone, in the accretionary complex provides important information on the provenance of clastic material (Mizutani, 1959; Adachi, 1973; Suzuki et al., 1991; Takeuchi, 2000). The following descriptions of the geology and chronology of the Kamiaso conglomerate are taken from Adachi (1971), Adachi et al. (1992), and Sano et al. (2013), to which the reader is referred for more detail.

The Kamiaso conglomerate is exposed along the gorge of the Hida River. Four horizons of the conglomerate beds, each several meters thick, have been mapped in this area (Fig. 33), but their lateral extent is limited to less than 1 km. The conglomerate beds, which are intercalated with a mudstone-rich distal turbidite, have sharp bases and are interpreted as channel-fill debris-flow deposits on a submarine fan. Similar conglomerates are known to
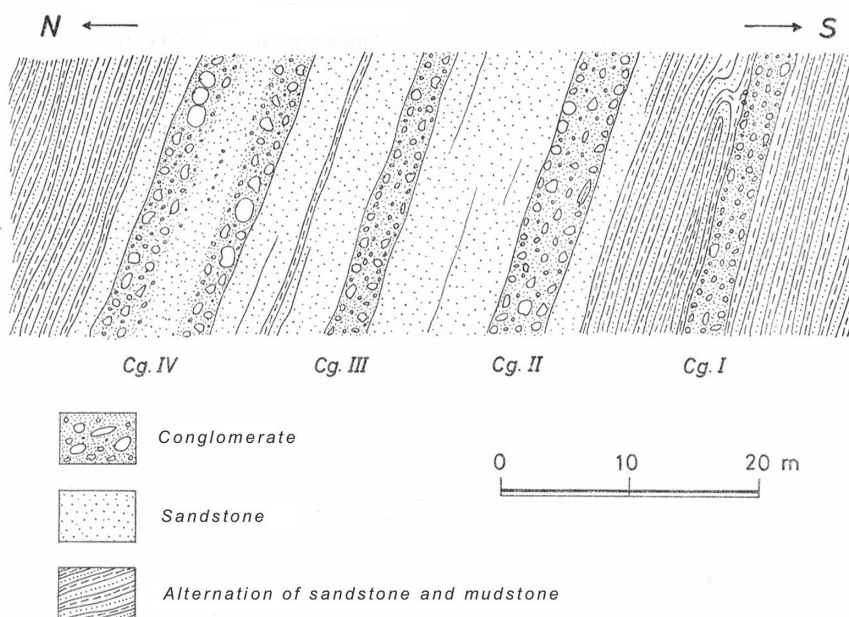
Fig. 33. Kamiaso conglomerate beds intercalated in turbiditic sandstone and mudstone along the Hidagawa River, Kamiaso (after Adachi, 1971).
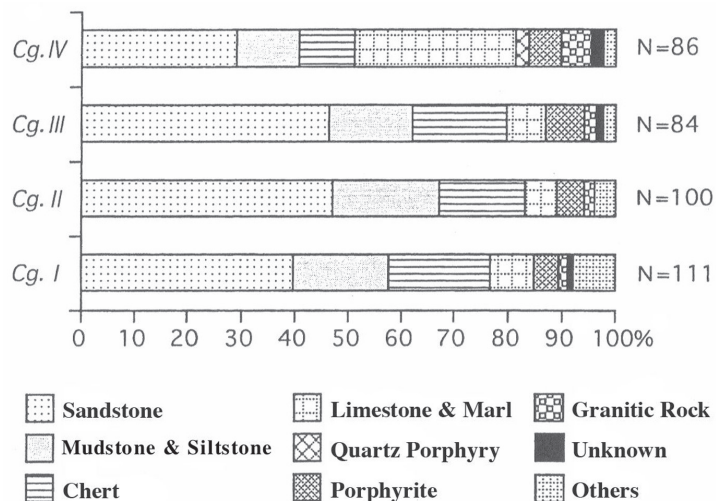
Fig. 34. Clast composition of the Kamiaso conglomerate. Others include orthoquartzite and basalt, and N means the total number of clast samples analyzed (after Sano et al., 2013).
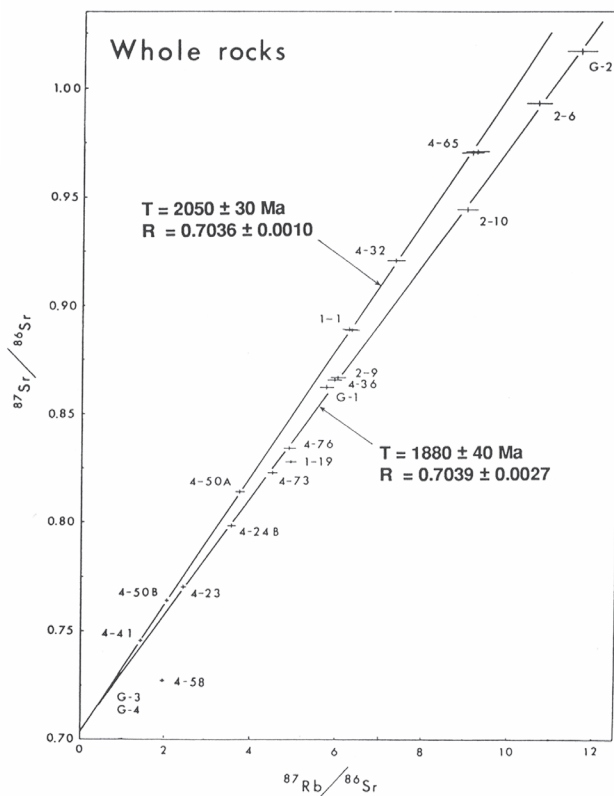
Fig. 35. Rb-Sr whole-rock isochrones for metamorphic and granitic clasts in the Kamiaso conglomerate (after Adachi et al., 1992).

occur at several localities in the Mino Belt. They record episodic events such as mega-earthquakes and mega-storms in the provenance areas, which transported coarse materials to the trench by debris flows.

The conglomerate contains polymictic clasts in a poorly sorted, sandy matrix-supported fabric. The clasts are 1–30 cm diameter, rarely greater than 50 cm. The clast composition is shown in Fig. 34. Intrabasinal rocks such as sandstone, mudstone, siltstone, chert, and limestone are common, and exceptional but key rock species include granitic rocks (including granitic gneiss), orthoquartzite, and marl, which are not components of the Mino accretionary complexes. One of the granitic gneiss clasts yielded a Rb–Sr whole-rock isochron age of 2050 ± 30 Ma (Fig. 35), which is the oldest radiometric age in Japan.

STOP 6. Hisuikyo

GPS coordinates: 35° 32'20"N, 137° 7'34"E.

We will observe the chert sequences at Hisuikyo along the Hida River, where the sequence is similar to that in the Inuyama area. As the Triassic to Jurassic radiolarian and
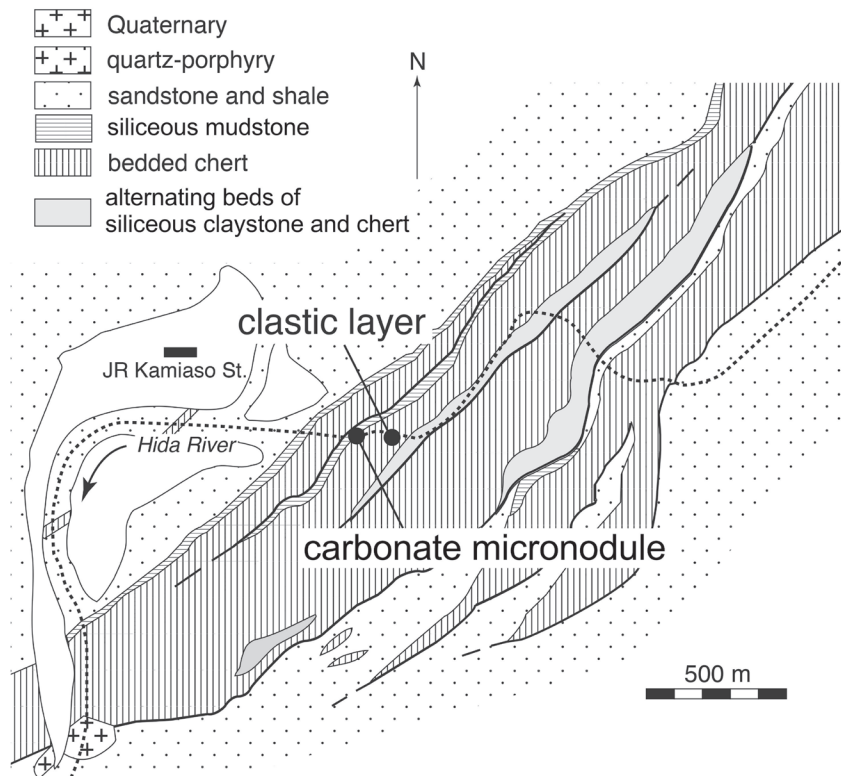
Fig. 36. Geologic map of the Hisuikyo area showing the locations of STOP 6-1 (clastic rock-bearing chert) and STOP 6-2 (manganese carbonate micronodule). Modified from Kido (1982).

conodont biostratigraphies of chert and siliceous mudstone were extensively examined along the Kiso River in the Inuyama area, we will concentrate on the clastic-rock-bearing chert formations and manganese carbonate micronodules at this stop (Fig. 36).

Stop 6-1: Clastic rock-bearing cherts

Chert in the Mino Belt is believed to be pelagic sedimentary rock, given that it lacks coarse clastic material. At some localities, however, the chert beds include clastic fragments such as chert, siliceous mudstone, volcanic rocks (probably basalt), polycrystalline quartz, plagioclase, dolomite, and glauconite (Kojima et al., 1999). In the lower part of the chert section there are 25 chert layers that contain clastic fragments (Fig. 37), although these are actually just 14 layers that have been folded and repeated (Fig. 38). Chert samples (JMP1379, 1380, 1412, and 1413: Fig. 38) yielded radiolarian fossils characteristic of the late Anisian to early Ladinian. The clastic-rock-bearing cherts, however, include both Triassic and Permian
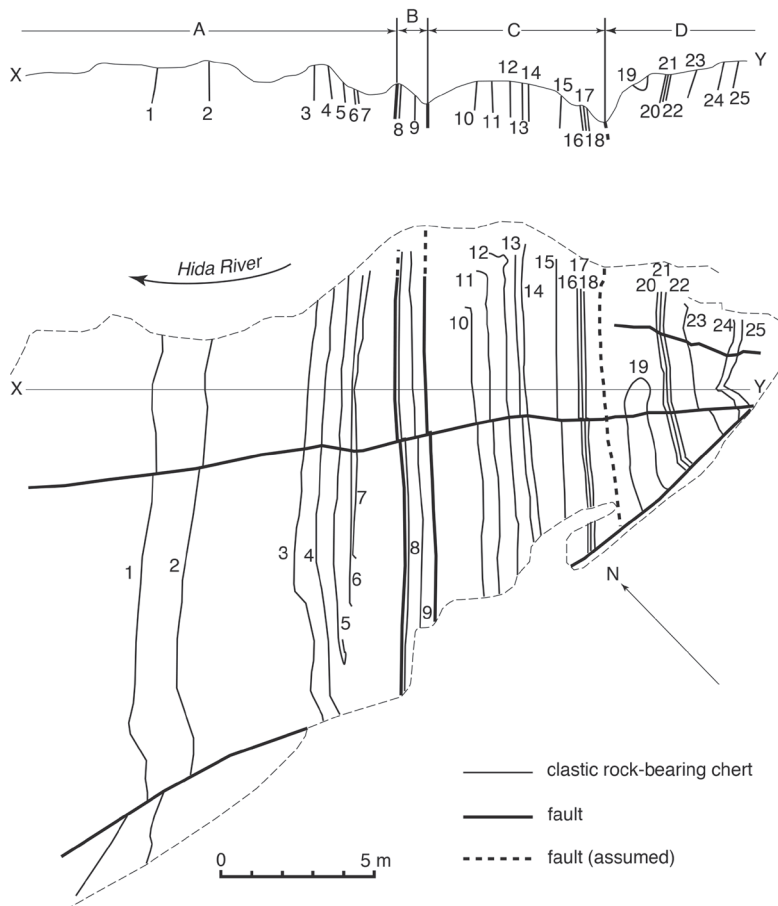
Fig. 37. Map showing occurrence of the clastic rocks-bearing chert in the Hisuikyo area (after Kojima et al., 1999).
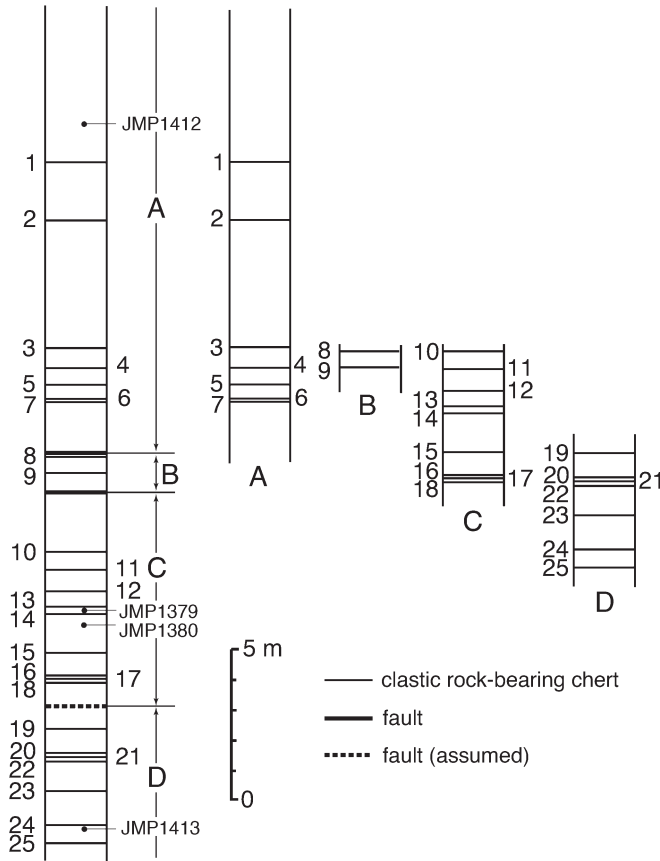
Fig. 38. Columnar sections showing repetition of chert formations in the Hisuikyo area. Left side column shows the apparent succession of the chert, and the other four columns show the correlation of the chert by using the clastic rock-bearing chert, and the numbers with JMP-prefix are horizons of biostratigraphically examined cherts (after Kojima et al., 1999).

— clastic rock-bearing chert
▬ fault
┈ fault (assumed)

Fig. 39. Occurrence of conodonts from the clastic rocks in chert of the Hisuikyo area (after Kojima et al., 1999).

conodonts (Fig. 39). Although it is difficult to estimate the provenance of the clastic fragments because of their wide variety and small grain size, Kojima et al. (1999) listed volcanic island, island arc, continental shelf, and older accretionary complexes as candidates.

Stop 6-2: Manganese carbonate micronodules

Manganese carbonate micronodules occur in a 10-cm-thick chert formation at the Hisuikyo locality (Figs. 36, 40). The nodules include well-preserved radiolarians, and Isozaki and Matsuda (1985) described new key species from the Early–Middle Jurassic: *Hsuum matsuokai, Laxtorum* (?) *hichisoense, Laxtorum* (?) *jurassicum*, and *Transhsuum hisuikyoense*

Fig. 40. Map showing the occurrence of manganese carbonate micronodules in the Hisuikyo section (after Isozaki and Matsuda, 1985).
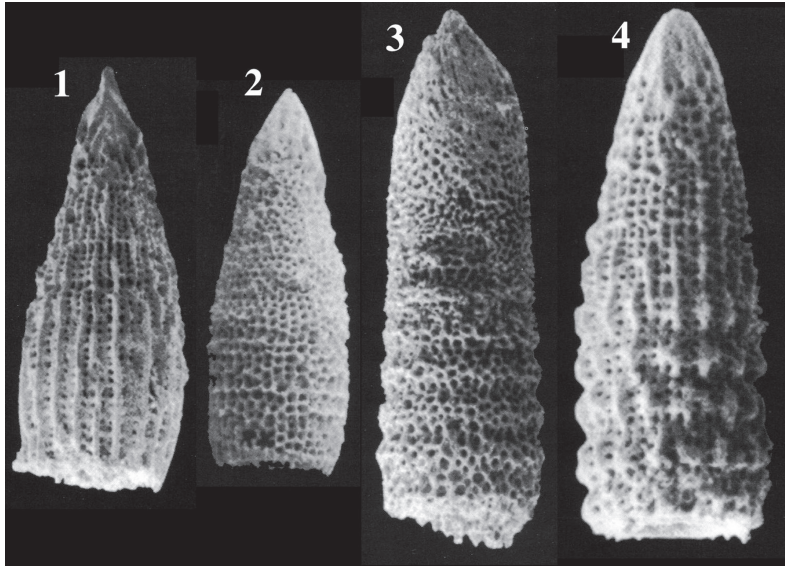
Fig. 41. Radiolarian fossils from the manganese carbonate micronodules in the Hisuikyo section (Reproduced from Isozaki and Matsuda, 1985). **1.** *Hsuum matsuokai*, **2.** *Laxtorum* (?) *hichisoense*, **3.** *Laxtorum* (?) *jurassicum*, **4.** *Transhsuum hisuikyoense*.

(Fig. 41). The micronodule-bearing chert occurs in the upper part of the chert section, and was assigned to the Late Pliensbachian to Bajocian? by Isozaki and Matsuda (1985) and to the Aalenian by Matsuoka (1995). Geochemical studies on the manganese carbonates in the Mino Belt (Sugisaki et al., 1991) suggest a hemipelagic depositional environment. The manganese carbonate nodules and layers always occur near the boundary between the chert and the overlying clastic rocks, and the interpretation by Sugisaki et al. (1991) is consistent with their stratigraphic position.

Concluding remarks

The Triassic–Jurassic chert sequences of the Mino Belt in the Inuyama–Kamiaso area, the Panthalassan pelagic sequences, are one of the most significant and complete records of their ocean environments. Many pioneer works in the 1980s and the early 1990s were shown in the excursion guidebook in previous InterRad held in Japan in 1994 (Matsuoka et al., 1994). Since the publication, further numerous study results have been accumulated, such as Early Triassic ocean anoxia and its recovery (Isozaki, 1997; Takahashi et al., 2009, 2013; Sato et al., 2011, 2012), Late Triassic Pluvial Event (Nakada et al., 2014), Late Triassic bolide impact and radiolarian faunal turnover (Onoue et al., 2012, 2016; Sato et al., 2016), and Triassic–Jurassic astronomical cycles with volcanism (Ikeda et al., 2010, 2015; Ikeda and Hori, 2014; Ikeda and Tada, 2014). We here show these results from the milestones in the

seminal stage to recent achievements on the cutting edge. We hope this excursion guidebook serves as a foundation and will encourage the further development of the studies in the Inuyama–Kamiaso area.

References

Abrajevitch, A., Hori, R. S. and Kodama, K., 2013, Rock magnetic record of the Triassic-Jurassic transition in pelagic bedded chert of the Inuyama section, Japan. *Geology*, **41**, 803–806.

Adachi, M., 1971, Permian intraformational conglomerate at Kamiaso, Gifu Prefecture, central Japan. *Jour. Geol. Soc. Japan*, **77**, 471–482.

Adachi, M., 1973, Pelitic and quartzo-feldspathic gneisses in the Kamiaso conglomerate - A study of Precambrian geology in Japan and East Asia. *Jour. Geol. Soc. Japan*, **79**, 181–203.

Adachi, M., Kojima, S., Wakita, K., Suzuki, K. and Tanaka, T., 1992, Transect of central Japan: from Hida to Shimanto. *29th IGC Field Trip Guide Book*, **1**, 143–178.

Ando, A., Kodama, K. and Kojima, S., 2001, Low-latitude and Southern Hemisphere origin of Anisian (Triassic) bedded chert in the Inuyama area, Mino terrane, central Japan. *Jour. Geophy. Res. Solid Earth*, **106**, 1973–1986.

Carter, E. S. and Hori, R. S., 2005, Global correlation of the radiolarian faunal change across the Triassic-Jurassic boundary. *Canad. Jour. Earth Sci.*, **42**, 777–790.

Carter, E. S., Gorican, S., Guex, J., O'Dogherty, L., De Wever, P., Dumitrica, P., Hori, R. S., Matsuoka, A. and Whalen, P. A., 2010, Global radiolarian zonation for the Pliensbachian, Toarcian and Aalenian. *Palaeogeogr. Palaeoclimat. Palaeoecol.*, **297**, 401–419.

Dal Corso, J., Mietto, P., Newton, R. J., Pancost, R. D., Preto, N., Roghi, G. and Wignall, P. B., 2012, Discovery of a major negative δ^{13}C spike in the Carnian (Late Triassic) linked to the eruption of Wrangellia flood basalts. *Geology*, **40**, 79–82.

Gröcke, D. R., Hori, R. S., Trabucho-Alexandre, J., Kemp, D. B. and Schwark, L., 2011, An open ocean record of the Toarcian oceanic anoxic event. *Solid Earth*, **2**, 245–257.

Hori, R., 1990, Lower Jurassic radiolarian zones of SW Japan. *Trans. Proc. Paleont. Soc. Japan. N. S.*, no. 159, 562–586.

Hori, R., 1992, Radiolarian biostratigraphy at the Triassic/Jurassic period boundary in bedded cherts from the Inuyama area, central Japan. *Jour. Geosci. Osaka City Univ.*, **35**, 53–65.

Hori, R. S., 1997, The Toarcian radiolarian event in bedded cherts from southwestern Japan. *Mar. Micropaleont.*, **30**, 159–169.

Hori, R. S., Cho, C.-F. and Umeda, H., 1993, Origin of cyclicity in Triassic-Jurassic radiolarian bedded cherts of the Mino accretionary complex from Japan. *Island Arc*, **3**, 170–180.

Hori, R. S., Kuroda, J., Ikehara, M. and Suzuki, K., 2016, Geochemical and Os isotopic studies on the pelagic Triassic-Jurassic mass extinction levels. *Goldschmidt Conference 2016 Yokohama Abstract*, 12i.

Ichikawa, K and Yao, A., 1976, Two new genera of Mesozoic cyrtoid radiolarians from Japan. *Spec. Publ., Progress Micropaleont.*, 110–117.

Igo, H. and Koike, T., 1975, Geological Age of the Kamiaso Conglomerate and New Occurrence of Triassic Conodonts in Mino Mountains. *Jour. Geol. Soc. Japan*, **81**, 197–198.

Ikeda, M., Tada, R. and Sakuma, H., 2010, Astronomical cycle origin of bedded chert: A middle Triassic bedded chert sequence, Inuyama, Japan. *Earth Planet. Sci. Lett.*, **297**, 369–378.

Ikeda, M. and Hori, R. S., 2014, Effects of Karoo–Ferrar volcanism and astronomical cycles on the Toarcian Oceanic Anoxic Events (Early Jurassic). *Palaeogeogr. Palaeoclimat. Palaeoecol.*, **440**, 725–733.

Ikeda, M. and Tada, R., 2014, A 70 million year astronomical time scale for the deep-sea bedded chert sequence (Inuyama, Japan): Implications for Triassic–Jurassic geochronology. *Earth Planet. Sci. Lett.*, **399**, 30–43.

Ikeda, M., Hori, R. S., Okada, Y. and Nakada, R., 2015, Volcanism and deep-ocean acidification across the end-

Triassic extinction event. *Palaeogeogr. Palaeoclimat. Palaeoecol.*, **440**, 725–733.

Imoto, N., 1984, Late Paleozoic and Mesozoic cherts in the Tamba Belt, Southwest Japan. Part 1. *Bull. Kyoto Univ. Educ. Ser. B*, **65**, 15–40.

Isozaki, Y., 1997, Permo-Triassic boundary superanixia and stratified superocean: Records from lost deep-sea. *Science*, **276**, 235–238.

Isozaki, Y., 2014, Memories of pre-Jurassic lost oceans: how to retrieve from extant lands. *Geoscience Canada*, **41**, 283–311.

Isozaki, Y. and Matsuda, T, 1982, Middle and Late Triassic conodonts from bedded chert sequences in the Mino-Tamba Belt, Southwest Japan. Part 1: *Epigondolella*. *Jour. Geosci. Osaka City Univ.*, **25**, 103–136.

Isozaki, Y. and Matsuda, T., 1983, Middle and Late Triassic conodonts from bedded chert sequences in the Mino-Tamba Belt, Southwest Japan. Part 2: *Misikella* and *Parvigondolella*. *Jour. Geosci. Osaka City Univ.*, **26**, 65–86.

Isozaki, Y. and Matsuda, T., 1985, Early Jurassic radiolarians from bedded chert in Kamiaso, Mino Belt, Central Japan. *Earth Sci. (Chikyu Kagaku)*, **39**, 429–442.

Ito, T., Zhang, L., Zhang, M.-H., Feng, Q.-L. and Matsuoka, A., 2017, *Guiuva sashidai* n. gen. n. sp., a probable colonial radiolaria from the Lopingian (Upper Permian) in South China. *Palaeoworld*, in press, http://dx.doi.org/10.1016/j.palwor.2017.04.001.

Kameda, J., Hina, S., Kobayashi, K., Yamaguchi, A., Hamada, Y., Yamamoto, Y., Hamahashi, M. and Kimura, G., 2012, Silica diagenesis and its effect on interplate seismicity in cold subduction zones. *Earth Planet. Sci. Lett.*, **317**, 136–144.

Kimura, K. and Hori, R., 1993, Offscraping Accretion of Jurassic Chert Clastic Complexes in the Mino-Tamba Belt, Central Japan. *Jour. Struct. Geol.*, **15**, 145–161.

Kido, S., Kawaguchi, I., Adachi, M. and Mizutani, S., 1982, On the *Dictyomitrella* (?) *kamoensis–Pantanellium foveatum* Assemblage in the Mino area, central Japan. *News Osaka Micropaleontol. Spec. Vol.*, no, 5, 195–210.

Koike, T., 1979, Biostratigraphy of Triassic conodonts. *Prof. Mosaburo Kanuma Mem. Vol.*, 21–77.

Kojima, S., Ando, H., Kida, M., Mizutani, S., Sakata, Y., Sugiyama, K. and Tsukamoto, H., 1999, Clastic rocks in Triassic bedded chert in the Mino terrane, central Japan: their petrographic properties and radiolarian ages. *Jour. Geol. Soc. Japan*, **105**, 421–434 (in Japanese with English abstract).

Kojima, S., Hayasaka, Y., Hiroi, Y., Matsuoka, A., Sano, H., Sugamori, Y., Suzuki, N., Takemura, S., Tsujimori, T. and Uchino, T., 2016, Pre-Cretaceous accretionary complexes. *In* Moreno, T., Wallis, S., Kojima, T. and Gibbons, W., eds., *The Geology of Japan*. Geological Society, London, 61–100.

Kozur, H., 2003, Integrated ammonoid, conodont and radiolarian zonation of the Triassic and some remarks to Stage/Substage subdivision and the numeric age of the Triassic stages. *Albertiana*, **28**, 57–74.

Kozur, H. and Mostler, H., 1994, Anisian to Middle Carnian radiolarian zonation and descrip- tion of some stratigraphically important radiolarians. *Geol. Paläont Mitt. Innsbruck*, **3**, 39–255.

Kubo, K., Isozaki, Y. and Matsuo, M., 1996, Color of bedded chert and redox condition of depositional environment: 57Fe Mössbauer spectroscopic study on chemical state of iron in Triassic deep-sea pelagic chert. *Jour. Geol. Soc. Japan*, **102**, 40–48 (in Japanese with English abstract).

Matsuda, T. and Isozaki, Y., 1991, Well-documented travel history of Mesozoic pelagic chert in Japan: from remote ocean to subduction zone. *Tectonics*, **10**, 475–499.

Matsuoka, A., 1995, Jurassic and Lower Cretaceous radiolarian zonation in Japan and in the western Pacific. *Island Arc*, **4**, 140–153.

Matsuoka, A., Hori, R., Kuwahara, K., Hiraishi, M., Yao, A. and Ezaki, Y., 1994, Triassic-Jurassic radiolarian-bearing sequences in the Mino terrane, central Japan. *Field trip guide book for the pre-conference excursion of INTERRAD VII, Osaka*, Organizing committee of INTERRAD VII, Osaka, 19–61.

Mizutani, S., 1959, Clastic plagioclase in Permian graywacke from the Mugi area, Gifu Prefecture, central Japan. *Jour. Earth Sci., Nagoya Univ.*, **7**, 108–136.

Mizutani, S. and Kido, S., 1983, Radiolarians in Middle Jurassic siliceous shale from Kamiaso, Gifu Prefecture, central Japan. *Trans. Proc. Palaeont. Soc. Japan, N. S.*, no. 132, 253–262.

Nakada, R., Ogawa, K., Suzuki, N., Takahashi, S. and Takahashi, Y., 2014, Late Triassic compositional changes of aeolian dusts in the pelagic Panthalassa: Response to the continental climatic change. *Palaeogeogr.*

Palaeoclimat. Palaeoecol., **393**, 61–75.

Nakae, S., 2000, Regional correlation of the Jurassic accretionary complex in the Inner Zone of Southwest Japan. *Mem. Geol. Soc. Japan*, no. 55, 73–98 (in Japanese with English abstract).

Nakao, K. and Isozaki, Y., 1994, Recovery history from the P/T boundary deep-sea anoxia recorded in pelagic chert in the Inuyama area, Mino Belt, Southwest Japan. *Jour. Geol. Soc. Japan*, **100**, 505–508.

Nakaseko, K. and Nishimura, A., 1979, Upper Triassic radiolaria from Southwest Japan. *Rep., Coll. Gen. Educ. Osaka Univ.*, **28**, 61–109.

Oda, H. and Suzuki, H., 2000, Paleomagnetism of Triassic and Jurassic red bedded chert of the Inuyama area, central Japan. *Jour. Geophys. Res.*, **105**, 25743–25767.

O'Dogherty, L., Carter, E. S., Gorican, S. and Dumitrica, P., 2010, Triassic radiolarian biostratigraphy. *In* Lucas, S.G., ed., *The Triassic Timescale*. Geol. Soc. London Spec. Publ., 163–200.

Ogg, J. G., 2012, Triassic. In Gradstein, F. M., Ogg, J., Schmitz, M. and Ogg, G., eds., *The Geologic Time Scale*. Elsevier, 681–730.

Okada, Y., Hori, R. S., Ikeda, M. and Ikehara, M., 2015, Geochemical study of Panthalassa deep-sea sedimentary rocks across the Triassic-Jurassic boundary. *News Osaka Micropaleontol. Spec. Vol.*, no. 15, 219–232 (in Japanese with English abstract).

Onoue, T., Sato, H., Nakamura, T., Noguchi, T., Hidaka, Y., Shirai, N., Ebihara, M., Osawa, T., Hatsukawa, Y., Toh, Y., Koizumi, M., Harada, H., Orchard, M.J. and Nedachi, M., 2012, Deep-sea record of impact apparently unrelated to mass extinction in the Late Triassic. *Proc. Nat. Acad. Sci. U.S.A.*, **109**, 19134–19139.

Onoue, T., Sato, H., Yamashita, D., Ikehara, M., Yasukawa, K., Fujinaga, K., Kato, Y. and Matsuoka, A., 2016, Bolide impact triggered the Late Triassic extinction event in equatorial Panthalassa. *Sci. Rep.*, **6**, doi: ARTN 2960910.1038/srep29609.

Payne, J. L., Lehrmann, D. J., Wei, J., Orchard, M. J., Schrag, D. P. and Knoll, A. H., 2004, Large Perturbations of the Carbon Cycle During Recovery from the End-Permian Extinction. *Science*, **305**, 506–509.

Rigo, M., Preto, N., Roghi, G., Tateo, F. and Mietto, P., 2007, A rise in the Carbonate Compensation Depth of western tethys in the Carnian (Late Triassic): Deep-water evidence for the Carnian pluvial event. *Palaeogeogr. Palaeoclimat. Palaeoecol.*, **246**, 188–205.

Sakuma, H., Tada, R., Ikeda, M., Kashiyama, Y., Ohkouchi, N., Ogawa, N.O., Watanabe, S., Tajika, E. and Yamamoto, S., 2012, High-resolution lithostratigraphy and organic carbon isotope stratigraphy of the Lower Triassic pelagic sequence in central Japan. *Island Arc*, **21**, 79–100.

Sano, H. and Kojima, S., 2000, Carboniferous to Jurassic oceanic rocks of Mino-Tamba-Ashio terrane, southwest Japan. *Mem. Geol. Soc. Japan*, no. 55, 123–144 (in Japanese with English abstract).

Sano, H., Kojima, S., Sato, H. and Rossana, M., 2013, *Guidebook for Field Excursion, Mino belt: Subduction-generated accretionary complex in central Japan, March 17-23, 2013*, Univ. Geneva, 121p., ISBN 978-2-940472-14-7.

Sano, H., Takano, A., Miyamoto, K. and Onoue, T., 2017, Depositional setting of the Upper Triassic siliceous micrite of the Mino-Tamba Belt. *Jour Geol. Soc. Japan*, **123**, 163–178 (in Japanese with English abstract)

Sato, T., Isozaki, Y., Shozugawa, K. and Matsuo, M., 2011, Fe-57 Mössbauer spectroscopic analysis of deep-sea pelagic chert: Effect of secondary alteration with respect to paleo-redox evaluation. *Jour. Asian Earth Sci.*, **42**, 1403–1410.

Sato, T., Isozaki, Y., Shozugawa, K., Seimiya, K., Matsuo, M., 2012, [57]Fe Mössbauer analysis of the Upper Triassic-Lower Jurassic deep-sea chert: Paleo-redox history across the Triassic-Jurassic boundary and the Toarcian oceanic anoxic event. *Hyperfine Interact*, **208**, 95–98.

Sato, H., Onoue, T., Nozaki, T. and Suzuki, K., 2013, Osmium isotope evidence for a large Late Triassic impact event. *Nature Commun.*, **4**, 2455, doi: 10.1038/ncomms3455.

Sato, H., Shirai, N., Ebihara, M., Onoue, T. and Kiyokawa, S., 2016, Sedimentary PGE signatures in the Late Triassic ejecta deposits from Japan: implications for the identification of impactor. *Palaeogeogr. Palaeoclimat. Palaeoecol.*, **442**, 36–47

Shibuya, H. and Sasajima, S., 1986, Paleomagnetism of red cherts: A case-study in the Inuyama area, central Japan. *Jour. Geophys. Res.*, **91**, 14105–14116.

Simms, M. J. and Ruffell, A. H., 1989, Synchroneity of climatic change and extinctions in the Late Triassic.

Geology, **17**, 265–268.

Simms, M. J. and Ruffell, A. H., 1990, Climatic and biotic change in the late Triassic. *Jour. Geol. Soc. London*, **147**, 321–327.

Sugisaki, R., Sugitani, K. and Adachi, M., 1991, Manganese carbonate bands as an indicator of hemipelagic sedimentary environments. *Jour. Geol.*, **99**, 23–40.

Sugiyama, K., 1992, Lower and Middle Triassic radiolarians from Mt. Kinkazan, Gifu Prefecture, Central Japan. *Trans. Proc. Palaeont. Soc. Japan, N. S.*, no. 167, 1180–1223.

Sugiyama, K., 1997, Triassic and Lower Jurassic radiolarian biostratigraphy in the siliceous claystone and bedded chert units of the southeastern Mino Terrane, Central Japan. *Bull. Mizunami Fossil Mus.*, no. 24, 79–193.

Suzuki, K., Adachi, M. and Tanaka, T., 1991, Middle Precambrian provenance of Jurassic sandstone in the Mino Terrane, central Japan: Th-U-total Pb evidence from an electron microprobe monazite study. *Sediment. Geol.*, **75**, 141–147.

Takahashi, S., Oba, M., Kaiho, K., Yamakita, S. and Sakata, S., 2009, Panthalassic oceanic anoxia at the end of the Early Triassic: A cause of delay in the recovery of life after the end-Permian mass extinction. *Palaeogeogr. Palaeoclimat. Palaeoecol.*, **274**, 185–195.

Takahashi, S., 2013, Palaeontological and geochemical studies on Permian–Triassic pelagic deep-sea sedimentary rocks. *Res. Org. Geochem.*, **29**, 1–16 (in Japanese with English abstract).

Takeuchi, M., 2000, Origin of Jurassic coarse clastic sediments in the Mino-Tanba Belt. *Mem. Geol. Soc. Japan*, no. 55, 107–121 (in Japanese with English abstract).

Takiguchi, T., Sugitani, K., Yamamoto, K. and Suzuki, K., 2006, Biogeochemical signatures preserved in ancient siliceous sediments; new perspectives to Triassic radiolarian bedded chert compositions. *Geochem. Jour.*, **40**, 33–45.

Tsukamoto, H., 1989, Lutecite in triassic bedded chert from the Southern Terrane, Central Japan. *Jour. Earth Sci. Nagoya Univ.*, **36**, 1–14.

Ujiie, K., Tabata, H., Kinoshita, T., Saito, T., Miyake, A. and Kouketsu, Y., 2015, Linkages between pelagic sedimentation and plate-boundary faulting. *Japan Geoscience Union Meeting 2015 Abstract*, SSS02-06.

Uno, K., Yamashita, D., Onoue, T. and Uehara, D., 2015, Paleomagnetism of Triassic bedded chert from Japan for determining the age of an impact ejecta layer deposited on peri-equatorial latitudes of the paleo-Pacific Ocean: A preliminary analysis. *Phys. Earth Planet. Int.*, **249**, 59–67.

Wakita, K., 1988, Origin of chaotically mixed rock bodies in the Early Jurassic to Early Cretaceous sedimentary complex of the Mino Terrane, central Japan. *Bull. Geol. Surv. Japan*, **39**, 675–757.

Wakita, K., Harayama, S., Kano, K., Mimura, K. and Sakamoto, T., 1992, *Geological map of Japan 1:200,000, Gifu.* Geol. Surv. Japan, 1 sheet.

Yamaguchi, A., Hina, S., Hamada, Y., Kameda, J., Hamahashi, M., Kuwatani, T., Shimizu, M. and Kimura, G., 2016, Source and sink of fluid in pelagic siliceous sediments along a cold subduction plate boundary. *Tectonophysics*, **686**, 146–157.

Yao, A., 1982, Middle Triassic to Early Jurassic radiolarians from the Inuyama area, central Japan. *Jour. Geosci. Osaka City Univ.*, **25**, 53–70.

Yao, A., Matsuda, T. and Isozaki, Y., 1980, Triassic and Jurassic radiolarians from the Inuyama area, central Japan. *Jour. Geosci. Osaka City Univ.*, **23**, 135–154.

Yao, A., Matsuoka, A. and Nakatani, T., 1982, Triassic and Jurassic radiolarian assemblages in Southwest Japan. *News Osaka Micropaleontol. Spec. Vol.*, no. 5, 27–43 (in Japanese with English abstract).

Yao, A. and Kuwahara, K., 1997, Radiolarian faunal change from Late Permian to Middle Triassic times. *News Osaka Micropaleontol. Spec. Vol.*, no. 10, 87–96 (in Japanese with English abstract).

Yoshida, H., 1986, Upper Triassic to Lower Jurassic radiolarian biostratigraphy in Kagamigahara City, Gifu Prefecture, central Japan. *Jour. Earth Sci. Nagoya Univ.*, **34**, 1–21.

Outline and history of the Itoigawa UNESCO Global Geopark in Niigata Prefecture in central Japan, with radiolarian occurrences in Itoigawa

Tsuyoshi ITO*, Yousuke IBARAKI** and Atsushi MATSUOKA***

Abstract

The Itoigawa UNESCO Global Geopark is located in Itoigawa City, Niigata Prefecture in central Japan. This geopark was approved as a Global Geopark in 2009, which is one of the first Global Geoparks in Japan. The Itoigawa–Shizuoka Tectonic Line, which divides the Japanese Islands into Southwest Japan and Northeast Japan in the Cenozoic tectonic framework, lies in the central part of the City of Itoigawa. Various rocks, ranging in age from the Cambrian to Quaternary, and cultural legacies can be observed in the 24 geosites in this geopark. Silurian, Permian, Triassic, and Jurassic radiolarians have been discovered from Itoigawa.

Key words: radiolaria, UNESCO Global Geopark, geosite, Fossa Magna Museum, Itoigawa, Niigata Prefecture

Introduction

According to the Global Geopark Network, "*UNESCO Global Geoparks are single, unified geographical areas where sites and landscapes of international geological significance are managed with a holistic concept of protection, education and sustainable development*" [URL1].

* Stratigraphy and Tectonics Research Group, Research Institute of Geology and Geoinformation, Geological Survey of Japan, AIST, Tsukuba 305-8567, Japan

** Fossa Magna Museum, Itoigawa 941-0056, Japan

*** Department of Geology, Faculty of Science, Niigata University, Niigata 950-2181, Japan
Corresponding author: T. Ito,
ito-t@aist.go.jp

Table 1. Timeline of the geopark work in Itoigawa since 1987.

Itoigawa	World	Event
1987		The "Fossa Magna Region Development Plan" designed
1989		"Itoigawa City Museum Plan" designed
		Construction of Itoigawa Geopark began under above policy
1990		Fossa Magana Park (Outcrop of fault) opened
1991		Geosites in the city called "Geopark"
1994		Fossa Magna Museum opened
1996		Omi Natural History Museum opened
2000		"Niigata Nippo Cultural Award" in recognition of finding two new minerals from Niigata Nippo (newspaper company)
	2000	European Geoparks Network founded
	2001	European Geoparks Network and UNESCO committed
2002		"Sakurai Award" in recognition of research on new mineral, itoigawaite, from Mineralogical Society of Japan
2003		"Geological Society of Japan Honorable Recognition" in recognition of conservation and education of important outcrops in Itoigawa
	2004	Global Geopark Network founded
2005		Itoigawa City, Nou Town, and Omi Town merged
	2007	Japanese Geopark Liaison Council founded
2007		Statement to aim to be Itoigawa Global Geopark expressed
2008		Seven areas (Itoigawa, Toya Caldera and Usu Volcano, Mt. Apoi, Minami Alps, San'in Kaigan, Muroto, Shimabara Peninsula) approved as Japanese Geopark
2009		Examination of Global Geopark
		Itoigawa Global Geopark approved
		Global Geoparks Network affiliated
		Official mascot characters "Geomaru" and "Nuna" designed
		Itoigawa and Hong Kong geoparks committed as friendship geoparks
2010		Conference of Japanese Geopark Network held at Itoigawa
2012		Re-approval of Japanese Geopark examined
2013		Itoigawa Japanese Geopark re-approved
		Re-approval of Global Geopark examined
		Itoigawa Global Geopark re-approved
2015		Itoigawa GeoStation GeoPal opened
		Fossa Magna Museum renewed
		Global Geopark program approved by UNESCO
2016		Geoparks Niigata International Forum held
2017		Re-aproval of UNESCO Global Geopark examined
		InterRad XV in Niigata held

The Global Geopark Network comprises 127 Geoparks in 35 Member States as of May 2017.

The Itoigawa UNESCO Global Geopark has been a current member of the Global Geopark Network since 2009 (Table 1), which is one of the first Global Geoparks in Japan. In fact, the Fossa Magna Park in Itoigawa was opened as a "Geopark" in 1990. The European Geopark Network was founded in 2000. Consequently, this "Geopark" in Itoigawa was the first use of the word in the world although they differed in meaning.

One of the main attractions of the Itoigawa UNESCO Global Geopark is the exposures of various rocks in a wide age range. Among them, Permian basement rocks have yielded radiolarians (e.g., Tazawa et al., 1984; Ujihara, 1985; Kawai and Takeuchi, 2001). Our research group, comprising Niigata University, Itoigawa City, and the Geological Survey of Japan, AIST, has mainly studied upper Mesozoic neritic strata and has reported the occurrences of Triassic and Jurassic radiolarians from clasts within the strata (Ito et al., 2012, 2014; Sakai et al., 2012). Recently, our research group discovered late Silurian radiolarian assemblages from a siliceous rock pebble of a float block of conglomerate (Ito et al., 2017a, 2017b).

This article introduces the geologic outline of Itoigawa and a brief history of the Itoigawa UNESCO Global Geopark, that is the first "Geopark" in the world. In addition, this article shows radiolarian occurrences in the previous studies in Itoigawa. Finally, we introduce briefly two geosites in the geopark. In the Itoigawa UNESCO Global Geopark, the word "geosite" is used to refer to a designated, thematic region of geological significance.

Geologic outline of Itoigawa

The Japanese Islands are located near the boundaries of four tectonic plates, Eurasian (Amur), North American (Okhotsk), Philippine Sea, and Pacific plates (Fig. 1). The Itoigawa–
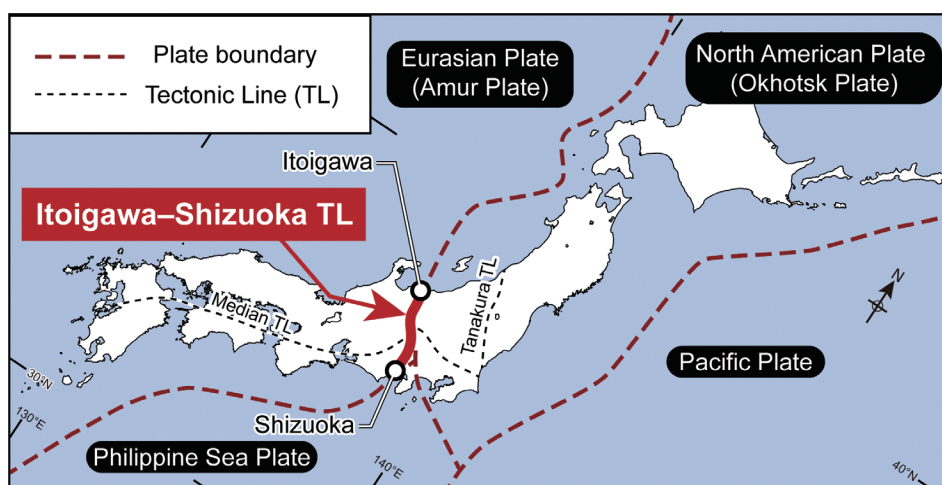
Fig. 1. Plate boundaries and major teconic lines of the Japanese Islands (based on Taira et al., 2016).
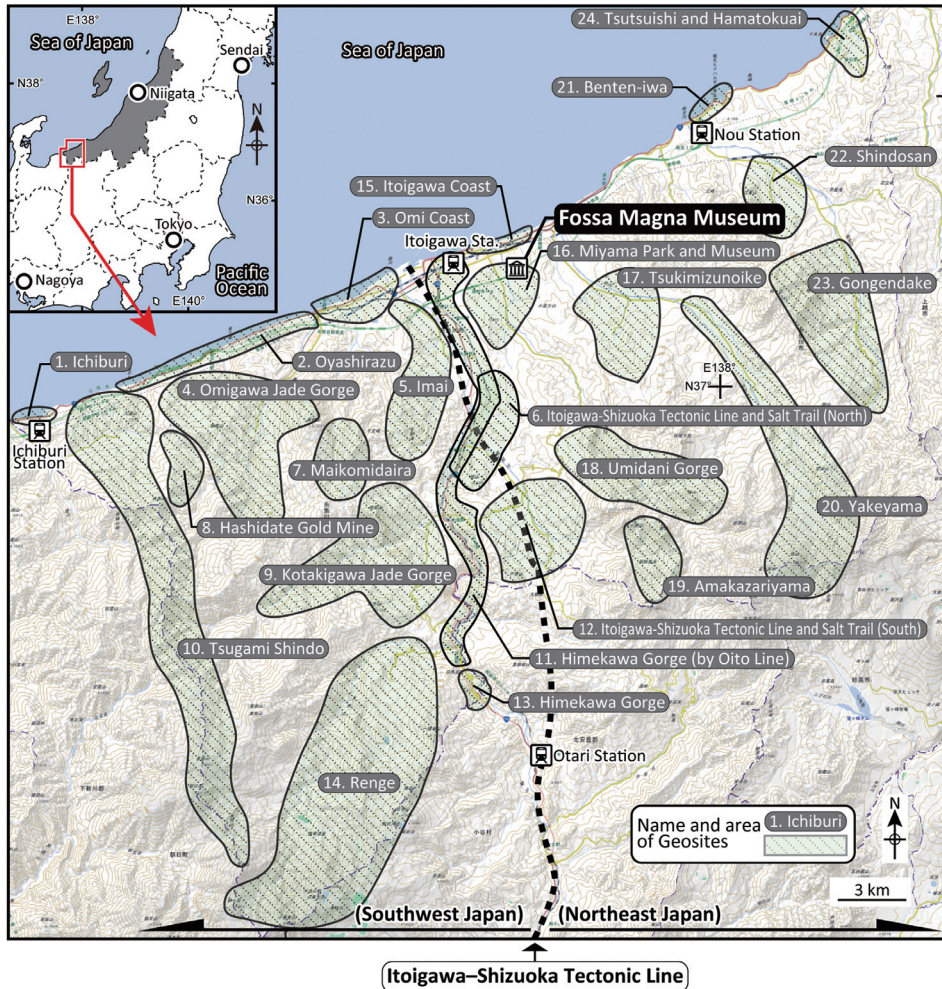
Fig. 2. Geosites in the Itoigawa UNESCO Global Geopark.

Shizuoka Tectonic Line, a massive fault line between the Eurasian and North American continental plates, lies in the central part of the City of Itoigawa. This tectonic line geologically divides the Japanese Islands into Southwest Japan and Northeast Japan in the Cenozoic tectonic framework (Fig. 2).

The City of Itoigawa, which borders the Sea of Japan, is located at the southwest end of Niigata Prefecture in central Japan. Various rocks are exposed in Itoigawa in spite of its small area (Fig. 3). This article follows the divisions of the geologic units, including their names and characters, shown by Nagamori et al. (2010) and Takeuchi et al. (2010, 2015a, 2015b). The Paleozoic and Mesozoic are mainly exposed in the west side of the Itoigawa–Shizuoka Tectonic Line whereas the Cenozoic is generally distributed over the east side of the line.

| Age | Stratigraphic divisions | Radiolarian occurrences |
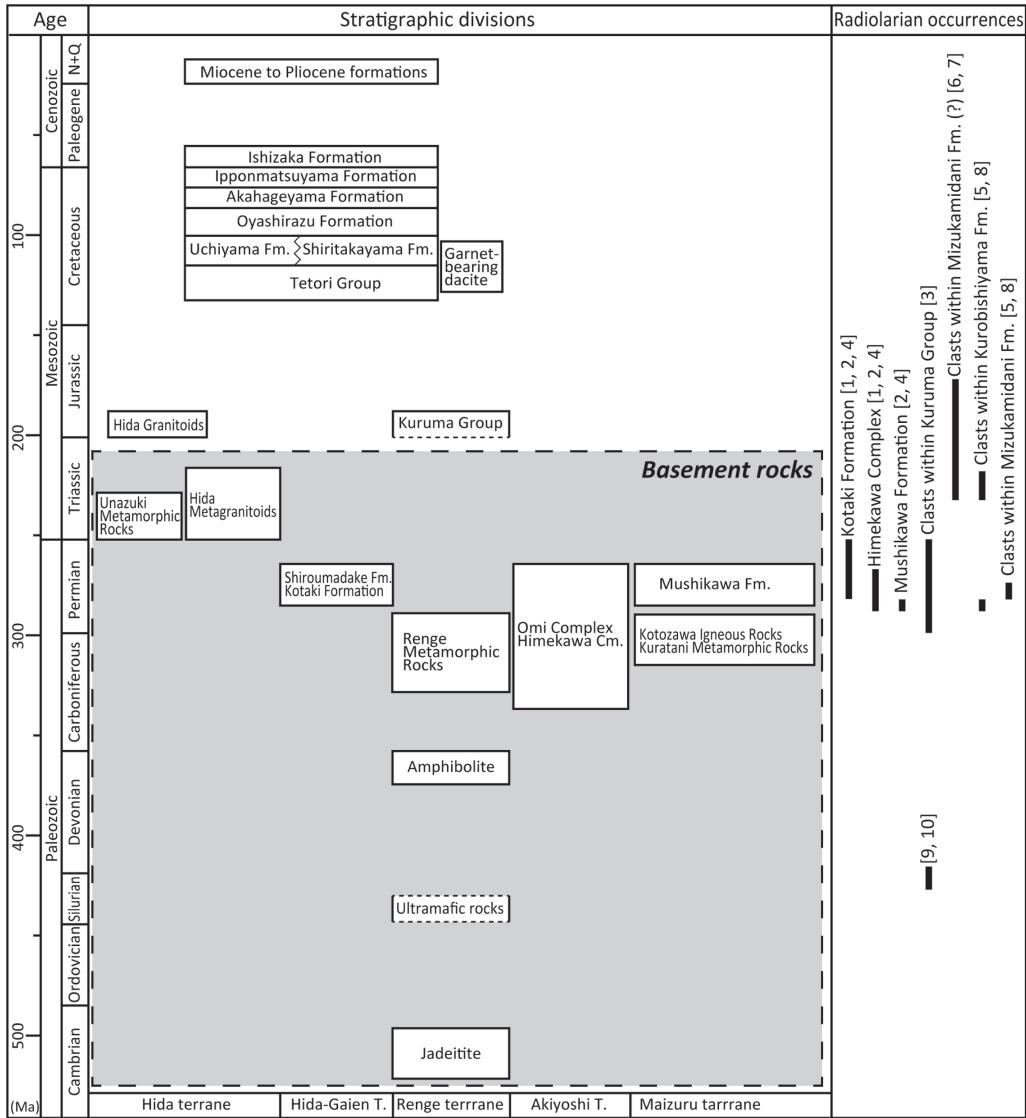
Fig. 3. Stratigraphic divisions of the Itoigawa (based on Nagamori et al., 2010; Takeuchi et al., 2010, 2015b), with previous radiolarian occurrences from tha area. Age is after Ogg et al. (2016). Quaternary deposits and the Quaternary Shirouma–Oike Volcano are omitted in this figure. Reference number: 1: Tazawa et al. (1984); 2: Ujihara (1985); 3: Kumazaki and Kojima (1996); 4: Kawai and Takeuchi (2001); 5: Tomita et al. (2007); 6: Ito et al. (2012); 7: Ito et al. (2014); 8: Takeuchi et al. (2015b); 9: Ito et al. (2017a); 10: Ito et al. (2017b).

1. Paleozoic

The Paleozoic is exposed mainly in the west part of Itoigawa. The Paleozoic in Itoigawa consists mainly of the following geologic terranes: Renge, Akiyoshi, Maizuru, and Hida-Gaien terranes.

The Renge terrane is composed mainly of the Carboniferous Renge Metamorphic Rocks, such as garnet amphibole schist, garnet biotite schist, chlorite schists, and muscovite schist,

and Ordovician–Carboniferous amphibolite. Ultramafic rocks, of which age is unknown, consist of serpentinite and peridotite. In some areas, serpentinite mélanges include exotic blocks of amphibolite, jadeitite, and the Renge Metamorphic Rocks.

The Akiyoshi terrane in Itoigawa comprises the Carboniferous–Permian Omi Complex (Nagamori et al., 2010) and the Permian Himekawa Complex (Kawai and Takeuchi, 2001; redefined by Nagamori et al., 2010). The former complex consists of limestones and basalts, while the latter complex shows the repetition of chert–clastic sequences.

The Permian Maizuru terrane is composed of the Kuratani Metamorphic Rocks (Nagamori et al., 2010), the Kotozawa Igneous Rocks (Nagamori et al., 2010), and the Mushikawa Formation (Ujihara, 1985; redefined by Nagamori et al., 2010). The Mushikawa Formation consists of clastics, such as mudstones, sandstones, and breccias.

The Hida-Gaien terrane is composed of the Permian Shiroumadake and Kotaki formations. The Shiroumadake Formation (Takeuchi et al., 2001; redefined by Takeuchi et al., 2004) in Itoigawa consists of felsic tuffs and felsic tuff breccias whereas the Kotaki Formation (Nagamori et al., 2010) is characterized by greenstones, sandstones, mudstones, felsic tuffs, and cherts.

2. Mesozoic

The Mesozoic is exposed mainly in the west part of Itoigawa and comprises mainly Lower Jurassic marine–terrestrial deposits, Cretaceous terrestrial deposits, and Upper Cretaceous volcanic and intrusive rocks.

The Lower Jurassic Kuruma Group (Kobayashi et al., 1957) in Itoigawa, which overlies the Renge Metamorphic Rocks and the ultramafic rocks, comprises the Gamaharazawa, Odokorogawa and Yoshinazawa formations (Shiraishi, 1992), in ascending order. This group consists mainly of clastic rocks, such as mudstones, sandstones, and conglomerates, with tuffs.

The Lower Cretaceous Tetori Group (Oishi, 1933) in Itoigawa comprises the Mizukamidani Formation (Kobayashi et al., 1957; redefined by Takeuchi et al., 2015a) and the Kurobishiyama Formation (Takeuchi et al., 2015a), in ascending order. The former consists mainly of conglomerates, sandstones, and mudstones, while the latter is composed of sandstones and conglomerates. The Mizukamidani Formation had been considered to belong to the Kuruma Group (Kobayashi et al., 1957); however, recent studies considered that it belongs to the Tetori Group (Chihara et al., 1979; Sakai et al., 2012; Takeuchi et al., 2015a, 2015b).

The middle Cretaceous Uchiyama Formation (Takeuchi et al., 2015a) consists of conglomerates and sandstones including andesite, rhyolitic pyroclastic rock, and lava. The middle Cretaceous Shiritakayama Formation (Yoshimura and Adachi, 1976; redefined by Takeuchi et al., 2015a) consists mainly of coarser sandstones including granules and pebbles.

The Uchiyama and Shiritakayama formations are contemporaneous heterotopic facies (Takeuchi et al., 2015a). The Cretaceous Oyashirazu Formation (Chihara, 1955; redefined by Takeuchi et al., 2015a) consists mainly of andesitic tuff breccia. This formation overlies conformably the Uchiyama and Shiritakayama formations. The Cretaceous Akahageyama Formation (Chihara et al., 1979), which covers the Mushikawa Formation, consists mainly of clastic rocks and tuffs. The Upper Cretaceous Ipponmatsuyama Formation (Chihara et al., 1979; redefined by Shiraishi, 1992) consists of andesitic and dacitic tuff breccias.

3. Cenozoic

The Cenozoic is exposed mainly in the east part of Itoigawa. The Cenozoic in Itoigawa consists mainly of Neogene marine–terrestrial deposits and Pleistocene intrusive rocks. As mentioned previously, the Itoigawa–Shizuoka Tectonic Line, geologically dividing the Japanese Islands into Southwest Japan and Northeast Japan in the Cenozoic tectonic framework, lies in central Itoigawa.

The Paleogene Ishizaka Formation (Tomizawa and Kitahara, 1967; redefined by Ishii, 1976) is composed mainly of lapilli tuffs with rhyolite lava and basal conglomerates. This formation overlies unconformably the Ipponmatsuyama Formation and the Paleozoic.

The Miocene to Pliocene formations (e.g., Tokurayama, Yamamoto, Imai, Senno-zawa, Nechi, Umikawa, Tanne, and Atosugiyama formations) are distributed over the north part of the Itoigawa area (Nagamori et al., 2010). These formations consist mainly of pyroclastics and clastics.

Quaternary stratovolcanos are present in Itoigawa. The Shirouma–Oike Volcano and the Yakeyama Volcano are located in the southwest and southeast parts in Itoigawa,
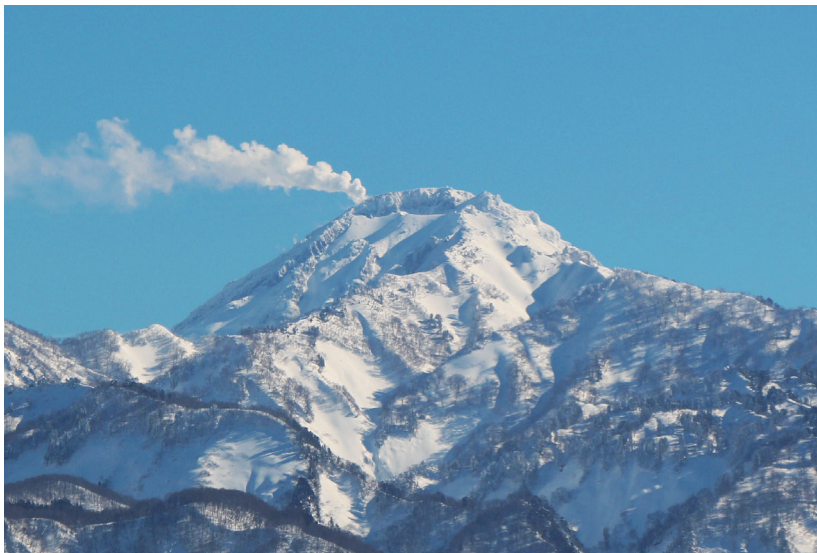
Fig. 4. Volcanic fume of the Yakeyama Volcano, photographed at January 1st 2016.

respectively. Both volcanos consist mainly of andesite and dacite lavas and pyroclastics. The Yakeyama Volcano is an active volcano and its first volcanic activity started ca. 3,000 years ago (Hayatsu, 1994). In recent years, the Yakeyama Volcano fumes constantly (Fig. 4) and the small-scale eruption was observed in July 2016. Quaternary deposits, such as terrace deposits and roams, cover the older geologic units.

Radiolarian occurrences from Itoigawa

Since Tazawa et al. (1984) discovered Permian radiolarians, some researchers have reported radiolarian occurrences from Itoigawa. Paleozoic and Mesozoic radiolarian occurrences from Itoigawa are summarized in Fig. 3 and described below.

1. Permian radiolarians from siliceous and argillaceous strata

Permian radiolarians occurred in siliceous and argillaceous strata in several geologic units in the Japanese Islands, such as the Akiyoshi terrane (e.g., Sano et al., 1987; Ito and Matsuoka, 2015a, 2016), Maizuru terrane (e.g., Nishimura and Ishiga, 1987), Hida-Gaien terrane (Niko et al., 1987; Umeda and Ezaki, 1997), Ultra-Tamba terrane (e.g., Sugamori, 2011), Tamba–Mino–Ashio terrane (e.g., Ishiga and Imoto, 1980; Kuwahara, 1997), and Chichibu composite terrane (e.g., Kuwahara, 1992; Ito and Matsuoka, 2015b). Likewise, the Kotaki Formation (Hida-Gaien terrane), Mushikawa Formation (Maizuru terrane), and Himekawa Complex (Akiyoshi terrane) in Itoigawa yielded Permian radiolarians (Tazawa et al., 1984; Ujihara, 1985; Kawai and Takeuchi, 2001).

Pseudoalbaillella sp. aff. *P. longicornis* Ishiga and Imoto occurred in mudstone of the Kotaki Formation of the Hida-Gaien terrane (Tazawa et al., 1984). The specimen shown by Tazawa et al. (1984) resembles the short form of *Pseudoalbaillella fusiformis* (Holdsworth and Jones) sensu Ito et al. (2015a). *Pseudoalbaillella fusiformis* occurred generally in the upper Cisuralian (lower Permian) to the Guadalupian (middle Permian) (e.g., Ishiga, 1990; Zhang et al., 2010; Wang and Yang, 2011; Ito et al., 2015a).

Ujihara (1985) discovered *Pseudotormentus* sp. from siliceous mudstone of the Kotaki Formation. Although Schwartzapfel and Holdsworth (1996) described *Pseudotormentus delawarensis* Schwartzapfel and Holdsworth obtained from the upper Mississippian (Lower Carboniferous), *Pseudotormentus* occurred generally in all of the Permian (Ito et al., 2016). Kawai and Takeuchi (2001) reported occurrence of *Follicucullus* sp. from chert and siliceous mudstone of the Kotaki Formation. *Follicucullus* occurred generally in the Lopingian (Upper Permian) (e.g., Ishiga, 1990; Zhang et al., 2014).

Kawai and Takeuchi (2001) discovered *Pseudotormentus* sp. from cherts of the Himekawa Complex (Akiyoshi terrane), *Pseudoalbaillella fusiformis*, *F. porrectus*, and *Pseudoalbaillella monacanthus* from siliceous mudstones of the complex, and *Albaillella asymmetrica* Ishiga

and Imoto from siliceous mudstone containing manganese carbonate spherules of the complex. *Pseudoalbaillella fusiformis*, *Pseudoalbaillella* sp. cf. *P. globosa* Ishiga and Imoto, *F. porrectus* Rudenko (originally described as *F. scholasticus* Ormiston and Babcock), and *Pseudoalbaillella monacantha* (Ishiga and Imoto) occurred in siliceous mudstones of the complex (Tazawa et al., 1984). The co-occurrence range of *Pseudoalbaillella fusiformis*, *Pseudoalbaillella monacantha*, and *F. porrectus* is restricted to the *F. porrectus* Interval Zone of the lower Capitanian, Guadalupian according to Zhang et al. (2014). The range of *A. asymmetrica* is restricted to the Kungurian of the Cisuralian according to Zhang et al. (2010).

　　Albaillella asymmetrica, Pseudoalbaillella fusiformis, and *Pseudoalbaillella longtanensis* Sheng and Wang occurred in mudstones of the Mushikawa Formation of the Maizuru terrane (Ujihara, 1985; Kawai and Takeuchi, 2001). These species co-occurred in the *P. longtanensis* Assemblage Zone of Ishiga (1990), corresponding to the Kungurian Age of the Cisuralian Epoch.

2. Permian–Jurassic radiolarians from clasts within the Mesozoic non-marine strata

　　Mesozoic non-marine strata in the Japanese Islands contain radiolarian-bearing clasts within conglomerate (e.g., Ishida et al., 2003; Ito et al., 2017c). Most previous studies have reported Permian–Jurassic radiolarian-bearing clasts within the Mesozoic in the Hokuriku region in central Japan (e.g., Saida, 1987; Takeuchi et al., 1991; Ito et al., 2015b). Siliceous and argillaceous rock clasts within the Kuruma Group and Mizukamidani (?) Formation in Itoigawa yielded Permian, Triassic, and Jurassic radiolarians (Kumazaki and Kojima, 1996; Tomita et al., 2007; Ito et al., 2012, 2014).

　　Kumazaki and Kojima (1996) reported *Pseudoalbaillella* sp. and *Pseudotormentus*? sp. occurred in siliceous mudstone clasts within conglomerates of the lower part of the Gamaharazawa Formation of the Kuruma Group. They however did not show their images. *Pseudoalbaillella* occurred in the Upper Carboniferous (Pennsylvanian) to the lower Permian (e.g., Holdsworth and Jones, 1980; Nazarov and Ormiston, 1986); *Pseudotormentus* occurred in the Permian (Ito et al., 2016).

　　Tomita et al. (2007) reported the occurrences of Permian and Triassic radiolarians, such as *Pseudoalbaillella* sp. cf. *P. fusiformis* and *Pseudostylosphaera japonica* Nakaseko and Nishimura, from chert clasts within the Lower Cretaceous Kurobishiyama Formation. Although Tomita et al. (2007) showed no radiolarian images, Takeuchi et al. (2015b) provided the images.

　　Follicucullus porrectus and *Pseudoalbaillella* sp. cf. *P. fusiformis* were discovered from mudstone clasts within the Lower Cretaceous Mizukamidani Formation (Tomita et al., 2007; Takeuchi et al., 2015b). These species occurred in the Guadalupian to Lopingian of the Permian (Zhang et al., 2014; Ito et al., 2015a).

　　Ito et al. (2012) found Middle to Late Triassic (Figs. 5.2, 6.5, 6.6) and Jurassic radiolarians
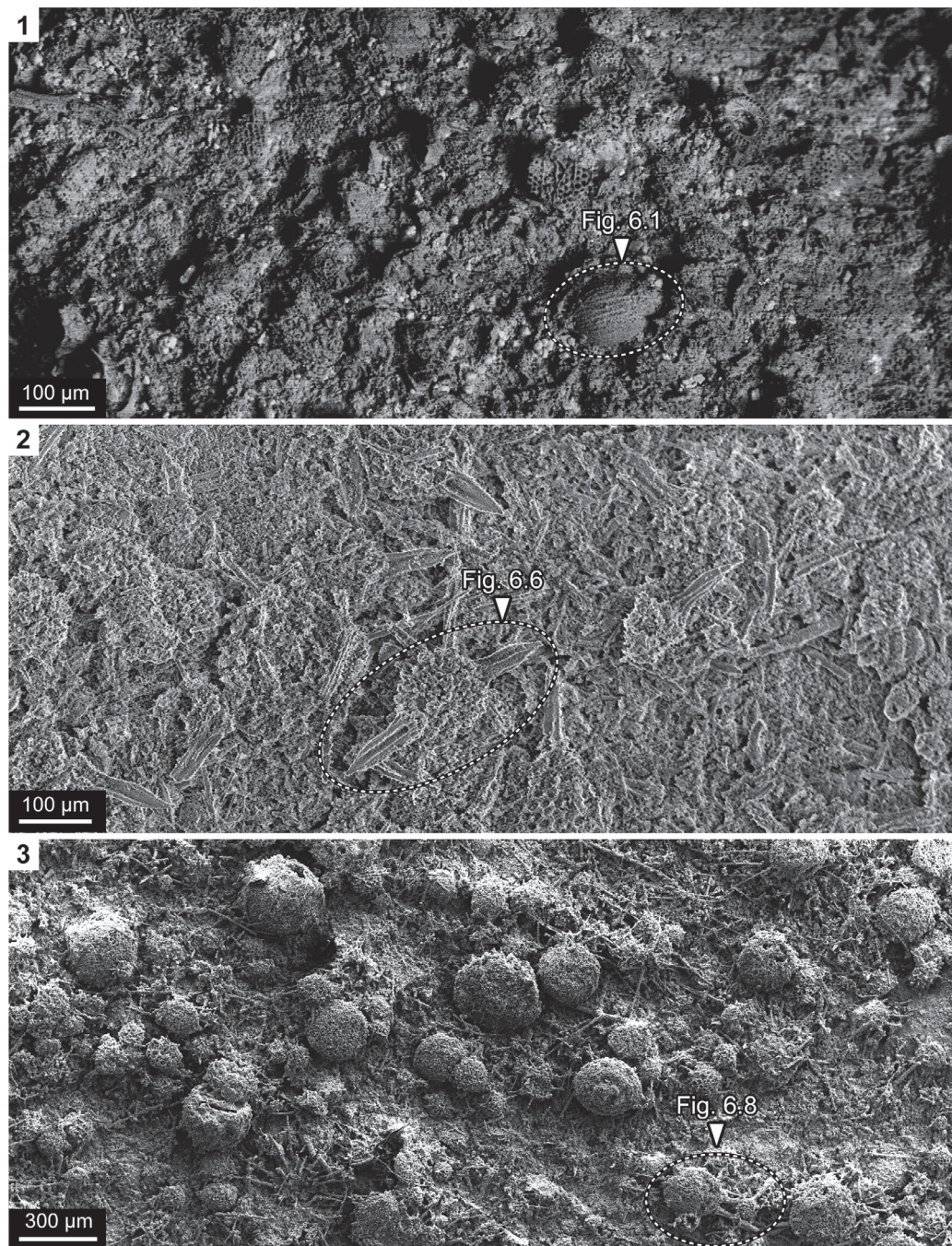
Fig. 5. Scanning electron microscope (SEM) images of the etched surfaces of pebbles within conglomerates in the Itoigawa area. **1:** Siliceous mudstone (IT12050102-1) from the Mizukamidani Formation (?) in Ichiburi; **2:** Chert (IT10050201-1) from the Mizukamidani Formation (?) in Ichiburi; **3:** Radiolarite (IY-FMM-K2) from float block in Kotaki.
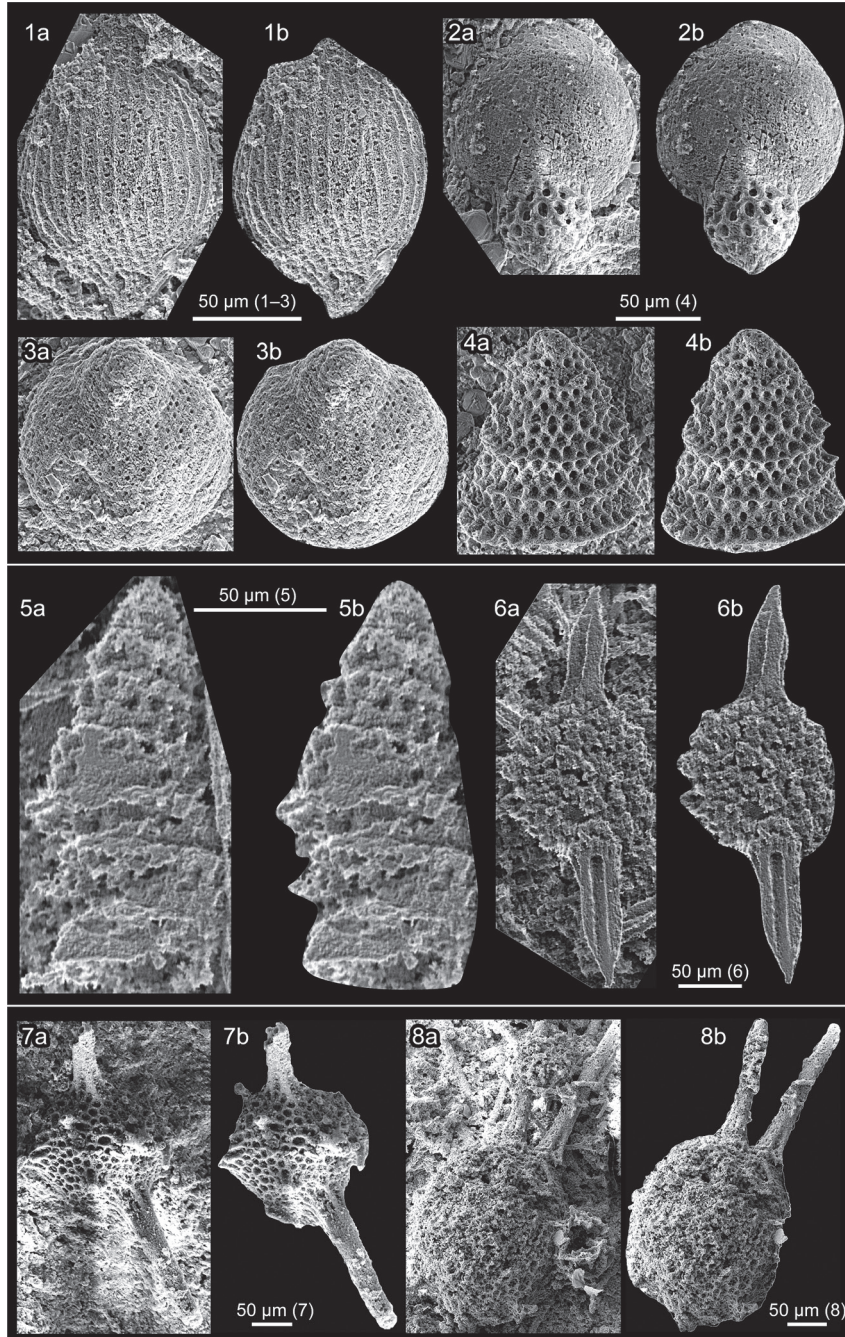
Fig. 6. Scanning electron microscope (SEM) images of radiolarians on etched surfaces (a) and trimmed images (b) from pebbles within conglomerates in the Itoigawa area. **1:** *Striatojaponocapsa plicarum* (Yao); **2:** *Cyrtocapsa mastoidea* Yao; **3:** closed nassellaria; **4:** *Parvicingula* sp.; **5:** multi-segmented Nassellaria; **6:** *Pseudostylosphaera* sp. cf. *P. japonica* Nakaseko and Nishimura; **7:** *Futobari morishitai* Furutani; **8:** Inaniguttidae gen. et sp. indet. 1–4: Siliceous mudstone (IT12050102-1) from the Mizukamidani Formation (?) in Ichiburi; 5, 6: Chert (IT10050201-1) from the Mizukamidani Formation (?) in Ichiburi; 7, 8: Radiolarite (IY-FMM-K2) from float block in Kotaki.

from chert clasts within conglomerates of sections exposed in the right bank of the Sakai River. Ito et al. (2014) obtained Bajocian to early Bathonian (Middle Jurassic) radiolarians (Figs. 5.1, 6.1–6.4) from siliceous mudstone clasts within the conglomerate of the same sections. Ito et al. (2012, 2014) assigned the conglomerate to the Mizukamidani Formation. Takeuchi et al. (2015a) however designated the sections as the type locality of the Shiritakayama Formation.

3. Silurian–Devonian radiolarians from a radiolarite clast within conglomerate of a float block

Ito et al. (2017a, 2017b) recently discovered a radiolarian assemblage from a radiolarite rock pebble of a float block of conglomerate, which was collected in the banks of the Kotaki River in the Kotaki area, Itoigawa. *Futobari morishitai* Furutani, Inaniguttidae gen. et sp. indet., and Palaeoscenidiidae gen. et sp. indet. were recognized on etched surfaces of the pebble (Figs. 5.3, 6.7, 6.8), whereas *Pseudospongoprunum* sp., *Zadrappolus* sp., and *Rotasphaera* sp. were discovered in residues obtained by chemically treating the conglomerate.

The former assemblage can be compared to that of the *Futobari solidus–Zadrappolus tenuis* Assemblage Zone of Kurihara (2004, 2007). The latter assemblage can be compared to that of the *Pseudospongoprunum tauversi* Assemblage Zone of Kurihara (2004, 2007). According to the U–Pb zircon dating by Manchuk et al. (2013), the age around the boundary between the *P. tauversi* and *F. solidus–Z. tenuis* assemblage zones is Ludlow to Pridoli (late Silurian).

The discovery was the first occurrence report of Silurian radiolarians in Niigata Prefecture, which was also the oldest fossil record in the prefecture. Additionally, the clasts are also one of the oldest radiolarian-bearing clasts within conglomerates of the Japanese Islands.

Stops in geosites

Twenty-four geosites are designated in the Itoigawa UNESCO Global Geopark (Fig. 1). These geosites deal with several themes ranging from geology to culture (Table 2). The City of Itoigawa is planning to publish pamphlets of all geosites. Among them, 21 geosites' pamphlets are currently published. They can be downloaded via the official webpage of the geopark [URL2]. In this section, we introduce outlines of two stops in the Geosite Nos. 9 and 16. Detailed explanations are shown in each pamphlet.

STOP 1. Kotakigawa Jade Gorge and Mt. Myojo (in Geosite No. 9)

The Kotakigawa Jade Gorge is located along the Kotaki River flowing along the south

Table 2. Geosites of the Itoigawa UNESCO Global Geopark and their themes .

No.	Name	Theme	Atractions
1	Ichiburi	Jade and Jurassic Fossils	Ichiburi Coast; Kikyoya Inn Site; Tamanoki Landslide; Ichiburi Customs Gate and Hackberry Tree; Jurassic fossils
2	Oyashirazu	A Cliff becomes a Highway	Tenken Oyashirazu; Oyashirazu Community Road; Katsuyama Fort Site; Letters on the Cliff; The Start of the Tsugami Shindo Trail
3	Omi Coast	Jomon Culture and Jade Coast	Omi Coast; Teraji Archeological Site; Lavender Beach; Suzawa Seaside Park and Omi Seaside Park; Salt Trail (Western Route)
4	Omigawa Jade Gorge	Geological Phenomena in the Depth of the Earth	Omigawa Jade Gorge; Albitite Boulders and New Minerals; Crystalline Schist Formations
5	Imai	Rocks and Formations Created alongside Fossa Magna	Fudotaki Falls; Mushikawa Customs Gate; Salt Trail (West Route); Suzawa Swamp Lanterns; Imai Mine Site; Yatsuroishi Quarry Site
6	Itoigawa–Shizuoka Tectonic Line and Salt Trail (North)	An Ancient Trail along a Gigantic Fault	Exposed Fault of the Itoigawa-Shizuoka Tectonic Line; Salt Trail (Matsumoto Highway); Pillow Lava; Utou
7	Maikomidaira	Karst Topography and Alpine Plants	Senrido Cave; Maikomidaira; Mt. Kurohimeyama; Byakurendo Cave
8	Hashidate Gold Mine	Remains of Itoigawa's Largest Gold Mine	Remains of the Gold Mine Office; Millstone used to crush ore; Sakata Toge Pass
9	Kotakigawa Jade Gorge	Jade Boulders and the Great Rock Face of Mt. Myojo	Mt. Myojo; Kotakigawa Jade Gorge; Takanami-no-ike Pond; Jade Gorge Fishing Park; Great Limestone Face
10	Tsugami Shindo	From Coast to Peak, 3,000 Vertical Meters of Geo Trail	Mt. Korenge; Mt. Yukikuradake; Mt. Asahidake; Alpine Plants; Jurassic Fossils
11	Himekawa Gorge via Oito Line	Geotourism via the Oito Line	Itoigawa Station; Himekawa Station; Kubiki Ono Station; Nechi Station; Kotaki Station; Hiraiwa Station
12	Itoigawa–Shizuoka Tectonic Line and Salt Trail (South)	An Ancient Trail along a Gigantic Fault	Salt Trail; Shiroike Pond; Mt. Tokurayama; Interbeds of sandstone and mudstone; Salt Trail Museum; Bokkajaya Tea House and Shionomichi Hot Spring
13	Himekawa Gorge	Erosion and Denudation of Giant Mountains	Collapsed geology (colluvium) at Kuzuha Pass; Bokka Horse Chestnut—Once an important landmark for travelers; Himekawa River; Cenotaph for the Debris Flow Disaster
14	Renge	Volcanic Fumaroles and Glacial Wetlands	Heimanotaira Wetlands; Renge Onsen Outdoor Hot Springs; Shiraike Pond; Former Site of Renge Mine
15	Itoigawa Coast	Vanished Sand Dunes and the Jade Coast	Itoigawa Coast (Jade Coast); Sea of Japan Sunset Lookout; Souma Gyofu House; Itoigawa Museum of History and Folklore; Tanimura Art Museum and Gyokusuien Garden; Amatsu Shrine
16	Miyama Park and Museum	Geopark Information Center	Miyama Park; Poetic Monument of Gyofu Soma; Fossa Magna Museum; Chojagahara Archeological Museum and Chojagahara Archeological Site; Observation Tower
17	Tsukimizunoike	Landslides, Terraced Rice Fields and Stone Images of Buddha	88 Stone Buddha Pilgrimage; The Yamaguchi House - A Historic Snow Country Residence; Tsukimizu-no-ike Pond; Nikkoji Temple; Former Site of Fudoyama Castle; Terraced Rice Fields
18	Umidani Gorge	Scenic Highlands and a Large Cross Section of Submarine Volcano	Umidani Highland; Umidani Sankyo Park; Cliff of Mt. Senjogatake; Mt. Hachiyama; Mt. Komagatake
19	Amakazariyama	One of the 100 Famous Mountains of Japan—Beloved by Climbers	Mt. Amakazariyama; Sasadaira; Amakazari Lodge and Amakazari Hot Spring
20	Yakeyama	Hot Springs and Disaster Prevention beneath an Active Volcano	Mt. Yakeyama; Erosion Control Dam; Carbonized Trees at Kamihayakawa Elementary School; Standing Beech Trees
21	Benten-iwa	Maritime Culture Fostered by Submarine Volcanoes	Benten-iwa; Hakusan Shrine; Tottoko-iwa; Site of the Kodomari Landslide; Road Station "Marine Dream Nou"
22	Shindosan	Submarine Volcanoes and Traditional Farmland Scenery	88 Stone Steps of Mt. Shindosan; Beech Forest; Mt. Hokogatake; Shindosan Park; Sacred Birthplace of Princess Nunakawa
23	Gongendake	Curious Area of Deformation in the Mountains	Mt. Gongendake; Avalanche Protection Fences; Avalanche Trenches; Maseguchi Hot Springs District; Commemorative monument of the 1986 Maseguchi Avalanche
24	Tsutsuishi Hamatokuai	Beautiful Stratification and Traditional Fishing Villages	Interbeds of sandstone and mudstone; Tsutsuishi Station; Weeping Cherry Tree Road; Tsutsuishi Fishing Port
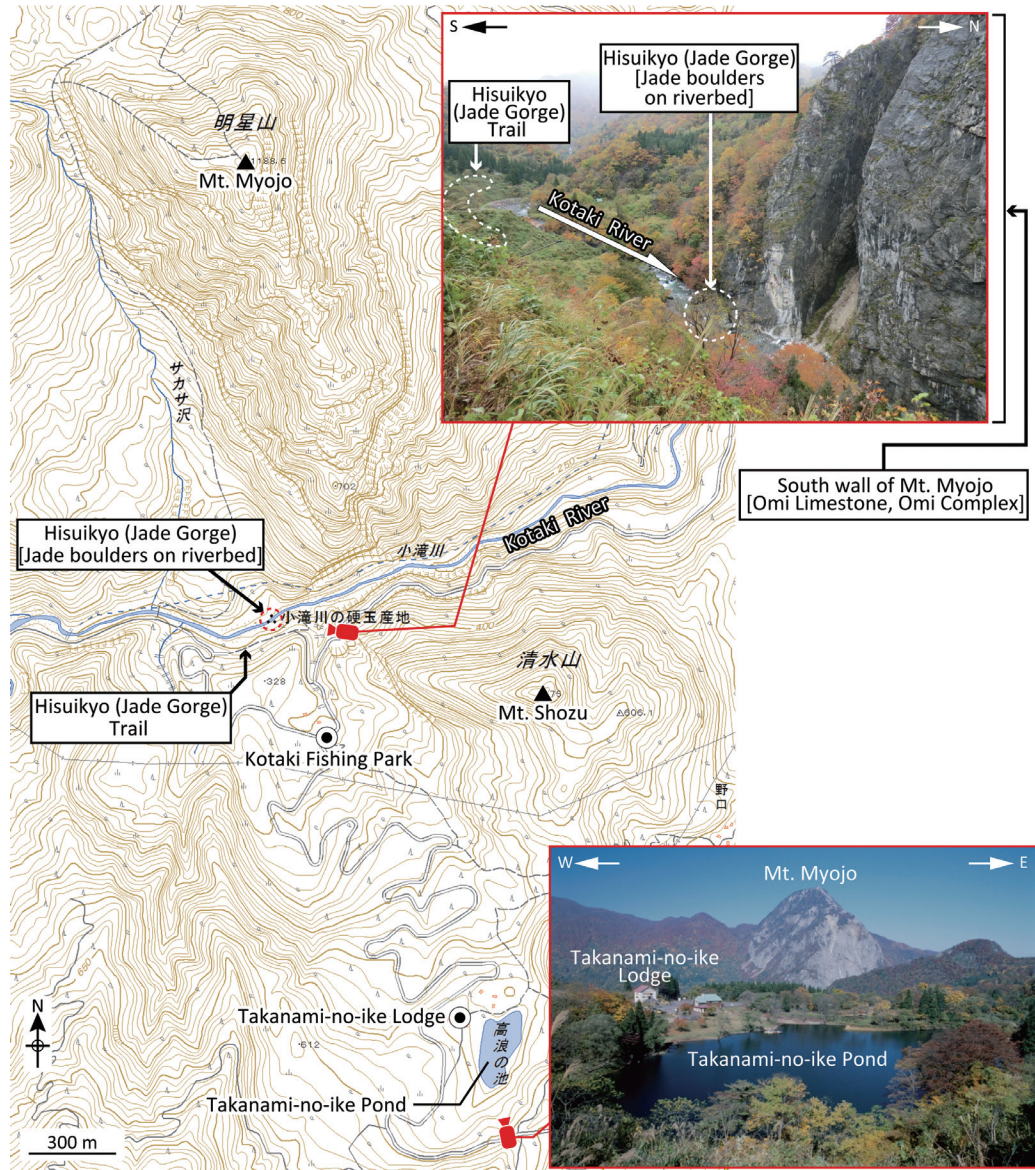
Fig. 7. Map of the Kotakigawa Jade Gorge Geosite (modified from topographic map "Kotaki" scale 1:25000 published by Geospatial Information Authority of Japan).

side of Mt. Myojo (Fig. 7). The Kotakigawa Jade Gorge was confirmed as the first natural source of jade in Japan in 1939 (Kawano, 1939), and was then designated as a natural monument of the nation in 1956 (Miyajima, 2010). Jade was established as the Municipal Stone of Itoigawa in 2008 and as the Niigata Prefectural Stone and National Stone of Japan in 2016.

Jadeitite, jadeite-albitite, and albitite lie as float blocks along the river bed of the Kotaki
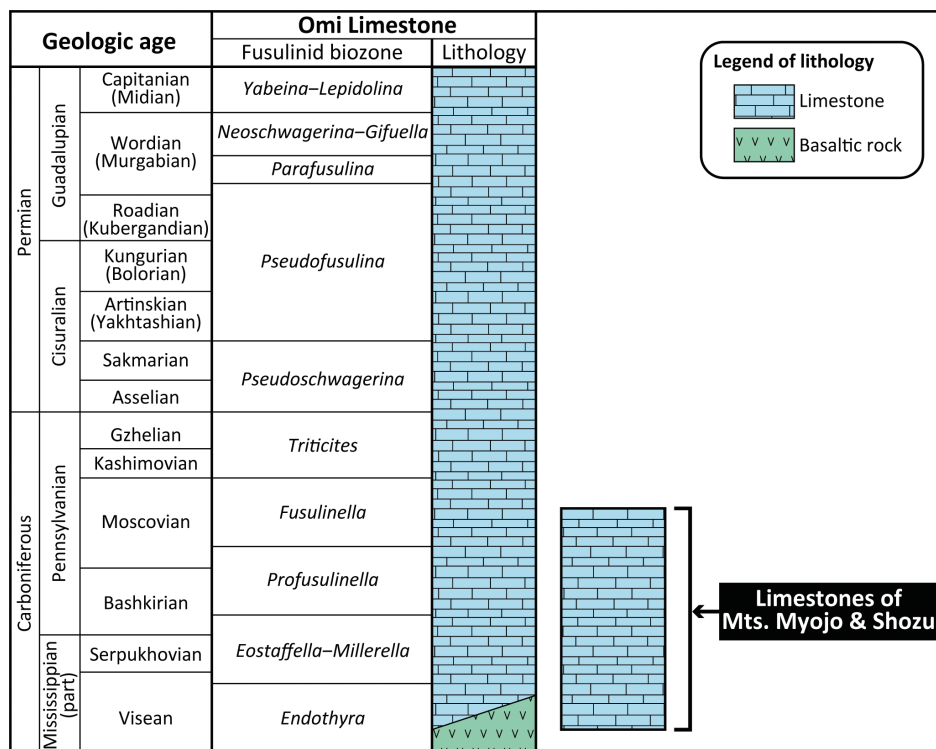
Fig. 8. Fusulinid biostratigraphy and lithology of the Omi Limestone with limestones of Mts. Myojo and Shozu (based on Hasegawa and Goto, 1990).

River (Takeuchi et al., 2015b). The jade-bearing rocks were derived from serpentines near the Kotaki River at the Kotakigawa Jade Gorge (Iwao, 1953). The serpentines are located between Carboniferous–Permian limestones of the Omi Complex of the Akiyoshi terrane and the Permian Kotaki Formation of the Hida Gaien belt (Takeuchi et al., 2015b).

Mounts Myojo and Shozu are located in the southernmost part of the distributional area of the Omi Limestone. The Omi Limestone, belonging to the Omi Complex of the Akiyoshi terrane, ranges from the Mississippian (Early Carboniferous) to the Guadalupian (Middle Permian) based on the fusulinid fossils (Hasegawa and Goto, 1990). Because of the absence of terrigenous clastics within the Omi Limestone, the seamount had been situated in an open-ocean setting (e.g., Nakazawa, 2001). Figure 8 shows fusulinid biostratigraphy of the Omi Limestone. Hasegawa and Goto (1990) stated that Mts. Myojo and Shozu are composed mainly of limestones of the *Endothyra*, *Eostaffella–Millerella*, *Profusulinella*, and *Fusulina–Fusulinella* zones.

A visitor can approach the Kotaki River from the Hisuikyo (Jade Gorge) Trail (Fig. 7). Several kinds of pebble and cobble are observable in the Kotaki River. Mount Myojo can be seen well from a viewing deck on opposite bank of Mt. Myojo.

STOP 2. Fossa Magna Museum (in Geosite No. 16)

The Fossa Magna Museum was opened in 1994 and then it was renovated in March 2015 (Table 1). The museum displays several exhibits (Fig. 9). Jade, the municipal stone of Itoigawa and national stone of Japan, can be seen in several places in the museum, such as in the courtyard (Fig. 9A) and the entrance of the exhibit rooms (Fig. 9B). Various fossils collected from Itoigawa and other areas are exhibited (Fig. 9C). Exhibits introduce the biography and works of Dr. H. E. Naumann, known as the discoverer of the Fossa Magna (Fig. 9D). A preparing peel of pyroclastic flow deposits of Mt. Yakeyama (Fig. 9E) and a replica of marine deposits in the Japan Sea (Fig. 9F) show geologic characteristics around Itoigawa.

The Fossa Magna Museum is located in Miyama Park, which is one of the geosites of the Itoigawa UNESCO Global Geopark. The Chojagahara Archaeological Museum and the Chojagahara Archaeological Site, a Nationally Designated Historical Site, are also in Geosite No. 16. The oldest jadeite artifacts in the world, made by Japanese indigenous Jomon people, were discovered from the Chojagahara Archaeological Site. The artifacts are exhibited in the Chojagahara Archaeological Museum.

Concluding remarks

Various rocks ranging in age from the Cambrian to Quaternary are exposed in Itoigawa, indicating its potential for several studies, such as geologic, paleontological, and petrological ones. Furthermore, the Itoigawa–Shizuoka Tectonic Line lies in the central part of the City of Itoigawa, also indicating the potential for studies of structural geology and Cenozoic tectonic framework in East Asia. In contrast to the investigative potential, there remains much to be researched in Itoigawa. We expect that several researchers will explore the frontiers of Itoigawa.

Acknowledgments

References

Chihara, K., 1955, Relations between sequence igneous activity of green tuff and metellogenetics: Niigata District*. *Jour. Geol. Soc. Japan*, **61**, 312 (in Japanese). *The title was translated by the authors.
Chihara, K., Komatsu, M., Uemura, T., Hasegawa, Y., Shiraishi, S., Yoshimura, T. and Nakamizu, M., 1979,
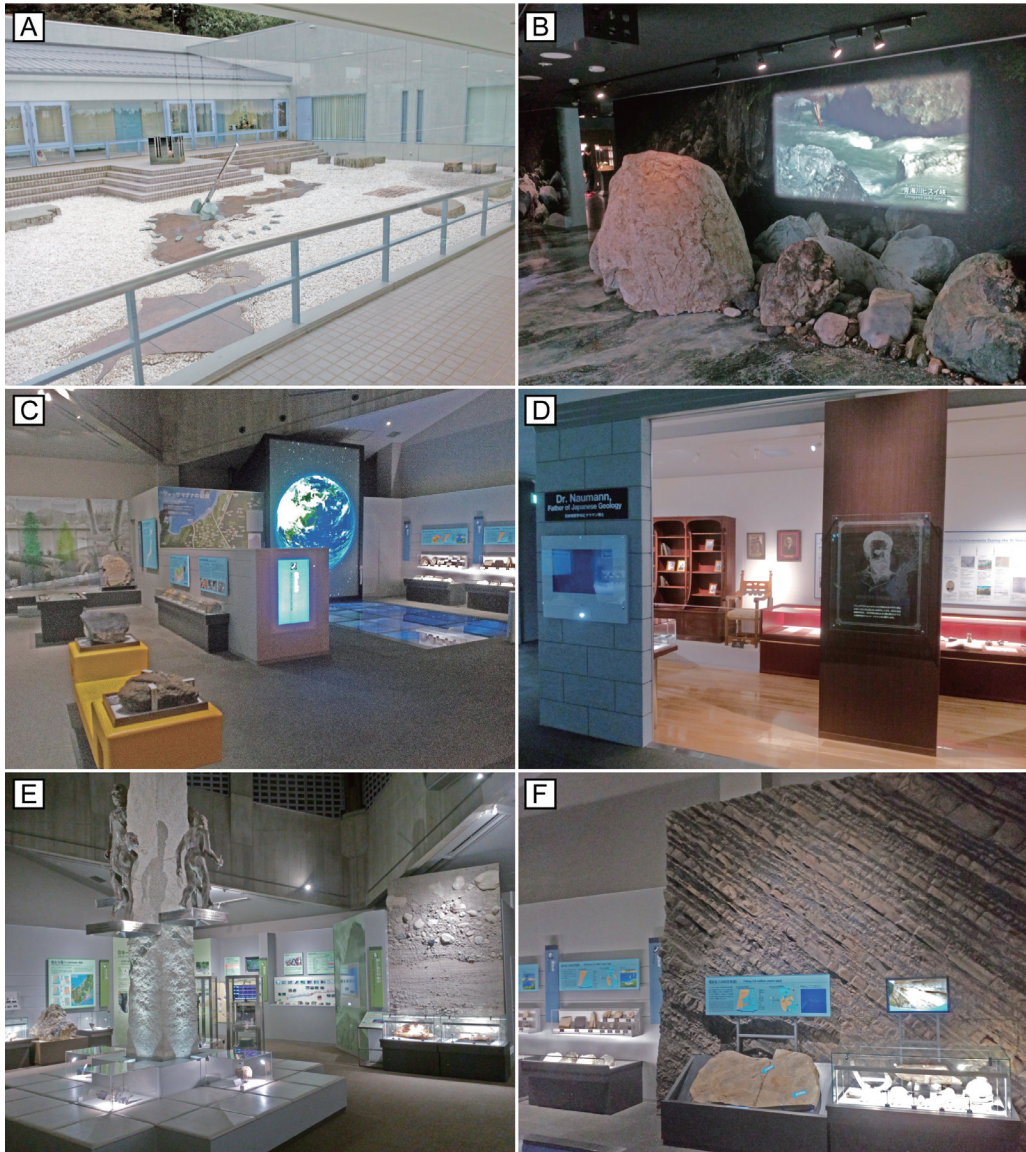
Fig. 9. Fossa Magna Musuem in Itoigawa, Niigata Prefecture, central Japan. **A:** Solar clock of jade stones on stone-clad Japanese Islands in the courtyard. **B:** Large jade gemstones at the entrance of the exhibit rooms. **C:** Fossa Magna Theater showing the birth of the Japanese Islands. **D:** Introduction of the lifetime of Dr. H. E. Naumann and exhibition of his works. **E:** Figures of hominids and preparing peel of pyroclastic flow deposits of Mt. Yakeyama. **F:** Replica of marine deposits in the Sea of Japan in 12 Ma.

Geology and tectonics of the Omi–Renge and Joetsu Tectonic Belts (5): Geology and tectonics of the Omi–Renge Tectonic Belt. *Sci. Rep. Niigata Univ., Ser. E*, no. 5, 1–60.

Hasegawa, Y. and Goto, M., 1990, Paleozoic and Mesozoic of Omi Region. *97th Ann. Meet. Geol. Soc. Japan, Excursion Guidebook*, 227–260 (in Japanese).

Hayatsu, K., 1994, The activity and age of Niigata-Yakeyama Volcano, central Japan. *Jour. Tokyo Geogr. Soc.*, **103**, 149–165 (in Japanese with English abstract).

Holdsworth, B. K. and Jones, D. L., 1980, Preliminary radiolarian zonation for the Late Devonian through Permian time. *Geology*, **8**, 281–285.

Ishida, K., Kozai, T., Park, S. O. and Mitsugi, T., 2003, Gravel bearing radiolarian as tracers for erosional events: a review of the status of recent research in SW Japan and Korea. *Jour. Asian Earth Sci.*, **21**, 909–920.

Ishiga, H., 1990, Paleozoic radiolarians. *In* Ichikawa, K., Mizutani, S., Hara, I., Hada, S. and Yao, A., eds., *Pre-Cretaceous Terrane of Japan*. Publication of IGCP project No. 224, Pre-Jurassic Evolution of Eastern Asia, 285–295.

Ishiga, H. and Imoto, N., 1980, Some Permian radiolarians in the Tamba District, southwest Japan. *Earth Sci. (Chikyu Kagaku)*, **34**, 333–345.

Ishii, H., 1976, The Ishizaka Rhyolite Formation and the Itoigawa–Shizuoka Tecotnic Line along the middle course of River Hime, Nagano Prefecture. *Bull. Osaka Mus. Nat. Hist.*, no. 30, 49–60 (in Japanese with English abstract).

Ito, T., Feng, Q. L. and Matsuoka, A., 2015a, Taxonomic significance of short forms of middle Permian *Pseudoalbaillella* Holdsworth and Jones, 1980 (Follicucullidae, Radiolaria). *Rev. Micropaleont.*, **58**, 3–12.

Ito, T., Feng, Q. L. and Matsuoka, A., 2016, Uneven distribution of *Pseudotormentus* De Wever et Caridroit (Radiolaria, Protozoa): Provincialism of a Permian planktonic microorganism. *Acta Geol. Sinica (English Edition)*, **90**, 1598–1610.

Ito, T., Kurihara, T., Hakoiwa, H., Ibaraki, Y. and Matsuoka, A., 2017a, Late Silurian radiolarians from a siliceous rock pebble within a conglomerate, Kotaki, Niigata Prefecture, central Japan. *Sci. Rep. Niigata Univ. (Geol.)*, no. 32, 1–14.

Ito, T., Kurihara, T., Hakoiwa, H., Ibaraki, Y. and Matsuoka, A., 2017b, Discovery of the oldest fossil in Niigata Prefecture of central Japan from the Kotaki area, Itoigawa: A report on collaboration research of Itoigawa City, Niigata University, and Geological Survey of Japan, AIST. *Bull. Itoigawa City Mus.*, no. 4, in press (in Japanese with English abstract).

Ito, T. and Matsuoka, A., 2015a, Imbricate structure of the Permian Yoshii Group in the Otakeyama area, Okayama Prefecture, southwest Japan. *Front. Earth Sci.*, **9**, 152–163.

Ito, T. and Matsuoka, A., 2015b, Swollen type of *Albaillella sinuata* Ishiga and Watase (Permian radiolaria) from a chert boulder in Ie-jima Island, Okinawa Prefecture, Japan. *News Osaka Micropaleontol. (NOM), Spec. Vol.*, no. 15, 207–217.

Ito, T. and Matsuoka, A., 2016, Ductilely deformed cherts within intrusive sandstones of the Yoshii Group of the Akiyoshi terrane in Southwest Japan: Consolidation time of Permian cherts. *News Osaka Micropaleontol. (NOM), Spec. Vol.*, no. 16, 95–104.

Ito, T., Sakai, Y., Feng, Q. L. and Matsuoka, A., 2015b, Middle Jurassic radiolarians from chert clasts within conglomerates of the Itsuki Formation of the Itoshiro Subgroup (Tetori Group) in the Taniyamadani Valley, Fukui Prefecture, central Japan. *Sci. Rep. Niigata Univ. (Geol.)*, no. 30, 1–13.

Ito, T., Sakai, Y., Feng, Q. L. and Matsuoka, A., 2017c, Review of microfossil-bearing clasts within upper Mesozoic strata in East Asia: staged denudation of mid-Mesozoic accretionary complexes. *Ofioliti*, **42**, 39–54.

Ito, T., Sakai, Y., Ibaraki, Y. and Matsuoka, A., 2014, Middle Jurassic radiolarians from a siliceous mudstone clast within conglomerate of the Tetori Group in the Itoigawa area, Niigata Prefecture, central Japan. *Sci. Rep. Niigata Univ. (Geol.)*, no. 29, 1–11.

Ito, T., Sakai, Y., Ibaraki, Y., Yoshino, K., Ishida, N., Umetsu, T., Nakada, K., Matsumoto, A., Hinohara, T., Matsumoto, K. and Matsuoka, A., 2012, Radiolarian fossils from siliceous rock pebbles within conglomerates in the Mizukamidani Formation of the Tetori Group in the Itoigawa area, Niigata Prefecture, central Japan. *Bull. Itoigawa City Mus.*, no. 3, 13–25 (in Japanese with English abstract).

Iwao, S., 1953, Albite and associated jadeite rock from Kotaki District, Japan: A study in ceramic raw material. *Rep. Geol. Surv. Japan*, no. 153, 26p.

Kawai, M. and Takeuchi, M., 2001, Permian radiolarians from the Omi area in the Hida-gaien Tectonic Zone, central Japan. *News Osaka Micropaleontol. (NOM), Spec. Vol.*, no. 12, 23–32 (in Japanese with English abstract).

Kawano, Y., 1939, First discovery of jade in Japan and its chemical character*. *Jour. Japan. Assoc. Mineral. Petrol. Ecol. Geol.*, **22**, 219–225. *The title was translated by the authors.

Kobayashi, T., Konishi, K., Sato, T., Hayami, I. and Tokuyama, A., 1957, On the Lower Jurassic Kuruma Group. *Jour. Geol. Soc. Japan*, **63**, 182–194 (in Japanese with English abstract).

Kumazaki, N. and Kojima, S., 1996, Depositional history and structure development of the Kuruma Group (lower Jurassic) on the basis of clastic rock composition. *Jour. Geol. Soc. Japan*, **102**, 285–302 (in Japanese with English abstract).

Kurihara, T., 2004, Silurian and Devonian radiolarian biostratigraphy of the Hida-gaien belt, central Japan. *Jour. Geol. Soc. Japan*, **110**, 620–639 (in Japanese with English abstract).

Kurihara, T., 2007, Uppermost Silurian to Lower Devonian radiolarians from the Hitoegane area of the Hida-gaien terrane, central Japan. *Micropaleontology*, **53**, 221–237.

Kuwahara, K., 1992, Late Carboniferous to Early Permian radiolarian assemblages from Miyagawa area, Mie Prefecture, Japan. *News Osaka Micropaleontol. (NOM), Spec. Vol.*, no. 8, 1–7 (in Japanese with English abstract).

Kuwahara, K., 1997, Upper Permian radiolarian biostratigraphy: Abundance zone of *Albaillella*. *News Osaka Micropaleontol. (NOM), Spec. Vol.*, no. 10, 55–75 (in Japanese with English Abstract).

Manchuk, N., Kurihara, T., Tsukada, K., Kochi, Y., Obara, H., Fujimoto, T., Orihashi, Y. and Yamamoto, K., 2013. U–Pb zircon age from the radiolarian-bearing Hitoegane Formation in the Hida Gaien Belt, Japan. *Island Arc*, **22**, 494–507.

Miyajima, H., 2010, Geotour of investigating jade in the Itoigawa Geopark: Enjoy and study of mysterious jade from different angles. *Jour. Geol. Soc. Japan*, **116**, Supplement, 193–216 (in Japanese).

Nakazawa, T., 2001, Carboniferous reef succession of the Panthalassan open-ocean setting: Example from Omi Limestone, central Japan. *Facies*, **44**, 183–210.

Nagamori, H., Takeuchi, M., Furukawa, R., Nakazawa, T. and Nakano, S., 2010, *Geology of the Kotaki district. Quadrangle Series, 1:50,000*, Geological Survey of Japan, AIST, 130p. (in Japanese with English abstract).

Nazarov, B. B. and Ormiston, A. R., 1986, Origin and biostratigraphic potential of the stauraxon polycystine radiolaria. *Marine Micropaleont.*, **11**, 33–54.

Niko, S., Yamakita, S., Otoh, S., Yanai, S. and Hamada, T., 1987, Permian radiolarians from the Mizuyagadani Formation in Fukuji area, Hida Marginal Belt and their significance. *Jour. Geol. Soc. Japan*, **93**, 431–433 (in Japanese).

Nishimura, K. and Ishiga, H., 1987, Radiolarian Biostratigraphy of the Maizuru Group in Yanahara area, Southwest Japan. *Mem. Fac. Sci. Shimane Univ.*, **21**, 169–188.

Ogg, J. G., Ogg, G. M. and Gradstein, F. M., 2016, A *Concise Geologic Time Scale 2016*. Elsevier, Amsterdam. 234p.

Oishi, S., 1933, The Tetori Series, esp. its biozone (2)*. *Jour. Geol. Soc. Japan*, **40**, 669–699 (in Japanese). *The title was translated by the authors.

Sakai, Y., Ito, T., Ibaraki, Y., Yoshino, K., Ishida, N., Umetsu, T., Nakada, K., Matsumoto, A., Hinohara, T., Matsumoto, K. and Matsuoka, A., 2012, Lithology and Stratigraphy of the Mizukamidani Formation of the Tetori Group in the right bank of the Sakai River in the Itoigawa area, Niigata Prefecture, Japan. *Bull. Itoigawa City Mus.*, no. 3, 1–11 (in Japanese with English abstract).

Saida, T., 1987, Triassic and Jurassic radiolarians in chert clasts of the Tetori Group in Tamodani area of Izumi Village, Fukui Prefecture, central Japan. *Jour. Geol. Soc. Japan*, **93**, 57–59 (in Japanese).

Sano, H., Iijima, Y. and Hattori, H., 1987, Stratigraphy of the Paleozoic rocks in the Akiyoshi Terrane of the central Chugoku Massif. *Jour. Geol. Soc. Japan*, **93**, 865–880 (in Japanese with English abstract).

Schwartzapfel, J. A. and Holdsworth, B. K., 1996, Upper Devonian and Mississippian radiolarian zonation and biostratigraphy of the Woodford, Sycamore, Caney and Goddard formations, Oklahoma. *Cushman Found. Spec. Publ.*, **33**, 1–275.

Shiraishi, S., 1992, The Hida Marginal Tectonic Belt in the middle reaches of the River Hime-kawa with special reference to the lower Jurassic Kuruma Group. *Earth Sci. (Chikyu Kagaku)*, **46**, 1–20 (in Japanese with English abstract).

Sugamori, Y., 2011, Late Permian radiolarians from the Ajima Formation of the Ultra-Tamba Terrane in the Sasayama area, southwest Japan. *Palaeoworld*, **20**, 158–165.

Taira, A., Ohara, Y., Wallis, S. R., Ishiwatari, A. and Iryu, Y., 2016, Geological evolution of Japan: an overview. *In* Moreno, T., Wallis, S. R., Kojima, S. and Gibbons, W., eds., *The Geology of Japan*, Geological Society of London, 1–24.

Takeuchi, M., Kawai, M., Noda, A., Sugimoto, N., Yokota, H., Kojima, S., Ohno, K., Niwa, M. and Ohba, H., 2004, Stratigraphy of the Permian Shiroumadake Formation and its structural relationship with serpentine in the Mt. Shiroumadake area, Hida Gaien belt, central Japan. *Jour. Geol. Soc. Japan*, **110**, 715–730 (in Japanese with English abstract).

Takeuchi, M., Ohkawa, M., Kawahara, K., Tomita, S., Yokota, H., Tokiwa, T. and Furukawa, R., 2015a, Redefinition of the Cretaceous terrigenous strata in the northeastern Toyama Prefecture based on U–Pb ages of zircon. *Jour. Geol. Soc. Japan*, **121**, 1–17 (in Japanese with English abstract).

Takeuchi, M., Saito, M. and Takizawa, F., 1991, Radiolarian fossils obtained from conglomerate of the Tetori Group in the upper reaches of the Kurosegawa River, and its geological significance. *Jour. Geol. Soc. Japan*, **97**, 345–356 (in Japanese with English abstract).

Takeuchi, M., Takenouchi, K. and Nakazawa, T., 2010, Geologic excursion in Itoigawa Geopark. *Jour. Geol. Soc. Japan*, **116**, supplement, 1–17 (in Japanese).

Takeuchi, M., Takenouchi, K. and Tokiwa, T., 2015b, Range Metamorphic rocks and the Mesozoic terrigenous strata. *Jour. Geol. Soc. Japan*, **121**, 193–216 (in Japanese).

Tazawa, J., Aita, Y., Yuki, T. and Otsuki, K., 1984, Discovery of Permian radiolarians from the "non-calcareous Paleozoic strata" of Omi, central Japan. *Earth Sci. (Chikyu Kagaku)*, **38**, 264–267 (in Japanese).

Tomita, S., Takeuchi, M. and Kametaka, M., 2007, Radiolarian fossils obtained from conglomerate of the Tetori Group in the northeastern part of Toyama Prefecture and its geological significance. *Abst. 114th Ann. Meet. Geol. Soc. Japan*, 243 (in Japanese).

Tomizawa, T. and Kitahara, I., 1967, On the geology in the environs of the middle course of the Hime-gawa River, Otari-mura, Kitaazumi-gun, Nagano Prefecture. *Jour. Geol. Soc. Japan*, **73**, 163–170 (in Japanese with English abstract).

Ujihara, M., 1985, Permian olistostrome and clastics along the Himekawa River in the northeast part of the Hida Gaien belt*. *Research report No. 2 -Joetsu terrane and Ashio terrane-*, 69–84 (in Japanese). *The title was translated by the authors.

Umeda, M. and Ezaki, Y., 1997, Middle Permian radiolarian fossils from the acidic tuffs of the Kanayama and Fukuji areas in the Hida "Gaien" Terrane, central Japan. *Fossils (Kaseki)*, no. 62, 37–44 (in Japanese with English abstract).

Wang, Y. J. and Yang, Q., 2011, Biostratigraphy, phylogeny and palaeobiogeography of Carboniferous–Permian radiolarians in South China. *Palaeoworld*, **20**, 134–145.

Yoshimura, T. and Adachi, H., 1976, Futomiyama Group in Niigata Prefecture. *Contrib. Dept. Geol. Mineral. Niigata Univ.*, no. 4, 131–136 (in Japanese with English abstract).

Zhang, N., Henderson, C. M., Wang, W. C., Wang, G. Q. and Shang, H. J., 2010, Conodonts and radiolarians through the Cisuralian–Guadalupian boundary from the Pingxiang and Dachongling sections, Guangxi region, South China. *Alcheringa*, **34**, 135–160.

Zhang, L., Ito, T., Feng, Q. L., Caridroit, M. and Danelian, T., 2014, Phylogenetic model of *Folliculullus* lineages (Albaillellaria, Radiolaria) based on high-resolution biostratigraphy of the Permian Bancheng Formation, Guangxi, South China. *Jour. Micropalaeont.*, **33**, 179–192.

[URL1] Global Geoparks Network (http://www.globalgeopark.org/aboutGGN/51.htm).

[URL2] Pamphlets & Publications of the Itoigawa UNESCO Global Geopark (http://www.geo-itoigawa.com/eng/about/dl.html).

Neogene biosiliceous sedimentary sequence and radiolarian biostratigraphy in the Tainai area, Niigata Prefecture

Isao MOTOYAMA*, Toshiyuki KURIHARA ** and Takuya ITAKI ***

Abstract

Middle Miocene–Pliocene biosiliceous and microfossil-bearing-siliciclastic sediments are exposed at the Natsui Section along the Tainai River. This outcrop comprises the Shimoseki, Uchisugawa, and Kuwae Formations. Radiolarians and other microfossils extracted from these formations have been investigated by many geologists and paleontologists for regional correlation and paleoenvironmental reconstruction of the Japan Sea. Here we present a radiolarian biostratigraphy of the Middle to Upper Miocene siliceous sedimentary sequence of the Natsui Section.

Key words: Miocene, Pliocene, Radiolaria, microfossil, Tainai River, Natsui Section, Niigata Prefecture

Introduction

In the Japan Sea side region of the Japanese Islands there are thick Neogene deposits that rest unconformably on pre-Neogene rocks. In this region the Neogene is made up of four depositional sequences; Lower Miocene pyroclastic and volcanic rocks deposited in terrestrial environments, uppermost Lower to lowermost Middle Miocene shallow marine deposits representing the initial transgression, Middle to Upper Miocene biogenic deep sea sediments, and Plio-Pleistocene siliciclastic sediments (Kobayashi and Tateishi, 1992;

* Faculty of Science, Yamagata University, Yamagata 990-8560, Japan

** Graduate School of Science and Technology, Niigata University, Niigata 950-2181, Japan

*** Geological Survey of Japan, AIST, Tsukuba, Ibaraki 305-8567, Japan
Corresponding author: I. Motoyama,
i-motoyama@sci.kj.yamagata-u.ac.jp

Kobayashi, 2002; Takano, 2002). This temporal facies change largely reflects the development of the Japan Sea, a marginal sea with deep basins (maximum water depth of 3,700 m), which probably did not exist before the Middle Miocene and was generated through the extension and opening of the eastern margin of the Asian Continent in
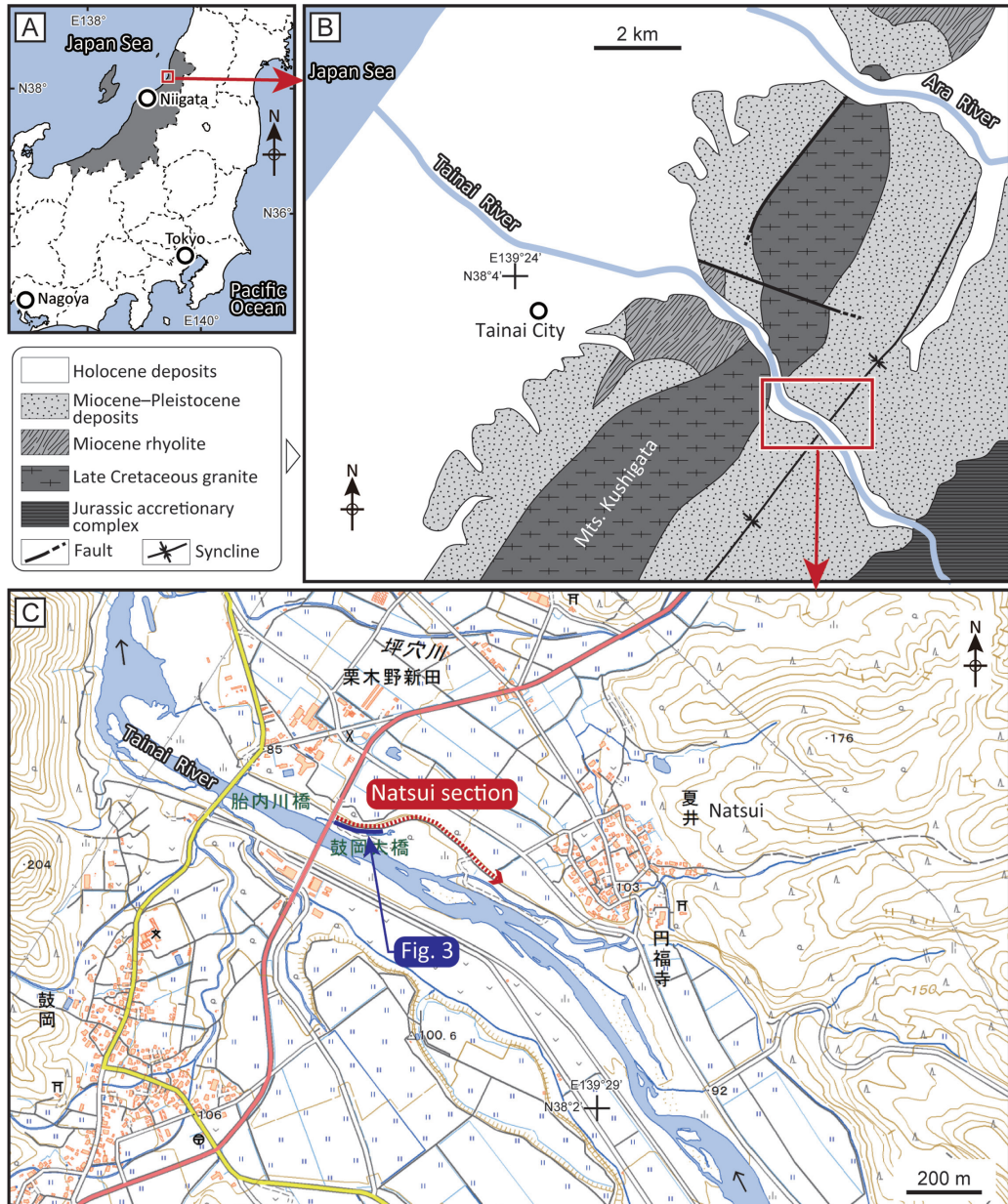
Fig. 1. Index map of the Tainai area of northern Niigata Prefecture. Map A: location of Niigata Prefecture (shaded area). Map B: schematic geologic map of the Tainai area (modified from Niigata Prefecture, 2000). Map C: location of the Natsui Section (modified from topographic map "Nakajo" scale 1:25,000 published by Geospatial Information Authority of Japan).

association with an ~500 km southeastward drift of the Japanese archipelago during a short time interval of one to two million years around 16–15 Ma (e.g., Van Horne et al., 2016). The basins subsided to bathyal depths (usually >1,000 m) after 15 Ma and accumulated biogenic siliceous sediments until the latest Miocene in nearshore areas or until the Pliocene in offshore areas (Yamaji and Sato, 1989; Iijima and Tada, 1990). Since the Pliocene, the basins of nearshore areas were buried with siliciclastic sediments that were brought from the emerged land areas as the Japanese Islands uplifted. These Neogene formations were finally uplifted and folded during the last two million years.

In the Tainai area, northern Niigata Prefecture (Fig. 1), the Neogene deposits are subdivided into the Kamagui, Shimoseki, Uchisugawa, and Kuwae Formations, in ascending order (Nishida and Tsuda, 1961) (Fig. 2). The Kamagui Formation consists of conglomerate and sandstone with fossils of subtropical fauna, representing the initial transgression as well as the mid-Miocene global warming event. The subsequent basinal deepening and climatic cooling resulted in deposition of the Shimoseki and Uchisugawa Formations which are composed of siliceous hard mudstone and diatomaceous mudstone, respectively. Local variations in the diagenesis of biogenic opal resulted in a diachronous boundary between these two formations across the region. The Pliocene Kuwae Formation is dominated by sandy siltstone occasionally including molluscan fossils and records facies changes in the outer shelf to slope environments reflecting local tectonics and relative sea-level changes (Takano et al., 2001). Radiolarians are common in the Uchisugawa Formation and rare in the Shimoseki and Kuwae Formations (Sugano and Nakaseko, 1971, 1972). Diatoms are abundant in the Uchisugawa and Kuwae Formations and calcareous microfossils are present within the Kuwae Formation (see the literature cited below for details).

Age		Tainai area
Pliocene		Kuwae Fm.
Miocene	Late	~unconformity~
		Uchisugawa Fm.
	Middle	Shimoseki Fm.
		Kamagui Fm.

Fig. 2. Schematic Neogene stratigraphy in the Tainai area.

The Natsui Section, comprising cliffs on both sides of the Tainai River, is located in the middle part of Tainai City, northern Niigata Prefecture (Fig. 1). A typical sedimentary sequence from the Shimoseki to Kuwae Formations is exposed there.

Geology and biostratigraphy of the Natsui Section

At the Natsui Section (Fig. 1C), Middle to Upper Miocene biosiliceous deposits of the Shimoseki and Uchisugawa Formations and Pliocene sandstone and sandy siltstone of the Kuwae Formation crop out in terrace cliffs along the Tainai River (Fig. 3). We will visit a cliff on the north side of the river. The Shimoseki Formation appears near the Tsuzumioka Bridge and is composed of bedded siliceous hard mudstone interbedded with rhyolitic tuffs.
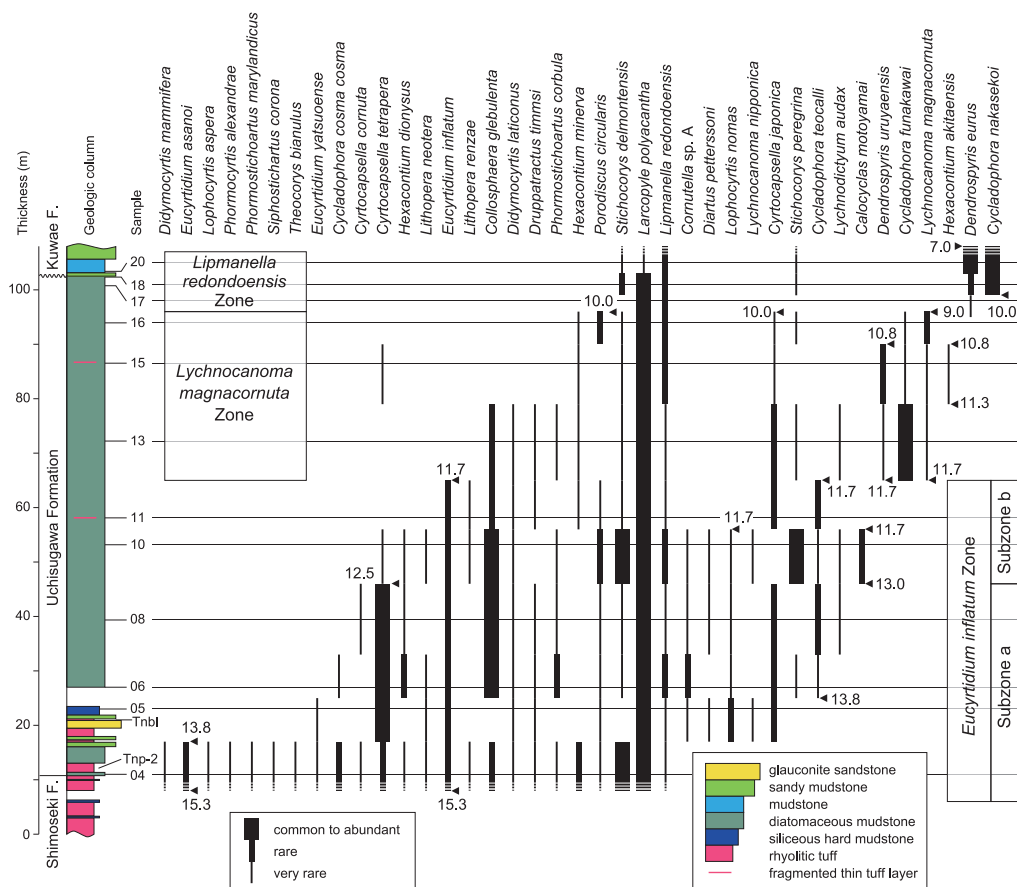
Fig. 3. Middle to Upper Miocene radiolarian biostratigraphy of the Uchisugawa Formation, Natsui Section. Relative abundances of species are estimated by eye under the transmitted light microscope. Tnp-2 and Tnbl are rhyolitic tuff layers described by Kurokawa et al. (1999). The Uchisugawa Formation can be divided into three zones, *E. inflatum*, *L. magnacornuta*, and *L. redondoensis* Zones. The lowest part of the Kuwae Formation belongs to the *L. redondoensis* Zone. Numerical ages (in Ma) for bioevents are those estimated by Kamikuri et al. (2007) and Kamikuri (2010). The location of the section is shown in Fig. 1C.
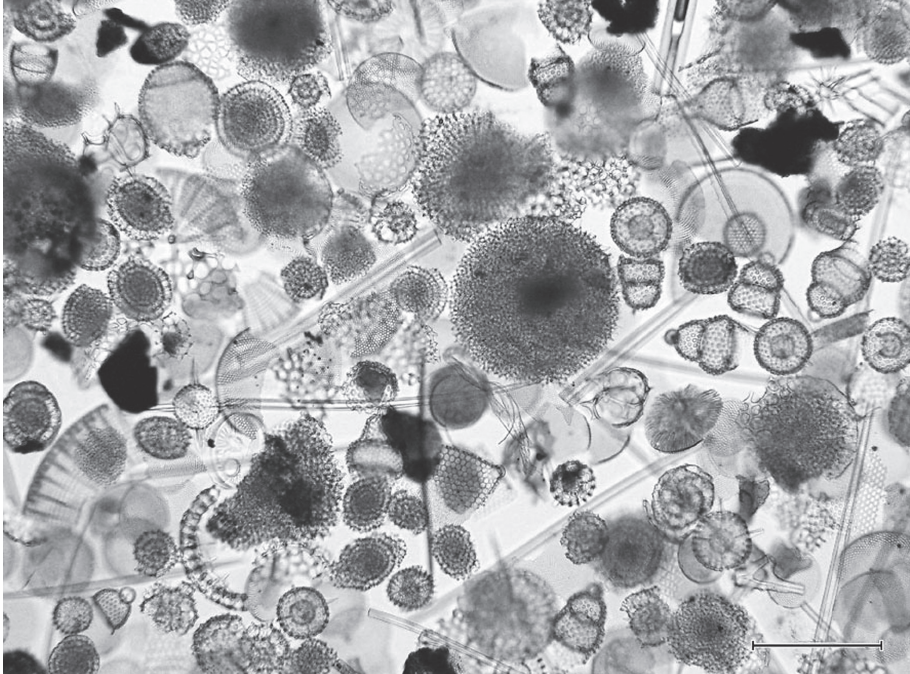
Fig. 4. Photograph of radiolarian assemblage of the Middle Miocene Subzone a of the *Eucyrtidium inflatum* Zone from Sample 04. Scale bar = 200 μm.
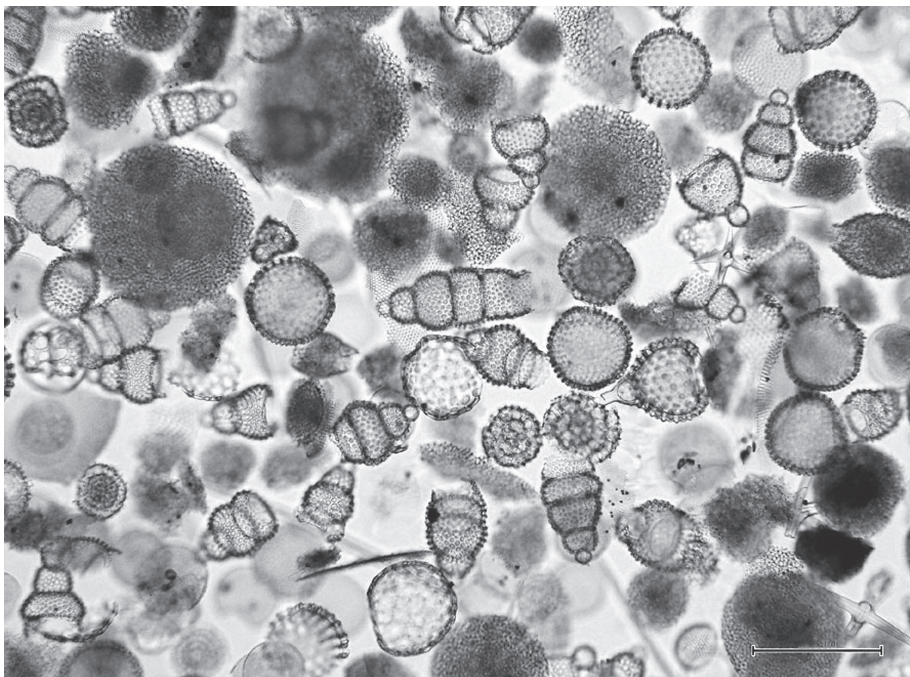
Fig. 5. Photograph of radiolarian assemblage of the Middle Miocene Subzone b of the *Eucyrtidium inflatum* Zone from Sample 10. *Stichocorys delmontensis/peregrina* dominates the assemblage. Scale bar = 200 μm.
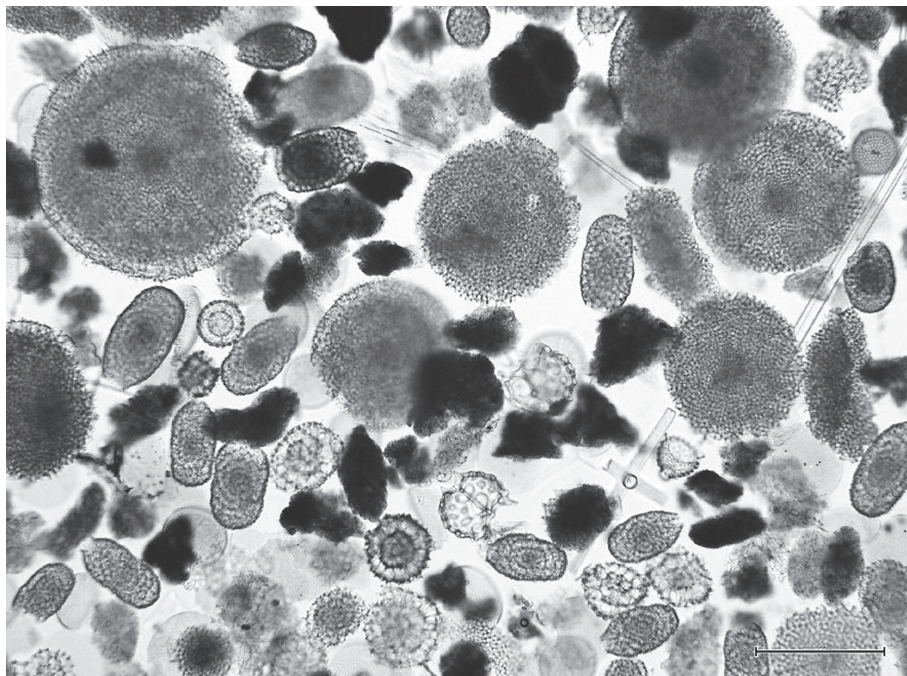
Fig. 6. Photograph of radiolarian assemblage of the Upper Miocene *Lychnocanoma magnacornuta* Zone from Sample 15. *Larcopyle polyacantha* is abundant. Large discoidal forms, *Spongopyle setosa* Dreyer, are remarkable. Scale bar = 200 μm.
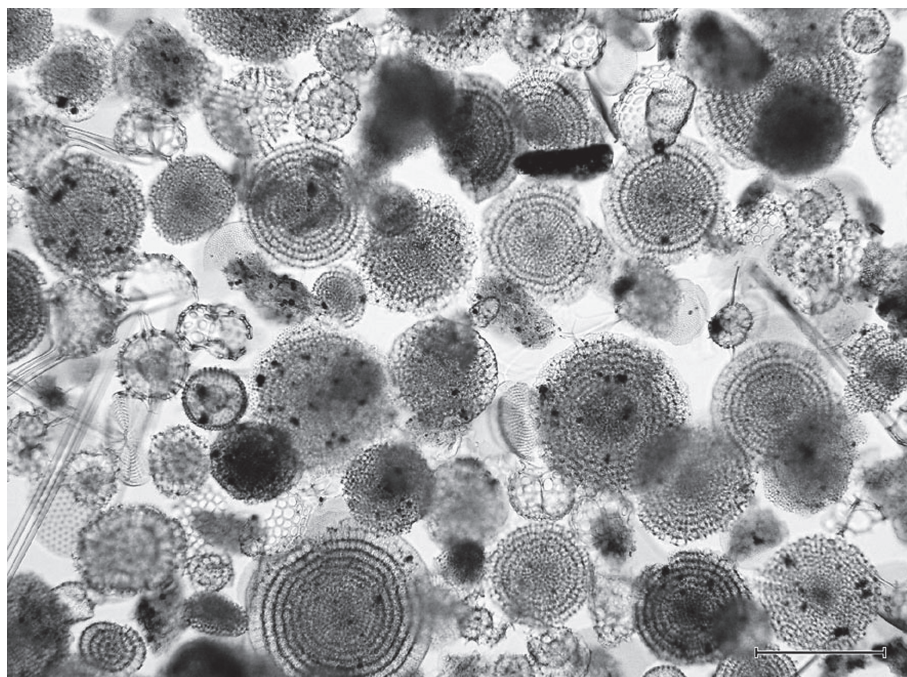
Fig. 7. Photograph of radiolarian assemblage of the Upper Miocene *Lychnocanoma magnacornuta* Zone from Sample 16. Discoidal forms with concentric rings, *Perichlamydium scutaeforme* Campbell and Clark, are dominant. Scale bar = 200 μm.
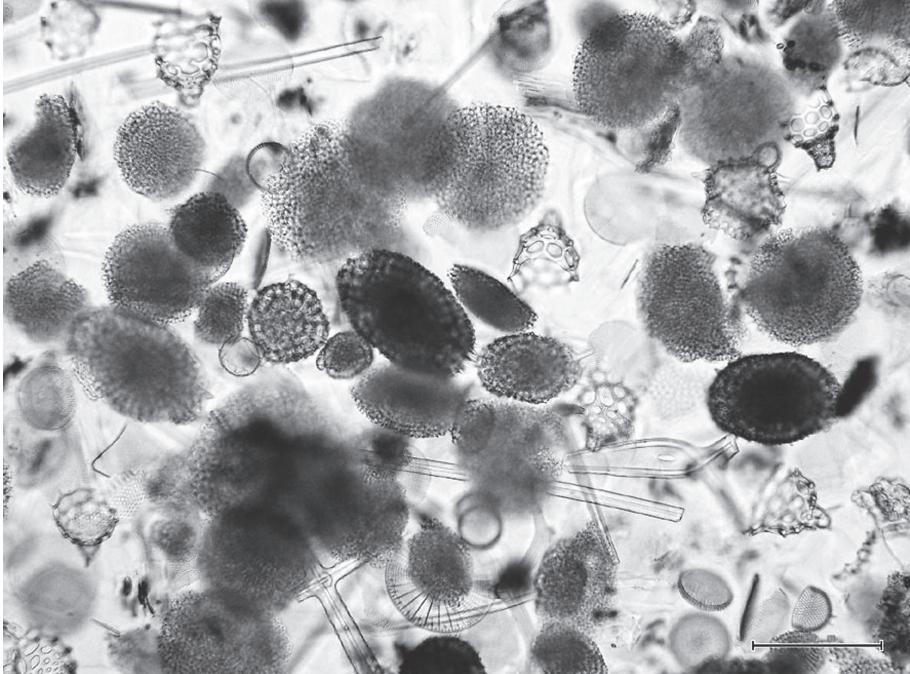
Fig. 8. Photograph of radiolarian assemblage of the Upper Miocene *Lipmanella redondoensis* Zone from Sample 18. *Larcopyle polyacantha* and *Spongodiscus* spp. are dominant. *Cycladophora nakasekoi* is characteristic. Scale bar = 200 μm.

The Uchisugawa Formation is a 90-m-thick sequence of massive olive-gray colored diatomaceous mudstone intercalated with a glauconitic sandstone bed, hard mudstones, and tuffs in its basal part. The Kuwae Formation, unconformably overlying the Uchisugawa Formation (Kobayashi and Watanabe, 1985; Hiramatsu and Miwa, 1998), consists of 200 m of gray to greenish-gray sandy siltstone and sandstone. Hiramatsu and Miwa (1998) suggested that this unconformity spans ~3.5 million years from 10 to 6.5 Ma. The Natsui Section belongs to the west wing of the syncline that lies between two topographic highs, Kushigata Mountains to the west and Iide Mountains to the east, and runs in a NNE to SSW direction (Fig. 1B). The strata from the Shimoseki to lower part of the Kuwae Formations at this section are steeply dipping to the east (80–70° E) and become gentler (40–10° E) closer to the synclinal axis.

Because of its accessible continuous exposure, the Natsui Section has been investigated for biostratigraphy and paleoenvironmental studies using various microfossils. These include a pioneering study of radiolarian biostratigraphy for the Niigata oil field by Sugano and Nakaseko (1972). The others are pollen stratigraphy (Yamanoi, 1976), diatom stratigraphy (Kobayashi and Watanabe, 1985; Hiramatsu and Miwa, 1998; Watanabe et al., 2003), planktonic foramaminiferal stratigraphy (Hiramatsu and Miwa, 1998; Miwa et al., 2004), calcareous nannofossil stratigraphy (Watanabe et al., 2003), and analysis of ostracoda fauna
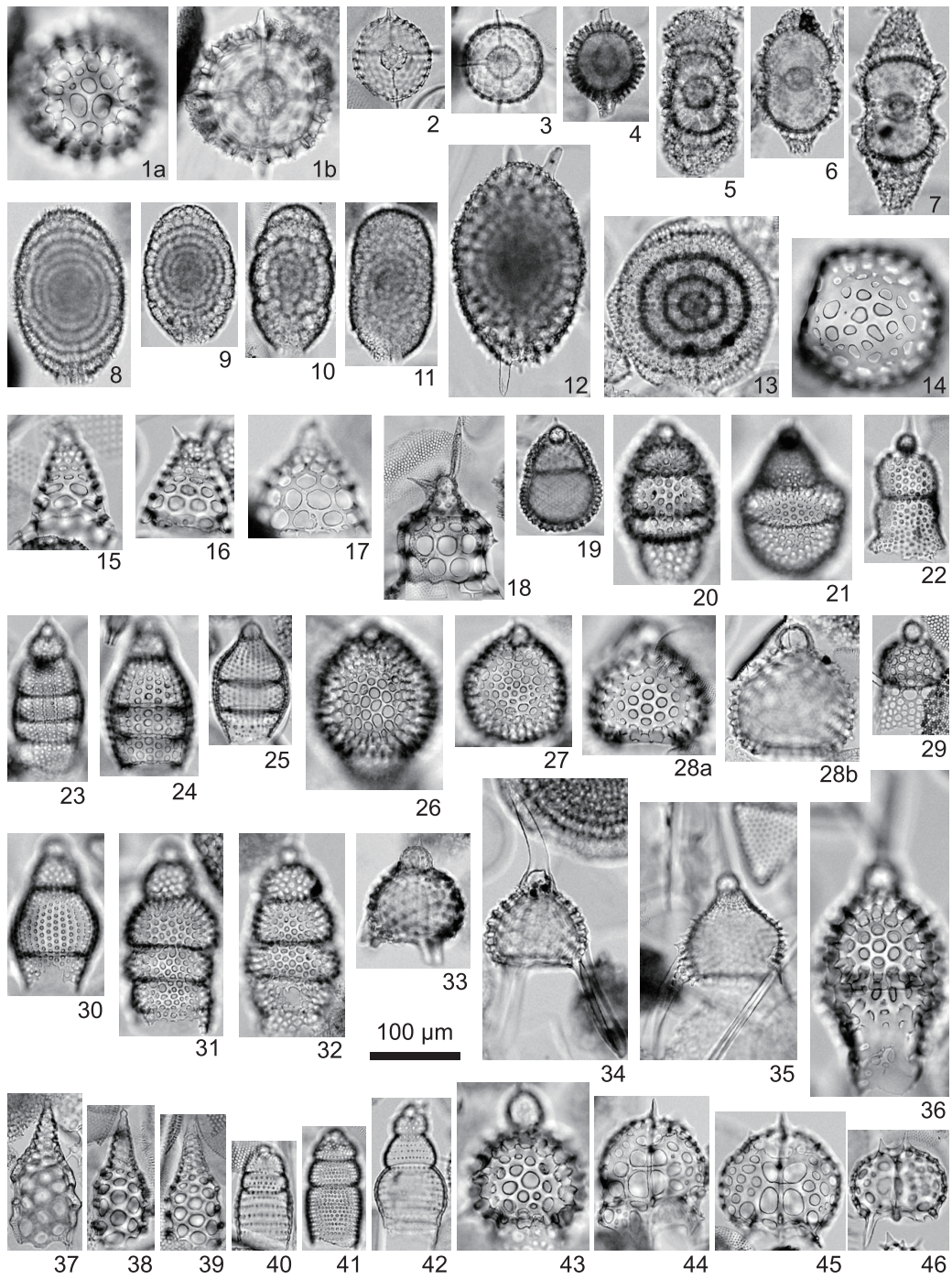
Fig. 9. Photographs of radiolarian species.

1. *Hexacontium akitaensis* (Nakaseko), Sample 15.
2. *Hexacontium dionysus* Kamikuri, Sample 6.
3. *Hexacontium minerva* Kamikuri, Sample 13.
4. *Druppatractus timmsi* (Campbell and Clark), Sample 4.
5. *Diartus petterssoni* (Riedel and Sanfilippo), Sample 5.
6. *Didymocyrtis mammifera* (Haeckel), Sample 4.
7. *Didymocyrtis laticonus* (Riedel), Sample 10.
8–12. *Larcopyle polyacantha* (Campbell and Clark) group: 8, 9, Sample 05; 10, Sample 13; 11, Sample 15; 12, Sample 18.
13. *Porodiscus circularis* Clark and Campbell, Sample 10.
14. *Collosphaera glebulenta* Bjørklund and Goll, Sample 8.
15. *Cycladophora cosma cosma* Lombari and Lazarus, Sample 4.
16. *Cycladophora teocalli* Kamikuri, Sample 10.
17. *Cycladophora funakawai* Kamikuri, Sample 13.
18. *Cycladophora nakasekoi* Motoyama, Sample 18.
19. *Cyrtocapsella japonica* (Nakaseko), Sample 11.
20. *Cyrtocapsella tetrapera* Haeckel, Sample 5.
21. *Cyrtocapsella cornuta* Haeckel, Sample 4.
22. *Lophocyrtis aspera* (Ehrenberg), Sample 4.
23. *Eucyrtidium asanoi* Sakai, Sample 4.
24. *Eucyrtidium inflatum* Kling, Sample 4.
25. *Eucyrtidium yatsuoense* Nakaseko. Sample 4.
26. *Lithopera renzae* Sanfilippo and Riedel, Sample 4.
27. *Lithopera neotera* Sanfilippo and Riedel, Sample 10.
28. *Lophocyrtis nomas* Sanfilippo and Caulet, Sample 8.
29. *Theocorys bianulus* O'Connor, Sample 4.
30. *Phormocyrtis alexsandrae* O'Connor, Sample 4.
31. *Stichocorys delmontensis* (Campbell and Clark), Sample 10.
32. *Stichocorys peregrina* (Riedel), Sample 10.
33. *Lychnocanoma nipponica* (Nakaseko), Sample 5.
34. *Lychnocanoma magnacornuta* Sakai, Sample 16.
35. *Lychnodictyum audax* Riedel, Sample 13.
36. *Calocyclas motoyamai* Kamikuri, Sample 10.
37–39. *Cornutella* sp. A, Sample 6.
40. *Phormostichoartus marylandicus* (Martin), Sample 4.
41. *Phormostichoartus corbula* (Harting), Sample 4.
42. *Siphostichartus corona* (Haeckel), Sample 4.
43. *Lipmanella redondoensis* (Campbell and Clark), Sample 16.
44, 45. *Dendrospyris eurus* Kamikuri, Sample 20.
46. *Dendrospyris uruyaensis* Kamikuri, Sample 13.

(Irizuki et al., 2007). Studies of tephrochronology (Kurokawa et al., 1999), magnetostraigraphy (Inoue et al., 2003), geochemistry (Sampei et al., 2009) and sequence stratigraphy (Takano et al., 2001) were also performed on this section.

Here, we present a new Middle to Upper Miocene radiolarian biostratigraphy for the Natsui Section along the north-side of the Tainai River (Fig. 3). The samples were treated with lamp oil and H_2O_2 and washed through a 63 μm mesh sieve. Disaggregated particles were pipetted onto a glass slide and mounted with a cover slip to make a permanent slide for transmitted light microscope observation.

Diatom and radiolarian fossils occurred abundantly through the sequence from the Uchisugawa Formation to the basal part of the Kuwae Formation (Figs. 3–9). The observed radiolarian assemblages are similar to those reported from the Middle to Upper Miocene sequences in the Japan Sea (Funayama, 1988; Motoyama, 1996; Kamikuri et al., 2017) and the middle-to-high latitude North Pacific (Motoyama, 1996; Kamikuri et al., 2004, 2007; Kamikuri, 2010). The studied sequence can be divided into three radiolarian zones, *Eucyrtidium inflatum*, *Lychnocanoma magnacornuta*, and *Lipmanella redondoensis* Zones in ascending order. A combination of the occurrence of *E. inflatum* and the absence of *L. magnacornuta* indicates the *E. inflatum* Zone (Samples 04 to 11). The *L. magnacornuta* Zone is defined by the total range of *L. magnacornuta* (Samples 13 to 16). The *L. redondoensis* Zone corresponds to the interval between the last occurrence of *L. magnacornuta* and the first occurrence of *Lychnocanoma parallelipes* (Samples 17 to 20). The *E. inflatum* Zone can be subdivided into Subzones a and b in ascending order. The rapid decrease of *Cyrtocapsella tetrapera* was recognized between Sample 08 and Sample 10, indicating the boundary between the two subzones. The contact between the Uchisugawa and Kuwae Formations falls within the *L. redondoensis* Zone, and thus we do not have any radiolarian evidence to support the unconformable relationship. The present radiolarian data, however, suggest that the time range represented by the unconformity is shorter than previously thought, being less than 2 million years in duration between 9.0 and 7.0 Ma.

Acknowledgements

References

Funayama, 1988, Miocene radiolarian stratigraphy of the Suzu area, northwestern part of the Noto Peninsula, Japan. *Contr. Inst. Geol. Paleontol., Tohoku Univ.*, no. 91, 15–41*.

Hiramatsu, C. and Miwa, M., 1998, Neogene microfossil biostratigraphy of the Kitakanbara area in Niigata Prefecture and the geomorphology of an unconformity at the base of the Kuwae Formation. *Jour. Japan. Assoc. Petrol. Technol.*, **63**, 302–314*.

Iijima, A. and Tada, R., 1990, Evolution of Tertiary sedimentary basins of Japan in reference to opening of the Japan Sea. *Jour. Fac. Sci. Univ. Tokyo, Sec. 2*, **22**, 121–171.

Inoue, H., Yamada, K., Takahashi, M., Motoyama, I. and Yanagisawa, Y., 2003, Magnetostratigraphy of the uppermost part of the Pliocene Kuwae Formation (Natsui Section) along the Tainai River, Kitakanbara area, Niigata Prefecture, central Japan. *Jour. Japan. Assoc. Petrol. Technol.*, **68**, 570–580*.

Irizuki, T., Kusumoto, M., Ishida, K. and Tanaka, Y., 2007, Sea-level changes and water structures between 3.5 and 2.8 Ma in the central part of the Japan Sea Borderland: Analysis of fossil Ostracoda from the Pliocene Kuwae Formation, central Japan. *Palaeogeogr., Palaeoclimatol., Palaeoecol.*, **245**, 421–443.

Kamikuri, S., 2010, New late Neogene radiolarian species from the middle to high latitudes of the North Pacific. *Rev. Micropaleontol.*, **53**, 85–106.

Kamikuri, S., Itaki, T., Motoyama, I. and Matsuzaki, M. K., 2017, Radiolarian biostratigraphy from middle Miocene to late Pleistocene in the Japan Sea. *Paleontol. Res.*, doi: 10.2517/2017PR001.

Kamikuri, S., Nishi, H., and Motoyama, I., 2007, Effects of late Neogene climatic cooling on North Pacific radiolarian assemblages and oceanographic conditions. *Palaeogeogr., Palaeoclimatol., Palaeoecol.*, **249**, 370–392.

Kamikuri, S., Nishi, H., Motoyama, I. and Saito, S., 2004, Middle Miocene to Pleistocene radiolarian biostratigraphy in the Northwest Pacific, Ocean Drilling Program Leg 186. *Island Arc*, **13**, 191–226.

Kobayashi, I., 2002, Outline of the Late Cenozoic stratigraphy and geohistorical events in the Honshu coastal region of the Japan Sea side, with an emphasis on the northern area of the Shin'etsu sedimentary province. *In* Tateishi, M. and Kurita, H. eds., *Development of Tertiary sedimentary basins around Japan Sea (East Sea)*, 1–21, Niigata Univ.

Kobayashi, I. and Tateishi, M., 1992, Neogene stratigraphy and paleogeography in the Niigata region, Central Japan. *Mem. Geol. Soc. Japan*, no. 37, 53–70*.

Kobayashi, I. and Watanabe, K., 1985, Geologic event in the eastern margin of Niigata Tertiary sedimentary basin, especially on Mio-Pliocene unconformity. *Sci. Rep. Niigata Univ., Ser. E (Geol. and Mineral.)*, no. 5, 91–103*.

Kurokawa, K., Nagata, R. and Yoshida, T., 1999, Volcanic ash layers in the Uchisugawa and Kuwae Formations in the northeastern Shibata City and along Tainai River, Niigata Prefecture, especially on the Znp-Ywg ash layer found from the Kuwae Formation. *Mem. Fac. Educ. Human Sci. (Natural Sci.), Niigata Univ.*, **2**, no. 1, 1–32*.

Miwa, M., Yanagisawa, Y., Yamada, K., Irizuki, T., Shoji, M. and Tanaka, Y., 2004, Planktonic foraminiferal biostratigraphy of the Pliocene Kuwae Formation in the Tainai River section, Niigata Prefecture and the age of the base of the No. 3 *Globorotalia inflata* bed. *Jour. Japan. Assoc. Petrol. Technol.*, **69**, 272–283*.

Motoyama, I., 1996, Late Neogene radiolarian biostratigraphy in the subarctic Northwest Pacific. *Micropaleontology*, **42**, 221–262.

Niigata Prefecture, 2000, *Geological Outline of the Niigata Prefecture*. 200p*.

Nishida, S. and Tsuda, K., 1961, The Neogene deposits in the Sakamachi district, Niigata Prefecture. *Professor Jiro Makiyama Mem. Vol.*, 107–113*.

Sampei, Y., Yamashita, Y., Irizuki, T., Ishida, K. and Tanaka, Y., 2009, Paleoceanography of the Japan Sea and organic carbon contents of the Pliocene Kuwae Formation along the Tainai River, Kitakanbara area, Niigata Prefecture, central Japan. *Geosci. Rept. Shimane Univ.*, **28**, 65–72*.

Sugano, K. and Nakaseko, K., 1971, On the assemblage of fossil Radiolaria in the neighbourhood of Kitakanbara Plain, Niigata Prefecture, Japan—Studies of fossil radiolarian stratigraphy of the Neogene formation, Niigata Prefecture, Japan (Part 3). *Mem. Osaka Kyoiku Univ. sec. III*, **20**, 63–79*.

Sugano, K. and Nakaseko, K., 1972, On the assemblage of fossil Radiolaria in the Kitakanbara Oil Field, Niigata Prefecture, Japan—Studies of fossil radiolarian stratigraphy of the Neogene formation, Niigata Prefecture, Japan (Part 5). *Mem. Osaka Kyoiku Univ. sec. III*, **21**, 181–197*.

Takano, O., 2002, Tectonostratigraphy and changes in depositional architecture through rifting and basin inversion in the Neogene Niigata-Shin'etsu basin, Northern Fossa Magna, central Japan: implications for

tectonic history of the Japan Sea marginal regions. *In* Tateishi, M. and Kurita, H. eds., *Development of Tertiary sedimentary basins around Japan Sea (East Sea)*, 157–181, Niigata Univ.

Takano, O., Moriya, S., Nishimura, M., Akiba, F., Abe, M. and Yanagimoto, Y., 2001, Sequence stratigraphy and characteristics of depositional systems of the Upper Miocene to Lower Pleistocene in the Kitakambara Area, Niigata Basin, central Japan. *Jour. Geol. Soc. Japan*, **107**, 585–604*.

Van Horne, A., Sato, H. and Ishiyama, T., 2016, Evolution of the Sea of Japan back-arc and some unsolved issues. *Tectonophysics*, http://dx.doi.org/10.1016/j.tecto.2016.08.020

Watanabe, M., Yanagisawa, Y., Tanaka, Y., Yamada, K., Irizuki, T. and Shoji, M., 2003, Diatom and calcareous nannofossil biostratigraphy of the Pliocene Kuwae Formation along the Tainai River, Kitakanbara area, Niigata Prefecture, central Japan. *Jour. Japan. Assoc. Petrol. Technol.*, **68**, 561–569*.

Yamaji, A and Sato, H., 1989, Miocene subsidence of the Northeast Honshu Arc and its mechanism. *Mem. Geol. Soc. Japan*, no. 32, 339–349*.

Yamanoi, T., 1976, Pollen analysis of the Neogene sediments—The Tainai River basin, Niigata Prefecture. *Sci. Rep. Niigata Univ., Ser. E (Geol. and Mineral.)*, no. 4, 197–206*.

*: in Japanese with English abstract

Excursion guide to the radiolarians of the East China Sea near Sesoko Island, Okinawa, Japan: An important research station for living radiolarian studies

Atsushi MATSUOKA[*1], Noritoshi SUZUKI[*2], Tsuyoshi ITO[*3],
Katsunori KIMOTO[*4], Akihiro TUJI[*5], Ryo ICHINOHE [*6] and Xin LI[*7]

Abstract

The Okinawa Radiolarian Tour, an annual workshop on living radiolarians, has been held at the Sesoko Station, the Tropical Biosphere Research Center of the University of the Ryukyus in Okinawa Prefecture, Japan, since 1997. More than 200 researchers and students have joined this tour to observe living radiolarians. The tours have provided valuable knowledge on living radiolarians, such as faunal characteristics, biological activities, skeletal growth, and molecular phylogeny. In this guide, brief histories of radiolarian biological research and the Okinawa Radiolarian Tour are given. Practical, latest information on oceanographic conditions, travel, safety, and handling and storage procedures for radiolarian studies will be given at the Sesoko Station.

Key words: Okinawa Radiolarian Tour, living radiolaria, East China Sea, Kuroshio Current, Sesoko Station, faunal characteristics, biological activities, skeletal growth, molecular phylogeny, culture experiment

[*1] Department of Geology, Faculty of Science, Niigata University, Niigata 950-2181, Japan
[*2] Department of Earth Science, Graduate School of Science, Tohoku University, Sendai 980-8578, Japan
[*3] Stratigraphy and Tectonics Research Group, Research Institute of Geology and Geoinformation, Geological Survey of Japan, AIST, Tsukuba 305-8567, Japan
[*4] Research and Development Center for Global Change (RCGC), JAMSTEC, Yokosuka 237-0061, Japan
[*5] Department of Botany, National Museum of Nature and Science, Tsukuba 305-0005, Japan
[*6] Graduate School of Science and Technology, Niigata University, Niigata 950-2181, Japan
[*7] State Key Laboratory of Palaeobiology and Stratigraphy, Nanjing Institute of Geology and Palaeontology, Chinese Academy of Sciences, Nanjing 210008, China
    Corresponding author: A. Matsuoka,
    amatsuoka@geo.sc.niigata-u.ac.jp

Introduction

Scientific interest in radiolaria, marine holoplanktonic protists, have goes back at least to Tilesius (1818), who illustrated a living radiolarian cell. As the radiolaria have not only a long geologic range (Cambrian to Recent) but also inhabit all water depths in all open oceans including the Arctic Ocean (e.g., De Wever et al., 2001; Suzuki and Aita, 2011; Suzuki and Not, 2015), they have played an important role in paleontology, geology, and marine ecology. In particular, knowledge of living radiolarian biology has great potential as a source of information to reconstruct the group's biologic history through the Phanerozoic.

One of the authors, Atsushi Matsuoka, has worked with living radiolarians at the Sesoko Station (Fig. 1) of the University of the Ryukyus since 1992. An annual workshop on living radiolarians in Sesoko, called the Okinawa Radiolarian Tour, has been held since 1997. As Table 1 indicates, living specimens recovered from surface waters around Sesoko Island have provided valuable knowledge on living radiolarians, such as faunal characteristics, biological activity, skeletal growth, and molecular phylogeny. The Sesoko Station is in fact one of the most important research stations for living radiolarian studies in the world.

The brief guide to observing radiolarians during this tour has already been published in both Japanese (Matsuoka, 2002) and English (Matsuoka, 2007). In this article, we first provide a brief history of radiolarian biological study. More practical details and latest information such as oceanographic conditions, travel, safety, handling and storage for radiolarian studies will be given at the Sesoko Station.
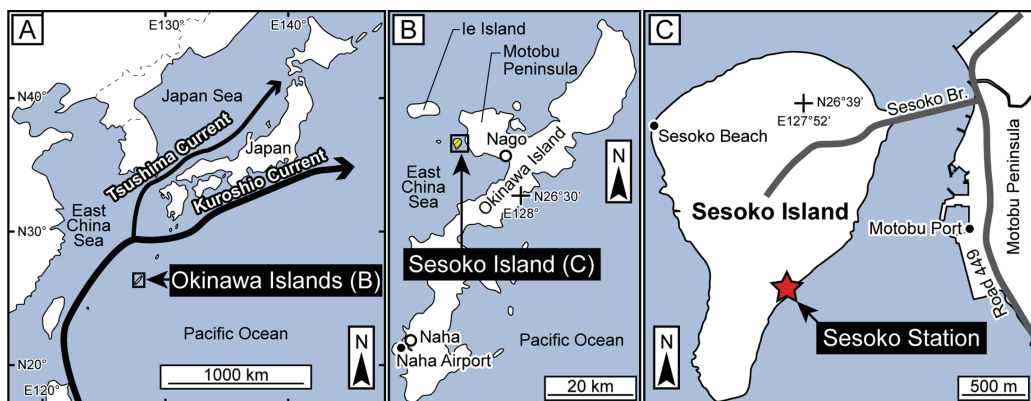
Fig. 1. Index map of the Sesoko Station with major warm ocean currents around the station.

Table 1. Major studies at the Sesoko Station.

Previous studies	Outline
Faunal characteristics	
Matsuoka (1993a)	Report of radiolarian fauna, composed of more than 30 species; comparison of the fauna with living radiolarians of the surface water near Barbados in the Caribbean Sea and indicating their similarities in the taxonomic components
Matsuoka (2009)	Observation of scanning electron microscopic images of radiolarian skeletons by using of sulfuric acid and showing ca. 60 species of the radiolarians
Matsuoka (2017)	Showing live and skeleton images of radiolarians (14 spumellarian and 15 nassellarian species) with transmitted light microscopy and scanning electron microscopy
Activities (Inc. feeding behavior and symbiosis)	
Matsuoka (1993a)	Observation of biological characters of nine species of living radiolarians; description of several biological characters of each species, such as activities of pseudopodia and color and size of symbionts
Suzuki and Sugiyama (2001)	Observation of axopodial activity of *Diplosphaera hexagonalis* Haeckel and recognition of cyclic extension and contraction of axopodia
Takahashi et al. (2003)	Observation of 29 species of living radiolarians to investigate their symbioses by using of epifluorescence microscope
Suzuki (2005)	Observation of axopodial activity of *Rhizosphaera trigonacantha* Haeckel having numerous fine axopodia (Type I axopodia) and few thick axopodia (Type II axopodia); clarification of the differences of these types of axopodia in shape and movement
Matsuoka (2007)	Finding a relationship between feeding behavior and shell morphology based on observation of living radiolarians
Sugiyama et al. (2008)	Observation of pseudopodial activities of *Eucyrtidium hexagonatum* Haeckel, *Pterocorys zancleus* (Müller), and *Dictyocodon prometheus* Haeckel; clarification of the relationships between pseudopodial activities and feeding behavior
Suzuki et al. (2009a)	Discovery of *Haliommilla capillaceum* (Haeckel) with a chain of extracellular cells; description of movement of the extracellular cells and pointed out the similarity to the sporogenesis of the host-specific parasitic dinoflagellate *Duboscquella* sp.
Suzuki et al. (2009b)	Report of distribution patterns of nuclei and symbionts of living radiolarians collected from the surface water around Sesoko Island and the Nansei Islands by using of C16H15N5 (DAPI)
Yuasa et al. (2012)	Observation and molecular anlysis on cyanobacterial symbionts within *Dictyocoryne profunda* Ehrenberg
Suzuki et al. (2013)	Discovery of novelty activity of *Streblacantha* sp. cf. *S. circumtexta* (Jørgensen)
Yuasa and Takahashi (2014)	Observation of repructive swarmers of *Sphaerozoum punctatum* (Huxley)
Yuasa and Takahashi (2015)	Description *Gymoxanthella radiolariae*, a symbiotic dinoflagellate from solitary polycystine radiolarians
Yuasa et al. (2016)	Observation of reproductive swarmers of *Didymocyrtis ceratospyris* Haeckel, *Pterocanium praetextum* (Ehrenberg), *Tetrapyle* sp., and *Triastrum aurivillii* Cleve
Skeletal growth	
Ogane et al. (2009)	Use of fluorescent compound $C_{20}H_{23}N_5O_3$ (PDMPO) to reveal skeletal growth of polycystine radiolarians
Ogane et al. (2010)	Applicaton of PDMPO to 50 cells from 22 species; clarification that skeletal thickening growth commonly occurs in polycystine radiolarians and that the patterns of skeletal growth differ by species
Ogane et al. (2014)	Discovery of assimilation of siliceous matter within pseudopodia; suggestion of 'pseudo silica absorption hypothesis'
Molecular phylogeny	
Takahashi et al. (2004)	Examination of the Family Spongodiscidae, including *Dictyocoryne profunda* Ehrenberg, *D. truncatum* (Ehrenberg), and *Spongaster tetras* Ehrenberg, with using of 18S ribosomal DNA sequence
Yuasa et al. (2004)	Examination of the Class Phaeodarea, including *Protocystis xiphodon* (Haeckel), *Challengeron diodon* Haeckel, and *Conchellium capsula* Borgert, with using of 18S ribosomal DNA sequence
Yuasa et al. (2005)	Examination of the Family Spongodiscidae (Class Polycystinea, Order Spumellarida) and the Family Pterocorythidae (Class Polycystinea, Order Nassellarida) with using of 16S ribosomal DNA sequence
Yuasa et al. (2006)	Examination of the Class Phaeodarea, including *Protocystis xiphodon* (Haeckel), *Challengeron diodon* Haeckel, and *Conchellium capsula* Borgert, with using of 18S ribosomal DNA sequence
Yuasa et al. (2009a)	Examination of *Hexacontium pachydermum* Jørgensen, *Cladococcus viminalis* Haeckel, *Arachnosphaera myriacantha* Haeckel, and *Astrosphaera hexagonalis* Haeckel with using of 18S ribosomal DNA sequence
Yuasa et al. (2009b)	Description of a simple method for obtaining 18S ribsomal DNA sequencs from a single radiolarian specimen

Histories of radiolarian biological research and the "Okinawa Radiolarian Tour"

There is a long history of study of radiolarian biology. Biological studies were carried out in Messina between Catania and the Italian Peninsula by German protozoologists as early as the 19th century (Müller, 1859; Haeckel, 1862; Hertwig, 1879), and led to discovery of yellowish brown photosynthetic microbiota, previously called "zooxanthella", for the first time in a marine organism - from the collodarian radiolarian *Collozoum inerme* (Brandt, 1881). Parasites were described from Taxopodia and Acantharia by German protozoologists (Koeppen, 1894; Borgert, 1898) and afterwards the cytological structure and parasites of radiolarians were detailed by French workers at the Villefranche-sur-mer Oceanological Observatory in 1950s–1960s (Hollande, 1953; Hollande and Enjumet, 1953, 1955, 1960; Cachon, 1964). Jean Cachon and Monique Cachon cooperated in clarifying the development of the cytoskeleton and its function in the 1970s (Cachon and Cachon, 1969, 1971, 1972a, 1972b, 1976, 1978, 1980). A Russian cytologist, Igor B. Raikov, summarized available knowledge of the radiolarian and phaeodarian nucleus in 1978, and the English version of this book was published four years later (Raikov, 1982). Despite these studies' progress on radiolarian cytology, little was known about physiological ecology at that time. Experimental physiology was studied mainly by Americans in 1970s to 1990s. Their results and interpretations were summarized in many publications (Anderson, 1978, 1980, 1983, 1984, 1986, 1993, 1994, 2012; Swanberg and Harbison, 1980; Anderson et al., 1983, 1984, 1986, 1989a, 1989b, 1989c; Swanberg, 1983; Swanberg et al., 1985, 1986, 1990; Swanberg, and Bjørklund, 1987; Swanberg and Caron, 1991; Swanberg and Eide, 1992; Caron et al., 1995; Michaels et al., 1995).

In the 1990s, A. Matsuoka and Kazuhiro Sugiyama independently stayed at the Lamont Doherty Geological Observatory of Columbia University and learnt how to work on living radiolarians under the guidance of O. Roger Anderson (Anderson and Matsuoka, 1992; Matsuoka, 1992; Matsuoka and Anderson, 1992; Sugiyama and Anderson, 1997). Just after coming back from the U.S., Matsuoka started making an effort to find suitable marine stations for the study of living radiolarians in Japan. Full-color images of living radiolarians around Japan were reported for the first time by Matsuoka (1993a) who collected these specimens in 1992 from surface waters in the East China Sea around Sesoko Island, Okinawa Prefecture, Japan (Table 2). From 1992 to 1996, Matsuoka prepared research equipment for living radiolarian research with the assistance of Satoshi Funakawa and Katsunori Kimoto. In 1997, he organized the first Observation Tour of Living Radiolarians at the Sesoko Station, the Tropical Biosphere Research Center, the University of the Ryukyus. The participants were K. Sugiyama, K. Kimoto, Katsuo Sashida, Osamu Takahashi, and Hideto Okuda. Since then this "tour" or workshop has been held more than 20 times almost every year. In 2002 the tour could not be organized due to reconstruction of buildings at the Sesoko Station. Most radiolarian workers in Japan have attended this tour and some of them

have become radiolarian biologists. The total number of the participants exceeds 200 people and includes American, Chinese, Filipino, French, and other foreigners.

The "Observation Tour of Living Radiolarians at Sesoko" is occasionally simply called "Okinawa Tour" or "Okinawa Radiolarian Tour". This tour efficiently contributed to living radiolarian and other protistan studies such as planktonic foraminifers and dinoflagellates (Suzuki and Sugiyama, 2001; Takahashi et al., 2003; Suzuki, 2005; Kimoto, 2005; Kimoto and Matsuoka, 2006; Sugiyama et al., 2008; Ogane et al., 2009, 2010, 2014; Suzuki et al., 2009a, 2009b, 2013; Probert et al., 2014; Biard et al., 2015; Takagi et al., 2016). The first molecular phylogenetic data of Spumellaria (exclusive of Collodaria) were also obtained from cells collected near Sesoko Island (Takahashi et al., 2004). After their participation in a couple of the tours, O. Takahashi and his colleague Tomoko Yuasa have regularly visited the Sesoko Station and successfully continue their own research (Yuasa et al., 2004, 2005, 2006, 2009a, 2009b, 2012, 2016; Yuasa and Takahashi, 2014, 2015).

The experience accumulated at the Sesoko Station has been transferred to other marine

Table 2. Participant numbers of the "Okinawa Radiolarian Tour" and major activities in Sesoko.

Year	Month	Tour number	Number of participants	Publication	Note
1992	Nov.		1		Matsuoka's first visit to the Sesoko Station
1993	-	-	-	Matsuoka (1993a)	
1994	-	-	-		
1995	Sept.		2		
1996	Sept.		3		
1997	Sept.	1st	6		Okinawa Radiolarian Tour starts
1998	Oct.	2nd	16		
1999	Sept.	3rd	12		
2000	July	4th	12		
2001	May-Sept.		6		Matsuoka's 5 months stay in Motobu
2002	March		4	Matsuoka (2002)	
	Nov.		6		
2003	May		1	Takahashi et al. (2003)	
	Nov.	5th	12		
2004	May		2		
	Nov.	6th	12		58th Symposium of Society of Science on Form
2005	April		2		
	Nov.	7th	7		
2006	Dec.	8th	11	Kouduka et al. (2006), Yuasa et al. (2006)	
2007	Nov.	9th	24	Matsuoka (2007)	
2008	Nov.	10th	21	Sugiyama et al. (2008)	Symposium for 10th Radiolarian Tour
2009	Nov.	11th	17	Matsuoka (2009), Ogane et al. (2009), Suzuki et al. (2009a, 2009b)	
2010	Dec.	12th	15	Ogane et al. (2010)	
2011	Dec.	13th	17		Japan-France Sympoium on Radiolarians
2012	Dec.	14th	5	Yuasa et al. (2012)	
2013	Dec.	15th	7		
2014	Dec.	16th	5		
2015	Nov.	17th	10		
2016	Oct.	18th	5		
2017	Oct.	19th		Matsuoka (2017)	Excursion of InterRad XV in Niigata 2017

stations in Japan. Matsuoka has carried out living radiolarian research at the Sado Marine Station of Niigata University since 2000 (Matsuoka et al., 2001, 2002; Itaki et al., 2003; Kurihara and Matsuoka, 2004, 2005, 2009, 2010; Kurihara et al., 2006, 2007, 2008). Although living radiolarians have been reported and studied from a variety of sampling locations (e.g., Sashida and Kurihara, 1999; Ishitani et al., 2011, 2012a, 2012b, 2012c, 2014; Ishitani and Takishita, 2015; Decelle et al., 2012a, 2012b, 2012c, 2013, 2014), studies in 2000s–2010s frequently used plankton samples collected around Sesoko Island (Tables 1, 2).

Location, climate, and oceanographic condition

Sesoko Island (26° 38' 46" N, 127° 51' 54"E) is located 600 m west of the Motobu Peninsula of Okinawa Island (Honto). Sesoko Island is a 7.3 km circumference pear-shaped island with a population of 800 people, which is connected with the Motobu Peninsula by the Sesoko Bridge (Sesoko-Oh-hashi; 762 m in total length). The Sesoko Station is located on the east coast of the island (Fig. 1).

Okinawa has a subtropical climate so that the air temperature is hot in summer (av. 28°C, min: 24°C, max: 33°C) and warm in winter (av.: 16°C, min: 10°C, max: 25°C). Late October is presumably 21–23°C on average. From July to early October, typhoons often cross over Okinawa. The temperature of surface water at the sampling site off Sesoko Island on 31 October in 2016 was 28.0°C.

Marine organisms around Sesoko are affected by the Kuroshio Current, a northward-flowing, strong western boundary current derived from the westward-flowing North Equatorial Current off the east coast of the Philippines (Fig. 1A). The Kuroshio Current is characterized by warm, high salinity and low nutrients; as a consequence, the radiolarians around Sesoko Island represent a subtropical fauna.

Travel information: transportation

The capital city of Okinawa, "Naha", is located in the south of the island, as is the Naha Airport. The Naha Airport is a hub airport for Okinawa and neighboring islands so that over 100 domestic flights are available every day. International flights are also available. The connection between the airport and city area of Naha is very easy via the Okinawa Urban Monorail (Yui Rail).

Public transit for Sesoko Island is not so convenient. A bus network exists on Okinawa Island but bus services to Sesoko Island are limited in number. Frequent bus services are available between Naha and Nago, located at the base of the Motobu Peninsula (Fig. 1B). Taking a taxi is the recommended way to get to Sesoko Station from the Nago Bus Terminal.

Life in the Sesoko Station

For the use of the Sesoko Station, you need to submit an application form prior to your visit. Detailed information is available at the following web page: "User Instructions for Sesoko Station, Tropical Biosphere Research Center, the University of the Ryukyus" [URL1].

1. Equipment

Guests can use a laboratory, a lecture room, and a galley in a building upon request. Any equipment such as beakers and Kleenex is not provided by the station (Table 3). Thus, the hosts or group leaders must bring all equipment and facilities including microscopes, bottles and consumables themselves. Furthermore, the hosts or group leaders must receive and dispatch baggage by themselves in the station. Other attendees are responsible only for private daily commodities like extra clothes and shoes.

2. Accommodations

Accommodations for "the Okinawa Tour" are arranged by the host or group leader.

3. Meals

There is no meal supply in the Sesoko Station, so that you need to go out for meals or prepare food by yourself. If your group gets permission to use the kitchen in the station, you can cook by yourself.

The day of sampling is special. In general, sampling will start in the morning (~ 9 o'clock) with the sailing of the boat. The boat will dock again by 11 o'clock. Onshore, the living radiolarians must be picked out from the sampling bottles as soon as possible to keep them healthy. For this reason, there is no time to have lunch, so light meals (e.g., snacks) might be better on sampling day.

From sampling to observations

This chapter explains the processes from preparation of sampling tools before a sampling day to observational methods and techniques for living radiolarians. For each process, an outline is given first, followed by the detailed steps.

1. Before the sampling day: Setup of the laboratory and checking sampling tools

Outline: All equipment and facilities, including a plankton net, should be checked by each sampling group and set up in the laboratory as compactly as possible, before the sampling day.

(1) All equipment and facilities should be set up in the laboratory at least one day before the

Table 3. Example list of equipment for collection and observation of living radiolarians.

Goods	Notes	Prepared by... participant	host
Microscope			
Inverted microscope	4X, 10X, 20X(LWD), 40X(LWD) objective lens		+
Digital video (or camera)	equiped to microscope		+
*Binocular microscope	If you pick up larger radiolarians		+
*Lights for bioncular microscope			+
*Upright microscope with water objective lens			+
USB flash drive	The people who want to bring back the captured photos	+	
*Tool kit	including tools to assemble and disassemble the microscope		+
Pick-up tools			
Adjustable Air Displacement Pipette	P20 (0-20 µL). Using to pick up radiolarians under a microscope		+
Disposable Tip	for your selected air displacement pipette		+
Transfer pipettes	variable sizes		+
Measuring pipettes	Move collected water to a dish. It is preferable to use the pipettes with larger opening at the tip (5 mL type preferable)		+
Glass petri dish	To find radiolairans cells from the collected water. Size is vabile for your purpose and microscopes		+
Plastic petri dish (or cell culture dish)	35 mm in diameter or like. This plastic petrish is used instead of large glass petri dish		+
Observation tools			
Flat bottom cell culture plates (=multiwell inesert system)	6-well (each cell diameter is 3.5 cm) and/or 12-well (2.26 cm), for hading radiolarian cells		+
*Glass bottom dish (= cell imaging dish)	The bottom of the dish is made of cover glass		+
Slide glass			+
Cover glass	18 mm x 18 mm, 24 mm x 32 mm		+
*Imaging plate cover glass (glass bottom well culture plate)	Similar to flat bottom cultureplates but its bottom is made of cover glass		+
Clear glass vials with screw caps (screw vials)	SV-20 is recommended		+
Consumers			
Aluminium foil			+
Dry wipes and cloths	To wipe on the desk, microscope and anywhere with sea water		+
waste bag			+
Sampling tools			
Cotton work gloves	To use on ship		+
Raincoat jacket and pants	For savety, you may not ware a long rain coat. Raincoat jacket and pants should be weared prior to your boarding.	+	
Shoes aviable wet conditions	Slippers, moccasins, ballet flats, sandals, high-heeled, and pump are strongly prohibited on boarding	+	
Plankton nets (hand net) with ropes	The length of rope is roughly 15 m		+
Wide mouth plastic bottle(jars) with screw plastic caps	1 L or 2 L. Keeping each towing sample onboard and in the labolatory		+
Bucket and water tank	Seawater at the sampling point is ready for labolatory work		+
GPS			+
Portable salinity meter, temperture meter, etc.			+
Travel sickness tablets		+	
Extra clothes for change after sampling	The station strongly prohibts to eneter into the building with wetted condition	+	
Towels	See above	+	
Protections for sunlight	sun glass, sunscreen	+	
Sorting tools			
Sieves	ca. 7.5 cm in diameter. 30–50 µm, 63–65 µm, and 1–4 mm openings are recommended		+
Stationery products			+
Chemicals and special equipment			
Ethanol	For DNA analysis		+
*Formalin	To examine stains		+
*Hydrogen peroxide	To revmoe protoplasm		+
*Sulfuric acid	To burn out protoplasm		+
*Millipore membrane filter holder assembly			+
*Manual operated vacuum pump			+
*Millipore membrane filter holder assembly	0.025 µm pore size for DNA and 0.45 µm pore size for other purposes		+
*Microtubes	To keep a single cell		+

planned sampling day.

(2) Size and material of the plankton net will depend on your research purpose. Matsuoka (2007) used 44 or 100 μm mesh plankton nets, while Suzuki et al. (2009) used a 38–43 μm mesh plankton net. We have also used larger cod-ends (the small, tip end) of the plankton nets for collecting living radiolarians.

(3) Sampling tools should also be prepared so that they can be easily transported to the research boat on the sampling day. The boat is so small that hosts and leaders should minimize the duplication of sampling tools, e.g. by sharing among sampling groups.

2. On the sampling day: Decisions and sailing

Outline: Going out or canceling the sampling trip is decided by the boat's captain. If we are given a go, we will put on our life-jackets and board on the boat with our sampling tools and personal bags. While cruising from the port to a sampling location, everyone must remain seated on the floor of the boat.

(1) The host will first discuss the sampling plan, date and hour with the captain of the boat at the Sesoko Station.

(2) The final decision on going or canceling sampling is made by the captain early in the morning of the chosen sampling day. The decision will depend largely on the weather forecast, especially on the sea surface roughness.

(3) As soon as we have the captain's approval to go out, our sampling tools should be brought quickly to the boat. Personal belongings will need to be put in a single waterproof bag.

(4) Shipboard participants should take along a change of clothes as well as a normal pair of shoes for after landing, which should be left somewhere outside of the building. Before boarding, we need to put on a rain jacket, coat, and a pair of shipboard shoes. Bring a drink as needed. It is obvious that while on board that we can become completely soaked with seawater, so that electric devices which are non-water proof such as mobile phones should be wrapped in a plastic bag or left in the building. If you get seasick easily, taking travel sickness tablets is recommended before boarding.

(5) Once the captain arrives, you will receive and put on the life-jacket from the lateral side of the boat (Fig. 2A), and take the sampling tools and your personal bag on board. Before you board on the boat, the safety instructions will be provided. Please follow the instructions to the letter for our safety.

(6) Soon after you board the boat in port (Fig. 2B), (a) you must sit down on the floor; (b) never stand up, never move, never go to the foremost part of the boat (bow); and (c) MUST keep your hand away from the any edge of the boat at all times (in particular, while in port). You may stand up and move when the boat stops at a sampling location.

(7) It may take 20 to 30 minutes to reach the sampling station from the port.

Fig. 2. Photographs of collecting and observational methods of living radiolarians. **A:** Sesoko Station and boat dock. **B:** Research boat for collecting living plankton. **C:** Plankton net streaming in the current. **D:** Pulling up the plankton net. **E:** Transferring plankton-bearing sea water to a bottle. **F:** Picking up radiolarians by using a binocular microscope. **G:** Transfer of a radiolarian individual to a flat bottom cell culture plate.

3. Work at the sampling station: Measuring water characteristics and collecting plankton-bearing seawater

Outline: At the sampling station, we will begin by measuring physical oceanic data. Then each sampling group will do their tows with the plankton net, each in their own working space. After several minutes (typically 5 minutes), each group will pull on the rope of the plankton net and quickly transfer the plankton-bearing seawater from a collecting bucket to a sampling bottle.

(1) When the boat arrives at the sampling station, the captain will stop the engine to avoid rolling the plankton nets together. People who get seasick should sit on the floor near the edge of the boat and try not to get in the way of the sampling. In particular, you must not lean over the boat edge all the time.

(2) At first, physical oceanic data (position, water depth, salinity, water temperature etc.) will be acquired. While this is being done, each sampling group should get their own plankton nets and work spaces ready. The spaces will be assigned by the host. Sampling groups can start sampling when ready. Tie the rope firmly to the boat to avoid losing your plankton net.

(3) Tow your plankton net carefully so as not to get entangled with other nets and ropes. Plankton nets are gently deployed into the sea with the opening facing into the direction of the wind (Fig. 2C). No gear to hoist the net out of the water is available on boat.

(4) The net should be towed from 3 to 7 mins (regularly 5 min) to capture a sufficient volume of plankton. The water depth to tow the net at depends on the sampling plan. During sampling, seawater will be collected in sampling bottles for use at the onshore laboratory.

(5) Recover the net at the end of the towing time by pulling on the rope (Fig. 2D). Before you completely pull it out the water, the interior cod-end of the net should be carefully washed with seawater to recover attached plankton. This attached plankton is handled differently depending on sampling purpose. For estimation of the total biomass, all plankton must be put into a collecting bucket. But for observing healthy radiolarians, one should never use the attached (= damaged) plankton from the net and the cod-end, so for studying healthy radiolarians do not put attached plankton in the collecting bucket.

(6) Soon after the plankton net is drawn back on the boat, the plankton in the collection bucket is gently transferred to the sampling bottle with additional fresh seawater (Fig. 2E), to decrease the planktonic density in the bottle. The bottles are kept in a cold box to maintain the freshness of the samples. The bottles with plankton should be full of seawater.

(7) Repeat towing several times as needed. However, we should go back to the Sesoko Station as soon as possible to begin the separation of specimens, so sampling repetitions should be limited.

4. Return to the Sesoko Station: Flushing seawater before entering the laboratory

Outline: On return the port, everything exposed to saltwater should be washed with freshwater. Participants should also take shower and change clothes.

(1) After we finish sampling, all things should be cleared up promptly as the boat may leave again.

(2) After we return the port, all tools and samples should be brought back to the laboratory. However, bringing things wet with seawater inside is strictly prohibited by station rules so that everything, including the participants, needs to be washed with fresh water before we enter in the building. A few members should be chosen to shower first so that they can bring the samples quickly inside. The remaining people can then bring the tools to the shower room where they are washed with freshwater. We then take our own showers and change to dry clothes and shoes.

(3) The washed but wet items should only be brought into the laboratory after being wiped out completely.

5. First few hours in the laboratory: First sorting and observation

Outline: The first step is to extract the fresh radiolarians from the collected seawater in the sampling bottles using binocular stereomicroscopes and/or inverted microscopes. The radiolarians are transferred to flat bottom cell culture plates.

(1) Living radiolarians will weaken quickly within a few hours under the "plankton soup" conditions that exist in the collecting bottles. Fresh radiolarians must thus be extracted as soon as possible. Due to this reason, we should separate radiolarians from other plankton before the making any observations.

(2) In order to settle the radiolarians at the bottom of the bottle, the sampling bottles are gently placed for 5–10 minutes near the sink for sea water in the laboratory.

(3) While waiting, fill each cell of the flat bottom cell culture plates with the seawater which was collected at the sampling location (2/3 height of each cell is enough). The flat bottom cell culture plates are sterilized, so they don't need to be washed when using a new one. This is true as well for the other observation and picking tools.

(4) To start, bring a glass petri dish or a plastic petri dish to the sink where a bottle is placed, transfer an appropriate volume of plankton soup into the dish, and then wipe off the dish bottom. The bottom of the dish must *always* be kept completely dry.

(5) The dish is carefully placed on the stage of a microscope.

(6) Two types of microscopes are used: the Niigata University research group regularly uses the binocular stereomicroscopes, while the Tohoku University research group uses the inverted microscopes.

   6a. Binocular stereomicroscope – Good for picking large radiolarians in a wide area.

   6b. Inverted microscope – Good for picking any size of radiolarians but view area is narrow.

(7) Start to pick-out radiolarians (Fig. 2F). If you are interested in polycystines, it is better for you to ignore acantharians because they are easily misidentified as spumellarians. Radiolarians can be picked up with an adjustable air displacement pipette (P20 and yellow disposable tips), transfer pipettes, or other tools.

(8) Once a radiolarian cell has been siphoned into a pipette, quickly transfer it to the flat bottom cell culture plate (Fig. 2G). Effective techniques to avoid damage to the radiolarian cell are as follows. 1) You don't need to check whether you successfully moved a cell or not. 2) You don't need to be concerned if other organisms get transferred along with the target radiolarian specimen. 3) If you use a 6-cell flat bottom cell culture plate, 10–20 radiolarian specimens can put together in a cell while 5–10 radiolarian specimens can be placed in cells of 12-cell flat bottom culture plates. 4) It is not recommended to mix unhealthy-looking specimens with fresh ones. The extraction process continues for several hours until radiolarians in the plankton soup are no longer viable, or nearly dead.

6. After first observation: Second sorting

Outline: If healthy radiolarians could not be found in the first order samples, examine the remaining liquid in the sampling bottle as a second sorting.

(1) If you could not find any healthy specimen in the first order samples, move to the second sorting. Before starting, another flat bottom cell culture plate is prepared with fresh seawater.

(2) Under an inverted microscope, carefully look for radiolarians (10x or 20x objective lenses are regularly used). Radiolarians tend to stay on the bottom of the periphery of a cell in the flat bottom cell culture plate. Very healthy-looking radiolarian specimens sometimes float in the middle or upper level of the seawater, so these specimens may be overlooked under an inverted microscope. In this case, carefully tap the flat bottom cell culture plate to shrink their pseudopodia, which causes them to settle.

(3) In the second sorting, it is important to pipette individuals without contaminant substances.

Important notice on the laboratory work

(1) When handling seawater, take special care not to spill it on the microscope, desk or anywhere else except in the sink. All spills must be quickly wiped up. Once seawater gets into microscopes and electric devices, they will be damaged.

(2) In the first sorting, spherical radiolarians are often found with a lot of attached organic matter. As some radiolarians can shed this attached organic matter, pick them up and transfer them into a separate cell of the flat bottom cell culture plate. These specimens should be kept separated from other "clean" radiolarian cells.

(3) Tiny radiolarians like the Plagiacanthidae, Lophophaenidae, Stephaniidae, and
    Sethophormidae tend to be passed over in the first sorting not only under the binocular
    stereomicroscope but also the inverted microscope.

(4) Pylonioidea specimens tend to be wrapped with gelatinous adhesive protoplasm and look
    immobile.

(5) Several radiolarian species can be only found with phase-contrast imaging.

Concluding remarks

   People generally find a fantastic plankton world under the microscope. We also have
been fascinated by beautiful radiolarians and have been giving more than a passing thought
to the long history of radiolarians and past climates. We believe anyone participating the
Okinawa Tour will have this experience. The Okinawa Tour is not only a simple hands-on
activity but also is one entrance to an important field in future radiolarian science. Matsuoka
(2007) pointed out that research on living radiolarians would provide us with fundamental
data for a better understanding of the past marine ecosystems. However, our knowledge on
the role of radiolarians, even in modern marine environments, is still limited. As Suzuki and
Not (2015) summarized in a recent research perspective on living radiolarians, very basic
information on their biology and ecology, such as life cycle and feeding behavior, are still
missing. As living radiolarians are found in open oceans just about everywhere in the world,
anyone can start to study them. We do hope that this paper contributes to being able to
handle living radiolarians as a first step towards your own studies.

References

Anderson, O. R., 1978, Light and electron microscopic observations of feeding behavior, nutrition, and reproduction in laboratory cultures of *Thalassicolla nucleata*. *Tissue & Cell*, **10**, 401–412.

Anderson, O. R., 1980, Radiolaria. *In* Levandowsky, M. and Hutner, S. H. eds., *Biochemistry and Physiology of Protozoa (2nd edition). Volume 3*, Academic Press, N.Y., 1–42.

Anderson, O. R., 1983, *Radiolaria*. Springer-Verlag, New York, 355p.

Anderson, O. R., 1984, Cellular specialization and reproduction in planktonic foraminifera and Radiolaria. *In* Steidinger, K. and Walker, L. eds., *Marine Plankton Life Cycle Strategies*, Chemical Rubber Co. Press, Boca Raton, Florida, 36–66.

Anderson, O. R., 1986, Silicification in Radiolaria-deposition and ontogenetic origins of form. *In* Leadbeater, B. S. and Riding, R. eds., *Biomineralization in Lower Plants and Animals*, Oxford University Press, Oxford, 375–391.

Anderson, O. R., 1993, The trophic role of planktonic foraminifera and Radiolaria. *Marine Microbial Food Webs*, **71**, 31–51.

Anderson, O. R., 1994, Cytoplasmic origin and surface deposition of siliceous structures in Sarcodina. *Protoplasma*, **181**, 61–77.

Anderson, O. R., 2012, Living together in the plankton: A survey of marine protist symbioses. *Acta Protozool.*, **52**, 1–10.

Anderson, O. R., Hemleben, C., Spindler, M. and Lindsey, J., 1986, A comparative analysis of the morphogenesis and morphometric diversity of mature skeletons of living *Didymocyrtis tetrathalamus tetrathalamus* and *Hexalonche amphisiphon*. *Marine Micropaleont.*, **11**, 203–215.

Anderson, O. R., Bennett, P., Angel, D. and Bryan, M., 1989a, Experimental and observational studies of radiolarian physiological ecology: 2. Trophic activity and symbiont primary productivity of *Spongaster tetras tetras* with comparative data on predatory activity of some Nassellarida. *Marine Micropaleont.*, **14**, 267–273.

Anderson, O. R., Bennett, P. and Bryan, M., 1989b, Experimental and observational studies of radiolarian physiological ecology: 1. Growth, abundance and opal productivity of the spongiose radiolarian Spongaster tetras tetras. *Marine Micropaleont.*, **14**, 257–265.

Anderson, O. R., Bennett, P. and Bryan, M., 1989c, Experimental and observational studies of radiolarian physiological ecology: 3. Effects of temperature, salinity and light intensity on the growth and survival of *Spongaster tetras tetras* Maintained in Laboratory Culture. *Marine Micropaleont.*, **14**, 275–282.

Anderson, O. R. and Matsuoka, A., 1992, Endocytoplasmic microalgae and bacteroids within the central capsule of the radiolarian *Dictyocoryne truncatum*. *Symbiosis*, **12**, 237–247.

Anderson, O. R., Swanberg, N. R. and Bennett, P., 1983, Assimilation of symbiont-derived photosynthates in some solitary and colonial Radiolaria. *Marine Biol.*, **77**, 265–269.

Anderson, O. R., Swanberg, N. R. and Bennett, P., 1984., An estimation of predation rate and relative preference for algal versus crustacean prey by a spongiose skeletal radiolarian. *Marine Biol.*, **78**, 205–207.

Biard, T., Pillet, L., Decelle, J., Poirier, C., Suzuki, N. and Not, F., 2015, Towards an Integrative Morpho-molecular Classification of the Collodaria (Polycystinea, Radiolaria). *Protist*, **166**, 374–388.

Borgert, A., 1898, Beiträge zur Kenntnis des in *Sticholonche zanclea* und Acanthometridenarten vorkommenden Parasiten (Spiralkörper Fol, *Amoebophrya* Köppen). *Zeit. wissen. Zool.*, **63**, 141–186.

Brandt, K., 1881, Untersuchungen an Radiolarien. *Monat. könig. Preuß. Akad. wissen. Berlin*, **1881**, 388–404.

Cachon, J., 1964, Contribution à l'étude des Péridiniens parasites. Cytologie, cycles évolutifs. *Ann. Sci. Natur., Sér. 12, Zool. Biol. Animal.*, **6**, 1–158.

Cachon, J. and Cachon, M., 1969, Révision systématique des Nassellaires Plectoidea à propos de la description d'un nouveau représentant, *Plectagonidium deflandrei* nov. gen. nov. sp. *Arch. Prot.*, **111**, 236–251.

Cachon, J. and Cachon, M., 1971, Le système axopodial des Radiolaries Nassellaires. *Arch. Prot.*, **113**, 80–97.

Cachon, J. and Cachon, M., 1972a, Le système axopodial des Radiolaires Sphaeroïdés. I. Centroaxoplastidiés. *Arch. Prot.*, **114** (1/2), 51–64.

Cachon, J. and Cachon, M., 1972b, Le système axopodial des Radiolaires Sphaeroïdés. II. Les Périaxoplastidiés,

III. Les Cryptoaxoplastidiés (Anaxopastidiés), IV. Les fusules et le système rhéoplasmique. *Arch. Prot.*, **114** (3), 291–307.

Cachon, J. and Cachon, M., 1976, Le Système axopodial des Collodaires (Radiolaires Polycystines) 1. Les exo-axoplastidíes. *Arch. Prot.*, **118**, 227–234.

Cachon, J. and Cachon, M., 1978, Constitution infrastrusturale des microtubules du systeme axopodial des Radiolaires. *Arch. Prot.*, **120**, 229–231.

Cachon, J. and Cachon, M., 1980, Axopod regeneration in *Sticholonche zanclea*: Transport and positioning mechanism of cytoplasmic structure. *Arch. Prot.*, **123**, 84–98.

Caron, D. A., Michaels, A. F., Swanberg, N. R. and Howse, F. A., 1995, Primary productivity by symbiont-bearing planktonic sarcodines (Acantharia, Radiolaria, Foraminifera) in surface waters near Bermuda. *Jour. Plankton Res.*, **171**, 103–129.

De Wever, P., Dumitrica, P., Caulet, J. P., Nigrini, C. and Caridroit, M., 2001, *Radiolarians in the Sedimentary Record*. Gordon and Breach Science Publishers, Amsterdam, 533p.

Decelle, J., Probert, I., Bittner, L., Desdevises, Y., Colin, S., de Vargas C, Gali, M., Simó, R. and Not, F., 2012a, An original mode of symbiosis in open ocean plankton. *PNAS*, **109** (44), 18000–18005.

Decelle, J., Siano, R., Probert, I., Poirier, C. and Not, F., 2012b, Multiple microalgal partners in symbiosis with the acantharian *Acanthochiasma* sp. (Radiolaria). *Symbiosis*, **57** (1-3), 233–244.

Decelle, J., Suzuki, N., Mahé, F., de Vargas C and Not, F., 2012c, Molecular phylogeny and morphological evolution of the Acantharia (Radiolaria). *Protists*, **163**, 435–450.

Decelle, J., Martin, P., Paborstava, K., Pond, D.W., Tarling, G., Mahé, F., de Vargas C, Lampitt, R. and Not, F., 2013, Diversity, ecology and biogeochemistry of cyst-forming Acantharia (Radiolaria) in the oceans. *PLoS One*, **81**, e53598.

Decelle, J., Romac, S., Sasaki, E., Not, F. and Mahé, F., 2014, Intracellular diversity of the V4 and V9 regions of the 18S rRNA in marine protists (radiolarians) assessed by high-throughput sequencing. *PLoS One*, **98**, e104297.

Haeckel, E., 1862, *Die Radiolarien (Rhizopoda Radiolaria). Eine Monographie. Tafel 1*. Reimer, Berlin, 572p.

Hertwig, R., 1879, *Der Organismus der Radiolarien*. Denkschriften der Medicinisch-Naturwissenschaflichen Gesellschaft zu Jena, 2(3), Gustav Fischer, Jena, 129–277, 1–10 pls.

Hollande, A., 1953, Compléments sur la cytologie des Acanthaires et des Radiolaires. *In* Grasse, P. P. ed., *Traite de Zoologie, Anatomie, Systematique, Biologie, volume 1(2)*, Masson, Paris, 1089–1100.

Hollande, A. and Enjumet, M., 1953, Contribution a l'etude biologique des spherocollides (Radiolaires Collodaires et Radiolaires Polysyttaires) et de leurs parasites. Pt. 1. Thalassicollidae, Physematidae, Thalasophysidae. *Ann. Sci. Natur., Ser. 11, Zool. Biol. Animal.*, **15**, 99–183.

Hollande, A. and Enjumet, M., 1955, Parasites et cycle évolutif des Radiolaires et des Acanthaires. *Bull. Trav. Publ. Stat. d'Aquicul. Pêch. Castigl.*, **7**, 151–176.

Hollande, A. and Enjumet, M., 1960, Cytologie, évolution et systématique des Sphaeroïdés (Radiolaires). *Arch. Mus. Nat. d'Hist. Natur., Sér.* 7, **7**, 1–134.

Ishitani, Y., Ishikawa, S. A., Inagaki, Y., Tsuchiya, M., Takahashi, K. and Takishita, K., 2011, Multigene phylogenetic analyses including diverse radiolarian species support the "Retaria" hypothesis — The sister relationship of Radiolaria and Foraminifera. *Marine Micropaleont.*, **81**, 32–42.

Ishitani, Y., Kamikawa, R., Yabuki, A., Tsuchiya, M., Inagaki, Y. and Takishita, K., 2012a, Evolution of Elongation Factor-Like (EFL) protein in Rhizaria is revised by radiolarian EFL gene sequences. *Jour. Eukaryot. Microbiol.,* **59**, 367–373.

Ishitani, Y., and Takishita, K., 2015, Molecular evidence for wide vertical distribution of the marine planktonic protist *Larcopyle buetschlii* (Radiolaria) in a semi-enclosed marginal sea. *Jour. Plankton Res.*, **37**, 851-856.

Ishitani, Y., Ujiié, Y., de Vargas C, Not, F. and Takahashi, K., 2012b, Phylogenetic relationships and evolutionary patterns of the Order Collodaria (Radiolaria). *PLoS One*, **7,** e35775.

Ishitani, Y., Ujiié, Y., de Vargas C, Not, F. and Takahashi, K., 2012c, Two distinctive lineages in the radiolarian Order Spumellaria having different ecological preference. *Deep-Sea Res. II,*, **61–64**, 172–178.

Ishitani, Y., Ujiié, Y., and Takishita, K., 2014, Uncovering sibling species in Radiolaria: Evidence for ecological partitioning in a marine planktonic protist. *Molecular Phylogenetics Evo.*, **78**, 215–222.

Itaki, T., Matsuoka, A., Yoshida, K., Machidori, S., Shinzawa, M. and Todo, T. 2003, Late spring radiolarian

fauna in the surface water off Tassha, Aikawa Town, Sado Island, central Japan, *Sci. Rep. Niigata Univ. (Geol.)*, no. 17, 41–51.

Kimoto, K. 2005. The ecology of living planktic foraminifera. (DVD) JAMSTEC Press.

Kimoto, K. and Matsuoka, A., 2006, Ecological study of living planktonic foraminifera by culture experiments. *Fossils (Kaseki)*, no. 79, 1–2 (in Japanese).

Koeppen, N., 1894, *Amoebophrya stycholonchae* nov. gen. et sp. *Zool. Anz.*, **17**, 417–424.

Kouduka, M., Matsuoka, A. and Nishigaki, K., 2006, Acquisition of genome information from single-celled unculturable organisms (radiolaria) by exploiting genome profiling (GP). *BMC Genomics*, **7**, 135. doi:10.1186/1471-2164-7-135

Kurihara T. and Matsuoka A., 2004, Shell structure and morphologic variation in *Spongosphaera streptacantha* Haeckel (Spumellaria, Radiolaria). *Sci. Rep. Niigata Univ. (Geol.)*, no. 19, 35–48.

Kurihara, T. and Matsuoka, A., 2005, Shell variability of *Pseudocubus obeliscus* Haeckel in the early autumn radiolarian fauna off Tassha, Sado Island, central Japan. *Sci. Rep. Niigata Univ. (Geol.)*, no. 20, 29–45.

Kurihara, T. and Matsuoka, A., 2009, A late-winter (March 10, 2008) living radiolarian fauna in surface-subsurface waters of the Japan Sea off Tassha, Sado Island, central Japan. *Sci. Rep. Niigata Univ. (Geol.)*, no. 24, 81–90.

Kurihara, T. and Matsuoka, A., 2010, Living radiolarian fauna of late autumn (November 13, 2008) in surface-subsurface waters of the Japan Sea off Tassha, Sado Island, central Japan. *Sci. Rep. Niigata Univ. (Geol.)*, no. 25, 83–92.

Kurihara, T., Shimotani, T. and Matsuoka, A., 2006, Water temperature, salinity, algal-chlorophyll profiles and radiolarian fauna in the surface and subsurface waters in early June off Tassha, Sado Island, central Japan. *Sci. Rep. Niigata Univ. (Geol.)*, no. 21, 31–46.

Kurihara, T., Uchida, K., Shimotani, T. and Matsuoka, A., 2007, Radiolarian faunas and water properties in surface and subsurface waters of the Japan Sea in September 2005, off Tassha, Sado Island, central Japan. *Sci. Rep. Niigata Univ. (Geol.)*, no. 22, 43–56.

Kurihara, T., Uchida, K., Shimotani, T. and Matsuoka, A., 2008, Radiolarian faunal characteristics in surface-subsurface waters of the Japan Sea off Tassha, Sado Island, central Japan in June 2007: inflowing radiolarians on the Tsushima Warm Current. *Sci. Rep. Niigata Univ. (Geol.)*, no. 23, 65–74.

Matsuoka, A., 1992, Skeletal growth of a spongiose radiolarian *Dictyocoryne truncatum* in laboratory culture. *Marine Micropaleont.*, **19**, 287–297.

Matsuoka, A., 1993a, Living radiolarians around the Sesoko Island, Okinawa Prefecture. *Fossils (Kaseki)*, no. 54, 1–9 (in Japanese with English abstract).

Matsuoka, A., 1993b, Observations of living radiolarians from the surface water in the Caribbean Sea. *News Osaka Micropaleontol. (NOM), Spec. Vol.*, no. 9, 349–363.

Matsuoka, A., 2002, Methods and research instruments for living radiolarian studies. *Fossils (Kaseki)*, no. 71, 19–27 (in Japanese).

Matsuoka, A., 2007, Living radiolarian feeding mechanisms: new light on past marine ecosystems. *Swiss Jour. Geosci.*, **100**, 273–279.

Matsuoka, A., 2009, Late autumn living radiolarian fauna from sub-tropical surface waters in the East China Sea off Sesoko Island, Okinawa, southwest Japan. *News Osaka Micropaleontol. (NOM), Spec. Vol.*, no. 14, 11–29.

Matsuoka, A., 2017, Catalogue of living polycystine radiolarians in surface waters in the East China Sea around Sesoko Island, Okinawa Prefecture, Japan. *Sci. Rep. Niigata Univ. (Geol.)*, no. 32, 57–90.

Matsuoka, A. and Anderson, O. R., 1992, Experimental and observational studies of radiolarian physiological ecology: 5. Temperature and salinity tolerance of *Dictyocoryne truncatum*. *Marine Micropaleont.*, **19**, 299–313.

Matsuoka, A., Shinzawa, M., Yoshida, K., Machidori, S., Kurita, H. and Todo, T., 2002, Early summer radiolarian fauna in surface waters off Tassha, Aikawa Town, Sado Island, central Japan. *Sci. Rep. Niigata Univ. (Geol.)*, no. 17, 17–25.

Matsuoka, A., Yoshida, K., Hasegawa, S., Shinzawa., M., Tamura, K., Sakumoto, T., Yabe, H., Niikawa, I. and Tateishi, M., 2001, Temperature profile and radiolarian fauna in surface waters off Tassha, Aikawa Town, Sado Island, central Japan. *Sci. Rep. Niigata Univ. (Geol.)*, no. 16, 83–93.

Michaels, A. F., Caron, D. A., Swanberg, N. R., Howse, F. A. and Michaels, C. M., 1995, Planktonic sarcodines (Acantharia, Radiolaria, Foraminifera) in surface waters near Bermuda: abundance, biomass and vertical flux. *Jour. Plankton Res.*, **171**, 131–163.

Müller, J., 1859, Über die Thalassicollen, Polycystinen und Acanthometren des Mittelmeeres. *Abh. könig. Akad. wissen. Berlin*, **1858**, 1–62.

Ogane, K., Tuji, A., Suzuki, N., Kurihara, T. and Matsuoka, A., 2009, First application of PDMPO to examine silicification in polycystine Radiolaria. *Plankton Benthos Res.*, **4**, 89–94.

Ogane, K., Tuji, A., Suzuki, N., Matsuoka, A., Kurihara, T. and Hori, R. S., 2010, Direct observation of the skeletal growth patterns of polycystine radiolarians using a fluorescent marker. *Marine Micropaleont.*, **77**, 137–144.

Ogane, K., Suzuki, N., Tuji, A. and Hori, R. S., 2014, Pseudopodial silica absorption hypothesis (PSA hypothesis): A new function of pseudopodia in living radiolarian polycystine cells. *Jour. Micropaleont.*, **33**, 143–148.

Probert, I., Siano, R., Poirier, C., Decelle, J., Biard, T., Tuji, A., Suzuki, N. and Not, F., 2014, *Brandtodinium* gen. nov. and *B. nutricula* comb. nov. (Dinophyceae), a dinoflagellate commonly found in symbiosis with polycystine radiolarians. *Jour. Phycol.*, **50**, 388–399.

Raikov, I. B., 1982, *The Protozoan Nucleus, Morphology and Evolution. Cell Biology Monographs, volume 9.* Springer-Verlag, Wien, 474p.

Sashida, K. and Kurihara, T., 1999, Recent radiolarian faunas in the surface water off the coat of Shimoda, Izu Peninsula, Japan. *Sci. Rep. Inst. Geosci., Univ. Tsukuba, sec. B=Geol. Sci.*, **20**, 115–144.

Sugiyama, K. and Anderson. O. R., 1997, Correlated fine structural and light microscopic analyses of living nassellarians *Eucyrtidium hexagonatum* Haeckel, *Pterocorys zancleus* (Müller) and *Spirocyrtis scalaris* Haeckel. *News Osaka Micropaleontol. (NOM), Spec. Vol.*, no. 14, 11–29.

Sugiyama, K., Hori, R. S., Kusunoki, Y. and Matsuoka, A., 2008, Pseudopodial features and feeding behavior of living nassellarians *Eucyrtidium hexagonatum* Haeckel, *Pterocorys zancleus* (Müller) and *Dictyocodon prometheus* Haeckel. *Paleont. Res.*, **12**, 209–222.

Suzuki, N., 2005, Physiological axopodial activity of *Rhizosphaera trigonacantha* Haeckel (a spheroidal radiolarian, Polycystina, Protista). *Marine Micropaleont.*, **54**, 141–153.

Suzuki, N. and Aita, Y., 2011, Radiolaria: achievements and unresolved issues: taxonomy and cytology. *Plankton Benthos Res.*, **6**, 69–91.

Suzuki, N., Kurihara, T. and Matsuoka, A., 2009a, Sporogenesis of an extracellular cell chain from the spheroidal radiolarian host *Haliommilla capillaceum* (Haeckel), Polycystina, Protista. *Marine Micropaleont.*, **72**, 157–164.

Suzuki, N. and Not, F., 2015, Biology and Ecology of Radiolaria. *In* Ohtsuka, S., Suzuki, T., Horiguchi, T., Suzuki, N. and Not, F., eds., *Marine Protists,* Springer, Tokyo, 81–108.

Suzuki, N., Ogane, K., Aita, Y., Kato, M., Sakai, T., Kurihara, T., Matsuoka, A., Ohtsuka, S., Go, A., Nakaguchi, K., Yamaguchi, S., Takahashi, T. and Tuji, A., 2009b, Distribution patterns of the radiolarian nuclei and symbionts using DAPI-fluorescence. *Bull. Natl. Mus. Nat. Sci., Ser.* B, **35**, 169–182.

Suzuki, N., Ogawa, K., Ogane, K. and Tuji, A., 2013, Patchwork silicification and disposal activity of siliceous fragments of a polycystine radiolarian. *Rev. Micropaléont.*, **56**, 63–74.

Suzuki, N. and Sugiyama, K., 2001, Regular axopodial activity of *Diplosphaera hexagonalis* Haeckel (spheroidal spumellarian, Radiolaria). *Paleont. Res.*, **5**, 131–140.

Swanberg, N. R., 1983, The trophic role of colonial Radiolaria in oligotrophic oceanic environments. *Limnol. Oceanogr.*, **28**, 655–666.

Swanberg, N. R., Anderson, O. R. and Bennett, P., 1985, Spongiose spumellarian Radiolaria: The functional morphology of the radiolarian skeleton with a description of *Spongostaurus*, a new genus. *Marine Micropaleont., **9**, 455–464.

Swanberg, N. R., Anderson, O. R. and Bennett, P., 1990, Skeletal and cytoplasmic variability of large spongiose spumellarian Radiolaria (Actinopodea: Polycystina). *Micropaleontology*, **364**, 379–387.

Swanberg, N. R., Bennett, P., Lindsey, J. L. and Anderson, O. R., 1986, A comparative study of predation in two Caribbean radiolarian populations. *Marine Microbial Food Webs*, **1**, 105–118.

Swanberg, N. R. and Bjørklund, K. R., 1987, The pre-cephalic development of the skeleton of *Amphimelissa setosa* (Actinopoda: Nassellarida). *Marine Micropaleont.*, **11**, 333–341.

Swanberg, N. R. and Caron, D. A., 1991, Patterns of sarcodine feeding in epipelagic oceanic plankton. *Jour. Plankton Res.*, **132**, 287–312.

Swanberg, N. R. and Eide, L. K., 1992, The radiolarian fauna at the ice edge in the Greenland Sea during summer, 1988. *Jour. Marine Res.*, **50**, 297–320.

Swanberg, N. R. and Harbison, G. R., 1980, The ecology of *Collozoum longiforme*, sp. nov., a new colonial radiolarian from the equatorial Atlantic Ocean. *Deep-Sea Res., Part A*, **27**, 715–731.

Takagi, H., Kimoto, K., Fujiki, T., Kurasawa, A., Moriya, K. and Hirano, H., 2016, Ontogenetic dynamics of photosymbiosis in cultured planktic foraminifers revealed by fast repetition rate fluorometry. *Marine Micropaleont.*, **122**, 44–52.

Takahashi, O., Mayama, S. and Matsuoka, A., 2003, Host-symbiont association of polycystine Radiolaria: Epifluorescence microscopic observation of living Radiolaria. *Marine Micropaleont.*, **49**, 187–194.

Takahashi, O., Yuasa, T., Honda, D. and Mayama, S., 2004, Molecular phylogeny of solitary shell-bearing Polycystinea (Radiolaria). *Rev. Micropaléont.*, **47**, 111–118.

Tilesius, W. G. von Tillenau, 1818, Ueber das nächtliche Leuchten des Meerwassers. *Ann. Wet. Gesel. ges. Natur.*, **3.1.3.2**, 360–372 & **4.2.1.2**, plates 20a, 20b.

Yuasa, T., Dolven, J. K., Bjørklund, K. R., Mayama, S. and Takahashi, O., 2009a, Molecular phylogenetic position of *Hexacontium pachydermum* Jørgensen (Radiolaria). *Marine Micropaleont.*, **73**, 129–134.

Yuasa, T., Horiguchi, T., Mayama, S., Matsuoka, A. and Takahashi, O., 2012, Ultrastructural and molecular characterization of cyanobacterial symbionts in *Dictyocoryne profunda* (polycystine radiolaria). *Symbiosis*, **57**, 51–55.

Yuasa, T., Horiguchi, T., Mayama, S. and Takahashi, O., 2016, *Gymnoxanthella radiolariae* gen. et sp. nov. (Dinophyceae), a dinoflagellate symbiont from solitary polycystine radiolarians. *Jour. Phycol.*, **52**, 89–104.

Yuasa, T. and Takahashi, O., 2014, Ultrastructural morphology of the reproductive swarmers of *Sphaerozoum punctatum* (Huxley) from the East China Sea. *European Jour. Protist.*, **50**, 194–204.

Yuasa, T. and Takahashi, O., 2015, Light and electron microscopic observations of the reproductive swarmers cells of nassellarian and spumellarian polycystines (Radiolaria). *European Jour. Protist.*, **54**, 19–32.

Yuasa, T., Takahashi, O., Dolven, J. K., Mayama, S., Matsuoka, A., Honda, D. and Bjørklund, K. R., 2006, Phylogenetic position of the small solitary phaeodarians (Radiolaria) based on 18S rDNA sequences by single cell PCR analysis. *Marine Micropaleont.*, **59**, 104–114.

Yuasa, T., Takahashi, O. and Mayama, S., 2004, PCR primers for the amplification of the nuclear small subunit ribosomal DNA sequences from polycystine radiolarians. *Japanese Jour. Protozool.*, **37**, 133–137.

Yuasa, T., Takahashi, O. and Mayama, S., 2009b, A simple technique for extracting small subunit ribosomal DNAs from both the host and symbiont of a single radiolarian specimen. *News Osaka Micropaleontol. (NOM), Spec. Vol.*, no. 14, 1–4.

Yuasa, T., Takahashi, O., Honda, D. and Mayama, S., 2005, Phylogenetic analyses of the polycystine Radiolaria based on the 18s rDNA sequences of the Spumellarida and the Nassellarida. *European Jour. Protistol.*, **41**, 287–298.

[URL1] User Instructions for Sesoko Station, Tropical Biosphere Research Center, the University of the Ryukyus (http://www.tbc.u-ryukyu.ac.jp/sesoko/user-information).
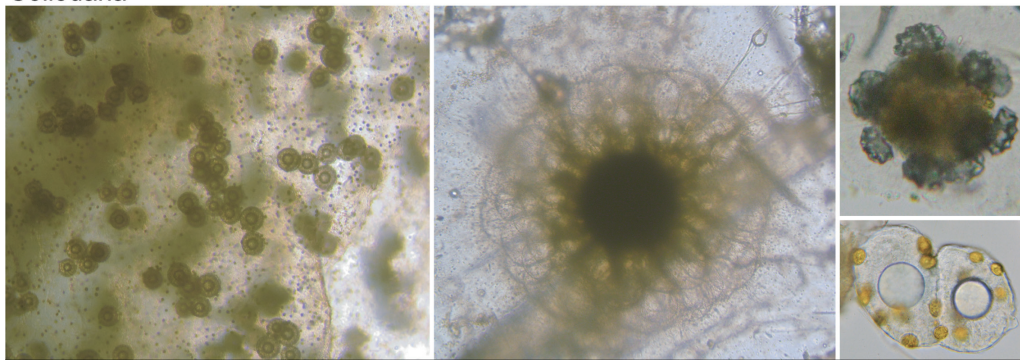
Collodaria

Spumellaria
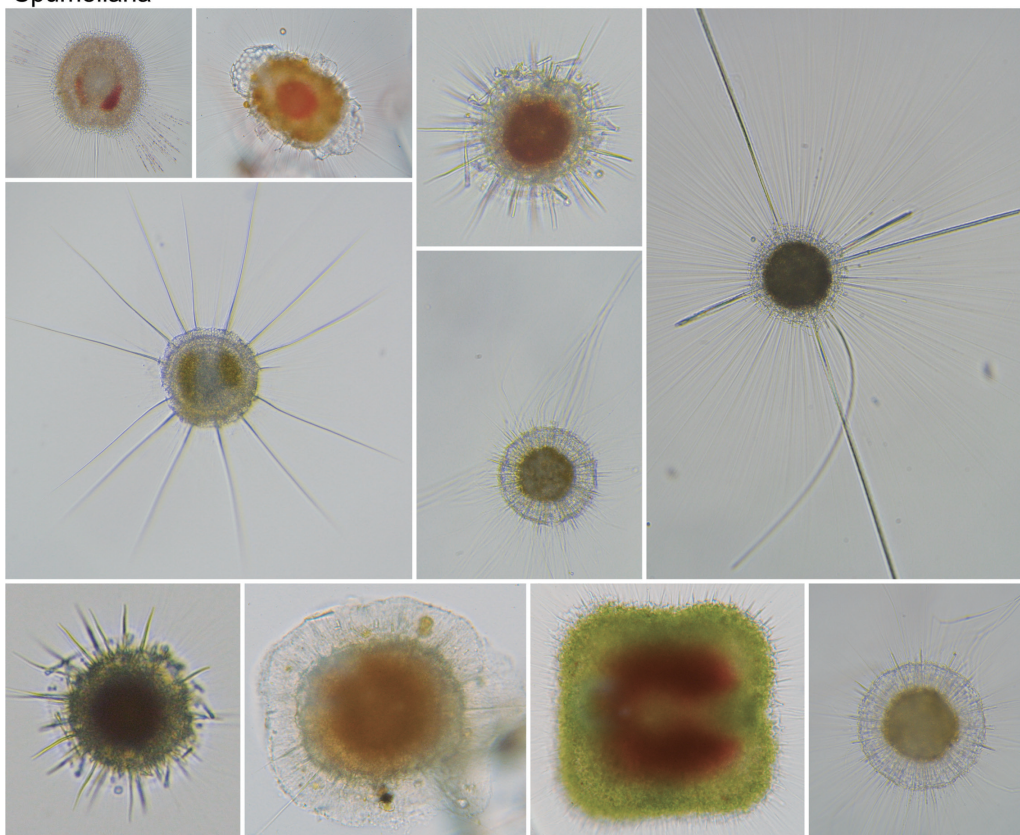
Appendix A. Photomicrographs of major living radiolarians (Collodaria and Spumellaria) collected from the sea water off Sesoko Island, Okinawa Prefecture, Japan.

Nassellaria

Acantharia

Taxopodia
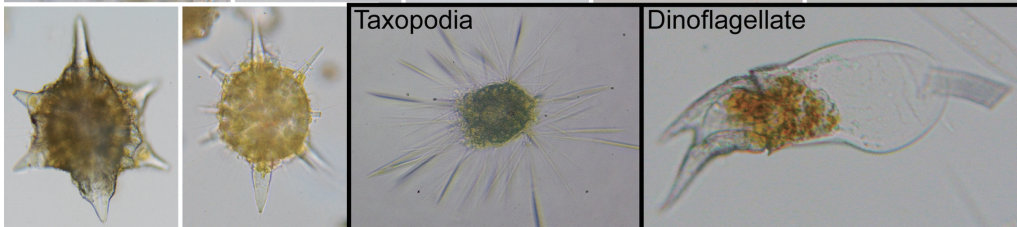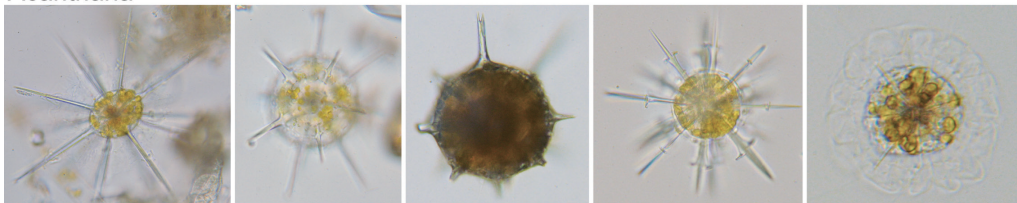
Dinoflagellate

Appendix B. Photomicrographs of major living radiolarians (Nassellaria and Acantharia) and other protists (Taxopodia and Dinoflagellate) collected from the sea water off Sesoko Island, Okinawa Prefecture, Japan.

Permian–Cretaceous radiolarians from Ie Island, Okinawa Prefecture, Japan

Tsuyoshi ITO* and Atsushi MATSUOKA**

Abstract

Ie Island in northwestern Okinawa Prefecture, Japan, mainly comprises of basement rocks (Gusukuyama Formation of the Southern Chichibu terrane) and the overlying Pleistocene Ryukyu Group. The bedded cherts of the Gusukuyama Formation in Mt. Gusuku in the central part of Ie Island have yielded radiolarians ranging from the *Neoalbaillella optima* Zone (Changhsingian, Lopingian, Permian) to the *Kilinora spiralis* Zone (JR6: Oxfordian, Upper Jurassic). Siliceous mudstones in the southern flank of Mt. Gusuku have yielded radiolarians of the *Pseudodictyomitra carpatica* Zone (KR1: uppermost Jurassic–lowermost Cretaceous). This age difference is assumed to indicate the presence of a thrust between Mt. Gusuku and the southern flank of the mountain. Red chert clasts are contained in the Pleistocene Ryukyu Group at Waji on the north coast of Ie Island, and Permian radiolarians have been obtained from chert clasts. In addition, a red bedded chert boulder at Waji yielded Cisuralian (Early Permian) radiolarians including dimorphic pair of *Albaillella sinuata* Ishiga and Watase.

Key words: Permian, Triassic, Jurassic, Cretaceous, radiolaria, dimorphism, accretionary complex, chert, Southern Chichibu terrane, Ryukyu Arc

---

* Stratigraphy and Tectonics Research Group, Research Institute of Geology and Geoinformation, Geological Survey of Japan, AIST, Tsukuba 305-8567, Japan

** Department of Geology, Faculty of Science, Niigata University, Niigata 950-2181, Japan
Corresponding author: T. Ito,
ito-t@aist.go.jp

Introduction

The Japanese Islands, located near a subduction zone in East Asia, mainly comprise accretionary complexes (Isozaki et al., 2010). Jurassic and Cretaceous accretionary complexes are distributed over the northwestern part of the Okinawa Islands (Nakae et al., 2010) (Fig. 1B). Konishi (1963) determined that the Jurassic accretionary complexes are an extension of the Southern Chichibu terrane. Oceanic rocks and terrigenous clastics of the Jurassic accretionary complexes are exposed mainly in Ie, Iheya, and Izena Islands and on the Motobu Peninsula (Fujita, 1989; Takami et al., 1999).

Ie Island is located to the northwest of the Motobu Peninsula of Okinawa Island and most of its area is covered with Pleistocene limestones. However, Mt. Gusuku exposed in the central part of the island is composed of Permian–Jurassic radiolarian-bearing bedded cherts (Ujiié and Oba, 1991a; Matsuoka et al., 1996; Shen et al., 1996). In addition, latest Jurassic–earliest Cretaceous radiolarian assemblages have occurred in siliceous mudstones on the southern flank of Mt. Gusuku, and chert clasts occurring within Pleistocene
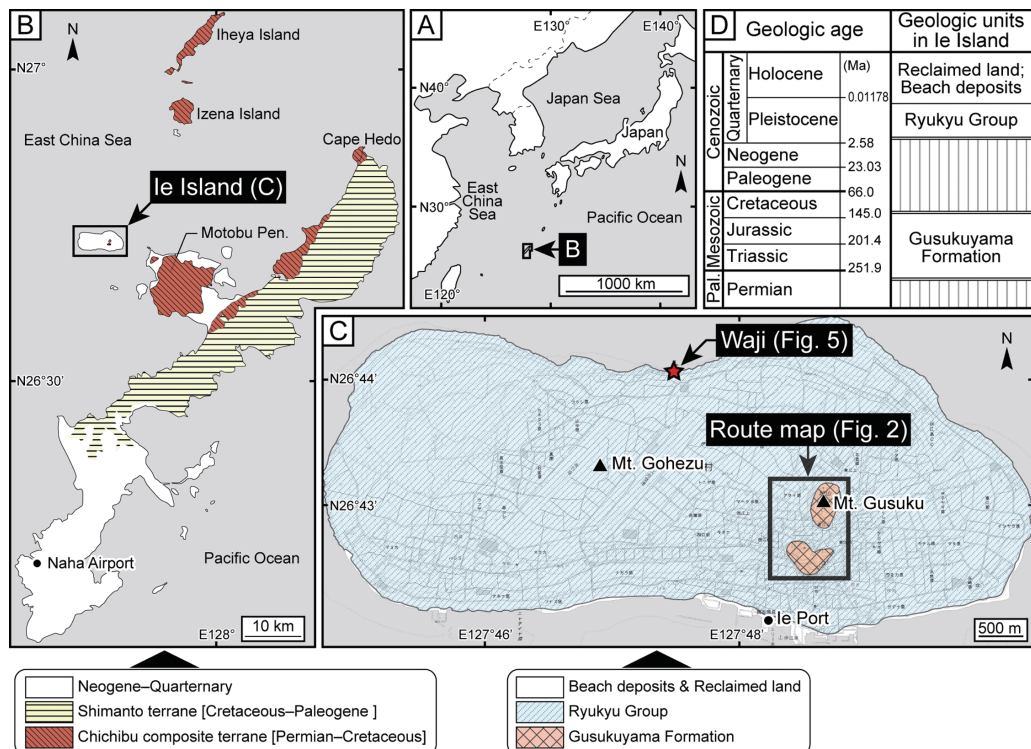
Fig. 1. Geologic maps of the Okinawa Islands and Ie Island and summary of geology of Ie Island. Geologic map of Okinawa Islands is after Nakae et al. (2010). Distribution of the Gusukuyama Formation in Mt. Gohezu is unshown because its distribution is narrow. Base map is from 1:50,000 topographic map "Ie-jima" published by Geospatial Information Authority of Japan. Numerical ages of the summary of geology are after Ogg et al. (2016).

limestones at Waji on the northern coast of the island have yielded Permian radiolarian assemblages (Ujiié and Oba, 1991a; Ito and Matsuoka, 2015). These include dimorphic pairs of the Albaillellaria (Ujiié and Oba, 1991a; Ito and Matsuoka, 2015) that have rarely been reported worldwide.

This article introduces the geologic outline of Ie Island and the radiolarian occurrences within two places, i.e., Mt. Gusuku and Waji.

Geologic outline

Ie Island is located approximately 9 km off northwest of the Motobu Peninsula. It is a small gourd-shaped island with a circumference of approximately 22 km. The northern coast of the island is topographically characterized by terrace plains with steep escarpments, while the southern area is low-pitched (Kinoshita, 2013).

The Ryukyu Group on Ie Island mainly comprises basal conglomerates, calcareous sandstones, and coral limestones in ascending order (Kinoshita, 2013), where limestones belonging to the Pleistocene Ryukyu Group cover most of the island (Fig. 1C). On the basis of boring data (Okinawa General Bureau, 1983) and rock exposure at Waji, the maximal thickness of the Ryukyu Group in Ie Island is known to be thicker than 50 m (Fujishiro, 1995). Basement rocks are exposed only around Mts. Gusuku and Gohezu. Limestones are slightly exposed around Mt. Gohezu whereas Mt. Gusuku is composed of bedded cherts. Outcrops comprising bedded cherts, siliceous mudstones, and sandstones are scattered in the south of Mt. Gusuku. Hashimoto et al. (1976) named the basement rocks around Mt. Gusuku the "Shiroyama Formation," although detailed characteristics were not described. Fujita (1989) then defined the Gusukuyama Formation as an equivalent of the pre-defined Shiroyama Formation. Fujita (1989) also named the basement rocks around Mt. Gohezu as the "Ie Formation," representing an extension of the Maedake, Iheya, and Izena formations in Iheya and Izena Islands, although the detailed characteristics were not described. Takami et al. (1999) proposed the unit division of accretionary complexes in Ie, Iheya, and Izena Islands and the Motobu Peninsula; according to this division, the basement rocks around Mt. Gusuku and Cape Bisezaki (the northwest end of the Motobu Peninsula) belong to the Ie unit. However, Nakae et al. (2010) followed the division of Fujita (1989) and named the basement rocks around Mt. Gusuku as the "Gusuykuyama Formation." Furthermore, Osozawa and Watanabe (2011) proposed the Ie Complex, which is distributed over both Mts. Gusuku and Gohezu, Cape Bisezaki, and the northeastern coast of Ie Island. The present study follows the description defined by Fujita (1989) and Nakae et al. (2010) in which the basement rocks in Ie Island are known as the Gusukuyama Formation. A geological summary of Ie Island is shown in Fig. 1D.

Bedded cherts are exposed at Waji on the north coast of Ie Island. Some researchers

have considered these cherts to be basement rocks (Ujiié and Hashimoto, 1983; Ujiié and Oba, 1991a; Shen et al., 1996; Takami et al., 1999). However, Osozawa and Watanabe (2011) and Ito and Matsuoka (2015) indicated that the cherts are contained as clasts within the Ryukyu Group at Waji but not basement rocks.

Stop descriptions

STOP 1. Mt. Gusuku

Mountain Gusuku is also known as "Tacchu" and is located in the central part of Ie Island. This mountain comprises bedded cherts, which generally strike W–E and dip 30° to 40°N, although several small folds are also recognized within the cherts. Limestones are exposed near stairs just south of the mountain (Fig. 2).

Permian, Triassic, and Jurassic radiolarians have been found to occur in the bedded cherts of Mt. Gusuku (Ujiié and Hashimoto, 1983; Fujita, 1989; Ujiié and Oba, 1991a, 1991b; Suzuki, 1992; Shen et al., 1996). *Neoalbaillella optima* Ishiga, Kito, and Imoto was obtained from chert near the start point of a climbing route for Mt. Gusuku (Shen et al., 1996), but the outcrop is currently covered by concrete (Fig. 2). *Neoalbaillella optima* is the diagnosed species from the *N. optima* Assemblage-Zone of the Changhsingian, Lopingian, upper Permian (Kuwahara et al., 1998). Although Triassic radiolarians were extracted, the occurrences were rare relative to the Jurassic radiolarian occurrences. For example, Ujiié and Oba (1991a) reported only one occurrence site of Triassic radiolarians; Shen et al. (1996) reported the Triassic radiolarian occurrences including *Palaeosaturnalis triassicus* (Kozur and Mostler) from three localities. *Palaeosaturnalis triassicus* ranges from the middle Carnian to the middle Norian (Dumitrica et al., 2010). In addition, Shen et al (1996) discovered *Kilinora spiralis* (Matsuoka), which is the diagnosis species of the *K. spiralis* Zone (JR6) of the Oxfordian, Upper Jurassic (Matsuoka, 1995), in the bedded cherts near the crest of Mt. Gusuku (Fig. 2).

In the south of the Mt. Gusuku, cherts and siliceous mudstones had been exposed near the Ie Junior High School, but most of these outcrops have now disappeared owing to land development. However, prior to the development, some researchers collected rock samples from the outcrops and conducted radiolarian preparation treatments (Ujiié and Hashimoto, 1983; Fujita, 1989; Ujiié and Oba, 1991b; Suzuki, 1992; Shen et al., 1996). The radiolarian age of the siliceous mudstones has been assigned as Tithonian–Berriasian by the researchers.

In this respect, Fig. 3 shows radiolarian photomicrographs from a siliceous mudstone sample that was collected at the northwest of Ie Junior High School in 1992 by A. Matsuoka. This radiolarian assemblage can be correlated to the *Pseudodictyomitra carpatica* Zone (KR1) of the Tithonian–Berriasian, uppermost Jurassic–lowermost Cretaceous (Matsuoka, 1995). The radiolarian age is thus consistent with the results of the above-mentioned previous studies.
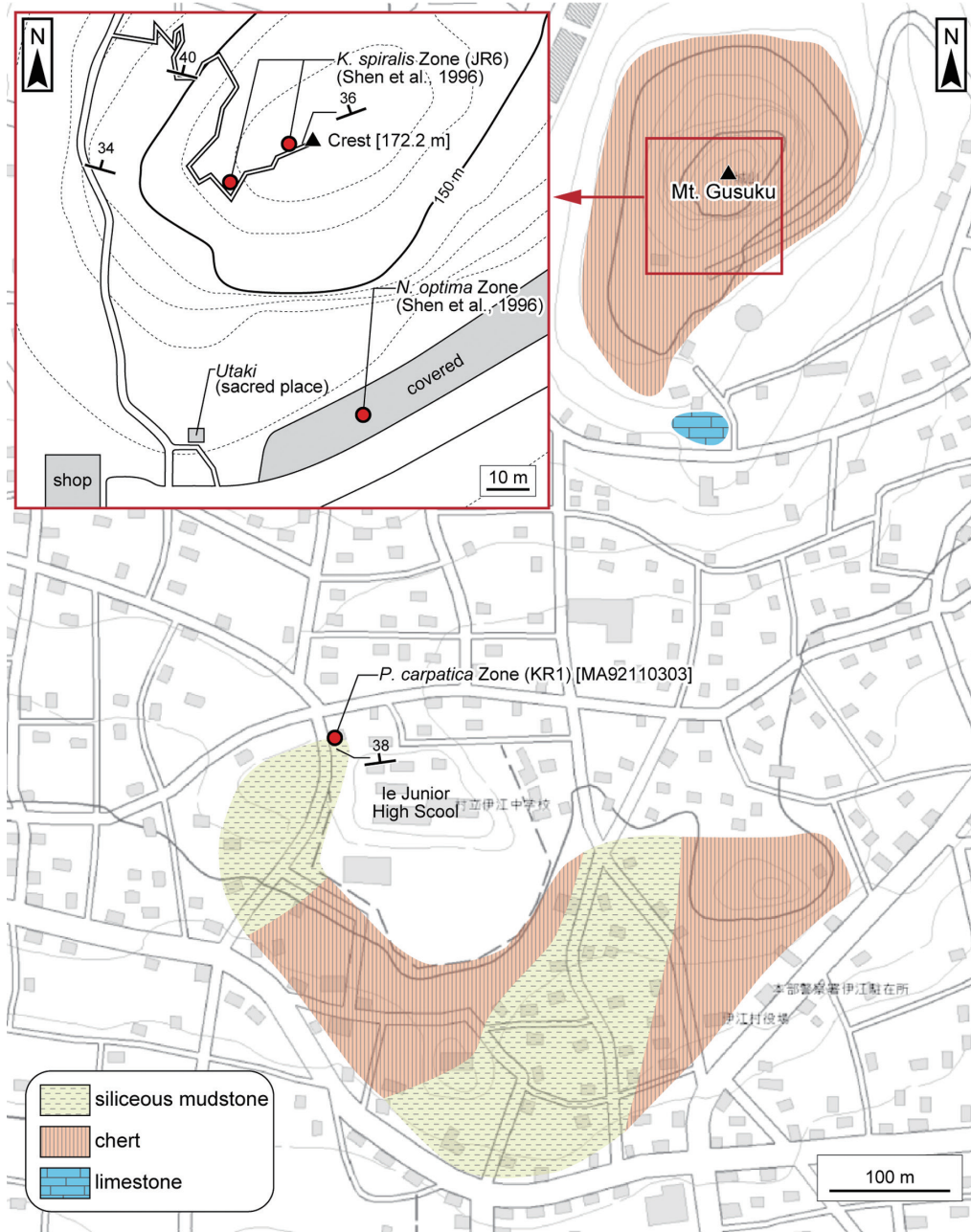
Fig. 2. Route map around Mt. Gusuku. Rock distribution around the Ie Junior High School is mainly based on Shen et al. (1996). Base map is from 1:50,000 topographic map "Ie-jima" published by Geospatial Information Authority of Japan.
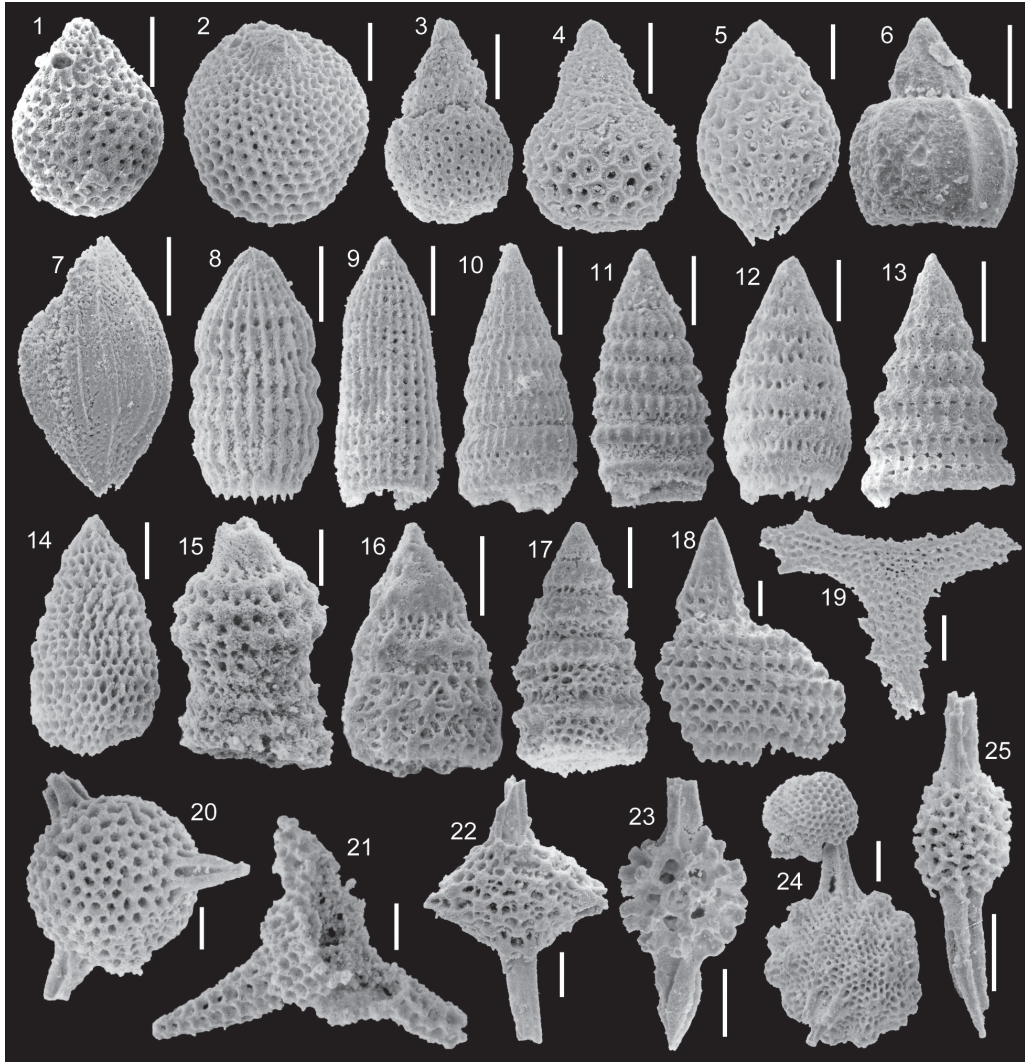
Fig. 3. Photomicrographs of radiolarian tests from MA92110303 collected at the west of the Ie Junior High School. **1:** *Zhamoidellum ovum* Dumitrica; **2:** *Cryptamphorella* sp.; **3:** *Hiscocapsa* sp.; **4:** *Hiscocapsa acuta* Hull; **5:** *Stichocapsa*(?) sp. aff. *S.*(?) *pulchella* (Rüst); **6:** *Eucyrtidiellum pyramis* (Aita); **7:** *Protunuma japonicus* Matsuoka and Yao; **8:** *Archaeodictyomitra minoensis* (Mizutani); **9:** *Archaeodictyomitra excellens* (Tan Sin Hok); **10:** *Loopus primitivus* (Matsuoka and Yao); **11:** *Pseudodictyomitra carpatica* (Lozyniak); **12:** *Loopus nudus* (Schaaf); **13:** *Praecaneta*(?) sp.; **14:** *Parvicingula*(?) sp.; **15:** *Ristola cretacea* (Baumgartner); **16:** *Xitus* sp.; **17:** *Cinguloturris carpatica* Dumitrica.; **18:** *Mirifusus dianae* (Karrer); **19:** *Paronaella*(?) *tubulata* Steiger; **20:** *Triactoma* sp.; **21:** *Podocapsa amphitreptera* Foreman; **22:** *Emiluvia* sp. cf. *E. chica* Foreman; **23:** *Pantanellium* sp.; **24:** *Acastea* sp.; **25:** *Archaeospongoprunum* sp. All scale bars are 50 μm.
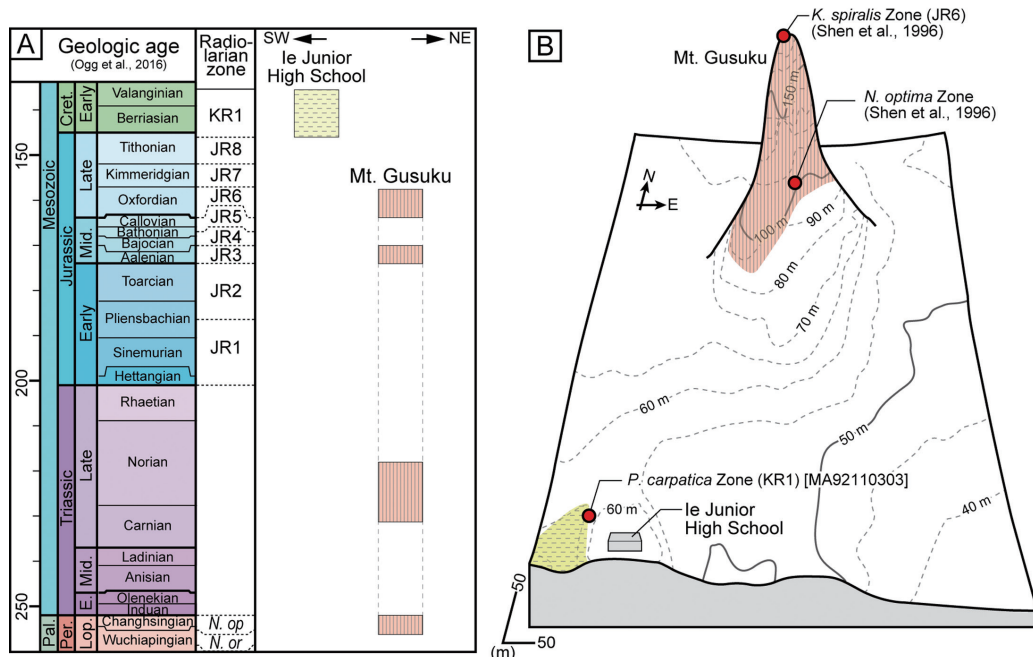
Fig. 4. Columnar and simplified three-dimensional graphic which show rock facies and age of the Gusukuyama Formation around Mt. Gusuku. Pal.: Paleozoic; Per.: Permian; Cret.: Cretaceous; E.: Early; Mid.: Middle.

On the basis of previous data and results of this present study (Fig. 4A), the bedded cherts at Mt. Gusuku range from the Changhsingian (Lopingian, upper Permian) to the Oxfordian (Upper Jurassic), whereas the siliceous mudstones near Ie Junior High School correspond to the Tithonian–Berriasian (uppermost Jurassic–lowermost Cretaceous). This implies that the younger siliceous mudstones near the Ie Junior High School are structurally located in a lower position than the older cherts at Mt. Gusuku (Fig. 4D). On the basis of this age difference, Shen et al. (1996) assumed the presence of a north-dipping thrust between these rocks and implied that the thrust represents an off-scrape accretionary process. However, as previously noted, the occurrence sites of Triassic radiolarians at Mt. Gusuku are a few relative to those of Jurassic radiolarians. If Mt. Gusuku is composed of a continuous succession of bedded cherts then this occurrence seems rather considerably uneven. It may imply the presence of other large faults within Mt. Gusuku.

STOP 2. Waji

Pleistocene limestones of the Ryukyu Group are well-exposed along the north coast of Ie Island. Red chert clasts, which vary in size ranging from several millimeters to approximately 6 m in diameter, are included within the limestones at Waji (Fig. 5). Ito and Matsuoka (2015) named the chert sequence (4.8 m in total thickness) found in the biggest
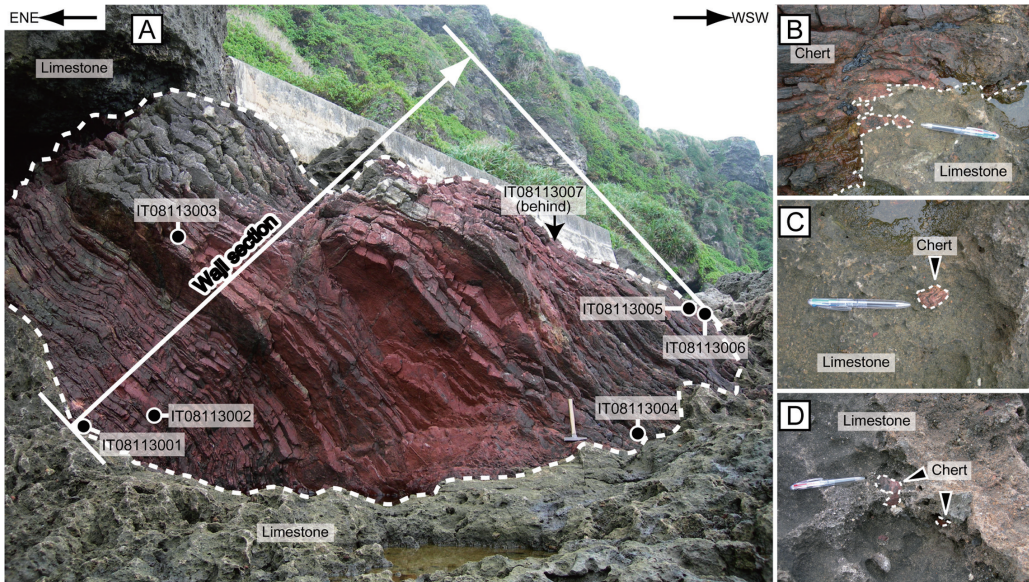
Fig. 5. Exposures of red cherts at Waji (after Ito and Matsuoka, 2015). **A:** Overall view of the Waji section; **B:** Boundary between chert boulder and limestone matrix; **C, D:** chert pebbles within limestone.

chert boulder at Waji the "Waji section" (Figs. 5A, 6A).

　　Permian radiolarians have been noted to occur in red cherts at Waji (Ujiié and Oba, 1991a; Shen et al., 1996; Ito and Matsuoka, 2015). Ujiié and Oba (1991a) reported Cisuralian (Early Permian) radiolarians such as *Albaillella sinuata* Ishiga and Watase and Capitanian (Guadalupian, Middle Permian) radiolarians such as *Pseudoalbaillella monacanthus* Ishiga and Imoto and *Follicucullus scholasticus* Ormiston and Babcock. Shen et al. (1996) obtained Changhsingian radiolarians such as *Albaillella triangularis* Ishiga, Kito, and Imoto. Ito and Matsuoka (2015) extracted Cisuralian radiolarians such as *A. sinuata* and *Pseudoalbaillella ishigai* Wang from the Waji section (Fig. 6).

　　Furthermore, Ujiié and Oba (1991a) and Ito and Matsuoka (2015) showed dimorphic pairs of the Order Albaillellaria. Ishiga (1991) had previously proposed and described that some taxa of the Albaillellaria are dimorphic represented by normal and swollen types. As the name suggests, swollen type specimens have a more swollen apical portion compared to normal type specimens (Fig. 6B). Ishiga (1991) also suggested the possibility that this dimorphism is caused by alternating generations, which is known in some living foraminifers (e.g., Leutenegger, 1977; Goldstein, 1999). Furthermore, the swollen type specimens have been recognized in some genera of the Albaillellidae and Follicucullidae (Table 1). The swollen type specimens are generally characterized by their rare occurrence and low population (2.1%–9.5%: Ishiga, 1991). However, the occurrence ratio of swollen type specimens of *A. sinuata* from one horizon in the Waji section is 27.1% (Ito and Matsuoka, 2015).
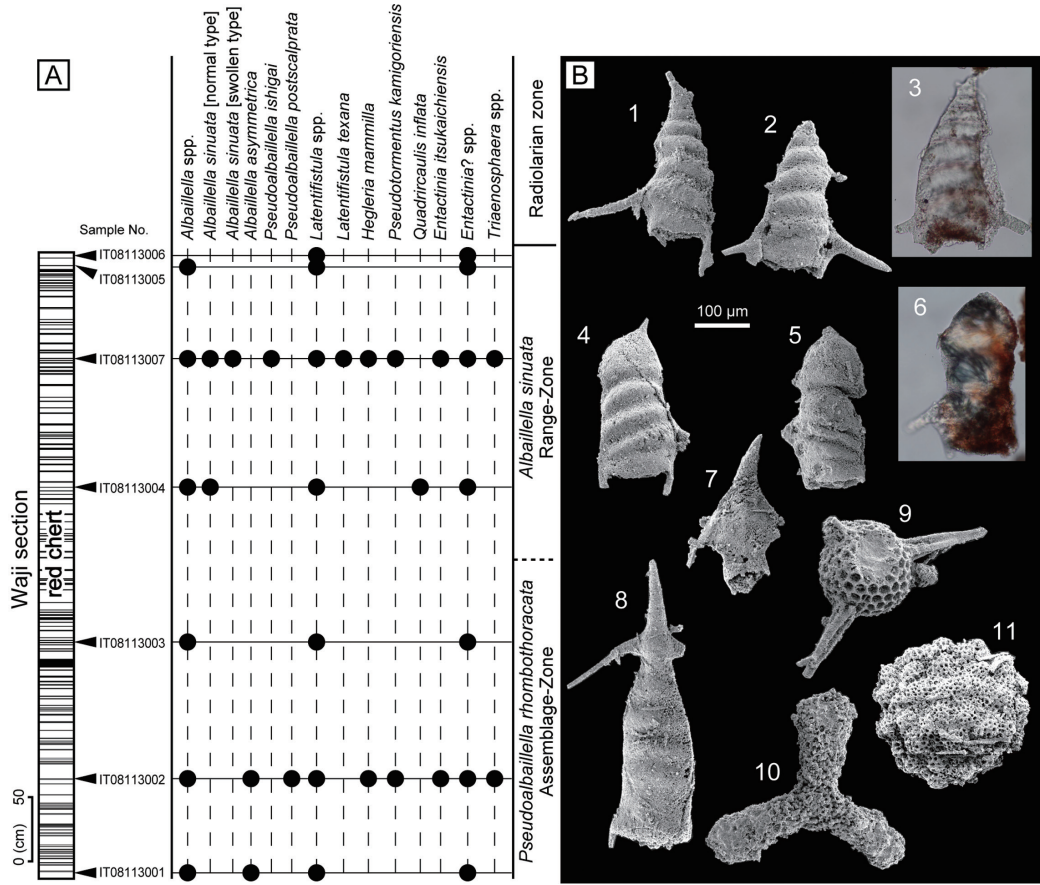
Fig. 6. Columnar of the Waji section and photomicrographs of major radiolarians obtained from the Waji section (modified from Ito and Matsuoka, 2015). **1–3:** Normal type of *Albaillella sinuata* Ishiga and Imoto; **4–6:** swollen type of *A. sinuata*; **7:** *Pseudoalbaillella postscalprata* Ishiga; **8:** *Pseudoalbaillella ishigai* Wang; **9:** *Triaenosphaera* sp.; **10:** *Latentifistula texana* Nazarov and Ormiston; **11:** *Hegleria mammilla* (Sheng and Wang). 1–6, 8–10: IT08113007; 7, 11: IT08113002.

Table 1. Illustrated Permian albaillellarian specimens of swollen-type in major previous studies.

Family	Genus	Species	Reference with plate and/or figure number	Age and locality	Original description
Albaillellidae Deflandre	*Albaillella* Deflandre	*A. sinuata* Ishiga and Watase	pl. 4, fig. 4, Ishiga et al., 1982a	Artinskian (Cisuralian), Tamba, Japan	*A.* sp. D
			pl. 4, figs. 9–10, Ujiié and Oba, 1991a	Artinskian (Cisuralian), Okinawa, Japan	Gen. et sp. indet.
			pl. 1, figs. 5–7, Xia and Zhang, 1998	Artinskian (Cisuralian), Guangxi, China	*A.* sp. aff. *A. sinuata*
			fig. 6.2, Zhang et al., 2002	Artinskian (Cisuralian), Guangxi, China	*A.* sp. aff. *A. sinuata*
			figs. 4.7–4.17, Ito and Matsuoka, 2015	Artinskian (Cisuralian), Okinawa, Japan	Swollen type of *A. sinuata*
		A. asymmetrica Ishiga and Imoto	pl. 3, figs. 10, 11, Ishiga et al., 1982a	Artinskian (Cisuralian), Tamba, Japan	*A. asymmetrica*
	Neoalbaillella Takemura and Nakaseko*	*N. optima* Ishiga, Kito and Imoto	pl. 1, fig. 32, Kuwahara and Yao, 1998	Changhsingian (Lopingian), Mino, Japan	*N.* sp. B
			pl. 1, fig. 5, Sashida et al., 2000	Changhsingian (Lopingian), Klaeng, Thailand	*N.* ? sp.
			pl. 1 fig. 12, Zhu et al., 2006	Changhsingian (Lopingian), N. Tibet, China	*N.* sp.
			fig. 3.10, Wu and Feng, 2008	Changhsingian (Lopingian), Guangxi, China	*N.* sp. A
			figs. 8.11–8.17, Wu et al., 2010	Changhsingian (Lopingian), Guangxi, China	*N. camarata* Wu and Feng
		N. pseudogrypa Sashida and Tonishi	pl. 1, fig. 12, Takemura et al., 2009	Changhsingian (Lopingian), Shikoku, Japan	Swollen type of *N. pseudogrypa*
		Neoalbaillella sp.**	pl. 34, figs. 2, 3, Takemura and Nakaseko, 1981	Changhsingian (Lopingian), Tamba, Japan	*N.* sp. A
			pl. 1, fig. 31, Kuwahara and Yao, 1998	Changhsingian (Lopingian), Mino, Japan	*N.* sp. A
			figs. 6.13–6.15, Jin et al., 2007	Changhsingian (Lopingian), Guangxi, China	*N.* sp. 1 and *N.* sp. 2
			figs. 8.18–8.21, 8.23, Wu et al., 2010	Changhsingian (Lopingian), Guangxi, China	*N. cephalota* Wu and Feng
Follicucullidae Ormiston and Babcock	*Pseudoalbaillella* Holdsworth and Jones***	*P. lomentaria* Ishiga and Imoto	pl. 2, figs. 14, 15, Ishiga and Imoto, 1980	Sakmarian (Cisuralian), Tamba, Japan	*P. lomentaria*
		P. sakmarensis Kozur	pl. 3, fig. 2, Ishiga and Imoto, 1980	Sakmarian (Cisuralian), Tamba, Japan	*P.* sp. A
		P. simplex Ishiga and Imoto or short form of *Pseudoalbaillella* species	pl. 1, fig. 19, Ishiga et al., 1984	Asselian? (Cisuralian), Tamba, Japan	*P. simplex*
		P. anfractus (Nazarov and Rudenko)	pl. 2, figs. 1–16, Panasenko and Rudenko, 1987	Sakmarian (Cisuralian), South Ural	*Haplodiacanthus anfractus*
		Short form of *P. fusiformis* (Holdsworth and Jones) sensu Ito et al., 2015	pl. 2, figs. 5, 7, Ishiga et al., 1982a	Roadian (Guadalupian), Tamba, Japan	*P.* sp. aff. *P. longicornis* Ishiga and Imoto
		P. ornata Ishiga and Imoto	pl. 1, figs. 2–4, Ishiga, 1991	Sakmarian (Cisuralian), Tamba, Japan	Swollen-type of *P. ornata*
		P. globosa Ishiga and Imoto	pl. 3, figs. 11, 12, Xia and Zhang, 1998	Roadian (Guadalupian), Guangxi, China	*P. globosa* m. II
	Follicucullus Ormiston and Babcock	*F. porrectus* Rudenko	pl. 3, fig. 2, Ujiié and Oba, 1991a	Capitanian (Guadalupian), Okinawa, Japan	*F. scholasticus* Ormiston and Babcock

* Ishiga (1991) noted the presence of swollen-type of *N. ornithoformis* Takemura and Nakaseko and *N. gracilis* Takemura and Nakaseko in the text. ** These specimens lack their pseudoabdomen and/or wings, so that their corresponding species are indeterminable. *** Ishiga (1991) noted the presence of swollen-type of *P. elongata* Ishiga and Imoto in the text.

Acknowledgements

References

Dumitrica, P., Tekin, U. K. and Bedi, Y., 2010, Eptingiacea and Saturnaliacea (Radiolaria) from the middle Carnian of Turkey and some late Ladinian to early Norian samples from Oman and Alaska. *Paläontologische Zeitschrift*, **84**, 259–292.

Fujishiro, N., 1995, The coral assemblages and developmental history of the Pleistocene coral reef of Ie Island, Okinawa Prefecture. *102nd Ann. Meet. Geol. Soc. Japan, Abstr.*, 190 (in Japanese).

Fujita, H., 1989, Stratigraphy and geologic structure of the pre-Neogene strata in the central Ryukyu Islands. *Jour. Sci. Hiroshima Univ. Ser. C*, **9**, 237–284.

Goldstein, S. T., 1999, Foraminifera: A biological overview. *In* Sen Gupta, B. K., ed., *Modern Foraminifera*. Kluwer Academic Publishers, pp. 50–68.

Hashimoto, S., Yoshida, K., Minoura, K. and Nakagawa, H., 1976, Geology of the northern part of Okinawa-jima – A preliminary report, Part I. *Geol. Study Ryukyu Isls.*, **1**, 9–20 (in Japanese).

Ishiga, H., 1991, "Dimorphic pairs" of Albaillellaria (Late Paleozoic Radiolaria), Japan. *Mem. Fac. Sci., Shimane Univ.*, **25**, 119–129.

Ishiga, H. and Imoto, N., 1980, Some Permian radiolarians in the Tamba District, southwest Japan. *Earth Sci. (Chikyu Kagaku)*, **34**, 333–345.

Ishiga, H., Imoto, N., Yoshida, M. and Tanabe, T., 1984, Early Permian radiolarians from the Tamba belt, Southwest Japan. *Earth Sci. (Chikyu Kagaku)*, **38**, 44–52.

Ishiga, H., Kito, T. and Imoto, N., 1982a, Middle Permian radiolarian assemblages in the Tamba district and an adjacent area, southwest Japan. *Earth Sci. (Chikyu Kagaku)*, **36**, 272–281.

Ishiga, H., Kito, T. and Imoto, N., 1982b, Permian radiolarian biostratigraphy. *News Osaka Micropaleontol. (NOM), Spec. Vol.*, no. 5, 17–26 (in Japanese with English abstract).

Isozaki, Y., Aoki, K., Nakama, T. and Yanai, S., 2010, New insight into a subduction-related orogen: A reappraisal of the geotectonic framework and evolution of the Japanese Islands. *Gondwana Res.*, **18**, 82–105.

Ito, T., Feng, Q. L. and Matsuoka, A., 2015, Taxonomic significance of short forms of middle Permian *Pseudoalbaillella* Holdsworth and Jones, 1980 (Follicucullidae: Radiolaria). *Rev. Micropaléont.*, **58**, 3–12.

Ito, T. and Matsuoka, A., 2015, Swollen type of *Albaillella sinuata* Ishiga and Watase (Permian radiolaria) from a chert boulder in Ie-jima Island, Okinawa Prefecture, Japan. *News Osaka Micropaleontol. (NOM), Spec. Vol.*, no. 15, 207–217.

Jin, Y. X., Feng, Q. L., Meng, Y. Y., He, Q. H. and Gu, S. Z., 2007, Albaillellidae (Radiolaria) from the Latest Permian in Southern Guangxi, China. *Jour. Paleont.*, **81**, 9–18.

Kinoshita, N., 2013, Studies on the Nagarabaru-Higashi shellmound: Iejima, Okinawa, during the 5th century through first half of 7th century. *Rep. Grant-in-Aid Sci. Res. (A) 2009‑2012, Japan*, 392p. (in Japanese).

Konishi, K., 1963, Pre-Miocene basement complex of Okinawa and tectonic belt of the Ryukyu Islands. *Sci. Rep. Kanazawa Univ.*, **8**, 569–602.

Kuwahara, K. and Yao, A., 1998, Diversity of Late Permian radiolarian assemblages. *News Osaka Micropaleont. (NOM), Spec. Vol.*, no. 11, 33–46 (in Japanese with English abstract).

Kuwahara, K., Yao, A. and Yamakita, S., 1998, Reexamination of Upper Permian radiolarian biostratigraphy. *Earth Sci. (Chikyu Kagaku)*, **52**, 391–404.

Leutenegger, S., 1977, Reproductive cycles of larger foraminifera and depth distribution of generations. *Utrecht Micropaleont. Bull.*, **15**, 27–34.

Matsuoka, A., 1995, Jurassic and Lower Cretaceous radiolarian zonation in Japan and the western Pacific.

Island Arc, **4**, 140–153.

Matsuoka, A., Aita, Y., Munasri, Wakita, K., Shen, G., Ujiié, H., Sashida, K., Vishnevskaya, V., Bragin, N. and Cordey, F., 1996, Mesozoic radiolarians and radiolarian-bearing sequences in the circum-Pacific regions: A report of the symposium 'Radiolarians and Orogenic Belts'. *Island Arc,* **5**, 203–213.

Nakae, S., Kaneko, N., Miyazaki, K., Ohno, T. and Komazawa, M., 2010, *Geological Map of Japan 1:200,000, Yaron Jima and Naha*. Geological Survey of Japan, AIST (in Japanese with English abstract).

Ogg, J. G., Ogg, G. M. and Gradstein, F. M., 2016, A *Concise Geologic Time Scale 2016*. Elsevier, Amsterdam, 234p.

Okinawa General Bureau, 1983, *Ground water of Okinawa Prefecture: hydrogeological map of Okinawa Prefecture**. 95p. (in Japanese). *The title was translated by the authors.

Osozawa, S. and Watanabe, Y., 2011, *Geology of Nago and Yambaru District*. Nago Museum, 209p. (in Japanese with English abstract).

Panasenko, E. S. and Rudenko, B. S., 1987, Systematic significance of some morphologic feature of Albaillellidae (Paleozoic). *Paleont. Jour.*, 13–21 (in Russian).

Sashida, K., Salyapongse, S. and Nakornsri, N., 2000, Latest Permian radiolarian fauna from Klaeng, eastern Thailand. *Micropaleontology*, **46**, 245–263.

Shen, G. P., Ujiié, H. and Sashida, K., 1996, Off-scraped Permian–Jurassic bedded chert thrust on Jurassic–early Cretaceous accretionary prism: Radiolarian evidence from Ie Island, central Ryukyu Island Arc. *Island Arc*, **5**, 156–165.

Suzuki, H., 1992, Mesozoic radiolarian fauna from the Ie Island, Okinawa Prefecture. *99th Ann. Meet. Geol. Soc. Japan, Abstr.*, 124 (in Japanese).

Takami, M., Takemura, R., Nishimura, Y. and Kojima, T., 1999, Reconstruction of oceanic plate stratigraphies and unit division of Jurassic–Early Cretaceous accretionary complexes in the Okinawa Islands, central Ryukyu Island Arc. *Jour. Geol. Soc. Japan*, **105**, 866–880 (in Japanese with English abstract).

Takemura, A. and Nakaseko, K., 1981, A new Permian radiolarian genus from the Tamba Belt, Southwest Japan. *Trans. Proceed. Palaeont. Soc. Japan, New Ser.*, no. 124, 208–214.

Takemura, A., Ueshima, S., Miyake, A., Takemura, S. and Yamakita, S., 2009, Late Permian radiolarian fauna from a phosphatic nodule in Northern Chichibu Belt, Shikoku, Southwest Japan. *News Osaka Micropaleontol. (NOM), Spec. Vol.*, no. 14, 583–594 (in Japanese with English abstract).

Ujiié, H. and Hashimoto, Y., 1983, Geology and radiolarian fossils of the inner "Motobu Belt" in the Okinawa-jima region. *Earth Monthly (Gekkan Chikyu)*, **5**, 706–712 (in Japanese).

Ujiié, H. and Oba, T., 1991a, Geology and Permo–Jurassic radiolaria of the Iheya zone, innermost belt of the Okinawa Island Region, Middle Ryukyu Island Arc, Japan. Part 1. Geology and Permian radiolaria. *Bull. Coll. Sci., Univ. Ryukyus*, no. 51, 35–55.

Ujiié, H. and Oba, T., 1991b, Geology and Permo–Jurassic radiolaria of the Iheya zone, innermost belt of the Okinawa Island Region, Middle Ryukyu Island Arc, Japan. Part 2. Mesozoic radiolaria and geological structure. *Bull. Coll. Sci., Univ. Ryukyus*, no. 52, 53–89.

Wu, J. and Feng, Q. L., 2008, Late Changhsingian radiolarian biostratigraphy from Guangxi, South China and its correlation to conodonts. *Sci. China Ser. D: Earth Sci.*, **51**, 1601–1610.

Wu, J., Feng, Q. L., Gui, B. W. and Liu, G. C., 2010, Some new radiolarian species and genus from Upper Permian in Guangxi Province, South China. *Jour. Paleont.*, **84**, 879–894.

Xia, W. C. and Zhang, N., 1998, Early to Middle Permian radiolarians from the Kuhfeng Formation in southeastern Guangxi, South China. *Earth Sci. (Chikyu Kagaku)*, **52**, 188–202.

Zhang, N., Xia, W. C. and Shao, J., 2002. Radiolarian successional sequences and rare earth element variations in Late Paleozoic chert sequences of South China: An integrated approach for study of the evolution of paleo-ocean basins. *Geomicrobiol. Jour.*, **19**, 439–460.

Zhu, T. X., Zhang, Q. Y., Dong, H., Wang, Y. J., Yu, Y. S. and Feng, X. T., 2006., Discovery of the Late Devonian and Late Permian radiolarian cherts in tectonic mélanges in the Cêdo Caka area, Shuanghu, northern Tibet, China. *Geol. Bull. China*, **25**, 1413–1418 (in Chinese with English abstract).

第15回国際放散虫研究集会
巡検案内書

CONTENTS

15th InterRad
Niigata
2017

15 October 2017